СИСТЕМНІ ДОСЛІДЖЕННЯ ТА ІНФОРМАЦІЙНІ ТЕХНОЛОГІЇ

МІЖНАРОДНИЙ НАУКОВО–ТЕХНІЧНИЙ ЖУРНАЛ

У номері:

• **Прогресивні інформаційні технології, високопродуктивні комп'ютерні системи**

• **Теоретичні та прикладні проблеми інтелектуальних систем підтримання прийняття рішень**

• **Проблемно і функціонально орієнтовані комп'ютерні системи та мережі**

• **Математичні методи, моделі, проблеми і технології дослідження складних систем**

In the issue:

- **Progressive information technologies, high-efficiency computer systems**

- **Theoretical and applied problems of intelligent systems for decision making support**

- **Problem- and function-oriented computer systems and networks**

- **Mathematical methods, models, problems and technologies for complex systems research**

Шановні читачі!

Навчально-науковий комплекс «Інститут прикладного системного аналізу» Національного технічного університету України «Київський політехнічний інститут імені Ігоря Сікорського» видає міжнародний науково-технічний журнал

«СИСТЕМНІ ДОСЛІДЖЕННЯ ТА ІНФОРМАЦІЙНІ ТЕХНОЛОГІЇ».

Журнал публікує праці теоретичного та прикладного характеру в широкому спектрі проблем, що стосуються системних досліджень та інформаційних технологій.

Провідні тематичні розділи журналу:

Теоретичні та прикладні проблеми і методи системного аналізу; теоретичні та прикладні проблеми інформатики; автоматизовані системи управління; прогресивні інформаційні технології, високопродуктивні комп'ютерні системи; проблеми прийняття рішень і управління в економічних, технічних, екологічних і соціальних системах; теоретичні та прикладні проблеми інтелектуальних систем підтримання прийняття рішень; проблемно і функціонально орієнтовані комп'ютерні системи та мережі; методи оптимізації, оптимальне управління і теорія ігор; математичні методи, моделі, проблеми і технології дослідження складних систем; методи аналізу та управління системами в умовах ризику і невизначеності; евристичні методи та алгоритми в системному аналізі та управлінні; нові методи в системному аналізі, інформатиці та теорії прийняття рішень; науково-методичні проблеми в освіті.

Головний редактор журналу — ректор Національного технічного університету України «Київський політехнічний інститут імені Ігоря Сікорського», академік НАН України Михайло Захарович Згуровський.

Журнал «Системні дослідження та інформаційні технології» включено до переліку фахових видань ВАК України.

Журнал «Системні дослідження та інформаційні технології» входить до таких наукометричних баз даних: Scopus, EBSCO, Google Scholar, DOAJ, Index Copernicus, реферативна база даних «Україніка наукова», український реферативний журнал «Джерело», наукова періодика України.

Статті публікуються українською та англійською мовами.

Журнал рекомендовано передплатити. **Наш індекс 23918.** Якщо ви не встигли передплатити журнал, його можна придбати безпосередньо в редакції за адресою: 03056, м. Київ, просп. Перемоги, 37, корп. 35.

Dear Readers!

Educational and Scientific Complex «Institute for Applied System Analysis» of the National Technical University of Ukraine «Igor Sikorsky Kyiv Polytechnic Institute» is published of the international scientific and technical journal

«SYSTEM RESEARCH AND INFORMATION TECHNOLOGIES».

The Journal is printing works of a theoretical and applied character on a wide spectrum of problems, connected with system researches and information technologies.

The main thematic sections of the Journal are the following:

Theoretical and applied problems and methods of system analysis; theoretical and applied problems of computer science; automated control systems; progressive information technologies, high-efficiency computer systems; decision making and control in economic, technical, ecological and social systems; theoretical and applied problems of intellectual systems for decision making support; problem- and function-oriented computer systems and networks; methods of optimization, optimum control and theory of games; mathematical methods, models, problems and technologies for complex systems research; methods of system analysis and control in conditions of risk and uncertainty; heuristic methods and algorithms in system analysis and control; new methods in system analysis, computer science and theory of decision making; scientific and methodical problems in education.

The editor-in-chief of the Journal is rector of the National Technical University of Ukraine «Igor Sikorsky Kyiv Polytechnic Institute», academician of the NASU Michael Zaharovich Zgurovsky.

The articles to be published in the Journal in Ukrainian and English languages are accepted. Information printed in the Journal is included in the Catalogue of periodicals of Ukraine.

СИСТЕМНІ ДОСЛІДЖЕННЯ ТА ІНФОРМАЦІЙНІ ТЕХНОЛОГІЇ

2 • 2024

ЗМІСТ

SYSTEM RESEARCH AND INFORMATION TECHNOLOGIES

2 • 2024

CONTENT

STRATEGY OF THE CYBER-PHYSICAL SYSTEM FOR THE SMALL BUSINESS ENTERPRISE GUARANTEED FUNCTIONING WITH THE DIGITAL TWIN SUPPORT

N.D. PANKRATOVA, G.S. TYMCHIK, Ye.V. PANKRATOV

Abstract. The article presents a strategy of the cyber-physical system guaranteed functioning for a small business enterprise (SBE), which is ensured by maintaining the digital twin and is due to its extremely high relevance in modern conditions. Business processes are linked to Industry 4.0 competencies. One of the innovations it implements is Digital Twin, a comprehensive facility support tool. Digital twin allows for tracking and effectively managing the entire cycle of an infrastructure project, from planning, procurement, and production to commissioning and maintenance of the facility. PEST, SWOT, SAW, TOPSIS, and VIKOR methods are used to build a strategy.

Keywords: Industry 4.0, digital twin, cyber-physical systems, strategy, internet of things, computer, physical and mathematical models.

INTRODUCTION

The development and changes in industry that ensure the automation of production and business processes in parallel with the development of computer technology are associated with the competencies of the Fourth Industrial Revolution, which has become a logical stage caused by the technological progress of the modern world [1]. Industry 4.0, characterised by sustainability, connectivity and real-time data processing, is the main driver of modern digital transformation. For manufacturing companies, it is crucial to correctly identify the most appropriate Industry 4.0 technologies that meet their operational schemes and production goals. To address this issue, various technology selection systems have been proposed, some of which are complex or require historical data from manufacturing enterprises that may not always be available. Paper [2] proposes an Industry 4.0 technology selection system that uses a fuzzy analytical hierarchy process and a fuzzy technique for ordering preferences by similarity to the ideal solution to rank different Industry 4.0 technologies based on their economic, social, and environmental impacts. The system is used to select the top three Industry 4.0 technologies out of eight technologies considered important for a manufacturing company. The results of the case study showed that cyber-physical systems, big data analytics, and autonomous/industrial robots occupy the top three places in the tech-

nology ranking with a proximity coefficient of 0.964, 0.928, and 0.601, respectively. digital twins (DTs) are used to support the guaranteed functioning of cyber-physical systems, which are used both to design new and maintain existing technical systems. The basic concept of a DT is the presence of a physical object, a virtual object and the exchange of information between them [3]. A DT can be created as a computer model of a physical object, using a set of forecasting procedures and a powerful hardware and software system. The mathematical description of DTs can be obtained by statistical and analytical modelling, machine learning [4; 5]. The development of a DTs can be based on the use of simulation modelling methods that provide the most realistic representation of a physical environment or object in the virtual world. The virtual nature of the object allows you to experiment with the model, build scenarios instead of real experiments without losing resources and risks.

The areas of application of DTs in small business include, in particular, the manufacturing sector: repair and production of bicycles, mopeds, household appliances, etc. The versatility of the technology allows it to be used at almost any enterprise. A small business enterprise's CPS is a comprehensive integration between physical production processes and their virtual representations, which allows for detailed modelling, monitoring, analysis and optimisation of SBE production. In this context, the DTs acts as a dynamic virtual representation of the physical system, which is constantly updated using data from sensors and data collection mechanisms in production. The real-time monitoring of the physical system by the DTs allows for detailed process analysis, forecasting of critical characteristics, which makes it possible to detect deviations from the normal situation in a timely manner, optimise production flows and improve overall production efficiency.

This SBE CPS includes not only automated assembly lines, but also quality management systems, logistics modules, production planning modules, and security systems. The use of DTs allows for real-time visualisation of the production process, analysis of various production scenarios, forecasting, and rapid response to changes in production conditions or orders. Such a cyber-physical system plays a key role in ensuring flexibility, efficiency and innovation at an SBE manufacturing facility, allowing not only to improve existing processes but also to implement the latest technological solutions to increase competitiveness and meet current market trends.

Gartner estimates that by 2027, more than 40% per cent of large companies worldwide will use DTs in their projects to increase revenue [6; 7]. Furthermore, Global Market Insight estimates that the DTs market size, which was worth $8 billion in 2022, will grow at an estimated 25% per cent CAGR between 2023 and 2032 [9]. According to another recent global technology research report, by 2028, the volume of solutions supporting diabetes in smart cities will reach $5.2 billion; more than 94% of all IoT platforms will contain some form of digital twinning; DTs will become a standard feature/functionality for implementing IoT applications; leading solutions for DTs include asset twinning, component twinning, system twinning, process twinning, and workflow twinning; more than 96% of suppliers recognise the need for IIoT APIs and platform integration with digital twinning functionality for industrial verticals; more than 42% of executives across a wide range of industry verticals understand the benefits of digital twinning, and 59% of them plan to implement it in their operations by 2028 [10].

The purpose of this paper is to develop a DTs strategy to support the guaranteed functioning of the cyber-physical system in the form of a small business enterprise.

RELATED PAPERS

The use of DTs technology is growing exponentially, and it is transforming the way we do business. For a detailed history of development, classification, applications, and prospects of this technology, see [11]. Over the past few years, vital business applications have been using DTs, and it is predicted that this technology will expand to more applications, use cases, and industries in the form of CFS. Among other things, organisations are implementing DTs, the main purpose of which is scenario analysis and support of business strategies [12]. The paper [12] also describes how DTs simplify intelligent automation in various industries, defines the concept, highlights the evolution and development of, examines its key technologies, explores trends and challenges, and explores its application in various industries. Today, this technology is used in many industries to provide an accurate virtual representation of objects and simulate operational processes. The growing scale and complexity of projects, the increasing number of stakeholders, globalisation, technological advancements, changing business models and declining profitability are forcing the construction industry to undergo a digital transformation. The DTs and the Internet of Things (IoT) are among the most significant digital developments of recent years. The purpose of the article [13] is to analyse the challenges of using the technologies of digitalisation and IoT in the construction sector, which offers significant benefits, such as improved project management, reduced errors and rework, and increased productivity and efficiency. On the other hand, implementation challenges include upfront costs, integrating the DTs with existing systems, managing IoT data, and a lack of standardisation and security. The growth of Internet of Things (IoT) systems is driven by their potential to improve efficiency, enhance decision-making, and create new business opportunities in various fields. The paper [14] identifies the main selection problems in IoT systems, the criteria used in multicriteria evaluation, and the multicriteria methods used to solve IoT selection problems. Next, a Hybrid Group Multicriteria Approach is proposed to solve selection problems in IoT systems. The approach includes the Best Worst Method (BWM) weighting method, the multicriteria Simple Additive Weighting (SAW) method, the Top Order Preference by Similarity to the Ideal Solution (TOPSIS) method, the All-Criteria Optimisation and Compromise Solution (VIKOR) method, the Comprehensive Proportional Assessment (COPRAS) method, and a method that combines the solutions obtained by the four considered multicriteria methods to obtain a single solution. The SAW, TOPSIS, VIKOR and COPRAS methods were analysed in terms of their advantages, disadvantages, inputs, outputs, measurement scale, normalisation type, aggregation method, parameters, complexity of implementation and interactivity. Technological advances in cyber-physical systems, digital manufacturing and Industry 4.0 are presented in [15]. It also presents some challenges and future research topics in these areas. In [16], it is argued that DCs rely on two key elements to create business value: digital data streams, a constant flow of digital images of events generated by sensors both inside and outside the phys-

ical object, and detailed digital models. The DTs provide many new opportunities for creating value by transferring software strategies to the physical world. In [17; 18], the possibility of controlling the modes of electrocuting (MCECT) was substantiated. It is shown that the peculiarities of the multifactorial influence of the control parameters of the melt treatment process on the structure formation of castings can only be revealed by numerical experiments using adequate computer models. The basic principles of constructing an automated MCECT system are formulated and the structure of an integrated three-component information system (ITIS) is developed for its implementation using computer models of many physical processes of EOT. Computer models serve as the system basis of the algorithmic paradigm laid down in the ITIS, which includes the identification of experimental casting samples with standard prototypes and predictive algorithms for controlling the modes of electric current melt treatment. Paper [19] presents general methods of DT technology and predictive maintenance technology, analyses the gap between them, and points out the importance of using DT technology to implement predictive maintenance. The article presents the method of predictive maintenance based on DTs, provides its characteristics and its differences from traditional predictive maintenance, and introduces the application of this method in smart manufacturing and in various industries.

MODELS AND METHODS

In today's conditions of rapid technological development and competitive business environment, the strategic identification of priority areas for the construction and use of a DT is becoming an integral part of the successful functioning of enterprises. The PEST, SWOT, SAW, TOPSIS, and VIKOR methods are used to build a strategy for the guaranteed functioning of the cyber-physical system of a small business enterprise with the support of a DT in the form of a computer model of a physical object. When analysing the subject area, PEST analysis [20] is used to identify the main factors, which is intended to identify political (P – political), economic (E – economic), social (S – social) and technological aspects of the external environment that affect the company's business. To find the strengths and weaknesses of this technology, opportunities and risks that accompany them, the SWOT analysis was used with further refinement by the VIKOR, TOPSIS methods.

A SWOT analysis is a critical part of the strategic management process, used to assess the strengths, weaknesses, opportunities and threats of an organisation or any activity. It is a key strategic planning tool that helps analyse internal and external factors. The purpose of a SWOT analysis is to formulate a business strategy, taking into account the existing conditions. The analysis includes four components: "Strengths", "Weaknesses", "Opportunities", "Threats", where strengths and weaknesses are internal factors of the organisation, and opportunities and threats are external. SWOT analysis helps to develop strategies that use strengths and opportunities to achieve the organisation's goals while minimising the impact of weaknesses and threats [21; 22].

The obtained results become the basis for strategic planning and implementation of the DTs, providing the enterprise with competitive advantages and sustainability in accordance with modern market requirements.

Implementation and results of the SWOT analysis procedure

In order to develop a strategy for the CPS of a small business enterprise with the support of a DT in the form of a computer model, using the results obtained by the PEST method, we formulate their characteristic critical strengths and weaknesses, opportunities and threats in the form of a SWOT matrix (Table 1).

T a b l e 1. SWOT-matrix for building a DTs' strategy

Internal controlled factors	
Strengths	Weaknesses
S_1 — increased accuracy and efficiency of production processes: DTs allows for detailed modelling and optimisation of all aspects of the production process, increasing overall productivity and potentially reducing equipment and personnel costs.	W_1 — high cost of development and implementation: the need for significant investments in the development and implementation of software and hardware, as well as support for their correct functioning
S_2 — ability to predict and prevent failures: the use of DTs allows you to identify potential problems in equipment and processes in advance, reducing the number of breakdowns, downtime and repair costs.	W_2 — dependence on data quality and availability: accurate, up-to-date and structured data for analysis is required, and a system for collecting and organising it is needed, which can be costly and difficult to implement
S_3 — flexibility and adaptability of production: DTs allow you to quickly adapt production lines to rapidly changing market requirements, including the military situation, production conditions of small businesses, such as bicycle shops, household appliances, etc.	W_3 — the need for highly skilled professionals: the need to have a staff with highly specialised personnel with relevant programming experience and an understanding of the development approaches that will be used.
S_4 — reducing the time required to repair and upgrade products: modifying, scaling and improving software, testing it quickly and safely.	W_4 — the need to integrate with existing information systems and processes: this can be a complex and time-consuming process, due to lack of proper documentation, inadequate existing systems and insufficient support.
S_5 — improving product quality: The use of DTs allows for the implementation of automated quality control systems, which will reduce the percentage of defects in the manufacture of spare parts at all stages.	W_5 — potential difficulty in managing change: resistance to change on the part of staff who may be resistant or not ready to implement new technologies due to the need to absorb new information and gain additional qualifications.
S_6 — the possibility of increasing efficiency. Automation of calculation and procurement tasks will lead to a significant increase in accuracy and sreduce the impact of the human factor, which will reduce the required resources and make more efficient use of existing ones.	W_6 — dependence on vendors: potential dependence on foreign suppliers of software, hardware and services used in the development and underlying operation of the software.

External uncontrollable factors	
Opportunities	Threats
O_1 — the growing popularity of digital technologies in the CFS sector and consumer demand for high-quality small business products.	T_1 — risks of cyberattacks and the possibility of data loss from servers or disruption of DTs operations.
O_2 — use of artificial intelligence and analytical tools that can improve the efficiency of the DTs computer model and its analytical capabilities.	T_2 — the threat of military attacks: problems with power supply, enemy air strikes and sabotage, and the risk of physical destruction of the infrastructure that supports operations.
O_3 — increasing business resilience: rapid adaptation of the computer model of the DTs to changes and challenges of the market during the war.	T_3 — the need to constantly update and adapt the computer model of the DTs to changing market conditions during the war.
O_4 — the potential to improve the quality of products and production processes through continuous improvement and upgrade of the computer model of the DTs.	T_4 — the possibility of technical problems in the software that may cause a DTs failure and lead to data loss, business interruption and other losses.
O_5 — the ability to attract new customers and markets through the introduction of advanced technologies and increase the company's competitiveness.	T_5 — insufficient support from the state for the introduction and use of DTs.
O_6 — government support: the opportunity to receive government grants or support for project activities in areas that are a priority for the state, such as the development of cycling infrastructure.	T_6 — economic instability: macroeconomic fluctuations can affect investment and budgets for innovation.

Let's form a matrix of comparison internal and external components of SWOT analysis based on estimates of the connection strength in the range [0.1] (Table 2).

T a b l e 2. Matrix for comparing the components of SWOT analysis

I/E components	T_1	T_2	T_3	T_4	T_5	T_6	O_1	O_2	O_3	O_4	O_5	O_6
S_1	0.2	0.0	0.5	0.2	0.2	0.3	0.5	0.8	0.7	0.2	0.0	0.3
S_2	0.7	0.3	0.4	0.3	0.3	0.3	0.6	0.7	0.5	0.3	0.0	0.3
S_3	0.3	0.0	1	0.5	0.7	0.2	0.7	0.9	1	0.5	0.6	0.6
S_4	0.6	0.0	0.9	0.4	0.6	0.5	0.8	0.8	0.9	0.6	0.5	0.5
S_5	0.7	0.0	0.6	0.6	0.5	0.6	0.7	0.6	0.5	0.2	0.7	0.4
S_6	0.2	0.0	0.1	0.2	0.3	0.5	0.2	0.2	0.3	0.3	0.0	0.7
W_1	0.8	0.7	0.7	0.5	0.7	0.9	0.3	0.9	0.8	0.8	0.6	0.8
W_2	0.9	0.0	0.6	0.7	0.0	0.5	0.1	1	0.5	0.7	0.0	0.2
W_3	0.5	0.5	0.7	0.5	0.0	0.7	0.0	0.8	0.2	1	0.0	0.5
W_4	0.6	0.4	0.3	0.7	0.0	0.6	0.2	0.6	0.4	0.6	0.0	0.6
W_5	0.6	0.0	0.8	0.6	0.4	0.3	0.0	0.3	0.7	0.3	0.0	0.5
W_6	0.7	0.3	0.7	0.6	1	0.6	0.4	0.7	0.6	0.7	0.2	0.6

Let us compare opportunities with strong and weak characteristics, as well as compare threats with strong and weak characteristics (Table 3).

T a b l e 3. Comparison of opportunities and threats with strong and weak characteristics

Opportunities	Strengths	Weaknesses
O_1	S_1, S_2, S_3, S_4, S_5, S_6	W_1, W_2, W_4, W_6
O_2	S_1, S_2, S_3, S_4, S_5, S_6	W_1, W_2, W_3, W_4, W_5, W_6
O_3	S_1, S_2, S_3, S_4, S_5, S_6	W_1, W_2, W_3, W_4, W_5, W_6
O_4	S_1, S_2, S_3, S_4, S_5, S_6	W_1, W_2, W_3, W_4, W_5, W_6
O_5	S_3, S_4, S_5	W_1, W_6
O_6	S_1, S_2., S_3, S_4, S_5, S_6	W_1, W_2, W_3, W_4, W_5, W_6
Threats	**Strengths**	**Weaknesses**
T_1	S_1, S_2, S_3, S_4, S_5, S_6	W_1, W_2, W_3, W_4, W_5, W_6
T_2	S_2	W_1, W_3, W_4, W_6
T_3	S_1, S_2, S_3, S_4, S_5, S_6	W_1, W_2, W_3, W_4, W_5, W_6
T_4	S_1, S_2, S_3, S_4, S_5, S_6	W_1, W_2, W_3, W_4, W_5, W_6
T_5	S_1, S_2, S_3, S_4, S_5, S_6	W_1, W_5, W_6
T_6	S_1, S_2, S_3, S_4, S_5, S_6	W_1, W_2, W_3, W_4, W_5, W_6

To determine the most important factors, let's calculate the impact of internal characteristics on the implementation of threats and opportunities F_j, G_k, D_i, H_m using the following formulas:

$$F_j = \left(\sum_i K_{S_j T_i} + \sum_m K_{S_j O_m} \right), \; G_k = \left(\sum_i K_{W_k T_i} + \sum_m K_{W_k O_m} \right), \; j = \overline{1,11}, k = \overline{1,8};$$

$$D_i = \left(\sum_j K_{S_j T_i} - \sum_k K_{W_k T_i} \right), \; H_m = \left(\sum_j K_{S_j O_m} - \sum_k K_{W_k O_m} \right), \; i = \overline{1,8}, \; m = \overline{1,9},$$

where $K_{S_j T_i}$ is the element of the matrix at the intersection of strength S_j and threat T_i; $K_{S_j O_m}$ is the element at the intersection of strength S_j and opportunity O_m; $K_{W_k T_i}$ is the the element at the intersection of the weakness W_k and the threat T_i; $K_{W_k O_m}$ is the element at the intersection of weakness W_k and opportunity O_m.

The calculation results are shown in Table 4.

T a b l e 4. Calculated critical factors by degree of importance

Strengths						
Factors	S_1	S_2	S_3	S_4	S_5	S_6
F	7.1	7.0	6.1	4.7	3.9	3.0
Weaknesses						
Factors	W_1	W_6	W_3	W_2	W_4	W_5
G	8.5	7.1	5.4	5.2	5.0	4.5
Opportunities						
Factors	O_1	O_5	O_3	O_2	O_6	O_4
H	2.5	1.0	0.7	-0.3	-0.4	-2.0
Threats						
Factors	T_2	T_1	T_4	T_6	T_3	T_5
D	-1.6	-1.4	-1.4	-1.2	-0.3	0.5

Based on the results of the SWOT analysis, it is possible to propose SO, WO, ST, WT strategies for developing DTs in small business in the form of the TOWS matrix [23] (Table 5).

T a b l e 5. TOWS matrix

	S_1	S_2	S_3	W_1	W_6	W_2
	SO-strategy			**WO-strategy**		
O_1 O_5 O_3	In order to build a strategy for small business DTs CPS taking into account all aspects of production processes, it is necessary to ensure the sustainability of business operations with rapid adaptation of the computer model of the DTs to changes and challenges of the market during the war, software modification and fast and safe testing, availability of a powerful forecasting unit involving artificial intelligence and analytical tools, and government support.			The high financial costs of developing and implementing, as well as maintaining the correct functioning of software and hardware, should be compensated by attracting highly qualified specialists, business investment, and assistance from friendly countries and foundations. Accelerate the creation of unified technical standards for DTs and legislative regulation of digitalisation. Determine the organisational and legal forms of operation of this technology, as well as quality and cyber-security standards.		
	WT-strategy			**WT-strategy**		
T_2 T_1 T_4	In the event of the threat of military attacks, cyber-attacks and the possibility of data loss from servers or disruption of the computer model of the DTs due to technical problems in the software, compensate with the ability to predict and prevent failures, relocate critical facilities to a protected area and attract qualified personnel, which allows the company to quickly adapt production lines to rapidly changing market requirements during martial law. This will ensure fast and high-quality project implementation and prevent cyber-attacks.			To search for available financial resources and work on standardising DTs technology at the legislative level and increase the transparency of corruption-prone processes. The state and business should establish cooperation with HEIs to train qualified IT specialists and ensure comfortable legal conditions for their work. The priority is to prevent inappropriate responses from the education system and corruption, as well as to ensure a high level of cyber-security. Ensure communication with international partners on possible threats to production and ways to overcome them.		

FINDING THE OPTIMAL STRATEGY FOR DEVELOPING A SMALL BUSINESS ENTERPRISE'S DTS CPS

TOPSIS method. Results of calculations

The TOPSIS and VIKOR methods have been applied to find the optimal strategy for developing the DTs CPS of a small business enterprise. The same results obtained by both methods in most cases indicate the sustainability of the decision.

The TOPSIS method is a multi-criteria decision-making tool that can be particularly useful for small businesses when choosing the best option from various alternatives. It helps small businesses find the solution that is closest to the ideal option and at the same time furthest from the undesirable one. The method includes the steps of data normalisation, weighting of criteria, identification of the ideal and worst solution options, and analysis of the distances to them for each proposal [24]. This allows small businesses to choose the most effective solutions, increase their competitiveness and efficiency.

The TOPSIS method is used to search for compromise strategies. Using the alternatives for implementing strategies, taking into account the results of the SWOT analysis and the TOWS matrix, we form a decision matrix a_{ij}, $i = \underline{1,4}$, $j = \underline{1,12}$, where the index i corresponds to the strategy (criterion) SO, WO, ST, WT, and the index j determines the alternative S_1, S_2, S_3,…, T_2, T_1, T_4 (Table 6).

The SAW method (Simple Additive Weighting Method) is a method of simple additive weighting that obtains the total score of each alternative by multiplying the value of the attribute for each alternative by the weight assigned to that attribute. The alternative with the highest score is the answer to the decision task. The weighting factors w_j, $j = \underline{1,12}$, which determine the importance of the factors for the decision maker and should sum to one, are shown in Table 6.

T a b l e 6. Decision matrix and weights of alternatives

Decision matrix											
i/j	S_1	S_2	S_3	W_1	W_6	W_3	O_1	O_5	O_3	T_2	T_1	T_4
SO	4.1	4.3	3.1	4.2	3.2	1.67	3.5	0.9	3.9	0.05	2.7	2.2
WO	3.5	3.6	2.6	3.9	3.1	1.52	0.15	0.27	2.2	1.27	2.1	1.6
ST	2.5	2.25	2.5	4.3	3.9	2.42	3.5	0.9	3.4	0.01	2.4	2.2
WT	2.3	2.12	2.3	3.9	3.3	2.12	0.61	0.21	2.8	1.17	3.8	3.3
Weights of alternatives											
w/j	S_1	S_2	S_3	W_1	W_6	W_3	O_1	O_5	O_3	T_2	T_1	T_4
w	0.1	0.09	0.09	0.1	0.09	0.09	0.07	0.08	0.08	0.09	0.07	0.05

Next, the decision matrix is normalised and weighted using formulas (Table 7)

$$r_{ij} = \frac{a_{ij}}{\sqrt{\sum_i^4 a_{ij}^{\,2}}}, \ \ i = \underline{1,4}, \ \ j = \underline{1,12} ;$$

$$v_{ij} = w_j r_{ij}, \quad \sum_{j}^{12} w_j = 1.$$

For each alternative $S_1, S_2, S_3, \ldots, T_2, T_1, T_4$ the ideal solution will be determined by the weighted normalised decision matrix as the maximum v_j^+ and minimum v_j^- values of the SO,WO,ST,WT criterion scores using formulas (Table 7)

$$v_j^+ = \max_i r_{ij}, j = \overline{1,12}; \quad v_j^- = \min_i r_{ij}, j = \overline{1,12},$$

v_j^+ and v_j^-, $j = \overline{1,12}$ can be interpreted as, respectively, the best and worst solutions for each criterion.

T a b l e 7. Weighted normalised decision matrix

j/i	SO	WO	ST	WT	v_j^+	v_j^-
S_1	0.06434	0.05492	0.03923	0.03609	0.06434	0.03609
S_1	0.06043	0.05059	0.03162	0.02979	0.06043	0.02979
S_3	0.05281	0.04429	0.04258	0.03918	0.05281	0.03918
W_1	0.05148	0.04780	0.05271	0.04780	0.05271	0.04780
W_6	0.04248	0.04115	0.05178	0.04381	0.05178	0.04115
W_3	0.03823	0.03480	0.05541	0.04854	0.05541	0.03480
O_1	0.04910	0.00210	0.04910	0.00855	0.04910	0.00210
O_5	0.05463	0.01638	0.05463	0.01274	0.05463	0.01274
O_3	0.04967	0.02802	0.04330	0.03566	0.04967	0.02802
T_2	0.00260	0.06616	0.00052	0.06095	0.06616	0.00052
T_1	0.03346	0.02602	0.02974	0.04709	0.04709	0.02602
T_4	0.02287	0.01663	0.02287	0.03430	0.03430	0.01663

Let us imagine an "ideal solution" that maximises all criteria simultaneously v^+ and a "worst case" v^-, that minimises all criteria

$$v^+ = (v_1^+, v_2^+, \ldots, v_{12}^+) = v_{ij}; \quad v^- = (v_1^-, v_2^-, \ldots, v_{12}^-) = v_{ij}.$$

For each realistic alternative, the Euclidean distance to the "ideal solution" D_i^+ and to the "worst solution" D_i^- is calculated using formulas, respectively:

$$D_i^+ = \sqrt{\sum_{j=1}^{12} (v_{ij} - v^+)^2};$$

$$D_i^- = \sqrt{\sum_{j=1}^{12} (v_{ij} - v^-)^2}.$$

In the TOPSIS method, a compromise alternative is selected based on the C_i indicator using formula. The results of the calculations are shown in Table 8.

$$C_i = \frac{D_i^-}{D_i^+ + D_i^-}.$$

T a b l e 8. Finding the best compromise strategy using the TOPSIS method

	Strategies in ascending order of performance			
	SO	**WO**	**WT**	**ST**
D^+	0.06884	0.07560	0.0753c5	0.07966
D^-	0.08049	0.07166	0.06858	0.06953
C	**0.53903**	0.48662	0.47648	0.46607

According to the TOPSIS method, the best compromise strategy for the guaranteed functioning of the cyber-physical system for a small business enterprise with the support of a DT is the SO strategy. It consists in the need to ensure business sustainability with the rapid adaptation of the computer model of the DTs to changes and challenges of wartime, software modification and fast and safe testing, the availability of a powerful forecasting unit involving artificial intelligence and analytical tools, possible state suspport.

The VIKOR method. Results of calculations

The use of the VIKOR method for multi-criteria decision-making can be useful for small business development, helping to select suppliers, assess the quality of services or define business strategies. VIKOR allows to optimize operations or strategic directions based on a systematic evaluation of available options against a set of criteria [25].

Let's search for compromise strategies using the VICOR method. Let us take the decision matrix a_{ij}, $i = \underline{1,4}$, $j = \underline{1,12}$ and the weights w_j, $j = \underline{1,12}$, which were taken for the TOPSIS method (Table 6). For all alternatives, the characteristics S_i, R_i, Q_i are calculated using formulas, respectively:

$$S_i = \sum_{j=1}^{20} \frac{w_j(a_j^+ - a_{ij})}{(a_j^+ - a_j^-)}, \text{ where } a_j^+ = \max_i a_{ij}, \ a_j^- = \min_i a_{ij};$$

$$R_i = \left(\frac{w_j(a_j^+ - a_{ij})}{(a_j^+ - a_j^-)} \right), \text{ where } a_j^+ = \max_i a_{ij}, \ a_j^- = \min_i a_{ij};$$

$$Q_i = \begin{cases} \dfrac{R_i - R^-}{R^+ - R^-}, & \text{if } S^+ = S^-, \\[2mm] \dfrac{S_i - S^-}{S^+ - S^-}, & \text{if } R^+ = R^-, \\[2mm] v\dfrac{S_i - S^-}{S^+ - S^-} + (1-v)\dfrac{R_i - R^-}{R^+ - R^-}, & \text{if } S^+ \neq S^- \text{ and } R^+ \neq R^-. \end{cases} \quad i = \overline{1,4}, \quad (1)$$

In formula (1), v is chosen in the range [0.1]. If there are no other conditions, $v = 0.5$, is assumed to be 0.5, which was done here. Next, Q_i are ordered in ascending order. The strategy with the minimum Q_i is assumed to be the best. The results of the calculations are shown in Table 9.

T a b l e 9. Finding the best compromise strategy using the VIKOR method

	Strategies in ascending order of performance			
	SO	ST	WT	WO
S	0.34353	0.44455	0.67679	0.74152
R	0.08714	0.09	0.1	0.1
Q	0	0.23801	0.91867	1

According to these results, the best strategy according to the VIKOR method is the SO strategy, since its value is minimal. In terms of all characteristics S, R, Q here is the same ordering of strategies SO, ST, WT, WO, with strategy SO being simultaneously the best in the ranking series by S and R, which emphasises the stability of the solution. Additionally, for the best alternative, the acceptable difference from the other alternatives is checked $\Delta Q = \dfrac{1}{4-1} = \dfrac{1}{3}$, which can be interpreted as a significant advantage of one alternative over the others. For VIKOR, the difference between the SO strategy and the ST strategy is $0.23801 < \dfrac{1}{3}$. For the other alternatives, the difference is significantly greater than $\dfrac{1}{3}$.

CONCLUSIONS

The carried out research allows to draw a conclusion about building a strategy for guaranteed functioning of the cyber-physical system for a small business enterprise with the support of a DT. Using PEST-analysis, the main factors in the subject area under consideration were identified, and with the help of SWOT analysis, the most significant strengths and weaknesses of the DTs technology, opportunities and threats associated with them were identified. Based on the results of the SWOT analysis, four strategies SO, ST, WO, WT were formed, on the basis of which the TOWS strategy matrix was built, and a decision matrix was formed. To find the optimal strategy, the multi-criteria decision-making methods TOPSIS and VIKOR with the involvement of the SAW method were used.

According to the results of calculations using the TOPSIS and VIKOR methods, the SO strategy was found to be the best compromise strategy for the guaranteed functioning of the cyber-physical system for a small business enterprise with the support of a DT. It consists in the need to ensure the sustainability of business operation with rapid adaptation of the computer model of the DTs to changes and challenges of the market during wartime related to possible cyber-attacks and the possibility of data loss from servers or disruption of the DTs due to technical problems of various nature, software modification and fast and safe testing, availability of a powerful forecasting unit involving artificial intelligence and analytical tools, and possible government support. This will ensure fast and high-quality execution of projects, orders, and new technical solutions.

In the future, it is planned to use the foresight and cognitive impulse modelling methodologies to build scenarios for the implementation of the strategy SO for guaranteed functioning of the SBE with the support of the DTs.

REFERENCES

1. H. Lasi, P. Fettke, H.-G. Kemper, T. Feld, and M. Hoffmann, "Industry 4.0", *Business & Information Systems Engineering*, vol. 6, pp. 239–242, Aug 2014. doi: 10.1007/s12599-014 0334-4
2. Parham Dadash Pour, Aser Alaa Ahmed, Mohammad A. Nazzal, and Basil M. Darras, "An Industry 4.0 Technology Selection Framework for Manufacturing Systems and Firms Using Fuzzy AHP and Fuzzy TOPSIS Methods," *Systems*, 11(4), 192, 2023. doi: 10.3390/systems11040192

3. M. Grieves, "Product lifecycle management: the new paradigm for enterprises," *International Journal of Product Development*, vol. 2, no. 1-2, 2005. doi: 10.1504/IJPD.2005.006669

4. N. Pankratova, I. Golinko, "Approach to Development of DTModel for Cyber-Physical System in Conditions of Conceptual Uncertainty," in *Zgurovsky M., Pankratova N. (eds) System Analysis and Artificial Intelligence. Studies in Computational Intelligence, Springer, Cham*, vol. 1107, pp. 3–25, 2023. doi: 10.1007/978-3-031-37450-0_1

5. Nataliya Pankratova, Igor Golinko, "Development of DTs to Support the Functioning of Cyber-physical Systems," *Computer Science Journal of Moldova 2023-12*. doi: 10.56415/csjm.v31.15

6. *Gartner survey reveals DTs are entering mainstream use.* 2019. Available: https://www.gartner.com/en/newsroom/press-releases/2019-02-20-gartner-survey-reveals-digital-twins-are-entering-mai

7. "The DTJourney: A smooth pathway to digital innovation," *Mevea*, 2022, May 10. Available: https://mevea.com/news-events/blog/the-digital-twin-journey-a-smooth-pathway-to-digital-innovation/

8. *Global Market Insight DTmarket.* (2022). Available: https://www.gminsights.com/industry-analysis/digital-twin-market

9. *Digital Twins Market by Technology, Twinning Type, Cyber-to-Physical Solutions, Use Cases and Applications in Industry Verticals 2023– 2028*. March 2023, 154 p.

10. N.D. Pankratova, K. Grishyn, and V. Barilko, "DTs: stages of concept development, areas of use, prospects," *System Research and Information Technologies*, no. 2, pp. 7–21, 2023. doi: 10.20535/srit.2308-8893.2023.2.01

11. Mohsen Attaran, Bilge Gokhan Gelik, "Digital Twin: Benefits, use cases, challenges and opportunities," *Decision Analytics Journal*, vol. 6, no. 100165, pp. 1–8, March 2023. doi: 10.1016/j.dajour.2023.100165

12. Vedat Nalioğlu, Hazal Tokdemi, and Deniz Artan, "Adopting DTand Internet of Things in the Construction Industry: A SWOT Analysis," *Lecture Notes in Civil Engineering (LNCE)*, vol. 350, June 2023. doi: 10.1007/978-3-031-32511-3_169

13. Constanta Zoie Radulescu, Marius Radulescu, "A Hybrid Group Multi-Criteria Approach Based on SAW, TOPSIS, VIKOR, and COPRAS Methods for Complex IoT Selection Problems," *Electronics*, 13(4), 789, 2024. doi: 10.3390/electronics13040789

14. Lidong Wang, Guanghui Wang, "Big Data in Cyber-Physical Systems, Digital Manufacturing and Industry 4.0," *International Journal of Engineering and Manufacturing*, 4, pp. 1–8, 2016. doi: 10.5815/ijem.2016.04.01

15. Federico Pigni, Richard Watson, and Gabriele Piccoli, "DTs: Representing the Future," *SSRN Electronic Journal*, 2021. doi: 10.2139/ssrn.3855535

16. Yu. Zaporozhets, A. Ivanov, Yu. Kondratenko, and V. Tsurkin, "Computer models for mode control of electric current treatment of melts at specified quality criteria for cast products. Part 1," *Electronic modeling*, vol. 42, no. 3, pp. 53–69, 2020. doi: 10.15407/emodel. 42.03.053

17. Yu. Zaporozhets, A. Ivanov, Yu. Kondratenko, and V. Tsurkin, "Computer models for mode control of electric current treatment of melts at specified quality criteria for cast products. Part 2," *Electronic modeling*, vol. 42, no. 4, pp. 49–70, 2020. doi: 10.15407/emodel. 42.04.049

18. D. Zhong, Z. Xia, Y. Zhu, and J. Duan, "Overview of predictive maintenance based on DTtechnology," *Heliyon*, 9(4), article e14534, 2023. doi: 10.1016/j.heliyon.2023.e14534

19. Carlos Diaz Ruiz, Jonathan J. Baker, Katy J. Mason, and Kieran Tierney, "Market-scanning and market-shaping: why are firms blindsided by market-shaping acts?" *Journal of Business & Industrial Marketing*, vol. 35, no. 9, pp. 1389–1401, 2020. doi: 10.1108/JBIM-03-2019-0130

20. David Pickton, Sheila Wright, "What's SWOT in strategic analysis?" *Strategic Change*, 7, pp. 101–109, 1998. doi: 10.1002/(SICI)1099-1697(199803/04)7:2< 101::AID-JSC332>3.0.CO;2-6

21. C.R. Sharath Kumar, K.B. Praveena, "SWOT ANALYSIS," *International Journal of Advanced Research*, 11, pp. 744–748, 2023. doi: 10.21474/IJAR01/17584

22. Jyoti Snehi, Abhinav Bhandari, and Gurpreet Singh, "iNIDS: SWOT Analysis and TOWS Inferences of State-of-the-Art NIDS solutions for the development of Intelligent Network Intrusion Detection System," *Computer Communications*, 195, 2022. doi: 10.1016/j.comcom.2022.08.022

23. Youssef Lamrani Alaoui, *Introduction to Multi Criteria Decision Making: TOPSIS Method*. 2019. doi: 10.13140/RG.2.2.36465.22882

24. Morteza Yazdani, Felipe Graeml, "VIKOR and its Applications: A State-of-the-Art Survey," *International Journal of Strategic Decision Sciences*, vol. 5, issue 2 pp. 56–83, April 2014. doi: 10.4018/ijsds.2014040105

INFORMATION ON THE ARTICLE

Nataliya D. Pankratova, ORCID: 0000-0002-6372-5813, Educational and Research Institute for Applied System Analysis of the National Technical University of Ukraine "Igor Sikorsky Kyiv Polytechnic Institute", Ukraine, e-mail: natalidmp@gmail.com

Gregory S. Tymchik, ORCID: 0000-0003-1079-998X, National Technical University of Ukraine "Igor Sikorsky Kyiv Polytechnic Institute", Ukraine, e-mail: deanpb@kpi.ua

Yevhen V. Pankratov, ORCID: 0009-0004-1508-3053, National Technical University of Ukraine "Igor Sikorsky Kyiv Polytechnic Institute", Ukraine, e-mail: pankratov.science@gmail.com

СТРАТЕГІЯ ГАРАНТОВАНОГО ФУНКЦІОНУВАННЯ КІБЕРФІЗИЧНОЇ СИСТЕМИ ПІДПРИЄМСТВА ДРІБНОГО БІЗНЕСУ ІЗ СУПРОВОДЖЕННЯМ ЦИФРОВОГО ДВІЙНИКА / Н.Д. Панкратова, Г.С. Тимчик, Є.В. Панкратов

Анотація. Наведено стратегію гарантованого функціонування кіберфізичної системи підприємства дрібного бізнесу, що забезпечується супроводженням цифрового двійника та зумовлено його надвисокою актуальністю у сучасних умовах. Бізнес-процеси пов'язані з компетенціями Industry 4.0. Одна з інновацій, яку вона впроваджує, є Digital Twin (цифровий двійник) – всеохопний інструмент супроводу об'єкта. Цифровий двійник дозволяє відстежувати та ефективно керувати повним циклом інфраструктурного проекту: від планування, закупівель, виробництва, до введення в експлуатацію та обслуговування об'єкта. Для побудови стратегії залучаються методи PEST, SWOT, SAW, TOPSIS та VIKOR.

Ключові слова: Індустрія 4.0, цифровий двійник, кіберфізичні системи, стратегія, інтернет речей, комп'ютерні, фізичні та математичні моделі.

MULTI-FACTOR FORECASTING OF STATISTICAL TRENDS FOR DATA SCIENCE PROBLEMS

O. PYSARCHUK, T. ANDREIEVA, O. GRINENKO, D. BARAN

Abstract. The article deals with the processes of multi-factor forecasting of statistical trends for Data Science problems. Most of the classic approaches to data processing consist of studying the consequences of phenomena rather than the factors of their appearance. At the same time, the factors affecting the behavior of the investigated process are assumed to be random and are not investigated. The article discusses the approach to forecasting the parameters of the trend of statistical time series, which consists of the study of factors that lead to changes in the dynamics of the studied process. This approach potentially has better indicators of adequacy, accuracy, and efficiency in obtaining final solutions than classical approaches. The implementation of this approach is shown using an example of the analysis of exchange rate changes. The obtained results show the practicality of considering multifactoriality in forecasting tasks.

Keywords: Data Science, multi-factor forecasting, statistical trends, currency rate forecasting.

INTRODUCTION

The development of information technologies has led to their implementation in many areas. One of the leading directions is the prediction of the indicators behavior of a certain controlled event. The examples of that can be: forecasting fluctuations in currency markets; control of changes in economic performance indicators of trading companies; forecasting the development of the epidemiological situation; forecasting parameters of the technical state of equipment of production lines, aviation systems, etc. All the listed applied tasks have the technological unity of Data Science stages: data acquisition (measurement); their accumulation (storage); data processing for the purpose of obtaining information about the models and behavior of the researched process (processing, forecasting); extraction of knowledge and its manipulation [1; 2]. Currently, the focus of Data Science issues is not on accumulation (measurement, storage), but on data processing with the aim of extracting from them adequate, accurate and operational information and knowledge. These processes in applied aspects of information technologies (IT) take place in the field of Big Data arrays and are manifested in the development of Back-End components of distributed ERP / CRM software systems with intellectual properties.

The key requirement of consumers for the final IT product is high quality indicators of the source information, which are manifested in strict requirements for the adequacy, accuracy and efficiency of the final solutions. It is possible to implement this only in the direction of applying effective mathematical models for processing Big Data arrays.

The experience shows that most classical approaches to data processing, regardless of their classes, directions of improvement and effective implementation to applied software systems, show their limitations [3–5]. They consist in the study of the consequences of phenomena, and not the factors of their appearance. For example, determining the trend and forecasting changes in the exchange rate based on the results of a retrospective analysis of their behavior. At the same time, the factors affecting the exchange rate are assumed to be random and are not investigated.

Therefore, there is a need to implement R&D processes for the development of mathematical support for modern ERP / CRM software systems capable of meeting the high demands of consumers regarding the adequacy, accuracy and efficiency of final solutions.

The article will consider an approach to predicting parameters of the trend of statistical time series, which potentially has better indicators of adequacy, accuracy and efficiency of obtaining final solutions, compared to classical approaches.

Analysis of existing approaches. In its formulated form, we have the classic task of applied statistical analysis / statistical learning: to build a mathematical model based on a statistical sample of data, that ensures the determination of predictive values for the process being studied [1–5]. The key hypothesis in this is the assumption of the random nature of the factors that affect the stochastic fluctuations of each discrete dimension and, accordingly, determine the behavior of the studied process outside the observation interval. As a rule, this happens due to the complex and sometimes unknown nature of cause-and-effect relationships, which determine the actual appearance of stochastic deviations and the development of the situation in the future. Overcoming this a priori uncertainty is classically implemented through assumptions about the general appearance of the trend model and the determination of its variables using complex algorithms, but the principle hypothesis of randomness remains unchanged. That is, the primary stochastic formalization of the problem has certain limitations in the accuracy of the final result, which are determined by data processing methods.

Formulation of the problem. Therefore, the task of improving the methods of statistical analysis / training in the direction of a detailed description and study of factors that lead to the essence of the change in consequences – the dynamics of the researched process – is urgent. The article examines the processes for multifactor forecasting of statistical trends for Data Science tasks. This is implemented in the applied field of economic analysis of exchange rate changes. The transition in statistical education from the analysis of consequences to factors requires the implementation of a complex of R&D processes: the formation of an informational model of factors that influence the change in currency rates; the establishment of indicators (indicators describing change) of factors and criteria; the measurement of indicators; and the statistical processing of indexes / indicators (determination of statistical characteristics, construction of a trend line, forecasting).

Thus, the goal of the article is the implementation of a complex of R&D processes for multifactor forecasting of statistical trends for Data Science tasks using the example of currency exchange analysis.

AN OVERVIEW OF THE MAIN MATERIAL

1. *To form the infographic model of factors that influence on the change of the currency exchange rates*. The ratio of the dollar (USD) to the hryvnia (UAH) was chosen as the exchange rate (hereinafter referred to as the exchange rate). On the basis of the cognitive analysis of primary sources [6–13] and the practice of currency trading, the factors affecting the exchange rate were determined.

Table 1. An infographic model of factors that influence the change in currency rates

N	Factor group	N	Factor in the group	Indicator	Data source, frequency of measurement
1	Sale/ purchase of foreign currency	1	Volume of sale/purchase of foreign currency	The official exchange rate of the hryvnia against the US dollar	The official website of the NBU[10], daily
				Saldo of transactions of the natural person on the sale/purchase of foreign currency	
				Saldo of NBU interventions	The official website of the NBU[10], weekly
2	Export of goods	1	Volume of the main Ukrainian export goods	Wheat export volume	Website of the Ministry of Agrarian Policy and Food of Ukraine[8], daily
				Barley export volume	
				Rye export volume	
				Corn export volume	
		2	Export prices for the main agricultural products of Ukraine	Wheat export price	Fenix Agro company website: fenix-agro.com; weekly
				Barley export price	
				Corn export price	
		3	Export prices for the main metal products of Ukraine	Hot-rolled steel export price	Information and analytical resource about industry: gmk.center, daily
				Armature export	
				Scrap steel export price	
				Iron ore raw materials export	
3	Import of goods	1	Global prices for the main imported goods	Oil global price	The website of the Ministry of Finance [12], daily
				Natural gas global price	
4	Foreign investments	1	Participation of non-residents in trading in hryvnia bonds of the domestic state loan	The volume of hryvnia government bonds in circulation at nominal and amortized cost with non-residents	The official website of the NBU[10], daily
				The amount of funds involved in the state budget for placement of domestic government bonds	Website of the Ministry of Finance of Ukraine [9], weekly
5	Interest rates	1	The level of inter-est rates on the interbank market	Interest rates on deposits in the national currency	The official website of the NBU[10], daily
				Interest rates on deposits in US dollars	
		2	Interest rates on deposits	NBU Key Policy Rate	The website of the Ministry of Finance [12], daily
				Ukrainian Overnight I ndex Average (UONIA)	
6	Stock Market	1	Stock indices of Ukraine	UX index	The website of the Ministry of Finance [12], daily
		2	World stock indices	Dollar index	Investing.com, daily

2. To set the indicators (parameters which describes the change) of factors and criteria is implemented as a result of the transformation of Table 1, based on the essence of a specific factor.

**T a b l e 2.** Indicators / parameters that describe the change of the factors and criteria

№	Group of factors	№	Indicators	Denotation	Criterion
1	Sale/ purchase of foreign currency	1	The official exchange rate of the hryvnia against the US dollar	ψ	$\psi \to$ min
		2	Saldo of transactions of the natural person on the sale/ purchase of foreign currency	φ	$\varphi \to$ max
		3	Saldo of NBU interventions	χ	$\chi \to$ min
2	Export of goods	4	Wheat export volume	E_{VW}	$E_{VW} \to$ max
		5	Barley export volume	E_{VB}	$E_{VB} \to$ max
		6	Rye export volume	E_{VR}	$E_{VR} \to$ max
		7	Corn export volume	E_{VC}	$E_{VC} \to$ max
		8	Wheat export price	E_{PW}	$E_{PW} \to$ max
		9	Barley export price	E_{PB}	$E_{PB} \to$ max
		10	Corn export price	E_{PC}	$E_{PC} \to$ max
		11	Hot-rolled steel export price	E_{PS}	$E_{PS} \to$ max
		12	Armature export	E_{PA}	$E_{PA} \to$ max
		13	Scrap steel export price	E_{PJ}	$E_{PJ} \to$ max
		14	Iron ore raw materials export	E_{P0}	$E_{P0} \to$ max
3	Import of goods	15	Oil global price	I_{POIL}	$I_{POIL} \to$ min
		16	Natural gas global price	I_{PGAS}	$I_{PGAS} \to$ min
4	Foreign investments	17	The volume of hryvnia government bonds in circulation at nominal and amortized cost with non-residents	INV_V	$INV_V \to$ max
		18	The amount of funds involved in the state budget for placement of domestic government bonds	INV_M	$INV_M \to$ max
5	Interest rates	19	Interest rates on deposits in the national currency	R_{DG}	$R_{DG} \to$ max
		20	Interest rates on deposits in US dollars	R_{DD}	$R_{DD} \to$ min
		21	NBU Key Policy Rate	P	$P \to$ max
		22	Ukrainian Overnight Index Average (UONIA)	UONIA	UONIA$\to$ max
6	Stock Market	23	UX index	UX	$UX \to$ max
		24	Dollar index	DX	$DX \to$ min

3. *The indicators in Table 2 were measured* on June 1, 2021. – November 1, 2022 according to the sources and frequency (discreteness) specified in Table 1. The result is a multidimensional Big Data array of a statistical training sample of 24 indicators of 156 values, 5 (weekly monitoring) – of 36 values. Technological

efficiency of further processing processes is ensured by saving the received data segment in the * format. xlsx file.

4. *The statistical processing* of indicators / parameters is implemented in the sequence of classical stages of statistical training: determination of statistical characteristics, construction of a trend line, forecasting. To increase the effectiveness of statistical training, a hierarchy of interconnected alternative and innovative stages is proposed (see the structural diagram in Figure). The structural scheme takes into account the features of multi-factor forecasting of statistical trends for Data Science tasks.

Processes for *i*-indicator
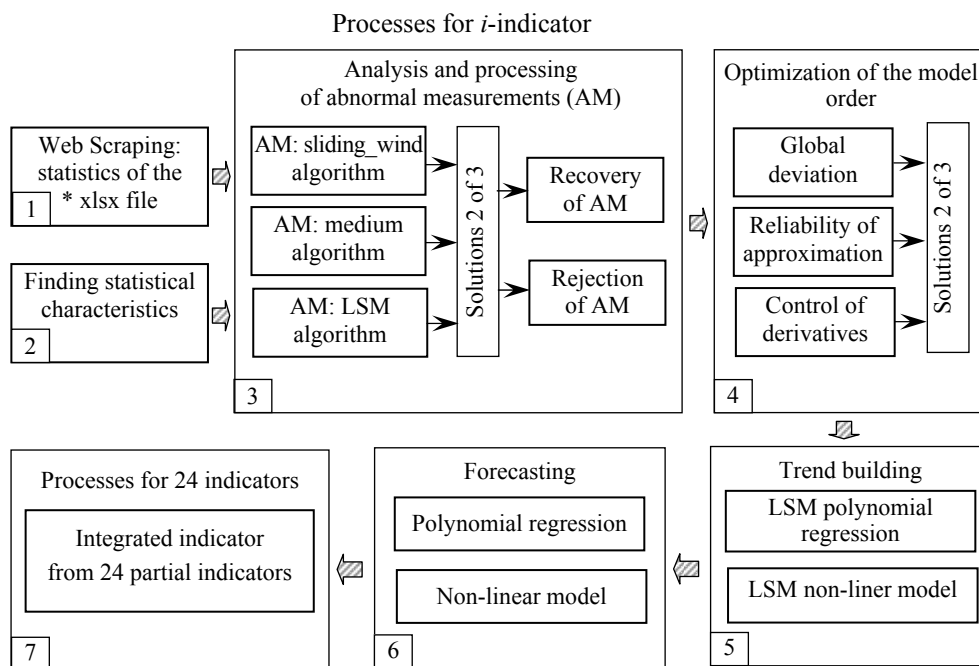
Structural diagram of the multi-factor forecasting process of statistical trends for Data Science tasks

The data obtaining (block 1 of the diagram, Figure) is implemented quickly from external sources using Web Scraping technologies.

Determination of the statistical characteristics of the obtained samples (block 2) is carried out a posteriori in the format of calculation: expected value, dispersion, standard deviation (SD), construction of a histogram of the law of distribution of the obtained samples. At the same time, the presence of a trend line is taken into account, which is removed using the Least Square Method (LSM) with a polynomial regression model [4].

Block 3 is intended for cleaning the statistical sample from anomalies. The use of three algorithms for detecting and cleaning anomalies [15] increases the reliability of the implementation of this process. Depending on the number of anomalies, the strategy of rejecting them is used (up to 10% of anomalous measurements – empirically obtained limits) and the recovery strategy (in other cases).

Optimizing the selection of the order of the trend line model (block 4) [14] is implemented with the control of the values of three indicators, which also increases the reliability of the final decisions.

The global linear deviation of the estimate is one that compares across multiple options:

$$\Delta = \frac{1}{n-1}\sum_{i=1}^{n}\left|y_i - \hat{y}_i\right|.$$

The accuracy of approximation R^2 (coefficient of determination) varies within $0...1$ and should be minimal:

$$R^2 = 1 - \frac{\sum_{i=1}^{n}(y_i - \hat{y}_i)^2}{\sum_{i=1}^{n}(y_i - \bar{y})^2},$$

where n is a sample size; $\bar{y}_i = \frac{1}{n}\sum_{i=1}^{n}y_i$, y_i is a measured value; $\hat{y}_i$ is LSM of estimating the measured value.

The derivatives of the higher orders are the controls of obtaining small values:

$$y_j^{(p)} = \frac{y_{j+1}^{(p-1)} - y_j^{(p-1)}}{\Delta t}, \quad j = \overline{1...m}, \; p = \overline{1...n}.$$

Determination of the trend line and forecasting (blocks 5, 6) is carried out using the algorithm of the least squares method (LSM) in classical polynomial [3; 4] or R&D nonlinear forms [4; 5].

For the presented research results, a nonlinear in parameters – transcendental model was chosen

$$f(t,c) = a_0 \cos \omega t + b_0 \sin \omega t,$$

where $c = \{a_0, b_0, \omega\}$ are the unknown parameters of the model. The procedure for determining the parameters of a nonlinear model consistent with the measured values is discussed in detail in [4; 5].

The calculation of the integrated assessment (unit 7) of the effect of factors on the controlled parameter — the exchange rate is carried out according to the scheme of multi-criteria / multi-factor assessment (SCOR) according to the nonlinear scheme of compromises [16]. The data format is a multidimensional discrete set of functions of 24 indicators.

According to the structural diagram of Fig. 1, an alpha version of the computing unit (Backend component) of the ERP system layout was created to support currency trading processes. The software component is implemented in the high-level python programming language with the use of technologies and libraries: Web Scraping, pandas — for obtaining data; numpy — for "raw" programming of data processing algorithms; matplotlib — for visualization of calculation results.

THE RESULTS OF THE CALCULATIONS AND THEIR ANALYSIS

1. The official exchange rate of the hryvnia against the US dollar

Chart	Statistical characteristics	Input stream	Estimation (polynomial of the 4th order) Coefficient of determination R^2=0,85
	Expected value	26.875997	26.875997
	Dispersion	0.15288	0.11475
	Standard deviation	0.39100	0.33875
	Distribution law		
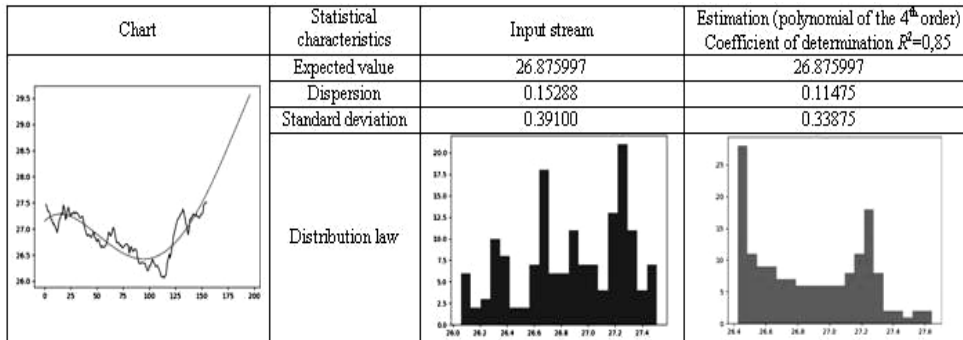
2. Saldo of operations of physical persons on the sale/purchase of foreign currency

Chart	Statistical characteristics	Input stream	Estimation (polynomial of the 2nd order) Coefficient of determination R^2=0,67
	Expected value	15.352169	7.847362
	Dispersion	137.10981	44.97901
	Standard deviation	11.70939	6.70664
	Distribution law		
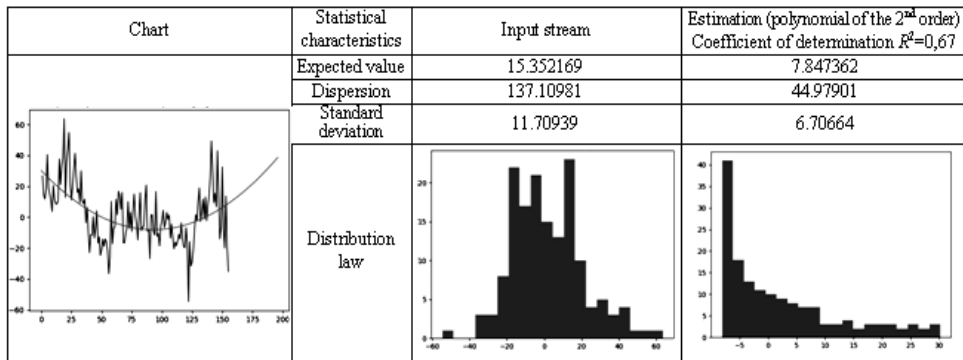
The indicator is calculated as the difference between the sale of foreign currency and its purchase.

3. Saldo of NBU interventions

Chart	Statistical characteristics	Input stream	Estimation (polynomial of the 2nd order) Coefficient of determination R^2=0,68
	Expected value	163.34	120.4238
	Dispersion	44296.145	6206.705
	Standard deviation	210.4665	78.7826
	Distribution law		
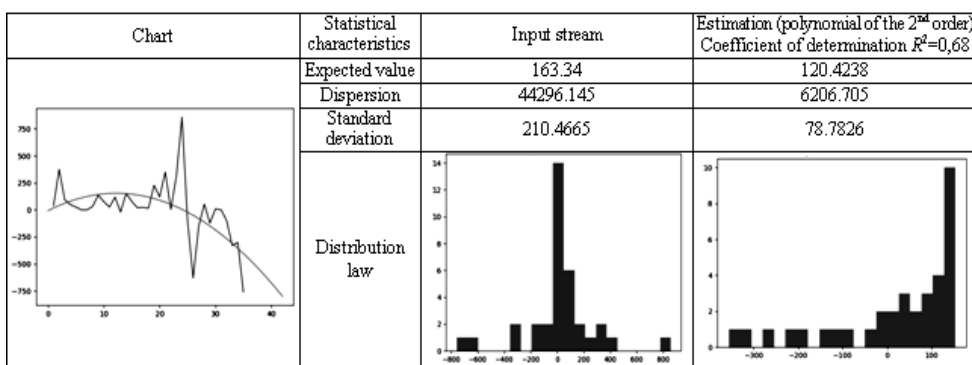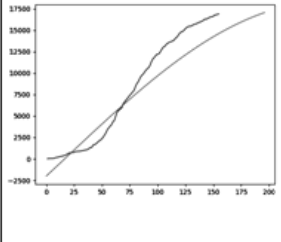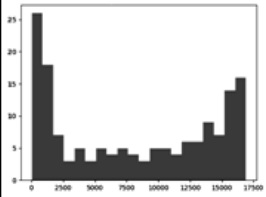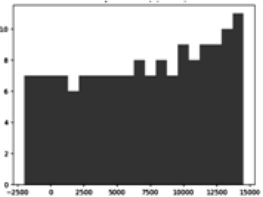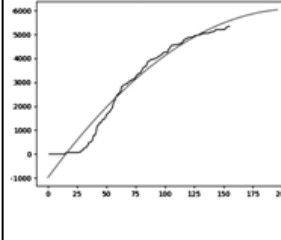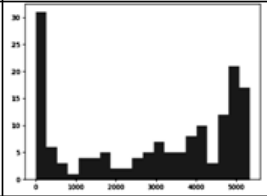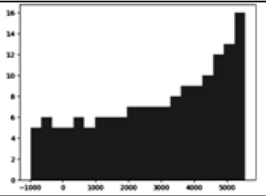
The indicator is calculated as the difference between the purchase of US dollars and their sale.

The volume of the main agricultural products of Ukrainian exports (indicators 4, 5, 6, 7) was calculated as the total volume of exported products, starting from June 1, 2021 (the beginning of the study)).
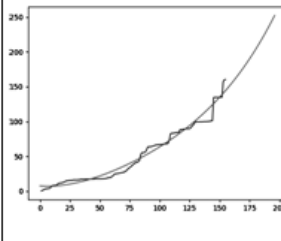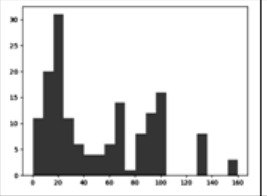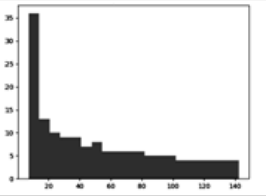
4. Wheat export volume

Chart	Statistical characteristics	Input stream	Estimation (non-linear smoothing) Coefficient of determination $R^2=0{,}91$
	Expected value	8045.29677	7103.56007
	Dispersion	37699035.022	20847045.489
	Standard deviation	6139.954	4565.856
	Distribution law		

5. Barley export volume

Chart	Statistical characteristics	Input stream	Estimation (polynomial of the 2nd order) Coefficient of determination $R^2=0{,}97$
	Expected value	2908.36129	3010.88877
	Dispersion	3804101.947	3088789.380
	Standard deviation	1950.411	1757.495
	Distribution law		

6. Rye export volume

Chart	Statistical characteristics	Input stream	Estimation (polynomial of the 4th order) Coefficient of determination $R^2=0{,}98$
	Expected value	51.96645	51.96645
	Dispersion	1650.4386	1605.4167
	Standard deviation	40.6256	40.0676
	Distribution law		

7. Corn export volume

Chart	Statistical characteristics	Input stream	Estimation (polynomial of the 4th order) Coefficient of determination $R^2=0{,}99$
	Expected value	4433.81935	4444.55952
	Dispersion	11837263.3093	11682804.9816
	Standard deviation	3440.5324	3418.0118
	Distribution law		

8. The export price of wheat

Chart	Statistical characteristics	Input stream	Estimation (polynomial of the 2nd order) Coefficient of determination R^2=0,90
	Expected value	293.657143	293.657143
	Dispersion	1165.19673	1002.00163
	Standard deviation	34.13498	31.65441
	Distribution law		

9. The export price of barley

Chart	Statistical characteristics	Input stream	Estimation (polynomial of the 4th order) Coefficient of determination R^2=0,93
	Expected value	268.514286	268.514286
	Dispersion	772.19265	701.16375
	Standard deviation	27.78835	26.47950
	Distribution law		

10. The export price of corn

Chart	Statistical characteristics	Input stream	Estimation (polynomial of the 4th order) Coefficient of determination R^2=0,85
	Expected value	274.228571	274.228571
	Dispersion	66.34775	50.32450
	Standard deviation	8.14541	7.09398
	Distribution law		

The export prices for all key agricultural products of Ukraine currently have a positive trend.
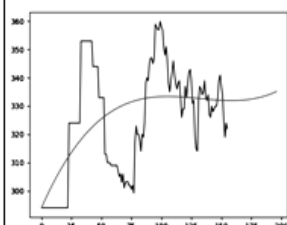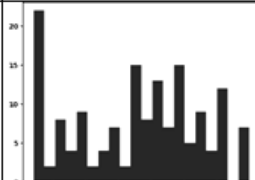
11. Export price of hot rolled steel

Chart	Statistical characteristics	Input stream	Estimation (polynomial of the 4th order) Coefficient of determination R^2=0,93
	Expected value	865.485806	865.485806
	Dispersion	7400.11969	6743.01622
	Standard deviation	86.02395	82.11587
	Distribution law		

12. The export price of armature

Chart	Statistical characteristics	Input stream	Estimation (polynomial of the 3rd order) Coefficient of determination R^2=0,84
	Expected value	753.474387	753.474387
	Dispersion	1145.28174	785.42695
	Standard deviation	33.84201	28.02547
	Distribution law		

13. Export price of scrap metal
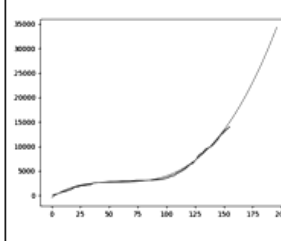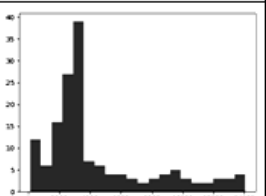
Chart	Statistical characteristics	Input stream	Estimation (polynomial of the 3rd order) Coefficient of determination R^2 = 0,63
	Expected value	325.413419	325.413419
	Dispersion	380.88411	115.86365
	Standard deviation	19.51625	10.76400
	Distribution law		

14. Export price for raw iron ore
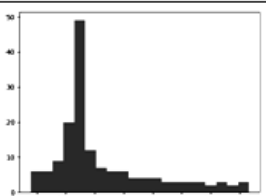
Chart	Statistical characteristics	Input stream	Estimation (polynomial of the 2nd order) Coefficient of determination R^2=0,92
	Expected value	147.064516	147.064516
	Dispersion	1994.07326	1766.70932
	Standard deviation	44.655048	42.03224
	Distribution law		

15. The global oil price
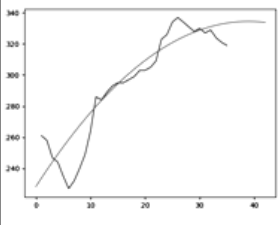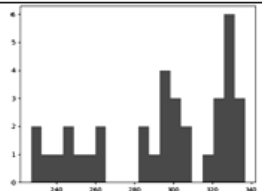
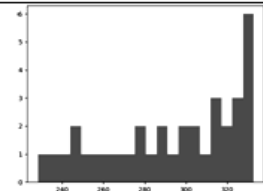| Chart	Statistical characteristics	Input stream	Estimation (polynomial of the 4th order) Coefficient of determination R^2 = 0,68
	Expected value	76.080774	76.080774
	Dispersion	24.02192	8.99828
	Standard deviation	4.90122	2.99971
	Distribution law		

16. The global natural gas price

Chart	Statistical characteristics	Input stream	Estimation (polynomial of the 4th order) Coefficient of determination $R^2 = 0,88$
	Expected value	4.398355	4.398355
	Dispersion	0.71180	0.58715
	Standard deviation	0.84368	0.76625
	Distribution law		

17. The volume of hryvnia government bonds in circulation at nominal and amortized cost with non-residents
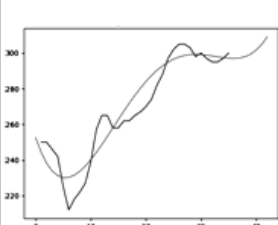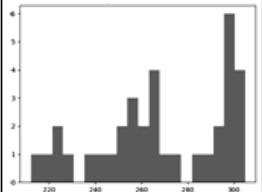
Chart	Statistical characteristics	Input stream	Estimation (polynomial of the 2nd order) Coefficient of determination $R^2 = 0,87$
	Expected value	98.620968	98.620968
	Dispersion	41.82890	33.12315
	Standard deviation	6.46752	5.75527
	Distribution law		
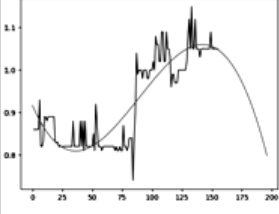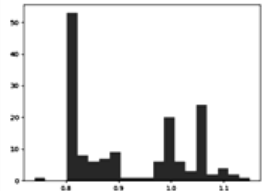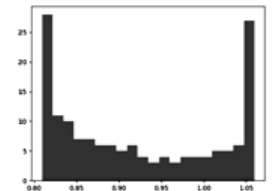
18. The amount of funds involved in the state budget for placement of domestic government bonds
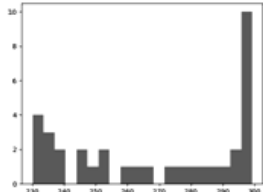
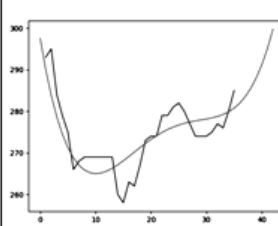| Chart	Statistical characteristics	Input stream	Estimation (polynomial of the 2nd order) Coefficient of determination $R^2 = 0,52$
	Expected value	7.054516	7.054516
	Dispersion	34.23411	3.17102
	Standard deviation	5.85099	1.78073
	Distribution law		
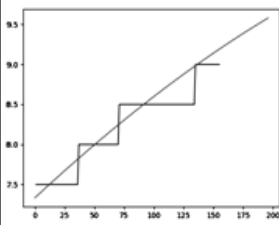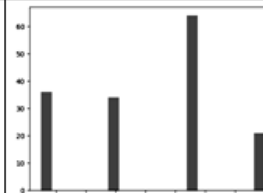
19. The interest rates on deposits in the national currency

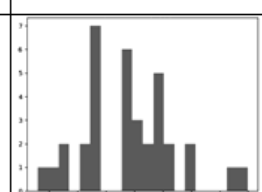| Chart	Statistical characteristics	Input stream	Estimation (polynomial of the 4th order) Coefficient of determination $R^2 = 0,85$
	Expected value	8.511806	8.511806
	Dispersion	0.07945	0.07362
	Standard deviation	0.28187	0.27133
	Distribution law		
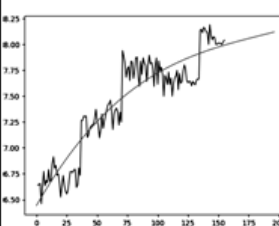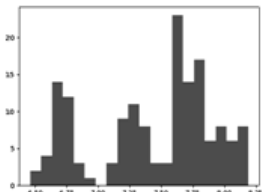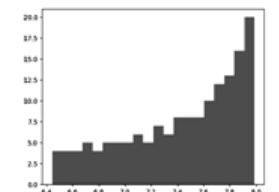
20. The interest rates on deposits in the USA dollars
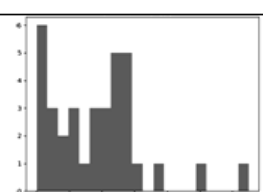
Chart	Statistical characteristics	Input stream	Estimation (polynomial of the 3rd order) Coefficient of determination $R^2 = 0,78$
	Expected value	0.923097	0.923097
	Dispersion	0.01054	0.00845
	Standard deviation	0.10268	0.09192
	Distribution law		
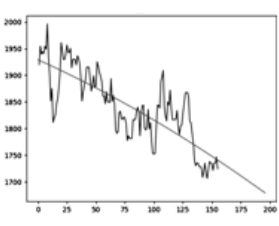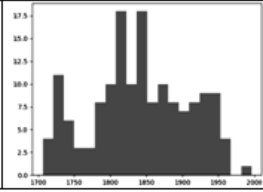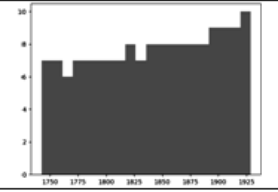
21. NBU Key Policy Rate

Chart	Statistical characteristics	Input stream	Estimation (non-linear smoothing) Coefficient of determination $R^2 = 0,90$
	Expected value	8.225806	8.304335
	Dispersion	0.24579	0.28948
	Standard deviation	0.49577	0.53804
	Distribution law		

22. Ukrainian Overnight Index Average (UONIA.
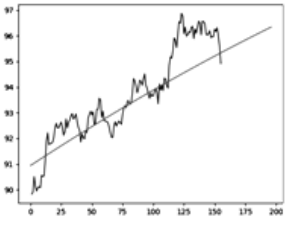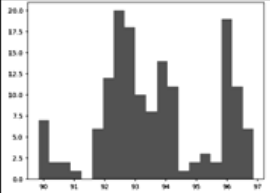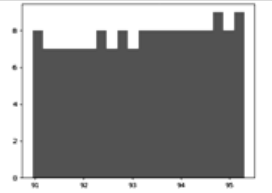
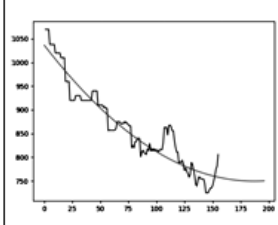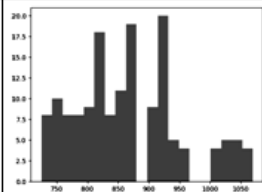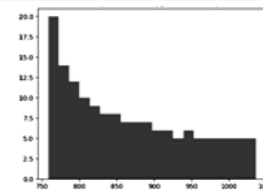| Chart	Statistical characteristics	Input stream	Estimation (polynomial of the 3rd order) Coefficient of determination $R^2 = 0,90$
	Expected value	7.432942	7.432942
	Dispersion	0.22817	0.19639
	Standard deviation	0.47768	0.44316
	Distribution law		

23. UX index

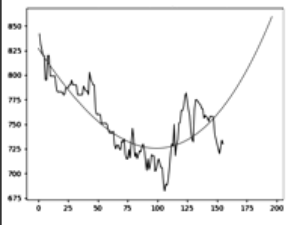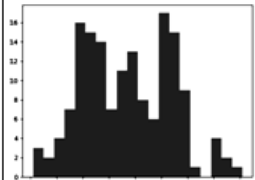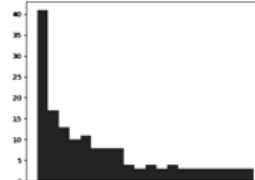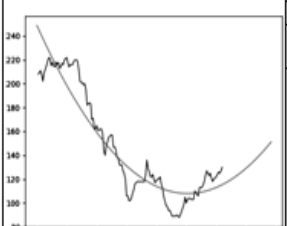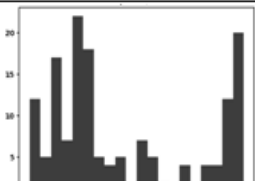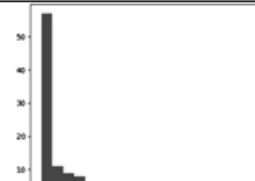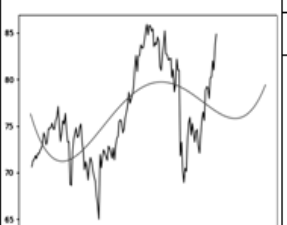| Chart	Statistical characteristics	Input stream	Estimation (polynomial of the 2nd order) Coefficient of determination $R^2 = 0,79$
	Expected value	1841.581226	1841.581226
	Dispersion	4564.20713	2951.12485
	Standard deviation	67.55892	54.32426
	Distribution law		

24. The dollar index

Chart	Statistical characteristics	Input stream	Estimation (non-linear smoothing) Coefficient of determination $R^2 = 0,83$
	Expected value	93.655419	93.204709
	Dispersion	3.17770	1.61243
	Standard deviation	1.78261	1.26981
	Distribution law		

CONCLUSIONS

The real data obtained and processed allow us to identify useful features. Statistical properties: parameters 1, 2, 3, 10, 11, 12, 23 (see histograms of distribution laws) are characterized by a normal distribution law, the others have combinatorial laws. This demonstrates the decomposition of the factors influencing the exchange rate into unitary and combinatorial components. Inherent natural presence of anomalous values of controlled parameters. The trend of the studied indicators is non-linear, and the dynamics of change may be conflicting according to the minimax analysis; that is, the improvement of certain indicators may be accompanied by the deterioration of others. So, once the infological model is formed, multifactorial consideration of the forecasting problem is appropriate. Further research will include the formation of an integrated indicator from partial factors and a comparison of its dynamics with the dominant effect, the exchange rate. At the same time, one should expect an increase in the accuracy and adequacy of predictive estimates of the studied parameters.

REFERENCES

1. Foster Provost and Tom Fawcett, *Data Science for Business*. Printed in the United States of America. Published by O'Reilly Media, Inc., 2013, 409 p.
2. David Dietrich, Barry Heller, and Beibei Yang, *Data Science & Big Data Analytics: Discovering, Analyzing, Visualizing and Presenting*. Indianapolis, Indiana: Data John Wiley & Sons, Inc., 2015, 420 p.
3. Trevor Hastie, Robert Tibshirani, and Jerome Friedman, *The Elements of Statistical Learning Data Mining, Inference, and Prediction;* 2nd edition. Springer, 2020, 768 p.
4. S.V. Kovbasyuk, O.O. Pisarchuk, and M.Yu. Rakushev, *The least squares method and its practical application*. Zhytomyr: NAU, 2008, 228 p.
5. O.O. Pisarchuk, V.P. Kharchenko, *Nonlinear and multicriterial modeling of processes in traffic control systems*. K.: Institute of Gifted Child, 2015, 248 p.
6. F.O. Zhuravka, *Monetary policy in the context of transformational changes in Ukraine's economy: monograph*. Sumy: "Business Perspectives," Ukrainian Academy of Banking of the National Bank of Ukraine, 2008, pp. 63–123.
7. S. Kulitsky, "Dynamics of US dollar exchange in Ukraine in 2019: attempted situational analysis," *Ukraine: Events, Facts, Comments*, no. 11, pp. 35–46, 2019. Available: http://nbuviap.gov.ua/images/ukraine/2019/ukr11.pdf
8. *Ministry of Agrarian Policy and Food of Ukraine* [official site]. Available: https://minagro.gov.ua
9. *Ministry of Finance of Ukraine* [official site]. Available: https://mof.gov.ua
10. *National Bank of Ukraine* [official site]. Available: http://bank.gov.ua

11. I. M. Sysoyeva, "The enterprise's profit forecasting depending on accounting policy methods," *Economics and State*, no. 10, pp. 93–94, 2010. Available: http://nbuv.gov.ua/UJRN/ecde_2010_10_26

12. *Ukrainian Information Portal on Finance and Investments "Minfin.com.ua"*. Available: https://minfin.com.ua

13. A. Khivrenko, *Exchange rate: how it is determined, who influences it and what should be guided*. Available: https://www.epravda.com.ua/publications/2020/09/19/665288/

14. O.O. Pysarchuk, O.V. Korochkin, and D.R. Baran, "Determining the order of a polynomial model for constructing a trend line in Data Science problems," *Problems of Informatization and Management*, 3(71), pp. 35–40, 2022. doi: 10.18372/2073-4751.71.17001.

15. O. Pysarchuk, Yu. Mironov, I. Pysarchuk, and D. Baran, "Algorithms of Statistical Anomalies Clearing for Data Science Applications," *System Research & Information Technologies*, no. 1, pp. 78–84, 2023. doi: 10.20535/SRIT.2308-8893.2023.1.06.

16. O. Pysarchuk, A. Gizun, A. Dudnik, V. Griga, T. Domkiv, and S. Gnatyuk, "Bifurcation Prediction Method for the Emergence and Development Dynamics of Information Conflicts in Cybernetic Space," *Proceedings of the International Workshop on Cyber Hygiene (CybHyg-2019) co-located with 1st International Conference on Cyber Hygiene and Conflict Management in Global Information Networks (CyberConf 2019). Kyiv, Ukraine, November 30, 2019*, pp. 692–709. Available: https://ceur-ws.org/Vol-2654/paper54.pdf

INFORMATION ON THE ARTICLE

Oleksii O. Pysarchuk, ORCID: 0000-0001-5271-0248, National Technical University of Ukraine "Igor Sikorsky Kyiv Polytechnic Institute", Ukraine, e-mail: PlatinumPA2212@gmail.com

Tetiana V. Andreieva, ORCID: 0009-0009-7033-9054, National Aviation University, Ukraine, e-mail: tetyanaandreieva@gmail.com

Olena O. Grinenko, ORCID: 0000-0001-9673-6626, National Aviation University, Ukraine, e-mail: gsa_ck@ukr.net

Danylo R. Baran, ORCID: 0000-0002-3251-8897, National Technical University of Ukraine "Igor Sikorsky Kyiv Polytechnic Institute", Ukraine, e-mail: danil.baran15@gmail.com

БАГАТОФАКТОРНЕ ПРОГНОЗУВАННЯ СТАТИСТИЧНИХ ТРЕНДІВ ДЛЯ ЗАДАЧ DATA SCIENCE / О.О. Писарчук, Т.В. Андреєва, О.О. Гріненко, Д.Р. Баран

Анотація. Розглянуто процеси багатофакторного прогнозування статистичних трендів для задач Data Science. Більшість класичних підходів до оброблення даних полягають у дослідженні наслідків явищ, а не факторів їх появи. При цьому фактори, що впливають на поведінку досліджуваного процесу, вважаються випадковими та не досліджуються. Розглянуто підхід до прогнозування параметрів тренду статистичних часових рядів, який полягає в дослідженні факторів, що призводять до зміни динаміки досліджуваного процесу. Такий підхід потенційно має кращі показники адекватності, точності і оперативності отримання кінцевих рішень порівняно з класичними підходами. Наведено реалізацію цього підходу на прикладі аналізу зміни курсу валют. Отримані результати розрахунків показують доцільність розгляду багатофакторності у задачах прогнозування.

Ключові слова: Data Science, багатофакторне прогнозування, статистичні тренди, прогнозування курсу валют.

POLARIZATION-BASED TARGET DETECTION APPROACH TO ENHANCE SMALL SURFACE OBJECT IDENTIFICATION ENSURING NAVIGATION SAFETY

M. STETSENKO, O. MELNYK, I. VOROKHOBIN, D. KORBAN, O. ONISHCHENKO, V. TERNOVSKY, I. IVANOVA

Abstract. This research introduces a groundbreaking approach to significantly enhance the performance of navigation radars under adverse weather conditions. Traditional ship radars, relying on horizontal polarization, encounter difficulties in effectively suppressing rain interference. In response, this study proposed an innovative method employing circular polarization for detecting navigation targets. This technique capitalizes on the distinct polarization properties exhibited by stable navigation targets and fluctuating interfering objects. Theoretical analysis and model experiments substantiate consistent ellipticity parameter values of scattered waves, independent of rain intensity, for both rain interferers and surface metallic objects. The practical implications of our research are highly promising. They enable detection irrespective of the noise-to-signal ratio by integrating an additional channel of circularly polarized waves and applying straightforward mathematical functions. This advancement marks a significant stride towards overcoming the challenges posed by rainy conditions in maritime navigation radar systems.

Keywords: safety of shipping, navigational safety, maritime transportation, radar interference, unfavorable weather conditions, rain and snow interference suppression, navigational targets, automonous surface vehicles, radiolocation principles, ship detection principles framework, radar accuracy.

INTRODUCTION

In today's global transportation landscape, approximately 80% of cargo is transported via oceangoing vessels, constituting a fleet of nearly 100 thousand units. Given this extensive maritime activity, ensuring navigation safety is paramount and involves adherence to specific technical requisites and construction guidelines. Central to these regulations is the inclusion of a navigation radar as standard equipment aboard seagoing vessels, serving as a critical tool for safeguarding navigation. The operator's ability to make precise decisions regarding vessel positioning, collision avoidance, and grounding prevention hinges significantly on the accuracy of radar-derived data.

Regrettably, the quality of data received is not consistently optimal. Operators frequently encounter challenges, particularly in adverse weather conditions such as heavy seas, rain, and snow. These atmospheric conditions introduce interference that affects radar performance. Presently, there exist various methods to mitigate rain and snow interference. The hardware approach employs a gain function, enabling operators to manually adjust signal strength to filter out low-amplitude signals. However, this manual intervention often results in unintended consequences, potentially filtering useful signals from small surface targets like small boats and floating objects.

To address this dilemma, contemporary radars employ algorithms designed to suppress rain and snow interference. Typically, interference from precipitation follows an even distribution pattern. The intensity of interference correlates with the severity of rain or snowfall. This interference can be effectively suppressed using a Constant False Alarm Rate (CFAR) approach. In low-resolution radars, the interference probability density aligns with a Rayleigh distribution. In high-resolution radars, it can be modeled by a Weibull distribution.

The CFAR mechanism enables the adjustment of interference control thresholds, allowing for a specified false alarm rate and enhancing target tracking capabilities. However, in scenarios where substantial noise fluctuations occur, the likelihood of false alarms rises. To sustain a consistent false alarm rate, it becomes imperative to elevate the detection threshold proportionally, subsequently augmenting the input signal-to-noise ratio. This adaptation, while crucial, does introduce a trade-off in the form of a potential loss of the consistent false alarm rate (LCFAR).

The literature review encompasses a diverse array of sources that significantly contribute to the radar technology field. Bohren and Huffman's seminal work, "Absorption and Scattering of Light by Small Particles" (1998), provides fundamental insights into the behavior of light with small particles. Their earlier 1983 paper underscores their enduring impact in the field. Reference [2] introduces a signal processing algorithm specifically tailored for ship navigation radar, with a focus on azimuth distance monitoring. Scientific work [3] delves into polarization invariants within the scattering matrix, emphasizing stability in aperture synthesis. Paper [4] critically distinguishes between forward propagation and backscattering in formulating the proper polarimetric scattering matrix for radar systems. Reference [5] demonstrates the practical application of polarimetric radar technology in target detection through a method based on polarimetric Synthetic Aperture Radar (SAR). Source [6] lays the foundation for understanding radiolocation principles, potentially exploring pivotal concepts and theoretical frameworks. Paper [7] centers on antenna miniaturization for radiolocation, suggesting advancements in antenna technology for enhanced radiolocation applications. Source [8] introduces a novel radiolocation method applicable to depth estimation, with potential applications in groundwater level analysis. Reference [9] discusses beamforming techniques within radio-telescope technology, signifying its relevance in radiolocation applications. Study [10] offers insights into radiolocation experiments within urban environments, potentially addressing challenges specific to this setting. Papers [11; 12] explore the directional radio response of a specific device guided by radiolocation, potentially contributing to advancements in device localization. They also introduce an algorithm for simultaneous radiolocation of multiple sources, indicating advancements in source localization techniques. Works [13; 14] present lightweight radar-based ship detection frameworks, potentially offering innovative methods for ship detection. They propose a unified approach to ship detection, combining optical and radar data, potentially advancing ship detection methods. Source [15] introduces a novel approach for estimating ship speed and heading using radar sequential images, potentially advancing ship tracking technology. Articles [16–18; 43] discuss inshore ship detection methods based on multi-modality saliency, potentially enhancing ship detection accuracy. They present a network designed for small ship detection in synthetic aperture radar imagery, indicating progress in ship detection algorithms. Additionally, they introduce a method for assessing the motion state of

ships and selecting appropriate radar imaging algorithms, potentially improving ship detection accuracy. Source [19] delves into calibration methods involving ground-based, ship-based, and spaceborne radars, potentially enhancing radar accuracy. In [20], the authors focus on estimating ship berthing parameters using a fusion of Multi-LiDAR and MMW radar data, potentially advancing ship docking technology. Articles [21–23] underscore the critical role of situational awareness in ensuring ship safety, addressing the optimization of ship speed for secure heavy cargo transportation under diverse weather conditions, and exploring the concept of autonomous ships and their steering control using mathematical models. Works [24–27] present assessment methodologies based on Markov models for navigational safety, offering a comprehensive approach to evaluating the vulnerability of critical ship equipment and systems. They examine information security risks in shipping to ensure safety in maritime transportation and investigate the environmental impact of ship operation in relation to efficient freight transportation. In [28–30], discussions encompass the use of fuzzy controllers in ship motion control systems for automation, the identification of energy-efficient operation modes for propulsion electrical motors in autonomous swimming apparatus, and the presentation of a straightforward technique for identifying parameters of vessel models.

Papers [31–33] introduce a decision support system concept for designing combined propulsion systems, explore challenges in creating energy-efficient positioning systems for multipurpose sea vessels, and investigate risk management mechanisms in higher education institutions using innovative project information support. Work [34] discusses a method for managing human resources in educational projects of higher education institutions. The article [35] focuses on modeling the creation of organizational energy-entropy. In [36], a model for creating a roadmap for enterprise development is constructed and analyzed. In [37], the dynamics of project portfolio structure in organizational development are examined, considering information entropy resistance. A model depicting the energy entropy dynamics of organizations is constructed and investigated in [38]. Studies on various forms of cooperation among participants in inland waterways cargo delivery in the Dnieper region and the development of a strategy for modernizing passenger ships by optimizing fund distribution are presented in [39; 40].

Recent advancements in system research and information technologies highlight significant developments across various domains where [41] introduced a novel modified kernel fuzzy c-means algorithm to enhance the detection of cotton leaf spots, demonstrating improved accuracy in agricultural diagnostics. The authors in [42] developed a multi-level decision-making framework for predicting and recommending treatments for heart-related diseases, providing a robust tool for healthcare applications. The work [43] proposed an interval type-2 generalizing fuzzy model for monitoring the states of complex systems using expert knowledge and [44; 45] applied optimal set partitioning theory to solve problems in artificial intelligence and pattern recognition, advancing methodologies in AI research.

In light of the aforementioned considerations, the research aims to enhance radar detection of navigation entities amidst atmospheric precipitation, irrespective of its intensity. A novel approach is proposed, focusing on recognizing and categorizing the polarization attributes of partially polarized waves to augment the information capacity of electromagnetic waves. This approach draws from

successful applications of statistical methods in the polarization analysis of rain clouds and precipitation, providing a basis for extending this methodology to the complex task of detecting and tracking intricate objects. By "complex object", we refer to a navigational entity situated against a backdrop of spatially dispersed reflectors that remain consistent throughout radar observations. The primary objective of this study is to establish a statistical correlation between the invariant characteristics of a polarized electromagnetic wave and an object on the sea surface, enveloped by spatially distributed reflectors like rain or other forms of precipitation. Resolving this requires determining the Stokes parameters for the scattered wave upon irradiation of the complex object. This transition from the energy traits to informative parameters such as polarization degree, azimuth, and ellipticity of the polarized wave holds significant promise.

MATERIALS AND METHODS

To describe all possible polarization states of a quasimonochromatic plane wave, four Stokes parameters can be used, which are determined through the components of the transverse electric field.

Let us write the electric vector of a plane monochromatic homogeneous wave in the form

$$\vec{E} = [E_x \, E_y] = 2 \left[\left(A_x e^{i\left(\omega\left(t - \frac{z}{v}\right) + \varphi_x\right)} \right) \left(A_y e^{i\left(\omega\left(t - \frac{z}{v}\right) + \varphi_y\right)} \right) \right],$$

where A_x, A_y denote amplitudes, and φ_x, φ_y denote phases of the components of plane wave.

Time-averaged values for the amplitude and phase of the parallel and transverse components of the vector $\vec{E}$ determine the known Stokes parameters I, Q, U, V:

$$I = |E_x|^2 + |E_y|^2 = A_x^2(t) + A_y^2(t),$$

$$Q = |E_x|^2 - |E_y|^2 = A_x^2(t) - A_y^2(t),$$

$$U = (E_x E_y^* + E_y E_x^*) = 2 A_x(t) A_y(t) \cos\cos[\varphi_x(t) - \varphi_y(t)],$$

$$V = i(E_x E_y^* - E_y E_x^*) = 2 A_x(t) A_y(t) \sin[\varphi_x(t) - \varphi_y(t)],$$

where the * sign means the complex conjugate, and the angle brackets mean time averaging: $A_x^2(t) = \dfrac{1}{T} \int\limits_0^T (t) \, dt \dots$.

The first component of the Stokes vector I characterizes the intensity of the light flux, the second component Q characterizes the degree of polarization (Fig. 1) [1; 2]. V component defines the direction of rotation of the polarization ellipse: a positive sign means right-handed rotation, and a negative sign means left-handed. The components of the Stokes vector are associated with ellipsometric parameters and have the following properties:

$$I \geq 0, \ I \geq \sqrt{Q^2 + U^2 + V^2},$$

$$\operatorname{tg}2\gamma = \frac{U}{Q}; \quad \operatorname{tg}2\eta = \frac{V}{\sqrt{Q^2 + U^2}},$$

where γ is the azimuth; $|tg\eta|$ is the ellipticity of the polarized wave $\left(-\frac{\pi}{4} \leq \eta \leq \frac{\pi}{4}\right)$.
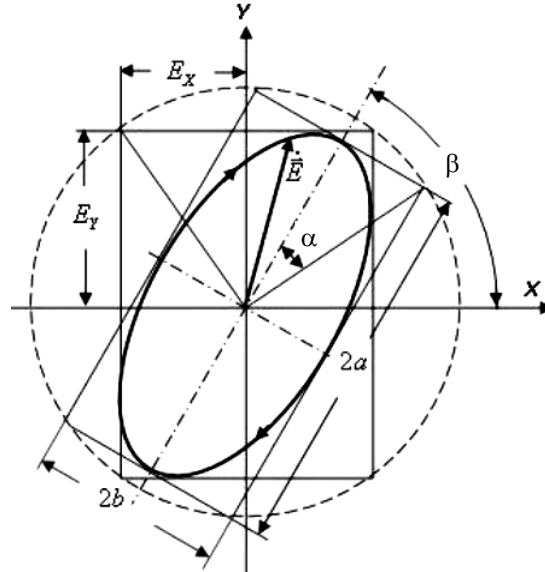
Fig. 1. Polarization ellipse of an electromagnetic wave

It is known that the Stokes parameters of a scattered wave are determined by the Muller scattering matrix. In general terms, the model of scattering of an electromagnetic wave by an arbitrary surface is described by the operator equation:

$$S = M S_0,$$

where $S_0 = \{I_0, U_0, V_0, U_0\}^{\mathrm{T}}$ is Stokes vector of incident radiation; $S = \{I, U, V, U\}^{\mathrm{T}}$ is the Stokes vector of scattered radiation; M is the scattering matrix characterizing the reflective properties of the scattering surface and the angle of incidence of the electromagnetic wave [2; 3; 4].

To compose the matrix of the linear scattering operator M, we consider the transformation of the components of the Stokes vector of the incident radiation according to the Fresnel formulas.

The intensities of the incident and scattered radiation are defined as

$$I_0 = \left|E_x^{inc}\right|^2 + \left|E_y^{inc}\right|^2; I = \left|E_x^{refl}\right|^2 + \left|E_y^{refl}\right|^2,$$

where E_x^{inc}, E_y^{inc} are the projections of the vector $\vec{E}^{inc}$ $(\vec{E} = E_x + iE_y)$ on the axis perpendicular to the direction of the incident electromagnetic wave space; alternatively, are the projections of scattered wave.

In turn, the amplitude Fresnel coefficients $\Phi_1 = \dfrac{E_x^{refl}}{E_x^{inc}}$ and $\Phi_2 = \dfrac{E_y^{refl}}{E_y^{inc}}$ are equal to the ratio of the amplitudes of the reflected and incident electromagnetic waves parallel and perpendicular to the scattering plane, respectively [4].

For the coefficients Φ_1 and Φ_2 the following expressions are true:

$$\Phi_1 = \frac{m_2 \cos\cos\phi - m_1 \cos\cos\varphi}{m_2 \cos\cos\phi + m_1 \cos\cos\varphi} \frac{m_2 \cos\cos\phi - m_1 \sqrt{m_2^2 - (m_1 \sin\sin\phi)^2}}{m_1 \cos\cos\phi + m_1 \sqrt{m_2^2 - (m_1 \sin\sin\phi)^2}}, \qquad (1)$$

$$\Phi_2 = \frac{m_1 \cos\cos\phi - m_2 \cos\cos\varphi}{m_1 \cos\cos\phi + m_2 \cos\cos\varphi} = \frac{m_1 \cos\cos\phi - m_2 \sqrt{m_2^2 - (m_1 \sin\sin\phi)^2}}{m_1 \cos\cos\phi + m_2 \sqrt{m_2^2 - (m_1 \sin\sin\phi)^2}}, \qquad (2)$$

where m_1 is the complex refractive index of the first medium; m_2 is the complex refractive index of the second medium; ϕ is the angle of incidence of the electromagnetic wave; φ is the angle of refraction of the electromagnetic wave.

Given the law of refraction for the refraction angle φ we write:

$$\sin\sin\varphi = \frac{m_1}{m_2} \sin\sin\phi\,;$$

$$\cos\cos\varphi = \sqrt{1 - \left(\frac{m_1}{m_2} \sin\sin\phi\right)^2}\,.$$

Since $E_x^{refl} = \Phi_1 E_x^{inc}$ and $E_y^{refl} = \Phi_2 E_y^{inc}$, it yields

$$I = \left|\Phi_1 E_x^{inc}\right|^2 + \left|\Phi_2 E_y^{inc}\right|^2 = \left|\Phi_1\right|^2 \left|E_x^{inc}\right|^2 + \left|\Phi_2\right|^2 \left|E_y^{inc}\right|^2.$$

Let us express $\left|E_x^{inc}\right|^2$, $\left|E_y^{inc}\right|^2$ through the components I_0, Q_0 of the incident wave Stokes vector. Since $I_0 = \left|E_x\right|^2 + \left|E_y\right|^2$, $Q_0 = \left|E_x\right|^2 - \left|E_y\right|^2$, then

$$\left|E_x^{inc}\right|^2 = \frac{I_0 + Q_0}{2}, \quad \left|E_y^{inc}\right|^2 = \frac{I_0 - Q_0}{2}\,.$$

Hence,

$$I = \left|\Phi_1\right|^2 \frac{I_0 + Q_0}{2} + \left|\Phi_2\right|^2 \frac{I_0 - Q_0}{2} = \frac{1}{2} I_0 (\left|\Phi_1\right|^2 + \left|\Phi_2\right|^2) + \frac{1}{2} Q_0 (\left|\Phi_1\right|^2 - \left|\Phi_2\right|^2)\,.$$

The second component of the Stokes vector of the scattered radiation is expressed through the components of the Stokes vector of the incident radiation as follows:

$$Q = \left|\Phi_1 E_x^{inc}\right|^2 - \left|\Phi_2 E_y^{inc}\right|^2 = \left|\Phi_1\right|^2 \left|E_x^{inc}\right|^2 - \left|\Phi_2\right|^2 \left|E_y^{inc}\right|^2 =$$

$$= \frac{1}{2} I_0 (\left|\Phi_1\right|^2 - \left|\Phi_2\right|^2) + \frac{1}{2} Q_0 (\left|\Phi_1\right|^2 + \left|\Phi_2\right|^2)\,.$$

We express the third component U of the Stokes vector through the components of the Stokes vector of the incident radiation:

$$U = (\Phi_1 \Phi_2^*)U_0 + (\Phi_2 \Phi_1^*)V_0.$$

And finally, for the fourth component of the Stokes vector of reflected radiation, we write

$$V = (\Phi_1 \Phi_2^*)U_0 + (\Phi_1 \Phi_2^*)V_0.$$

Thus, for the Stokes vector of scattered radiation, the following expression is obtained:

$$S = \left(\frac{1}{2}I_0(|\Phi_1|^2 + |\Phi_2|^2) + \frac{1}{2}Q_0(|\Phi_1|^2 - |\Phi_2|^2)\frac{1}{2}I_0(|\Phi_1|^2 - |\Phi_2|^2) + \right.$$

$$\left. + \frac{1}{2}Q_0(|\Phi_1|^2 + |\Phi_2|^2) \; (\Phi_1\Phi_2^*)U_0 + (\Phi_2\Phi_1^*)V_0 \; (\Phi_1\Phi_2^*)U_0 + (\Phi_1\Phi_2^*)V_0 \right).$$

We compose the Mueller scattering matrix for reflective metal surfaces:

$$M = (M_{11}\,M_{12}\,0\,0\,M_{21}\,M_{22}\,0\,0\,0\,0\,M_{33}\,M_{34}\,0\,0\,M_{43}\,M_{44}\,),$$

where

$$M_{11} = M_{22} = \frac{|\Phi_1|^2 + |\Phi_2|^2}{2}; \quad M_{12} = M_{21} = \frac{|\Phi_1|^2 - |\Phi_2|^2}{2};$$

$$M_{33} = M_{44} = (\Phi_2\Phi_1^*), \quad M_{34} = -M_{43} = (\Phi_2\Phi_1^*).$$

Mueller scattering matrix for a raindrop with a spherical shape

It is convenient to decompose the vector of the incident electric field E^{inc} into parallel $E_|^{inc}$ and perpendicular $E_\perp^{inc}$ components, and present the relationship between the incident and scattered fields in the matrix form:

$$(E_|^{refl}\,E_\perp^{refl}\,) = \frac{e^{ik(r-z)}}{-ikr}(S_2\,S_3\,S_4\,S_1\,)(E_|^{inc}\,E_\perp^{inc}\,), \tag{3}$$

where k is the wave vector, r is the path travelled by the wave, and S_j $(j = 1, 2, 3, 4)$ are the elements of the amplitude scattering matrix that depend on the scattering angle θ and azimuth γ.

Then, for scattering of an electromagnetic wave by a spherical particle, taking into account the principle of reciprocity, expression (3) can be written as

$$(E_|^{refl}\,E_\perp^{refl}\,) = \frac{e^{ik(r-z)}}{-ikr}(A_2\,0\,0\,A_1\,)(E_|^{inc}\,E_\perp^{inc}\,), \tag{4}$$

where

$$A_1 = \frac{1}{2}\sum_n (2n+1)(a_n + b_n); \tag{5}$$

$$A_2 = \frac{1}{2}\sum_n^{n=\infty} (2n+1)(a_n + b_n)(\cos\cos\theta). \tag{6}$$
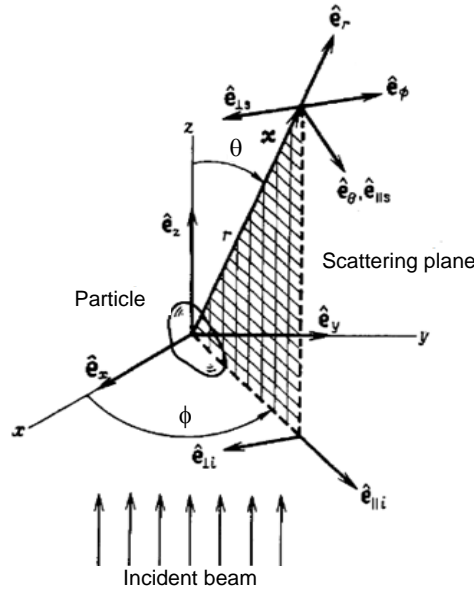
Fig. 2. Interaction processes

In formulas (5), (6), the coefficients of the scattering series a_n and b_n are found using the following expressions:

$$a_n = \frac{m\psi_n(mx)\psi'_n(\eta x) - \psi_n(mx)\psi'_n(mx)}{m\psi_n(mx)\xi'_n(x) - \xi_n(x)\psi'_n(mx)};$$

$$b_n = \frac{\psi_n(mx)\psi'_n(mx) - m\psi_n(mx)\psi'_n(mx)}{\psi_n(mx)\xi'_n(x) - m\xi_n(x)\psi'_n(mx)},$$

where $\psi_n(\eta x)$, $\xi_n(x)$ are the Riccati–Bessel functions, and x and m denote the diffraction parameter and relative refractive index, respectively.

Where in

$$x = ka = \frac{2\pi m_2 a}{\lambda};\tag{7}$$

$$m = \frac{m_1}{m_2},\tag{8}$$

where a is the particle radius, m_1 and m_2 are the refractive indices of the particle and medium (air), respectively.

We expand the functions included in the coefficients a_n and b_n in the power series and save only the terms of order x^6. The first four obtained coefficients are as follows:

$$a_1 = -\frac{i2x^3}{3}\frac{m^2-1}{m^2+2} - \frac{i2x^5}{5}\frac{(m^2-2)(m^2-1)}{(m^2+2)^2} + \frac{4x^6}{9}\left(\frac{m^2-1}{m^2+2}\right)^2;$$

$$b_1 = -\frac{ix^5}{45}(m^2-1);\quad a_2 = -\frac{ix^5}{15}\frac{m^2-1}{2m^2+3};\quad b_1 \approx 0.$$

If $|m|x < 1$, then $|b_1| < |a_1|$; under this assumption, the elements of the amplitude matrix up to terms of the order of x^3 are equal to

$$A_1 \frac{3}{2} a, \tag{9}$$

$$A_2 = \frac{3}{2} a_1 \cos\cos\theta, \tag{10}$$

$$a_1 = -\frac{i2x^3}{3} \frac{m^2 - 1}{m^2 + 2}. \tag{11}$$

From (4) follows the relation connecting the Stokes parameters of the incident and scattered electromagnetic waves:

$$(I_s\, Q_s\, U_s\, V_s) =$$

$$= \frac{1}{k^2 r^2}(S_{11}\, S_{12}\, 0\, 0\, S_{12}\, S_{11}\, 0\, 0\, 0\, 0\, S_{33}\, S_{34}\, 0\, 0\, -S_{34}\, S_{33})(I_i\, Q_i\, U_i\, V_i),$$

where

$$S_{11} = \frac{1}{2}(|S_2|^2 + |S_1|^2), \quad S_{12} = \frac{1}{2}(|S_2|^2 - |S_1|^2),$$

$$S_{33} = \frac{1}{2}(S_2^* S_1 + S_2 S_1^*), \quad S_{34} = \frac{i}{2}(S_1 S_2^* - S_2 S_1^*).$$

In view of (9), (10), the scattering matrix for a spherical particle takes the form

$$\frac{9|a|^2}{4k^2 r^2}\left(\frac{1}{2}(1+\theta)\frac{1}{2}(\theta-1)\,0\,0\,\frac{1}{2}(1-\theta)\frac{1}{2}(1+\theta)\,0\,0\,0\,0\cos\cos\theta\,0\,0\,0\,0\cos\cos\theta\right). \tag{12}$$

Note that if the incident electromagnetic wave of intensity I_0 is not polarized, then the law of Rayleigh scattering determines the intensity of the scattered wave from (12):

$$I = \frac{8\pi^4 m_2 a^6}{\lambda^4 r^2}\left|\frac{m^2 - 1}{m^2 + 2}\right|^2 (1+\theta)I_0.$$

The relationship between the rain intensity and the radius of the drops is conveniently represented as an empirical function of the average size distribution of raindrops, and written as follows:

$$F(a) = 1 - e^{-\left(\frac{a}{\alpha}\right)\cdot\eta}, \tag{13}$$

where the function $F(a)$ characterizes that part of the total volume of water that falls on drops of radius from 0 to a; η is the constant equal to 2.25.

The parameter α depends on the rain intensity I_r as listed below:

I_r, $mm/hour$	0.5	1.0	2.5	5.0	10	25
α	1.11	1.3	1.61	1.89	2.22	2.74

Determining the complex refractive index of water and metal object

The complex refractive index and the complex dielectric constant are related to each other as follows:

$$\varepsilon = \varepsilon' + i\varepsilon''; \quad \varepsilon = m^2; \tag{14}$$

$$m = n - i\chi, \tag{15}$$

where ε' is the real part of the complex dielectric constant and ε'' is the imaginary part of it, n is the refractive index, χ is the extinction coefficient.

From (14), (15) we obtain following expressions:

$$\varepsilon' = n^2 - \chi^2; \quad \varepsilon'' = 2n\chi;$$

$$n^2 = \frac{1}{2}\varepsilon'\left[1 + \sqrt{1 + \left(\frac{\varepsilon''}{\varepsilon'}\right)^2}\right]; \tag{16}$$

$$\chi = \frac{\varepsilon''}{2n}. \tag{17}$$

In order to use formulas (14) and (15) for calculating complex refractive index of water drop, we need to look at dipole theory.

According to the Debye dipole theory, the real part of the complex dielectric constant is expressed by the following formula:

$$\varepsilon' = n_0^2 + \frac{\varepsilon - n_0^2}{1 + \left(\dfrac{\lambda_s}{\lambda}\right)^2}, \tag{18}$$

and the imaginary part is

$$\varepsilon'' = \frac{\lambda_s}{\lambda}\frac{\varepsilon_0 - n_0^2}{1 + \left(\dfrac{\lambda_s}{\lambda}\right)^2}, \tag{19}$$

where n_0 is the optical refractive index, ε_0 is the permittivity of free space, λ is the wavelength, and λ_s is the so-called "shocks wave" which corresponds to the maximum value of the imaginary part of the dielectric constant.

Numerous measurements show that $\varepsilon_0 = 80.8$, $n_0^2 = 1.8$ and $\lambda_s = 1.6$. Above expressions allow to calculate complex refractive index for water drop.

For metal object, complex refractive index is often expressed as

$$m^2 = \varepsilon\mu\mu_0 = \left(\varepsilon' - \frac{i\sigma}{2\pi f\varepsilon_0}\right)\mu\mu_0, \tag{20}$$

where f is the wave frequency, σ is the relative conductivity of a material, μ is the relative permeability of a material, μ_0 is the magnetic permeability of free space, $\mu_0 = 1.2566 \cdot 10^{-6}$ H/m.

Neglecting the real part in (20), which is true for navigation radar frequencies, complex refractive index for metal objects is obtained as follows:

$$m = \sqrt{-\frac{i\sigma}{2\pi f \varepsilon_0} \mu \mu_0} \; . \tag{21}$$

Generalized Muller matrix for a composite target

Suppose that against the background of precipitation in the form of rain with intensity I_r, there is a navigational target, the radar cross-section (RCS) of which is less than or comparable with the total RCS of rain drops. In this case, expression (4) in Cartesian dimensions is written as follows:

$$(E_x^{refl} \; E_y^{refl}) = \frac{e^{ik(r-z)}}{-ikr} \left[\sum_{l=1}^{N} (A_2 \, 0 \, 0 \, A_1) + (\Phi_1 \, 0 \, 0 \, \Phi_2) \right] \times$$

$$\times (\cos\cos\gamma \; \sin\sin\gamma \; \sin\sin\gamma \; -\cos\cos\gamma)(E_|^{inc} \; E_\perp^{inc}) , \tag{22}$$

where N is the number of rain drops in the irradiated volume, γ is the azimuth.

It is easy to determine the number N from the considerations that in one cubic meter the number of raindrops and drizzle drops rarely exceeds 1000. Then for N we find,

$$N = 1000[V_{irr}] = 500 \left[\pi \left(\frac{r^2\lambda^2}{4A} \right) c\tau \right],$$

where V_{irr} is the irradiated volume, A is the effective area of the radar antenna, c is the speed of light, τ is the duration of the probe pulse, and […] sign denotes ceiling function.

RESULTS AND DISCUSSION

Using formulas (7)–(11) and (13)–(19), we have estimated numeric values of refraction and extinction parameters as well as scattering coefficient a_1 for a typical rain drop sizes. Results are summarized in Table 1 for both *X*-band and *S*-band radar frequencies.

As expected, extinction and scattering rise with the carrier frequency. Within same wavelength, size of rain drop is directly proportional to the scattered wave amplitude.

T a b l e 1. Influence of raindrop size on permittivity, refraction, extinction, and scattering coefficient for *X*-band and *S*-band radar frequencies

a, mm	a_1	λ, cm	ε'	ε''	ε	m_2
1.5	$3.794\cdot10^{-4} + 0.02i$					
2	$8.994\cdot10^{-4} + 0.047i$	3	63.461	32.803	81	$8.213 - 1.997i$
3	$3.035\cdot10^{-3} + 0.159i$					
1.5	$3.072\cdot10^{-6} + 5.379\cdot10^{-4}i$					
2	$7.282\cdot10^{-5} + 1.913\cdot10^{-3}i$	10	79.023	12.324	81	$8.916 - 0.691i$
3	$2.458\cdot10^{-5} + 4.564\cdot10^{-3}i$					

As an example, let us calculate the scattering matrix for 1 m³ of rain drops with radius of 1.5 mm irradiated by plain wave with wavelength of 3 cm and scattering angle $\theta = 0°$ over the time τ. Refractive index for air is $m_1 = 1$.

Muller matrix coefficients have been obtained as follows:

$$(I_s\,Q_s\,U_s\,V_s\;) = \frac{1}{k^2 r^2}(892.526 - 0.045\,0\,0 -$$

$$-0.045\,892.526\,0\,0\,0\,0\,892.526\,0\,0\,0\,0\,892.526\;)(I_i\,Q_i\,U_i\,V_i\;). \tag{23}$$

As can be seen from (23), scattering matrix has six nonzero elements, and only two independent ones. Since the main contribution is done by diagonal elements of the matrix, we can consider it diagonal.

Now, if radar beam will meet a metal object, the scattering matrix (23) will transform in new one:

$$(I_s\,Q_s\,U_s\,V_s\;) = \frac{1}{k^2 r^2}(893.583 - 1.126\,0\,0 - 1.126\,893.583\,0\,0\,0\,0\,891.587\,59.684\,0\,0 -$$

$$-59.684\,891.587\;)(I_i\,Q_i\,U_i\,V_i\;). \tag{24}$$

Numerical values of Φ_1 and Φ_2 from (22) were obtained using formulas (20), (1) and (2). In (20), the relative conductivity was taken $\sigma = 7690000$ Ohm^{-1}m^{-1}, and the relative permeability of the metal material is $\mu = 100$ (carbon steel).

It can be seen from (24), another pair of nonzero elements has appeared. This suggests practical improvement of the navigation target detection method. By determining ellipsometric parameters of the scattered wave within radar's signal processing algorithm, target existence would be discovered easily.

For this purpose, circular polarized (CP) or $\pm 45^\circ$ polarized ($\pm 45^\circ$P) incident probing radiation is required. As can be seen from Table 2, CP and $\pm 45^\circ$P X-band probing results in zero values for azimuth and ellipticity irrespective to the rain intensity, if target is not available. However, presence of target results in nonzero values for those two parameters.

T a b l e 2. Ellipsometric parameters of scattered circular and 45° polarized 3 cm waves at different environmental and navigational conditions

I_r, mm/hour		0.5	1	2.5	5
Rain	Azimuth (CP)	0	0	0	0
	Ellipticity (CP, ±45°P)	0	0	0	0
Rain + object	Azimuth (CP)	2	2.1	2.2	2.5
	Ellipticity (CP, ±45°P)	0.134	0.056	0.029	0.017

Improving navigation safety through statistical target detection in atmospheric precipitation involves the use of advanced radar technologies and data processing techniques. For Maritime Autonomous Ships (MAAS) in particular, this approach can significantly improve situational awareness and collision avoidance capabilities:

• Advanced radar systems. MAAS are equipped with advanced radar systems capable of operating in a variety of weather conditions, including rain and snow. These radars utilize special technologies to distinguish between real targets (such as other vessels) and interference caused by precipitation.

• Statistical signal processing. This method is based on statistical signal processing algorithms. These algorithms analyse radar signals and use statistical models to distinguish between real targets and interference caused by precipitation. Statistical models are created based on extensive data analysis and experimentation.

- Constant False Alarm Rate (CFAR). A key component of this method is the use of constant false alarm rate (CFAR) technology. CFAR algorithms dynamically adjust the target detection threshold based on the statistics of received radar signals. This maintains a constant false alarm rate even in the presence of interference.

- Probability Density Functions. In low resolution radars, the probability density function of interference often follows a Rayleigh distribution. For high resolution radars, the Weibull distribution may be more appropriate. These probability density functions are used to model the statistical behaviour of radar signals.

- Adaptive thresholding. The radar system continuously adapts its detection threshold depending on the prevailing environmental conditions. When heavy precipitation is detected, the system dynamically raises the detection threshold to screen out interference. This ensures that targets of interest remain visible.

- Integration with sensor fusion. Radar data processed using the statistical target detection method is integrated with data from other sensors on board the MAAS. These can be cameras, LiDAR, GPS and AIS (automatic identification system). This integration of data from multiple sensors increases overall situational awareness.

- Real-time decision-making. The processed information is fed into the MAAS decision-making algorithms. These include collision avoidance, route planning, and other navigation functions. When a potential collision hazard is detected, MAAS can autonomously take evasive action.

- Continuous Learning and Adaptation. Statistical models and algorithms are designed to learn and adapt over time. As MAAS encounters different environmental conditions and navigation scenarios, the system refines its statistical models to achieve even greater accuracy.

This enables MAAS to navigate safely even in unfavourable weather conditions where traditional radar systems may encounter interference from precipitation. The integration of statistical signal processing and CFAR techniques enhances MAAS' ability to accurately detect and respond to potential collision risks, which significantly improves navigation safety.

CONCLUSIONS

The findings presented in this study unveil a remarkable phenomenon in electromagnetic wave scattering: when a spherical raindrop is illuminated at different angles, there is an absence of depolarization in the incident wave. This stands in stark contrast to the partial depolarization exhibited by a metal target, resulting in distinct azimuth and ellipticity characteristics of the scattered wave. Leveraging this polarization contrast holds tremendous promise for advancing navigation radar technology, offering a notable boost in the precision and reliability of target detection.

One of the most significant merits of this method lies in its capability to facilitate target detection regardless of atmospheric precipitation intensity and the accompanying noise-to-signal ratio. This resilience stems from the invariant nature of the parameter, which remains unaffected by Radar Cross Section (RCS) variations.

However, it is important to note that the implementation of this method necessitates a navigation radar station equipped with at least two channels, specifi-

cally with horizontal polarization and 45° polarization. While this may entail increased costs and operational complexity for shipboard radar systems, the benefits in terms of heightened navigational security significantly outweigh this drawback, particularly in the realm of high-speed maritime transportation. The potential gains in safety and accuracy of navigation far outweigh the associated investment, marking a substantial step forward in maritime technology.

REFERENCES

1. Craig Bohren, Donald Huffman, *In Absorption and Scattering of Light by Small Particles*. 1983. doi: 10.1002/9783527618156
2. Yuxin Qin, Yu. Chen, "Signal processing algorithm of ship navigation radar based on azimuth distance monitoring," *International Journal of Metrology and Quality Engineering*, 2019. doi: 10. 12. 10.1051/ijmqe/2019010
3. V. Tatarinov, "Polarization Invariants of the Scattering Matrix and Stability of their Statistical Characteristics in the Aperture Synthesis Problem," *Proc. of the European Conference synthetic Aperture Radar, March 26 – 28, 1996, Königswinter, Germany*, pp. 113–115.
4. E. Luneburg, S.R. Cloude, and W.-M. Boerner, "On the proper polarimetric scattering matrix formulation of the forward propagation versus backscattering radar systems description," *IGARSS'97. 1997 IEEE International Geoscience and Remote Sensing Symposium Proceedings. Remote Sensing - A Scientific Vision for Sustainable Development, Singapore, 1997*, vol. 4, pp. 1591–1593. doi: 10.1109/IGARSS.1997.608965
5. Genwang Liu, Xi Zhang, and Junmin Meng, "A Small Ship Target Detection Method Based on Polarimetric SAR," *Remote Sensing*, 11(24), 2938, 2019. doi: 10.3390/rs11242938
6. Stanisław Rosłoniec, *Radiolocation and Its Basic Principles*. 2023. doi: 10.1007/978-3-031-10631-6_1
7. Jerry Jose, A. Rekh, and M.J. Jose, "Demonstrating Antenna Miniaturisation for Radiolocation Applications using Double Elliptical Patches," *Defence Science Journal*, 71, pp. 515–523, 2021. doi: 10.14429/dsj.71.16276
8. N. Ayuso et al., "A new radiolocation method for precise depth estimation and its application to the analysis of changes in groundwater levels in Colonia Clunia Sulpicia," *Archaeological Prospection*, vol. 29, issue 3, 2022. doi: 10.1002/arp.1858
9. Aleksander Droszcz, Konrad Jedrzejewski, Julia Kłos, Krzysztof Kulpa, and Mariusz Pożoga, "Beamforming of LOFAR Radio-Telescope for Passive Radiolocation Purposes," *Remote Sensing*, 13(4), 810, 2021. doi: 10.3390/rs13040810
10. Douglas N. Travers, M. Pike Castles, and William M. Sherrill, "Radiolocation Experiments in an Urban Environment," *IEEE Transactions on Electromagnetic Compatibility*, vol. EMC-12, issue 4, pp. 174–177, 1970. doi: 10.1109/TEMC.1970.303054
11. Danko Antolovic, "Directional radio response of a 802.11b device guided by radiolocation," *PORTABLE-POLYTRONIC 2008 - 2nd IEEE International Interdisciplinary Conference on Portable Information Devices and the 2008 7th IEEE Conference on Polymers and Adhesives in Microelectronics and Photonics*. doi: 10.1109/PORTABLEPOLYTRONIC.2008.4681258
12. Danko Antolovic, "An Algorithm for Simultaneous Radiolocation of Multiple Sources," *2009 IEEE 70th Vehicular Technology Conference Fall*, pp. 1–5. doi: 10.1109/VETECF.2009.5378896
13. Nanjing Yu, Haohao Ren, Tianmin Deng, and Xiaobiao Fan, "A Lightweight Radar Ship Detection Framework with Hybrid Attentions," *Remote Sensing*, 15, 2743, 2023. doi: 10.3390/rs15112743
14. Mikhail Popov, Sergey Stankevich, Valentyn Pylypchuk, Kun Xing, and Chunxiao Zhang, *Unified Approach to Inshore Ship Detection in Optical/radar Medium Spatial Resolution Satellite Images*. 2023. doi: 10.1007/978-981-99-4098-1_8

15. Xueqian Xu, Bing Wu, Lei Xie, A.P. Teixeira, and Xinping Yan, "A Novel Ship Speed and Heading Estimation Approach Using Radar Sequential Images," *IEEE Transactions on Intelligent Transportation Systems*, pp. 1–14, 2023. doi: 10.1109/TITS.2023.3281547

16. Zhe Chen, Zhiquan Ding, Xiaoling Zhang, Xiaoting Wang, and Yuanyuan Zhou, "Inshore Ship Detection Based on Multi-Modality Saliency for Synthetic Aperture Radar Images," *Remote Sensing*, 15, 3868, 2023. doi: 10.3390/rs15153868

17. Yongsheng Zhou, Hanchao Liu, Fei Ma, Zongxu Pan, and Fan Zhang, "A Sidelobe-Aware Small Ship Detection Network for Synthetic Aperture Radar Imagery," *IEEE Transactions on Geoscience and Remote Sensing*, pp. 1-1, 2023. doi: 10.1109/TGRS.2023.3264231

18. Tianyi Zhang, Shujiang Liu, Zegang Ding, Yongpeng Gao, and Kaiwen Zhu, "A Motion State Judgment and Radar Imaging Algorithm Selection Method for Ship," *IEEE Transactions on Geoscience and Remote Sensing*, 60, pp. 1–18, 2022. doi: 10.1109/TGRS.2022.3212674

19. Alain Protat, Valentin Louf, Joshua Soderholm, Jordan Brook, and William Ponsonby, "Three-way calibration checks using ground-based, ship-based, and space-borne radars," *Atmospheric Measurement Techniques*, 15, pp. 915–926, 2022. doi: 10.5194/amt-15-915-2022

20. Zhuolin Wang, Yingjun Zhang, "Estimation of ship berthing parameters based on Multi-LiDAR and MMW radar data fusion," *Ocean Engineering*, 266, 113155, 2022. doi: 10.1016/j.oceaneng.2022.113155

21. O. Melnyk, Y. Bychkovsky, and A. Voloshyn, "Maritime situational awareness as a key measure for safe ship operation," *Scientific Journal of Silesian University of Technology. Series Transport*, 114, pp. 91–101, 2022. doi: https://doi.org/10.20858/sjsutst.2022.114.8

22. S. Onyshchenko, O. Melnyk, "Efficiency of Ship Operation in Transportation of Oversized and Heavy Cargo by Optimizing the Speed Mode Considering the Impact of Weather Conditions," *Transport and Telecommunication*, 23 (1), pp. 73–80, 2022. doi: 10.2478/ttj-2022-0007

23. O. Melnyk et al., "Autonomous Ships Concept and Mathematical Models Application in their Steering Process Control," *TransNav*, 16 (3), pp. 553–559, 2022. doi: 10.12716/1001.16.03.18

24. O. Melnyk, S. Onyshchenko, "Navigational safety assessment based on Markov-model approach," *Scientific Journal of Maritime Research*, 36 (2), pp. 328–337, 2022. doi: https://doi.org/10.31217/p.36.2.16

25. O. Melnyk, S. Onyshchenko, O. Onishchenko, O. Lohinov, and V. Ocheretna, "Integral approach to vulnerability assessment of ship's critical equipment and systems," *Transactions on Maritime Science*, 12(1), 2023. doi: 10.7225/toms.v12.n01.002

26. O. Melnyk et al., "Review of Ship Information Security Risks and Safety of Maritime Transportation Issues," *TransNav*, vol. 16, no. 4, pp. 717–722, 2022. doi: 10.12716/1001.16.04.13

27. O. Melnyk et al., "Study of Environmental Efficiency of Ship Operation in Terms of Freight Transportation Effectiveness Provision," *TransNav*, vol. 16, no. 4, pp. 723–729, 2022. doi: 10.12716/1001.16.04.14

28. O. Melnyk et al., "Application of Fuzzy Controllers in Automatic Ship Motion Control Systems," *International Journal of Electrical and Computer Engineering*, vol. 13, no. 4, pp. 3958–3968, 2023. doi: 10.11591/ijece.v13i4.pp3948-3957

29. Y. Volyanskaya, S. Volyanskiy, A. Volkov, and O. Onishchenko, "Determining energy-efficient operation modes of the propulsion electrical motor of an autonomous swimming apparatus," *Eastern-European Journal of Enterprise Technologies*, 6 (8-90), pp. 11–16, 2017. doi: 10.15587/1729-4061.2017.118984

30. V.A. Golikov, V.V. Golikov, Y. Volyanskaya, O. Mazur, and O. Onishchenko, "A simple technique for identifying vessel model parameters," *IOP Conference Series: Earth and Environmental Science*, 172 (1), art. no. 012010, 2018. doi: 10.1088/1755-1315/172/1/012010

31. V. Budashko, V. Nikolskyi, O. Onishchenko, and S. Khniunin, "Decision support system's concept for design of combined propulsion complexes," *Eastern-European Journal of Enterprise Technologies*, 3 (8-81), pp. 10–21, 2016. doi: 10.15587/1729-4061.2016.72543

32. V. Budashko, T. Obniavko, O. Onishchenko, Y. Dovidenko, and D. Ungarov, "Main Problems of Creating Energy-efficient Positioning Systems for Multipurpose Sea Vessels," *2020 IEEE 6th International Conference on Methods and Systems of Navigation and Motion Control, MSNMC 2020 - Proceedings*, art. no. 9255514, pp. 106–109, 2020. doi: 10.1109/MSNMC50359.2020.9255514

33. V. Piterska, D. Lohinov, and L. Lohinova, "Risk Management Mechanisms in Higher Education Institutions Based on the Information Support of Innovative Projects," *International Scientific and Technical Conference on Computer Sciences and Information Technologies, 2022-November*, pp. 410–413, 2022. doi: 10.1109/CSIT56902.2022.10000551

34. V. Piterska, A. Shakhov, O. Lohinov, and L. Lohinova, "The Method of Human Resources Management of Educational Projects of Institution of Higher Education," *International Scientific and Technical Conference on Computer Sciences and Information Technologies*, 2, art. no. 9321912, pp. 123–126. doi: 10.1109/CSIT49958.2020.9321912

35. Alla Bondar, Natalija Bushuyeva, Sergey Bushuyev, and Svitlana Onyshchenko, "Modelling of Creation Organisational Energy-Entropy," *International Scientific and Technical Conference on Computer Sciences and Information Technologies*, 2, art. no. 9321997, pp. 141–145, 2020. doi: 10.1109/CSIT49958.2020.9321997

36. S. Onyshchenko, A. Bondar, V. Andrievska, N. Sudnyk, and O. Lohinov, "Constructing and exploring the model to form the road map of enterprise development," *Eastern-European Journal of Enterprise Technologies*, 5 (3-101), pp. 33–42, 2019. doi: 10.15587/1729-4061.2019.179185

37. S. Bushuyev, S. Onyshchenko, N. Bushuyeva, and A. Bondar, "Modelling projects portfolio structure dynamics of the organization development with a resistance of information entropy," *International Scientific and Technical Conference on Computer Sciences and Information Technologies*, 2, pp. 293–298, 2021. doi: 10.1109/CSIT52700.2021.9648713

38. A. Bondar, S. Onyshchenko, O. Vishnevska, D. Vishnevskyi, S. Glovatska, and A. Zelenskyi, "Constructing and investigating a model of the energy entropy dynamics of organizations," *Eastern-European Journal of Enterprise Technologies*, 3 (3-105), pp. 50–56, 2020. doi: 10.15587/1729-4061.2020.206254

39. O. Scherbina, O. Drozhzhyn, O. Yatsenko, and O. Shybaev, "Cooperation forms between participants of the inland waterways cargo delivery: a case study of the dnieper region," *Scientific Journal of Silesian University of Technology. Series Transport*, 103, pp. 155–166, 2019. doi: 10.20858/sjsutst.2019.103.12

40. A. Shibaev, S. Borovyk, and I. Mykhailova, "Developing a strategy for modernizing passenger ships by the optimal distribution of funds," *Eastern-European Journal of Enterprise Technologies*, 6 (3-108), pp. 33–41, 2020. doi: 10.15587/1729-4061.2020.219293

41. M. Stetsenko et al., "Improving Navigation Safety by Utilizing Statistical Method of Target Detection on the Background of Atmospheric Precipitation" *Trends in Sustainable Computing and Machine Intelligence - Proceedings of ICTSM 2023.* doi: https://doi.org/10.1007/978-981-99-9436-6_8

42. P.M. Paithane, S.J. Wagh, "Novel modified kernel fuzzy c-means algorithm used for cotton leaf spot detection," *System Research and Information Technologies*, no. 4, pp. 85–99, 2023. doi: 10.20535/SRIT.2308-8893.2023.4.07

43. V. Sharma, S.S. Samant, "A multi-level decision-making framework for heart-related disease prediction and recommendation," *System Research and Information Technologies*, no. 4, pp. 7–20, 2023. doi: 10.20535/SRIT.2308-8893.2023.4.01

44. N.R. Kondratenko, O.O. Snihur, and R.M. Kondratenko, "Interval type-2 generalizing fuzzy model for monitoring the states of complex systems using expert knowl-

edge," *System Research and Information Technologies*, no. 2, pp. 63–73, 2023. doi: 10.20535/SRIT.2308-8893.2023.2.05

45. E.M. Kiseleva, O.M. Prytomanova, and L.L. Hart, "Application of optimal set partitioning theory to solving problems of artificial intelligence and pattern recognition," *System Research and Information Technologies*, no. 4, pp. 91–101, 2021. doi: 10.20535/SRIT.2308-8893.2021.4.07

INFORMATION ON THE ARTICLE

Maksym S. Stetsenko, ORCID: 0000-0001-8155-2947, National University "Odesa Maritime Academy", Ukraine

Oleksiy M. Melnyk, ORCID: 0000-0001-9228-8459, Odesa National Maritime University, Ukraine, e-mail: m.onmu@ukr.net

Igor I. Vorokhobin, ORCID: 0000-0001-7066-314X, National University "Odesa Maritime Academy", Ukraine

Dmytro V. Korban, ORCID: 0000-0002-6798-2526, National University "Odesa Maritime Academy", Ukraine

Oleg A. Onishchenko, ORCID: 0000-0002-3766-3188, National University "Odesa Maritime Academy", Ukraine

Valentin B. Ternovsky, ORCID: 0000-0002-4402-4157, Odesa National Maritime University, Ukraine

Iryna M. Ivanova, ORCID: 0000-0002-1751-7781, Odesa National Maritime University, Ukraine

ВИКОРИСТАННЯ ПОЛЯРИЗАЦІЙНОГО ПІДХОДУ ДО ВИЯВЛЕННЯ ЦІЛЕЙ З МЕТОЮ ПІДВИЩЕННЯ ЕФЕКТИВНОСТІ ІДЕНТИФІКАЦІЇ МАЛИХ НАДВОДНИХ ОБ'ЄКТІВ ТА ЗАБЕЗПЕЧЕННЯ БЕЗПЕКИ СУДНОПЛАВСТВА / М.С. Стеценко, О.М. Мельник, І.І. Ворохобін, Д.В. Корбан, О.А. Онищенко, В.Б. Терновський, І.М. Іванова

Анотація. Досліджено новаторський підхід, що дає змогу значно підвищити ефективність навігаційних радіолокаційних станцій за несприятливих погодних умов. Традиційні суднові радари, які використовують горизонтальну поляризацію, стикаються з труднощами в ефективному придушенні дощових перешкод. Запропоновано інноваційний метод, що використовує кругову поляризацію для виявлення навігаційних цілей. Цей метод використовує відмінні поляризаційні властивості, які демонструють стабільні навігаційні цілі і флуктуаційні об'єкти, що заважають. Теоретичний аналіз і модельні експерименти обґрунтовують узгоджені значення параметра еліптичності розсіяних хвиль, незалежні від інтенсивності дощу, як для дощових перешкод, так і для поверхневих металевих об'єктів. Практичні наслідки таких досліджень є дуже перспективними, адже вони уможливлюють виявлення об'єктів незалежно від співвідношення шум/сигнал шляхом інтегрування додаткового каналу циркулярно поляризованих хвиль і застосування простих математичних функцій. Такий підхід знаменує собою значний крок до подолання проблем ідентифікації малих надводних об'єктів, пов'язаних із метеорологічними умовами в морських навігаційних радіолокаційних системах.

Ключові слова: безпека судноплавства, навігаційна безпека, морські перевезення, радіолокаційні перешкоди, несприятливі погодні умови, придушення перешкод, навігаційні цілі, автономні надводні транспортні засоби, принципи радіолокації, виявлення суден, точність радіолокації.

A HYBRID MODEL OF ARTIFICIAL INTELLIGENCE INTEGRATED INTO GIS FOR PREDICTING ACCIDENTS IN WATER SUPPLY NETWORKS

Yu. ZAYCHENKO, T. STAROVOIT

Abstract. The search for an effective and reliable model for predicting accidents on water supply networks by determining their exact locations has always been important for effectively managing water distribution systems. This study, based on the adaptive neuro-fuzzy logical inference system (ANFIS) model, was developed to predict accidents in the city of Kyiv (Ukraine) water supply network. The ANFIS model was combined with genetic algorithms and swarm optimization (ACO) methods and integrated into a GIS to visualize results and determine locations. Forecasts were evaluated according to the following criteria: mean absolute error (MAE), root mean square error (RMSE), and coefficient of determination (R^2). Depending on the amount and type of input data, ANFIS optimization with genetic algorithms and swarm optimization (ACO) can, on average, increase the accuracy of ANFIS predictions by 10.1% to 11%. The obtained results indicate that the developed hybrid model may be successfully applied to predict accidents on water supply networks.

Keywords: ANFIS, ACO, GA, spatial objects, geodatabase, metaheuristics, spatiotemporal analysis, water loss.

INTRODUCTION

Forecasting accidents in water distribution systems is important in the management of water resources, as it makes it possible to identify problem areas in the network and eliminate them in advance. Intelligent predictive systems are models and algorithms that provide valuable information about the future performance of a system as a decision support system. With the development of supervisory control and data acquisition (SCADA) systems, real-time monitoring of pressure and data flows is commonly used to detect pipe bursts. Machine learning [5] and cluster analysis models were developed for optimal assessment. Failures in the network can also be analyzed using hydraulic models [6].

The techniques mentioned above were successful in detecting accidents, but not in pinpointing their exact locations [7]. The model-based approach relies heavily on the accuracy of hydraulic models [8] and may not be suitable for larger water supply systems. Other methods that utilize pressure/flow measurements and GIS have also been proposed. For instance, [9] utilized triangle-based cubic interpolation to establish a pressure drop surface during network breaks to locate the

source of the problem. In [10] the measuring zone's rupture location in the water supply network was identified by assessing the sensitivity of various pressure/flow measurements in relation to emergency leaks. [11] employed a multivariate graphical model that utilized data from multiple pressure gauges to identify potential accident locations, employing a combination of Gaussian and geostatistical methods. Typically, fluctuations in demand can make it difficult to detect hydraulic indicators resulting from accidents. Therefore, these methods can only provide a general idea of where network breaches may occur, with an error range of hundreds of meters and several pipes. Unfortunately, this is not precise enough to quickly locate and fix network issues, resulting in delayed system restoration.

A more accurate method is needed to locate pipe bursts, which involves gathering detailed information about the water system's behaviour in potential locations to detect anomalies. This can be achieved by placing accelerometer sensors and analyzing acoustic signals, which can automatically determine the location of the rupture or leak [12]. However, the reliability of this method depends on the characteristics of the leakage conditions, such as pressure and flow rate, and the detection range is limited by the clarity and correlation of the acoustic signals. Another approach is based on transient processes [13], which analyzes characteristic transient waves to determine the location of accidents. However, background noise or other activities in the system can interfere with transient signals caused by discontinuity, especially if the number of channels to be analyzed increases [7]. Hence, methods based on transient processes may not be suitable for locating pipe breaks with exact precision.

Many researchers have explored the use of machine learning in water resources research [14], but there is no consensus on the best model for predicting water supply network emergencies. To address this, a forecasting model was developed that can pinpoint the exact location of potential emergencies. Artificial neural networks are commonly used in water resource assessment due to their computational efficiency [15–17], but they may produce errors in some cases due to poor prediction or overtraining [15]. Therefore, it is necessary to optimize the ANN and look for new approaches and new classes of neural networks.

Studies [18–20] have proposed a high-precision hybrid model called ANFIS, which combines artificial neural networks (ANN) and fuzzy logic. The hybrid ANFIS model has better performance than the two separate models, but it has certain limitations in finding the best weight parameters, which greatly affect the prediction performance [15]. Furthermore, different optimization algorithms yield varying results based on the geoenvironmental factors of the area being studied. Therefore, developing new hybrid algorithms to determine the best weights and produce reliable results is fundamental for flow modeling processes.

The purpose of this work is the development of a new model of artificial intelligence and the study of its effectiveness in the tasks of predicting accidents on water supply networks with the determination of exact locations. This research is conducted for the first time on the water distribution system of the city of Kyiv.

MODEL DEVELOPMENT AND TRAINING METODOLOGY

Data set collection for spatial modeling

The proposed modeling method is applied to the GIS water supply system of the city of Kyiv (Ukraine). The length of the water supply networks in the city is in-

creasing due to the inclusion of street and intra-quarter networks from enterprises. As of 2019, the total length of the networks was 4,284.8 km.

In the structure of the city's water supply networks, the main part is street networks — 2614.8 km or 61% of the total length of pipes; intra-quarter networks — 1275.1 km or 29.8%; water pipes — 394.9 km or 9.2%. The vast majority of pipelines, namely 65.9%, are made of cast iron; 30.5% — from steel and only 3.6% — from plastic materials.

21.4% of the pipes of the water supply network have been operated for more than 50 years and another 33.2% — about 50 years; the service life of 27.1% is up to 35 years, 12.3% — up to 25 years, 4.6% — up to 15 years, and only 1.4% — up to 5 years. According to the degree of wear, 50.4% of the pipes are worn by more than 90%; 24.3% of pipes — by 50–75%; 15.5% — by 75–90%; 6.3% — by 25–50%; 3.5% — less than 25%.

Pipelines made of cast iron have the longest average age — 46.8 years, pipelines made of steel — 45.4 years, the smallest — made of plastic — 15 years. According to the pipe depreciation indicator, the water distribution system is characterized as follows: the average degree of wear of steel pipes is 90%, cast iron pipes are 75%, and plastic pipes are 23%.

The accident rate, which is determined by the number of accidents per unit length of the network, has fluctuated in the range of 2.0–2.2 accidents/km in recent years, and the tendency to increase the number of accidents was observed specifically for water pipes.

The methodology of this study is shown in Fig. 1, and includes the following stages:

1) preparation of input data;

2) separation of data into training (70%) and test (30%) sets;

3) training of ANFIS neuro-fuzzy network;

4) optimization of the ANFIS model by genetic algorithms and the swarm optimization algorithm (ACO);

5) checking the accuracy of ANFIS, ANFIS-GA and ANFIS-ACO models.
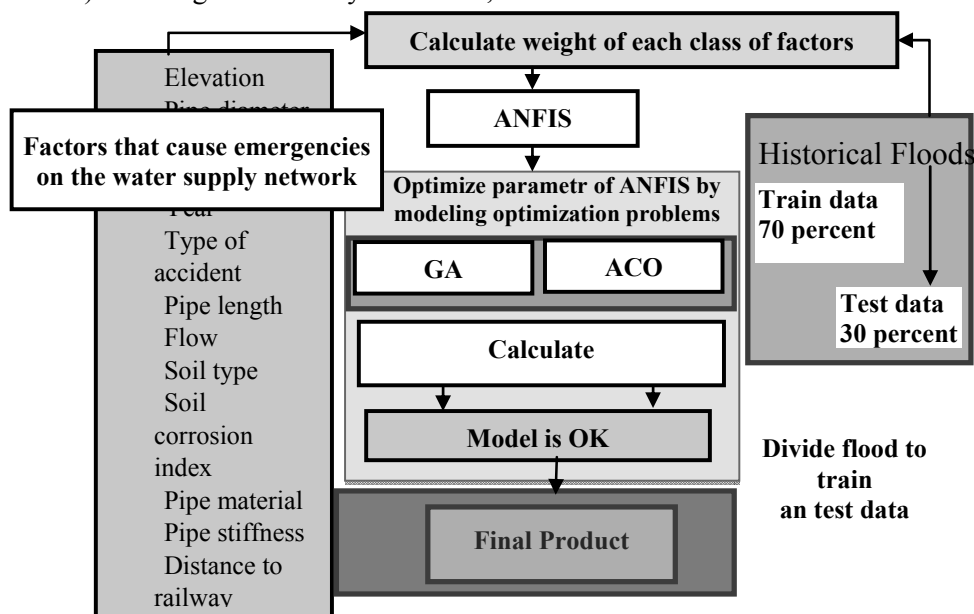
Fig. 1. Structural diagram of the development and optimization of the ANFIS model

It is important to consider how the problem occurs in relation to other factors to make accurate spatial predictions. Table 1 shows the data used in our predictive model, with some entered into the GIS and the rest determined through hydraulic modeling based on the GIS model.

T a b l e 1. Factors and conditions used in the model that impact the emergence of issues in the water supply network

Factors/conditions	Units	Description
The degree of proximity of the location to railway tracks/	m	When trains are in motion, the ground vibrates, causing pipes to crack and gate valves to be damaged.
Age	year	Year of laying the pipe
Length	m	Length of a pipe
Diameter	mm	Size of a pipe
Soil type index	NA	Soil type
Geoposition	NA	Geospatial location
Accident date	year	Accident date on network
Pressure	bar	Pressure from hydraulic calculation results
Volume of consumption	m^3/hour	Volume of water consumption per hour
Volume of consumption	m^3/month	Volume of water consumption per month
Demand	NA	Water demand
flow rate	NA	Flow rate according to hydraulic calculation
Pipe materials rigidity	NA	rigidity coefficient
Consumers	NA	Individuals and legal persons

It is probable that certain factors may affect the occurrence of pipe ruptures or damages in specific parts of the network, while leaving other areas unaffected. One such factor could be the presence of railway tracks. The vibrations caused by freight trains passing by can lead to frequent failures in the water supply network, resulting in pipe ruptures or damage to fittings. Additionally, the type of pipe material used also plays a significant role in determining its lifespan. Steel pipes typically last for 25 years, while plastic or cast iron pipes can last up to 50 years.

PREPARATION OF DATA SET FOR TRAINING AND TESTING

In order to check if the model is practical, the data set for analysis should be split into two groups: one for building the model (called the training data set) and the other for testing it (called the test data set) [21]. To create the training data set, 70% of locations with and without previous accidents on the network (a total of 313 locations) were randomly chosen and combined.

The remaining 30% were then used to create the test dataset. Both data sets were originally in vector format but were converted to csv format for further analysis. For both data sets, the value 1 was assigned to indicate the presence of an accident on the network, while 0 was assigned to indicate the absence of accidents.

We conducted a statistical analysis to thoroughly examine the data and improve the intelligent model.

We performed a statistical analysis of spatial data in order to determine the parameters of the membership function for training the ANFIS network and its optimization (Fig. 2).
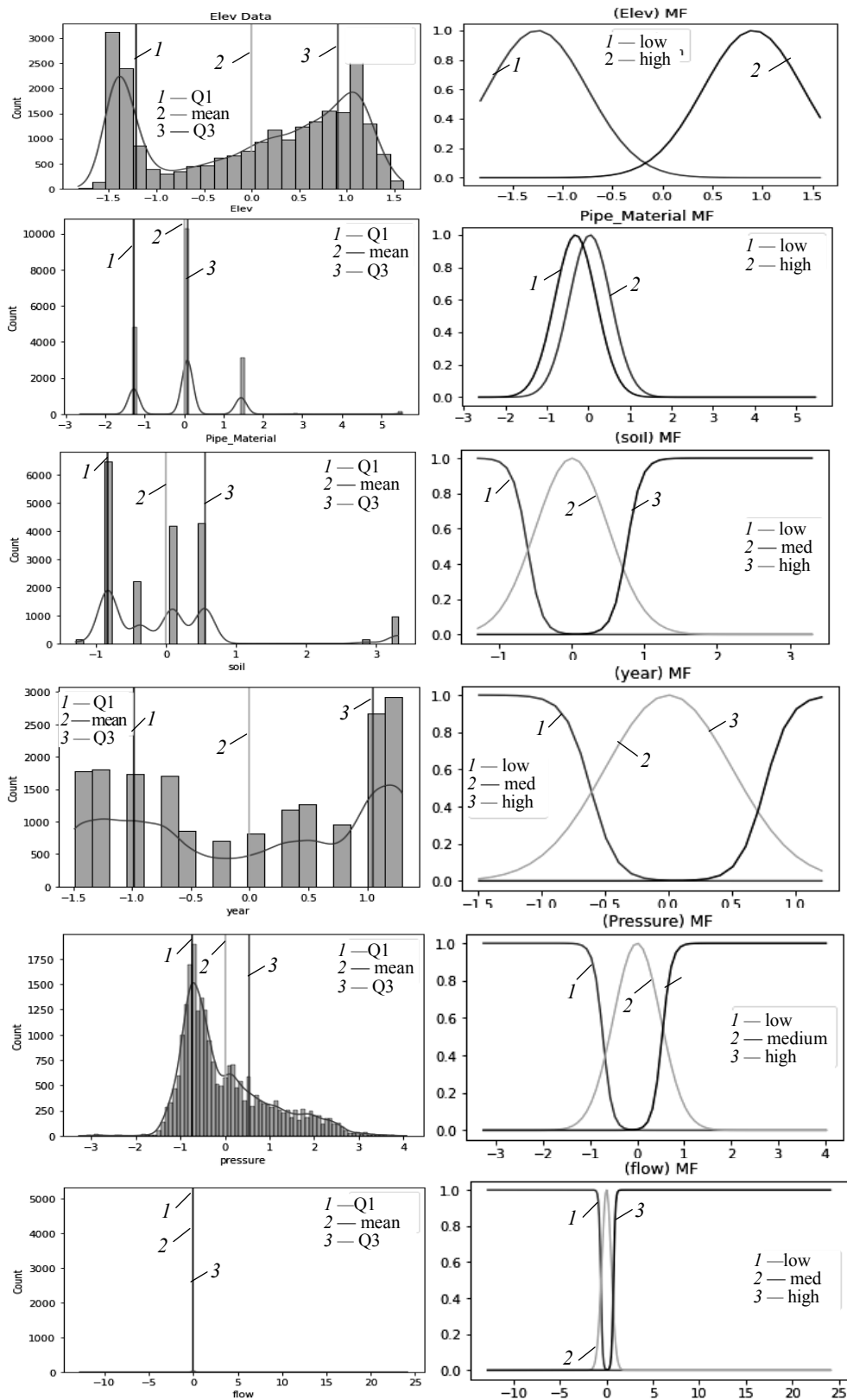
Fig. 2. Statistical analysis of the spatial data

DEVELOPMENT OF THE ANFIS MODEL AND ALGORITHMS FOR ITS OPTIMIZATION

Adaptive neuro-fuzzy logical inference system

ANFIS (Adaptive Network Based Fuzzy Inference System) is an adaptive fuzzy logical inference system proposed by Sugeno based on IF-THEN rules. It is a method that combines artificial neural networks (ANNs) with fuzzy ones. This neural network is used for membership function tuning and rule base tuning in a fuzzy expert system. Below is the Sugeno model of fuzzy logic inference (Fig. 3).
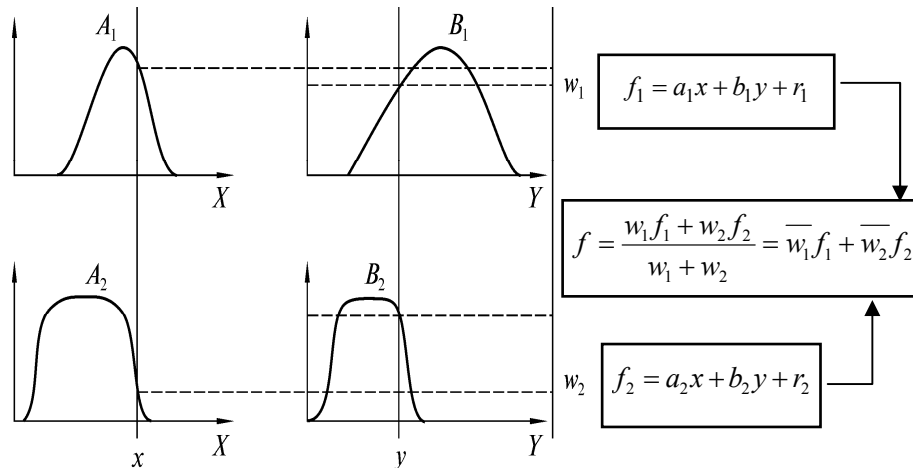
Fig. 3. Sugeno's fuzzy logic model

The layers of this fuzzy neural network perform the following functions.
Layer 1. Membership Function Layer
In this layer, each neuron uses a membership function (fuzzifier) to transform the input signal x or y. The most commonly used functions are the bell-shaped function or the Gaussian function:

$$\mu_{A_i}(x) = \frac{1}{1 + \left[\left(\dfrac{x - c_i}{a_i}\right)^2\right]};$$

$$\mu_{A_i}(x) = \exp\left[-\left(\frac{x - c_i}{a_i}\right)^2\right].$$

Layer 2. Antecedent Layer
Each neuron is represented by the symbol Π. It performs an intersection between sets of input signals, which simulates a logical AND operation. The neuron then sends an output:

$$w_i = \mu_{A_i}(x) \times \mu_{B_i}(y), \quad i = i = 1, 2, .., n.$$

In fact, any *T*-norm operator that generalizes the AND operation can be used in these neurons.

Layer 3. Normalization Layer

Each neuron in this layer calculates the normalized strength of the rule:

$$\underline{w_i} = \frac{w_i}{\sum_i w_i}, \quad i = 1,2,..,n \,.$$

Layer 4. Consequent Layer

The values of output variables are formed in neurons:

$$O_i^4 = \underline{w_i} f_i = \underline{w_i}(a_i x + b_i y + r_i)\,.$$

Layer 5. Aggregation Layer

We receive the output signal of the neural network and perform defuzzification of the results:

$$O^5 = \text{overall output} = \sum \underline{w_i} f_i = \frac{\sum_i w_i f_i}{\sum_i w_i}\,.$$

The neural network of the ANFIS architecture is trained using the gradient descent method.

OPTIMIZATION OF ANFIS WEIGHTING COEFFICIENTS AND OFFSETS BY THE ANT COLONY ALGORITHM

Ant Colony Optimization (ACO) is a probabilistic method for solving complex computational problems that find optimal parameters in a search environment. This algorithm, which was proposed by Marcus Dorigo in 1996, imitates the behaviour of ants in finding the optimal path from their nest to a food source. In [22; 23], the author optimizes the weighting coefficients of an artificial neural network using ACO and investigates the performance of the network. In the search space, a population of weights is created which is considered as an objective function and is found according to the formula:

$$\text{SEP} = 100 \frac{O_{\max} - O_{\min}}{n_o n_p} \sum_{p=1}^{n_p} \sum_{i=1}^{n_o} (t_i^p - o_i^p)^2,$$

where t_i^p and o_i^p are the expected and actual value of the output neuron and for the template p.

The terms $O_{\max}$, and $O_{\min}$ represent the highest and lowest values of the output signal from a specific neuron, while n_o and n_p refer to the number of output neurons.

The ACO algorithm is a tool for optimizing neural network parameters such as synaptic weights, number of layers, and number of hidden neurons. It begins by randomly selecting decisions from a predefined set of data, which are then evaluated and assigned to the decision space based on their fitness values. New solutions are created using information from previous iterations, with a higher likelihood of selecting values with a greater concentration of pheromones [23]. This process generates a matrix of size $M \times N$, where M represents the decision population size and N represents the number of decision variables.

$$\text{Population} = \begin{bmatrix} X_1 \\ X_2 \\ \vdots \\ X_j \\ \vdots \\ X_M \end{bmatrix} = \begin{bmatrix} x_{11} & x_{12} & \ldots & x_{1i} & \ldots & x_{1N} \\ x_{21} & x_{22} & \ldots & x_{2i} & \cdots & x_{2N} \\ \ldots & \ldots & \ldots & \vdots & \ldots & \ldots \\ x_{j1} & x_{j2} & \ldots & x_{ji} & \cdots & x_{jN} \\ \ldots & \ldots & \ldots & \vdots & \ldots & \ldots \\ x_{M1} & x_{M2} & \ldots & x_{Mi} & \ldots & x_{MN} \end{bmatrix},$$

where $X_j = j$-th solution, $x_{ji} - i$-th solution variable for the j-th solution, and M is the size of the number of solutions. The value x_{ji} is chosen randomly from the set V_i:

$$V_i = \{v_{i1}, v_{i2}, ..., v_{id}, v_i D_i\}, \ i = 1, 2, ..., N,$$

where V_i = set of predefined values for the i-th decision variable, $v_{id} = d$-th possible value for the i-th decision variable, and D_i = total number of possible values for the i-th decision variable [23].

GENETIC ALGORITHMS

Genetic algorithms develop optimal solutions by sampling from all possible solutions. The best of these solutions are then combined using the genetic operators of crossover and mutation to generate new solutions. This process continues until a certain termination condition is met [4]. The diagram of the GA process is shown in Fig. 4. The first step is the initial state in which we want to find the Hamiltonian cycle with the smallest sum of weights. In the second step, the fitness function estimates the Hamiltonian cycles, with lower cost functions indicating the best individuals. Finally, in the third step, the most adapted individual is identified.
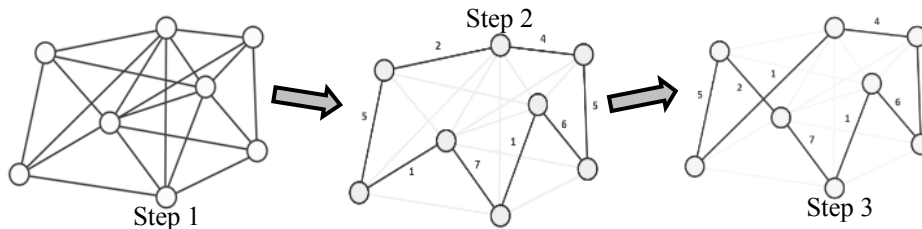
Fig. 4. Scheme of the process of genetic algorithms

GA can be used to optimize various parameters in water distribution systems. It uses the following mechanisms: crossover, mutation, selection. The goal of training is to minimize the root mean square error:

$$E(W) = \frac{1}{M} \sum_{k=1}^{M} (d_k - y_k(w))^2 \ ;$$

$$W = [W_I, W_O] \ ;$$

$$W_I = \left\| w_{ij}^I \right\| \ ;$$

$$W_O = \left\| w_{ij}^O \right\| .$$

We set the initial population in which any individual is represented by the corresponding weights of N individuals: $[W_I(0),...,W_i(0),...,W_N(0)]$.

We calculate the fitness index (Fitness Index) and evaluate the quality of forecasting:

$$FI(W_i) = C - E(W_i) \rightarrow \max ,$$

where C — constant.

IMPLEMENTATION OF THE MODEL

The technique of forecasting with a combination of GIS and artificial intelligence methods were applied to predict accidents on the water supply network of the city of Kyiv. The Sugeno method was used, as it shows better accuracy. The optimal membership function was chosen by trial and error. The ANFIS method was optimized by GA and ACO to improve accuracy.

The performance of the ANFIS, ANFIS-GA, ANFIS-ACO models was determined from the resulting mean absolute error (MAE), which indicates a risk metric corresponding to the expected value of the absolute error loss or the loss rate:

$$MAE(y,\hat{y}) = \frac{1}{n_{samples}} \sum_{i=1}^{n_{samples}} \left| y_i - \hat{y}_i \right| .$$

The mean squared error indicates the risk indicator corresponding to the expected value of the squared error or loss:

$$RMSE(y,\hat{y}) = \frac{1}{n_{samples}} \sum_{i=0}^{n_{samples}} (y_i - \hat{y}_i)^2 .$$

The R^2 function calculates the coefficient of determination, which represents the proportion of variance (y) that was explained by the independent variables in the model:

$$R^2(y,\hat{y}) = 1 - \frac{\sum_{i=1}^{n}(y_i - \hat{y}_i)^2}{\sum_{i=1}^{n}(y_i - \underline{y})^2} .$$

The function explained variance calculates the estimate of the explained variance:

$$explained\_variance\ (y,\hat{y}) = 1 - \frac{\text{var}\{y,-\hat{y}\}}{\text{var}\{y\}} .$$

RESULTS

Spatial-temporal assessments and prediction of the occurrence of accidents on the water supply network of the city of Kyiv

Spatiotemporal GIS analysis and modeling are essential for studying and predicting future events. For modeling, we used the ESRI GIS package: ArcGIS Pro 2.7. The first step was data acquisition and preparation. The obtained information was

summarized in the netCDF data structure, which was used for spatial statistical analysis and creation of a space-time cube (Fig. 5) [24] .
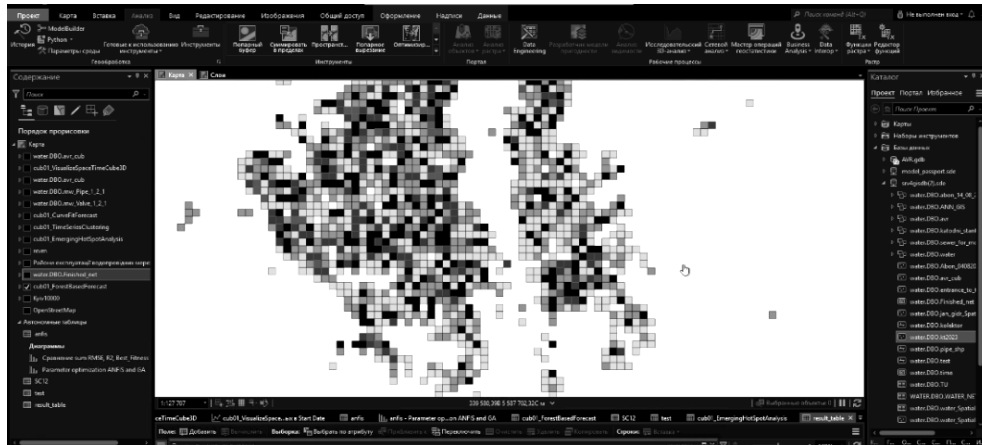
Fig. 5. The result of spatial forecasting

A space-time cube is a well-known model in ArcGIS that combines spatial data and time into a three-dimensional data structure of the netCDF (total network shape) format, containing an array of bins with absolute location and absolute time [24]. So, we aggregated incidents of accidents on the water supply network within a grid size of 500×500 m^2 (distance interval) with an absolute step interval of 1 month. This approach made it possible to investigate cases of accidents on the water supply network of the city of Kyiv (Ukraine).

We applied the space-time cube to a forest-based prediction model, which generated a 2D object class indicating the predicted locations within the original space-time cube. Each location is predicted individually (as shown in Fig. 5) and has its own schedule (as seen in Fig. 6).
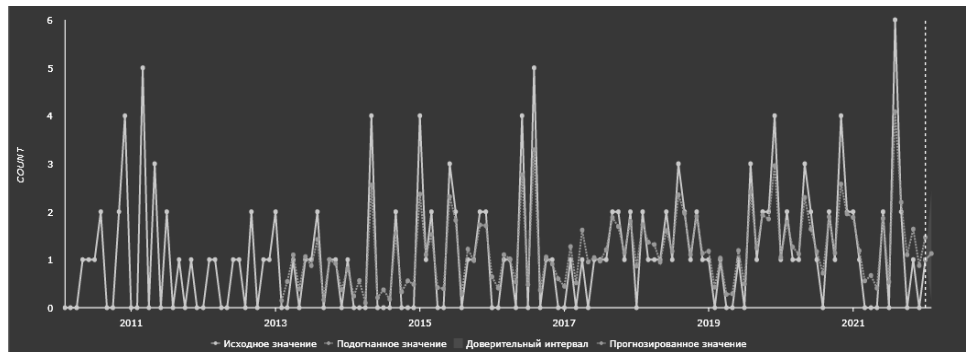
Fig. 6. Graph of the values of the locations of the space-time cube

In Fig. 6, the graph displays the input, data gaps restored as a result of calculations, predicted values and confidence intervals. Confidence intervals are created for each predicted time step, which are presented as fields of output objects.

The upper and lower bounds of the confidence intervals for the first predicted time step are calculated using quantile random forest regression. To predict values for a future time, observations from each leaf of the tree are averaged together. The confidence interval of the second forecast is calculated in a similar way, but is adjusted taking into account the confidence interval of the first fore-

cast [25]. The real confidence interval of the second forecast is calculated by adding the lengths of the limits of the confidence interval of the two forecasts. Subsequent time steps are calculated by adding previous predictions. The real confidence level of these intervals is at least 90%, but in reality the accuracy may be higher [25].

The result of the assessment of the total accuracy of the forecast in different locations, using the forest-based method, is shown in Table 2.

T a b l e 2. The result of the overall assessment of forecast accuracy in different locations

Category	Min	Max	Mean	Median	Mean sq. dev.
RMSE of the prediction	0.00	1.25	0.26	0.24	0.15
RMSE of validation	0.00	2.89	0.56	0.48	0.45

This forecasting method is best used for time series with a complex shape and trends that are difficult to model using simple mathematical functions. The correct selection of time steps during model validation is important. The more time steps that are excluded, the less time it takes to evaluate the validation model. However, if too few time steps are included, the RMSE value will be estimated using less data and may be misleading. Also, this tool can produce unstable and unreliable forecast results if the same value is repeated too often in time series [25]. To optimize and improve the accuracy of the predictive model, we combined GIS methods with hybrid artificial intelligence methods.

Configuration of hybrid models

In this study, we integrated the ANFIS model with GA and ACO algorithms, and compared the performance of the models. The algorithms are implemented in the Spyder environment (Anaconda 3). In order to test the model with different optimization algorithms, the data were organized into separate training and test datasets, which were divided into 70% and 30% (Fig. 7).
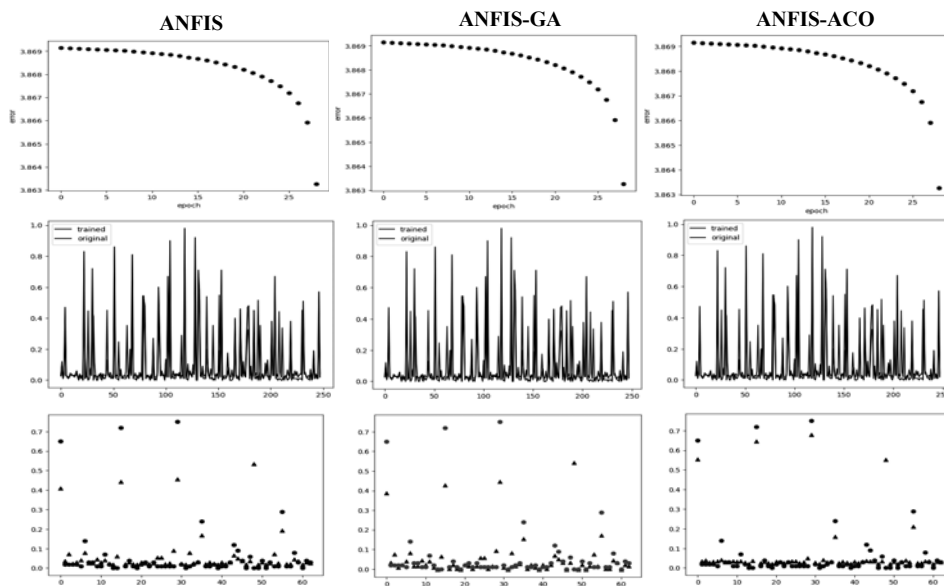
Fig. 7. Results of model training

Fig. 7 shows the result of model training: change in error frequency during training; comparing predicted values with actual data on the training set and comparing predicted values with actual data on the test set.

The first step was to import the training data into the ANFIS, ANFIS-GA, ANFIS-ACO models to reveal the hidden relationships between the factors affecting the emergency of the water supply network. As a next step, the validation data were used to test the performance and predictive capabilities of the models. MAE, RMSE, R^2, and explained_variance were used to measure accuracy. Table 3 shows the result of learning hybrid models (the first 5 iterations in GA and ACO).

T a b l e 3 . Comparison and performance testing of models

Model	Test data				Train data			
	MAE	RMSE	R^2	Cov	MAE	RMSE	R^2	Cov
ANFIS	0.043	0.094	0.613	0.613	0.062	0.125	0.576	0.578
	Study time:				0:00:06.19			
ANFIS-GA	0.041	0.097	0.599	0.600	0.061	0.124	0.575	0.574
	Study time:				0:00:08.31			
	0.042	0.098	0.583	0.585	0.061	0.124	0.575	0.577
	Study time:				0:00:08.98			
	0.041	0.098	0.587	0.589	0.061	0.125	0.575	0.577
	Study time:				0:00:09.09			
	0.044	0.098	0.585	0.587	0.062	0.124	0.573	0.575
	Study time:				0:00:08.41			
	0.042	0.098	0.584	0.586	0.061	0.125	0.575	0.576
	Study time:				0:00:08.24			
ANFIS-ACO	0.041	0.096	0.593	0.595	0.061	0.124	0.573	0.575
	Study time:				0:00:11.96			
	0.042	0.097	0.585	0.587	0.061	0.124	0.574	0.576
	Study time:				0:00:11.86			
	0.043	0.098	0.585	0.586	0.062	0.125	0.572	0.575
	Study time:				0:00:12.22			
	0.041	0.098	0.586	0.588	0.061	0.125	0.576	0.577
	Study time:				0:00:11.92			
	0.042	0.097	0.585	0.587	0.062	0.125	0.573	0.575
	Study time:				0:00:12.21			

The MAE values for the ANFIS, ANFIS-GA, and ANFIS-ACO models were calculated for both the test and training data. The results show that the ANFIS-GA model had the best performance with a MAE value of 0.042 for the test data and 0.061 for the training data. The GA algorithm was found to be more efficient than the ACO algorithm, which had a similar performance but required twice as much training time. It's important to note that these results may vary based on the input data. Overall, the ANFIS-GA model is stable, efficient, and has a fast convergence rate.

CHECKING AND COMPARING MODELS

We used three different optimization models, namely ANFIS, ANFIS-GA, and ANFIS-ACO, which were developed and implemented in Spyder (Anaconda3).

The results obtained from these models were then visualized in ArcGIS Pro 2.7. To train these models, we divided the pointed objects of accidents into two categories: 30% for training and 70% for testing. We used the training data set to establish relationships between the occurrence of accidents (1) and the absence of accidents (0).

We checked the accuracy and performance of hybrid intelligent models by calculating the mean absolute error of MAE. Fig. 8 shows the membership functions of the input variables of the ANFIS model. Fig. 9 illustrates the graph of the change in the loss function depending on the number of iterations. Membership functions indicate the fuzziness of the inputs. A comparison of the accuracy scores in Fig. 8 shows that the ANFIS network performs well.
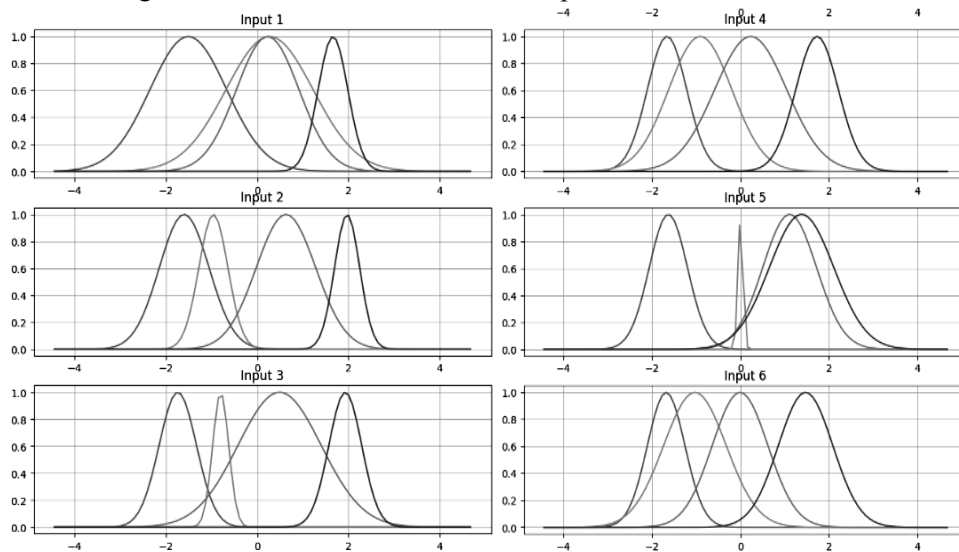
Fig. 8. Membership functions of the used input variables

As a result, the accuracy of the ANFIS model was 95.49%. The accuracy decreases when the number of inputs increases, so to increase the accuracy, it is necessary to improve the network with optimization algorithms.
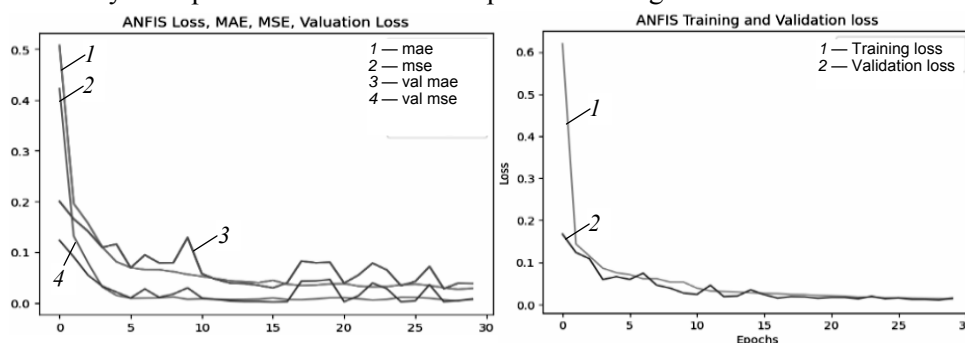
Fig. 9. The graph of the change of the loss function depending on the number of iterations

The result of training the ANFIS-GA and ANFIS-ACO models was not much better than the classic ANFIS, moreover, the ANFIS-ACO model required much more time. In ANFIS-GA, the training time was the same as in ANFIS (one iteration on average 0:00:06.24), while in ANFIS-ACO the total training time took 0:58:19.69 (0:00:12.38 one iteration). Overall, the predictions aligned well

and matched the experimental data accurately. It's worth mentioning that the test results demonstrate the developed models' proficiency in forecasting data beyond the training range.

Compared to GIS forecasting methods, developed artificial intelligence models provide an opportunity to expand and increase forecast accuracy, and indicate specific problematic pipes. Also, the developed models can be easily integrated into ArcGIS Pro in the form of geoprocessing tools, and published on corporate geoportals.

CONCLUSIONS

Adaptive neural fuzzy logic inference system (ANFIS) and its hybrid learning methods: ANFIS-GA, ANFIS-ACO were used to predict water supply network accidents. This model was integrated into GIS (ArcGIS Pro) to visualize and determine the exact locations of possible accidents and was verified in practice (all predicted accident locations for the next three days coincided with accidents that occurred on the Kyiv water supply network). The following conclusions can be drawn from the forecasting model described above:

- Performance evaluation and model validation results of selected metrics: R2, RMSE, and MAE for both training and testing on a small amount of data showed that the hybrid models did not outperform ANFIS model.

- When the amount of input data increased, the accuracy of the ANFIS model decreased and it became necessary to optimize the ANFIS with genetic algorithms and the swarm optimization algorithm (ACO). This optimization increased the accuracy of ANFIS prediction by 10.1%, 11%.

- The results of ANFIS, ANFIS-GA, and ANFIS-ACO intelligent models combined with GIS indicate a large information potential that can support real-time operational control of water supply systems. Fuzzy models of emergency forecasts have a significant advantage as they require less information about water supply systems than conventional probabilistic models. In addition, this information may be vague and inaccurate. The ANFIS model is suitable for modeling complex problems, especially when the relationship between factors is unknown. It is especially useful for identifying threats and providing advance warnings about the likelihood of an accident.

REFERENCES

1. C.M. Fontanazza, V. Notaro, V. Puleo, P. Nicolosi, and G. Freni, "Contaminant intrusion through leaks in water distribution system: experimental Analysis," *Procedia Eng.*, 119, pp. 426–433, 2015. doi: 10.1016/j.proeng.2015.08.904.
2. "Urban Water Statistics Yearbook 2017," (in Chinese), *CUWA*.
3. Dung H. Tran, A.W.M. Ng, and B.J.C. Perera, "Neural networks deterioration models for serviceability condition of buried stormwater pipes," *Engineering Applications of Artificial Intelligence*, 20(8), pp. 1144–1151, 2007. doi: 10.1016/j.engappai.2007.02.005.
4. M. van Dijk, S.J. van Vuuren, J.E. van Zyl, "Optimising water distribution systems using a weighted penalty in a genetic algorithm", *Water SA*, 35(5), pp. 537–548, 2008. doi: 10.4314/wsa.v34i5.180651.
5. M. Romano, Z. Kapelan, and D.A. Savic, "Evolutionary algorithm and expectation maximization strategies for improved detection of pipe bursts and other events in

water distribution systems," *J. Water Resour. Plan. Manag.*, 140 (5), pp. 572–584, 2014. doi: 10.1061/(ASCE)WR.1943-5452.0000347.

6. J. Meseguer et al., "A decision support system for on-line leakage localization Environ," *Environmental Modelling & Software*, vol. 60, pp. 331–345, 2014. doi: 10.1016/j.envsoft.2014.06.025.

7. Y. Wu and S. Liu "A review of data-driven approaches for burst detection in water distribution systems," *Urban Water J.*, 14 (9), pp. 972–983, 2017. doi: 10.1080/1573062X.2017.1279191.

8. C.J. Hutton, Z. Kapelan, L. Vamvakeridou-Lyroudia, and D.A. Savic, "Dealing with uncertainty in water distribution system models: a framework for real-time modeling and data assimilation," *J. Water Resour. Plan. Manag.*, 140 (2), pp. 169–183, 2014. doi: 10.1061/(ASCE)WR.1943-5452.0000325.

9. S.R. Mounce, A. Khan, A.S. Wood, A.J. Day, P.D. Widdop, and J. Machell, "Sensor-fusion of hydraulic data for burst detection and location in a treated water distribution system," *Inf. Fusion*, 4 (3), pp. 217–229, 2003. doi: 10.1016/S1566-2535(03)00034-4.

10. B. Farley, S.R. Mounce, and J.B. Boxall, "Development and field validation of a burst localization methodology," *J. Water Resour. Plan. Manag.*, 139 (6), pp. 604–613, 2013. doi: 10.1061/(ASCE)WR.1943-5452.0000290.

11. M. Romano, Z. Kapelan, and D.A. Savic "Geostatistical techniques for approximate location of pipe burst events in water distribution systems" *J. Hydroinf.*, 15 (3), pp. 634–651, 2013. doi: 10.2166/hydro.2013.094.

12. J. Kang, Y.J. Park, J. Lee, S.H. Wang, and D.S. Eom, "Novel leakage detection by ensemble cnn-svm and graph-based localization in water distribution systems," *IEEE Trans. Ind. Electron.*, 65 (5), pp. 4279–4289, 2018. doi: 10.1109/TIE.2017.2764861.

13. A.F. Colombo, P. Lee, and B.W. Karney, "A selective literature review of transient-based leak detection methods," *J. Hydro Environ. Res.*, 2 (4), pp. 212–227, 2009. doi: 10.1016/j.jher.2009.02.003.

14. H.R. Maier, A. Jain, G.C. Dandy, and K.P. Sudheer, "Methods used for the development of neural networks for the prediction of water resource variables in river systems: Current status and future directions. Environ," *Model. Softw.*, 25, pp. 891–909, 2010. doi: 10.1016/j.envsoft.2010.02.003.

15. D.T. Bui, B. Pradhan, H. Nampak, Q.-T. Bui, Q.-A. Tran, Q.-P. Nguyen, "Hybrid artificial intelligence approach based on neural fuzzy inference model and metaheuristic optimization for flood susceptibilitgy modeling in a high-frequency tropical cyclone area using GIS," *J. Hydrol.*, 540, pp. 317–330, 2016. doi: 10.1016/j.jhydrol.2016.06.027.

16. H. Ghalkhani, S. Golian, B. Saghafian, A. Farokhnia, and A. Shamseldin, "Application of surrogate artificial intelligent models for real-time flood routing," *Water Environ. J.*, 27(4), pp. 535–548, 2013. doi: 10.1111/j.1747-6593.2012.00344.x

17. M. Rezaeianzadeh, H. Tabari, A.A. Yazdi, S. Isik, and L. Kalin, "Flood flow forecasting using ANN, ANFIS and regression models," *Neural Comput. Appl.*, 25(1), pp. 25–37, 2013. doi: 10.1007/s00521-013-1443-6.

18. F.-J. Chang and M.-J. Tsai, "A nonlinear spatio-temporal lumping of radar rainfall for modeling multi-step-ahead inflow forecasts by data-driven techniques," *J. Hydrol.*, vol. 535, pp. 256–269, 2016. doi: 10.1016/j.jhydrol.2016.01.056.

19. Y.S. Güçlü and Z. Şen, "Hydrograph estimation with fuzzy chain model," *J. Hydrol.*, vol. 538, pp. 587–597, 2016. doi: 10.1016/j.jhydrol.2016.04.057.

20. A. Lohani, R. Kumar, and R. Singh, "Hydrological time series modeling: A comparison between adaptive neuro-fuzzy, neural network and autoregressive techniques," *J. Hydrol.*, vol. 442–443, pp. 23–35, 2012. doi: 10.1016/j.jhydrol.2012.03.031.

21. C.-J.F. Chung and A.G. Fabbri, "Validation of spatial prediction models for landslide hazard mapping," *Nat. Hazards*, vol. 30, pp. 451–472, 2003. doi: 10.1023/B:NHAZ.0000007172.62651.2b.

22. K. Socha and C. Blum, "An ant colony optimization algorithm for continuous optimization: application to feed-forward neural network training," *Neural Computing and Applications*, vol. 16(3), pp. 235–247, 2007. doi: 10.1007/s00521-007-0084-z.

23. C. Blum and K. Socha, "Training feed-forward neural networks with ant colony optimization: An application to pattern classification," in *Fifth International Conference on Hybrid Intelligent Systems (HIS'05), IEEE, 2005, November*. doi: 10.1109/ICHIS.2005.104.

24. Omid Bozorg-Haddad, Mohammad Solgi, and Hugo A. Loáiciga, *Meta-heuristic and Evolutionary Algorithms for Engineering Optimization*. 2017. doi: DOI:10.1002/9781119387053.

25. "ArcGIS analysis workflows for public safety," *ESRI*.

INFORMATION ON THE ARTICLE

Yuriy P. Zaychenko, ORCID: 0000-0001-9662-3269, Educational and Research Institute for Applied System Analysis of the National Technical University of Ukraine "Igor Sikorsky Kyiv Polytechnic Institute", Ukraine, e-mail: zaychenkoyuri@ukr.net

Tetiana V. Starovoit, ORCID: 0009-0008-6335-7679, Educational and Research Institute for Applied System Analysis of the National Technical University of Ukraine "Igor Sikorsky Kyiv Polytechnic Institute", Ukraine, e-mail: starovoyt.tania@lll.kpi.ua

ГІБРИДНА МОДЕЛЬ ШТУЧНОГО ІНТЕЛЕКТУ ІНТЕГРОВАНА В ГІС ДЛЯ ПРОГНОЗУВАННЯ АВАРІЙ НА МЕРЕЖАХ ВОДОПОСТАЧАННЯ / Ю.П. Зайченко, Т.В. Старовойт

Анотація. Пошук ефективної та надійної моделі прогнозування аварій на мережах водопостачання з визначенням їх точних розташувань завжди був важливим для ефективного керування системами розподілу води. Дослідження, засноване на моделі адаптивної нейронечіткої системи логічного висновку (ANFIS), розроблено для прогнозування аварій на мережі водопостачання міста Києва (Україна). Модель ANFIS поєднано з генетичними алгоритмами та методами ройової оптимізації (ACO) та інтегрували в ГІС для візуалізації результатів і визначення їх розташування. Прогнози оцінювали за такими критеріями: середньої абсолютної похибки (MAE), середньої квадратичної похибки (RMSE) та коефіцієнтом детермінації (R^2). Залежно від кількості та вигляду вхідних даних оптимізація ANFIS генетичними алгоритмами та алгоритмом ройової оптимізації (ACO) може в середньому збільшувати точність передбачення ANFIS на 10,1%, 11%. Отримані результати свідчать про те, що розроблена гібридна модель може бути успішно застосована для прогнозування аварій на мережах водопостачання.

Ключові слова: геоінформаційні системи, ANFIS, ACO, GA, просторові об'єкти, просторово-часовий аналіз, втрати води.

INTERACTIVE DECISION SUPPORT SYSTEM FOR LUNG CANCER SEGMENTATION

V. SYDORSKYI

Abstract. This paper studies Clinical Intelligent Decision Support Systems (CIDSSs) for lung cancer segmentation, which are based on deep neural nets. A new interactive CIDSS is proposed and compared with previous approaches. Additionally, the purpose uncertainty problem in building interactive systems is discussed, and criteria for measuring both quality and amount of user feedback are proposed. In order to automate system evaluation, a new algorithm was used to simulate expert feedback. The proposed interactive CIDSS outperforms previous approaches (both interactive and noninteractive) on the task of lung lesion segmentation. This approach looks promising both in terms of quality and expert user experience. At the same time, this paper discusses a bunch of possible modifications that can be done to improve both evaluation criteria and proposed CIDSS in future works.

Keywords: clinical decision support systems, deep learning, open system, interactive segmentation.

INTRODUCTION

Decision support systems (DSS) stand out as instrumental across various domains of human activities [1–3]. These systems combine the advantages of big data, statistical models, big informational systems, classical machine learning, and deep learning technologies. Of particular academic and practical interest are the emerging Intelligent DSS. Characterized by their reliance on neural networks, these systems promise enhanced analytical depth and precision, setting the stage for transformative applications across diverse sectors.

A significant portion of recent research [4] has been dedicated to the application of machine learning and deep learning in medical imaging. These studies primarily focus on architecting neural networks and formulating optimization policies to improve diagnostic accuracy. However, it is important to consider deep learning models as part of DSS systems and sub-systems in medical applications. Being a part of IDSS, they can benefit from advances in computer science, system analysis, and decision-making in scientific and practical spheres. IDDS, based on neural nets, can provide accurate medical insights, a user-friendly interface, and an interactive and adaptive mechanism for decision-making.

To address the problem of building IDSS based on deep learning approaches, using expert feedback to improve the initial results of the proposed system, the task of lung cancer segmentation is considered. The main contributions of this paper are:

- Integration of a segmentation neural net into an interactive intelligent decision support system.

- Adaptation of the previous interactive segmentation approach [5] to the task of lung cancer segmentation.
- Improvement of the previous approach by the usage of two types of segmentation neural nets.
- Formulate a purpose uncertainty problem [6] in the construction of such a DSS and propose a set of criteria for DSS assessment, including a special algorithm for expert feedback simulation.

Also, it is important to mention that the proposed system can be adapted for other types of cancer diagnosis. Such adaptions will be considered in future works.

RELATED WORK

The application of clinical decision support systems (CDSS) was proposed in recent studies in order to help with the diagnosis and treatment of oncology diseases [7], modifications in order to adapt to cancer treatment in developing countries [8], and specialized DSS, for example for brain tumors treatment [9]. All these works are focused on building complete decision support systems. Still, at the same time, they focus less on particular intelligent subsystems, which hugely benefit the precision of the overall system.

The latest research in computer science proposes a wide variety of deep learning algorithms [10], which can be utilized in order to improve the quality of CDSS. Starting from classical U-Net [11], FPN [12], and DeepLab [13] architectures, which made a breakthrough in semantic image segmentation in the sphere of medical imaging, ending with the latest Unet++ [14], UNet 3+ [15] and UNETR [16] architectures, which rely on complex skip and residual connections and on processing the whole image volume altogether (3D Nets). Additionally, different Hybrid and Neuro-Fuzzy Networks were applied to the task of lung and brain tumor segmentation and detection in combination with classical 2D, MIL, and 3D approaches [17].

At the same time, interactive segmentation methods propose guiding deep learning algorithms with user feedback. Segment Anything Model [18] proved that neural nets can generalize to the segmentation of many different objects in completely different scenarios. However, there is doubt that it can segment precise medical images, especially in the presence of very tiny and hard distinguishable objects, like lung cancer lesions. Other more specialized approaches were proposed [19; 5] and showed success in medical image segmentation.

INTERACTIVE INTELLIGENT DECISION SUPPORT SYSTEM FOR LUNG CANCER SEGMENTATION

This work considers modern deep learning algorithms to build an interactive intelligent decision support system for lung cancer segmentation. The proposed approach operates on CT scans from different manufacturers and incorporates user feedback to increase the segmentation quality. Finally, three possible architectures of DSS are compared by several criteria.

First, let's formalize the main problem that the segmentation system should solve. This system receives a pre-processed CT scan — x, which is a 3D image, where dimensions refer to the width, height, and depth of the image matrix:

$$x = \{x_{ijk}\}, \ i = 0,...,height, \ j = 0,...,width, \ k = 0,...,n\_slices.$$

In the proposed approach, the Multi-Instance Learning (MIL) [17; 20] approach is used, where each instance refers to a slice of the scan. So, the basic deep learning model — H should approximate mask pixel distribution for each slice based on several scan slices:

$$H(x_K) = \widehat{y_k}, \ x_K = x_{IJK}, \ \widehat{y_k} = \widehat{y_{IJk}},$$

$$I = \{0,1,...,height\}, \ J = \{0,1,...,width\}, \ K = \{k_1, k_2,..., k_l\},$$

where K refers to some set of indexes that define slices, which are used for the prediction of each slice mask, k refers to some fixed slice index, and $\widehat{y_k}$ refers to an approximated slice mask.

In order to make the system interactive, it is required to introduce additional input to the network, which refers to the expert feedback on initially approximated slice masks. One of the ways to incorporate such feedback is to allow expert to select pixels that, he thinks, are misclassified. An expert can simply click on pixels that he thinks should be assigned to foreground — lesion region or background — non lesion region. Also, an expert can erase the whole slice mask. Formalization of expert's feedback:

- Two sets of clicks are provided by the expert: c_p — "positive" clicks, which refer to the foreground ($c\_p = \{i, j\}, \ i \in \{0,1,...,height\}, \ j \in \{0,1,...,width\}$) and c_n — "negative" clicks, which refer to the background ($c\_n = \{i, j\}, \ i \in \{0,1,...,height\}, \ j \in \{0,1,...,width\}$).

- Click mask — cm ($cm = \{cm_{ij}\}, \ i = 0,...,height, \ j = 0,...,width, cm_{ij} \in [0, +\infty)$).

- Algorithm for encoding clicks into click mask $C2M$ ($C2M(c\_p) = cm\_p$ OR $C2M(c\_n) = cm\_n$).

- New model — H_I ($H\_I(cm\_p, cm\_n, \widehat{y_k}, x_K) = \widehat{y\_f_k}$).

It is important to mention that H_I takes the previous predicted mask $\widehat{y_k}$ on input, which allows to incorporate both information from the previous step and expert feedback. The interactive procedure can be applied several times: redefine $\widehat{y_k} := \widehat{y\_f_k}$ and ask expert for new c_p and c_n. Such an iterative procedure creates a certain trade-off: more iterations result in better segmentation masks while taking more expert's time. Also, to receive the initially predicted mask, two approaches can be used: predicted masks from H or initialize $\widehat{y_k}$ as zero mask and ask an expert to define foreground areas without the initially predicted mask.

So there are three possible structures of segmentation DSS:

1. Noninteractive (Fig. 1).
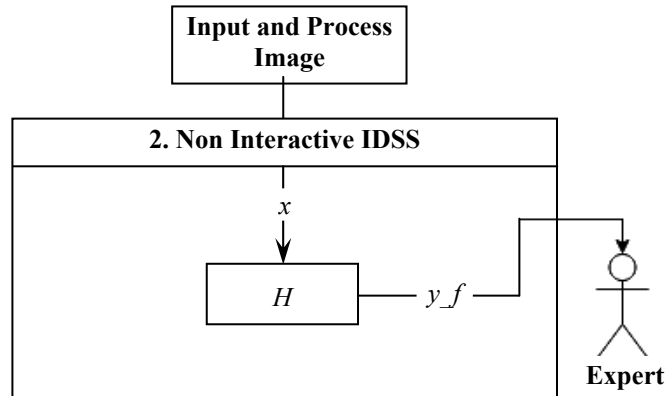
Fig. 1. Structure of noninteractive IDSS

2. Interactive, without the initially predicted mask (Fig. 2).
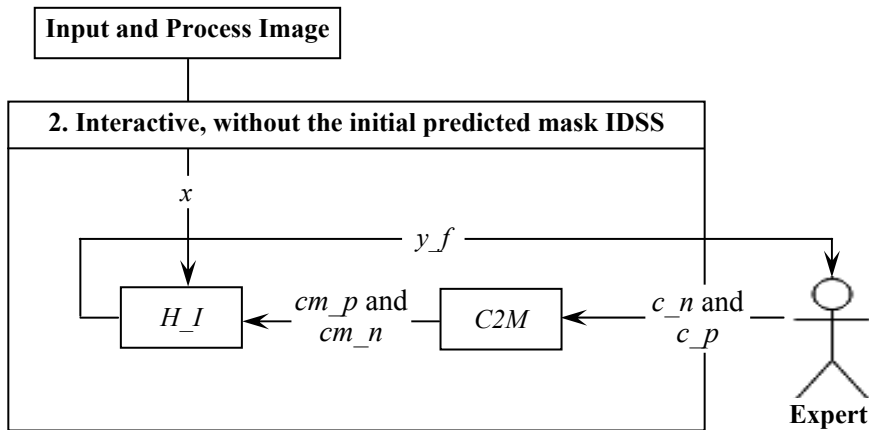
Fig. 2. Structure of interactive IDSS, without the initially predicted mask

3. Interactive with initially predicted mask, received from H (Fig. 3).
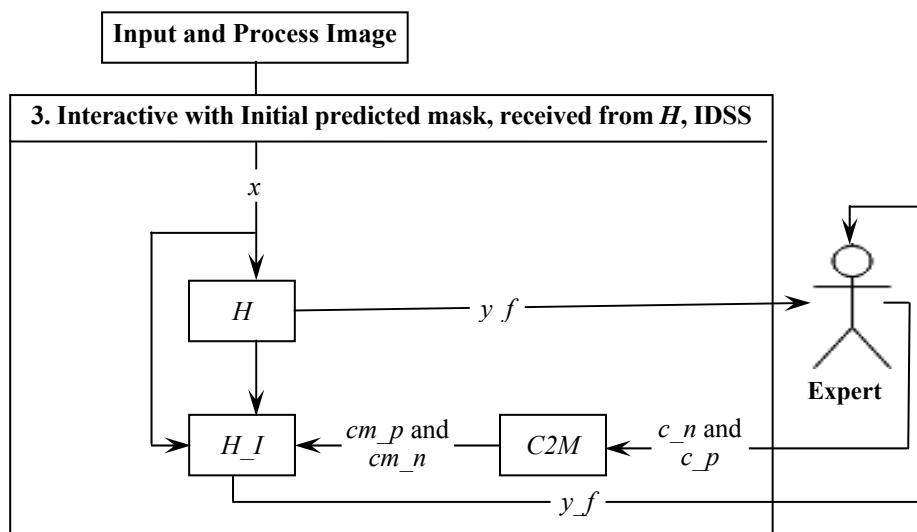
Fig. 3. Structure of interactive IDSS with initially predicted mask received from H

Although, it is important to mention that proposed segmentation DSSs are open systems because they explicitly have information exchange in the form of user feedback. While utilizing this user feedback, entropy in the system is decreasing. This can be easily tracked by the improvement of quality metrics, which will be discussed in Experiments section.

Purpose uncertainty problem. One of the problems in building such an IDSS is purpose uncertainty [6] because there is a trade-off between the amount of user interaction and the quality of the final mask. In this task, different ways of expert interaction require different amounts of effort:

– Making a positive click is the most challenging action because it requires an understanding of precise lesion location, while the initial mask, produced by DSS, can bias the expert.

– Making negative clicks requires less effort because, in most cases, finding a healthy region is an easier task.

– Erasing the whole mask is the most straightforward action because it does not require selecting a particular region.

Considering quality metrics, there is also some uncertainty because the proposed systems will be tested on a series of CT scans, but it is important to track both average quality results and a number of poorly segmented masks. In order to handle this problem, median metric values and the whole metric distribution will be considered in Evaluation section.

DETAILED NEURAL NET SETUP

First of all, K set for selecting input instances should be defined. In the proposed approach $K = \{k-2,\, k-1,\, k,\, k+1,\, k+2\}$, k refers to target slice.

So, the neural net will operate on the target slice and two previous and next slices. Initial experimental results proved that using more slices does not improve segmentation quality and only leads to optimization and inference overheads and overfitting. To feed selected slices in regular 2D Convolutions, slices will be stacked on channel dimension so the resulting input will have the following form:

$$x\_k = x\_KIJ,\ I = \{0,1,...,height\},\ J = \{0,1,...,widt\}\,.$$

In this paper, classical Encoder-Decoder segmentation neural nets will be used: EfficientNet B3 [21] encoder and Unet++ [14], DeepLabV3+ [22] decoders. Different setups will be evaluated in Experiments section, and the best one will be chosen according to the proposed criteria. After the final fully connected layer, the sigmoid will constrain outputs of each pixel prediction to [0; 1] range, and thresholding by 0.5 will be applied.

To design click-to-mask transformation, "Gaussian" masks will be used, as proposed in [5] — equations:

$$DM_{c_l} = \{d_{ij}\},\ d_{ij} = d((i,j), c_l)\,;$$

$$CM_{c_l} = \{cm_{ij}\},\ cm_{ij} = e^{(-d_{ij}{}^2 /(2sigma^2))}\ \text{ if }\ d_{ij} < clip\_radius\ \text{ else } 0\,;$$

$$CM = \sum_{c_l} CM_{cl}\,,$$

where DM_{c_l} is a distance transform for each click c_l; d — euclidean distance; CM_{c_l} — click mask for each click c_l; *sigma* — "Gaussian standard deviation"; *clip_radius* parameter, which zeros out mask pixels, which are too far from the center; CM final click mask for several clicks. In the proposed approach, separate masks for positive and negative clicks are used. Finally, to feed clicks masks and previously predicted masks to an interactive neural net H_I, all inputs are stacked channel-wise, so H_I has three more additional input channels compared to H.

DETAILED OPTIMIZATION SETUP

For training both H and H_I Adam optimizer [23] and reducing the learning rate with the OneCycleCosine learning rate scheduler, starting with 1e-3 and finishing with 1e-6, are used. Neural nets are trained for 191000 steps. Batch size is set to 32, and a distributed data parallel [24] mechanism on two A100 GPUs is used.

It is important to consider the data distribution of masked regions, which is typical for most medical segmentation tasks. In most cases, regions with lesions take only a very small partition of the whole image area, so there are many more negative pixels than positive ones. This work proposes to sample slices with and without lesions with equal probability to reduce class imbalance for the optimization procedure.

In order to optimize both neural nets, the sum of BCE and Jaccard [25] losses is used.

Also, a transfer learning mechanism is used, and the encoder is initialized with weights received from a noisy student learning procedure [26].

For training noninteractive net (H) horizontal and vertical flip augmentations are used, and on the inference stage, the same test time augmentation [27] is applied to improve prediction quality. For training interactive net (H_I) any augmentations are not used.

Another important part is the click-sampling strategy. This work mostly follows strategies proposed in [5] but with several modifications specific to the medical imaging domain. Initially, there are not previously predicted masks, so first clicks should be initialized by some "cold start" strategy. For positive clicks, the center masses of each lesion are selected; if there are several lesions on one slice, the lesion with the biggest area is picked. For negative clicks, random points within d_0 distance from the lesion are selected. Other negative click sampling strategies from [5] were not considered because of task specifications:

- Sampling from another object is not possible in this task because there is only one type of object to segment.
- Sampling from the target object border is also inefficient because the lesion area is pretty tiny, and its border may contain a big part of this area.

After sampling clicks, a click mask for the current interaction can be created and saved to the click cache for the next interactions. Predicted masks for click sampling are used only after the first epoch. Having previously predicted masks

and previous clicks, it is possible to use other sampling strategies. For selecting a positive click, the algorithm uses false negative pixels connected regions and selects the biggest area region and sample click, which is located on the largest distance both from the region border and previous clicks:

$$c_l = \arg\max{}_p(\min(\min{}_{p_t}d(p,p_r),\min{}_{p_c}d(p,p_c))), \qquad (1)$$

where c_l refers to click to select; p — all possible points; p_t — points of the region; p_c — previous clicks from the cache. The algorithm follows the same logic for negative clicks, but here, false positive masks are used as mislabeled masks. To introduce diversity and ensure that the neural net can work only with a few clicks, the algorithm randomly resets the click cache for each image with a probability of 0.3. Also, the maximum number of positive and negative clicks is constrained to 12 separately. It is done to reduce RAM overhead and ensure that the neural netdoes not abuse the usage of lots of clicks.

EXPERIMENTAL RESULTS

In this section, the following points are described:

– Lung lesions dataset, which is used for training neural networks and testing proposed DSSs;

– Metric that is used for evaluation and solution for purpose uncertainty issue;

– An algorithm for simulating feedback from an expert;

– Results of the proposed approach.

Dataset. To experiment with the proposed IDSS, the Lung Image Database Consortium image collection (LIDC-IDRI) [28] is used, which consists of diagnostic and lung cancer screening thoracic computed tomography (CT) scans with marked-up annotated lesions. In this research, only CT scans and marked-up annotated lesions are used.

The whole dataset contains 1018 scans from 1010 unique patients. So, in most cases, there is one CT scan for one patient. The dataset annotation was obtained from four independent experts. To get the final mask, the consensus of the majority of annotators [29] was used. The examples of original and masked images are presented in Fig. 4.
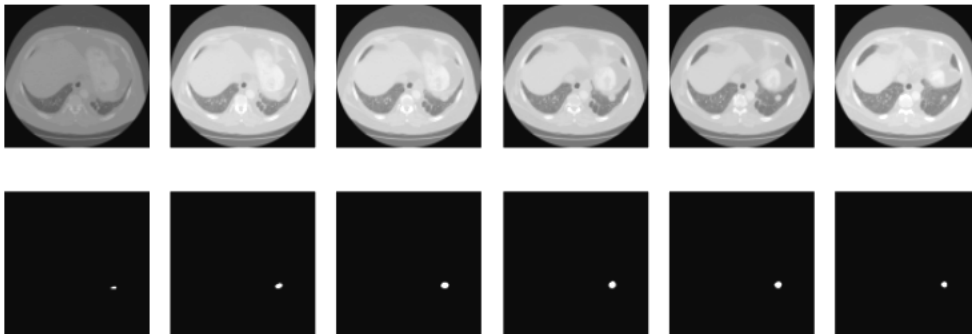
Fig. 4. Examples of CT scans with annotation. First row — original scans. Second row — annotation

All CT scans have 512×512 height and width, but they all differ in the number of slices. Slices distribution can be seen in Fig. 5.
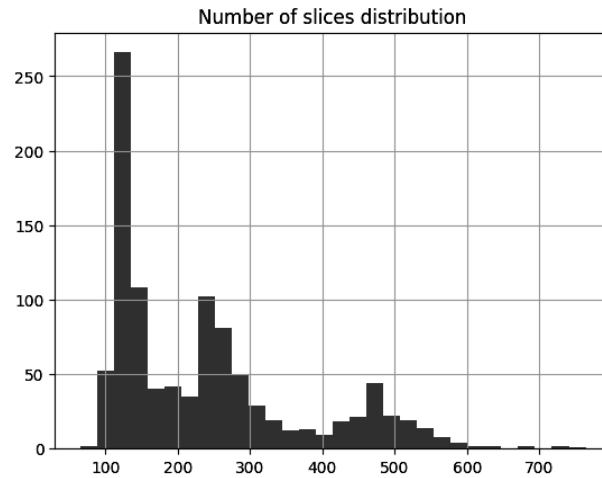
Fig. 5. Distribution of the number of slices across the dataset

As mentioned before, the biggest problem in lesion segmentation is a severe class imbalance — most of the pixels are background pixels. Moreover, most of the slices do not contain lesions: the median number of slices in the scan is 203.5, and the median number of slices with lesions is 40. Also, the area of lesions is pretty small; the median of the relative area of the foreground area to the whole scan area across all dataset images is 8.7683e-06. So, such class imbalance should be considered during model optimization and evaluation.

Evaluation. Two main criteria to evaluate results will be considered: quality and amount of expert feedback.

For quality evaluation, the Intersection over Union (IoU) [30] metric is used, which is computed for each scan separately and averaged across all scans. If the scan does not contain lesions and the predicted mask is empty — IoU is equal to 1. This work also outlines the median, first (Q_1), and third (Q_3) quartiles of IoU scores and overall distribution.

For the amount of expert feedback evaluation, three types of feedback, outlined in Purpose uncertainty problem section, are considered. The feedback score equation (2) includes different weights for feedback types. These weights are proposed based on personal perception of the process and can be tuned in future work.

$$Feedback\ Score = Number\ of\ Positive\ Clicks +$$

$$+ Number\ of\ Negative\ clicks\ *0.85 +$$

$$+ Number\ of\ Masks\ erasements\ *0.75 .\qquad(2)$$

This score should be minimized.

The dataset is split into train and test sets with stratification by relative area of foreground area and grouping by patients (so scans of one patient are only in the test or train set). After the split, there are 203 scans in the test set and 815 scans in the train set, so approximately 20% of the data is used for model assessment.

Algorithm for simulating expert feedback. This algorithm is needed to test our second and third types of IDSS. The proposed algorithm behaves as an "ideal" expert. The algorithm makes one optimal click for each slice in each scan

on each iteration. Such an approach is impossible in the real scenario, but professional radiologists should behave near the "ideal" behavior. This work proposes possible improvements for future work:

• Introduce the probability of making positive, negative clicks or mask erased.

• Introduce some probability distribution of click coordinate.

• Condition both previous distributions on lesion size, number of ground truth, and predicted lesions in the particular CT scan.

• Reduce the probability of correct feedback with iteration number.

Let's formalize optimal positive and negative clicks. First, false positive pixels connected regions for positive click and false negatives connected regions for negative are computed. If there are no such regions for a particular scan or the whole region consists only of its border (single-pixel line), the algorithm just omits clicking. Otherwise, it selects the biggest mislabeled region using the technique proposed in equation (1).

If no feedback was done for a particular slice, a mask from the previous iteration or an empty mask if we have a "cold start" scenario is used.

Experiments. Both different systems and different decoders for neural networks H and H_I will be compared by evaluation metrics proposed in Evaluation section

Quality metrics are outlined in Table 1.

T a b l e 1. Quality metrics

System and Decoder	*Mean IoU* $\uparrow$	*Median IoU* $\uparrow$	Q_1 *IoU* $\uparrow$	Q_3 *IoU* $\uparrow$
System 1 Unet++ Decoder	0.4083	0.4385	0.1507	0.5993
System 1 DeepLabV3+ Decoder	0.3929	0.4104	0.1202	0.6103
System 2 Unet++ Decoder	0.7031	0.6904	0.6154	0.7729
System 2 DeepLabV3+ Decoder	0.6868	0.6679	0.5925	0.7587
System 3 Unet++ Decoder	**0.7182**	**0.7039**	**0.6351**	**0.7945**
System 3 DeepLabV3+ Decoder	0.6986	0.6833	0.6063	0.7844

DeepLabV3+ and Unet++ decoders are compared because the first one was used in [5]. From the IoU score, it is obvious that Unet++ outperforms the DeepLabV3+ decoder for all systems, which is logical because the model can benefit from lots of skip connections in Unet++ architecture. Bootstrapped cross-entropy [31] loss was also tested in this work, but the results were worse than the proposed loss setup. Comparing different systems, the proposed System 3 outperforms all other systems by all quality metrics and with all proposed decoders. It is essential to pay attention to Mean IoU, and Q_1 IoU : we can see that the interactive approach introduces more than 0.3 improvements in mean score and a bit less than 0.5 improvement in Q_1 score, which is a huge increase in quality.

Next, we can observe IoU scores distribution for System 1 Unet++ Decoder, System 2 Unet++ Decoder, and System 3 Unet++ Decoder in Fig. 6.
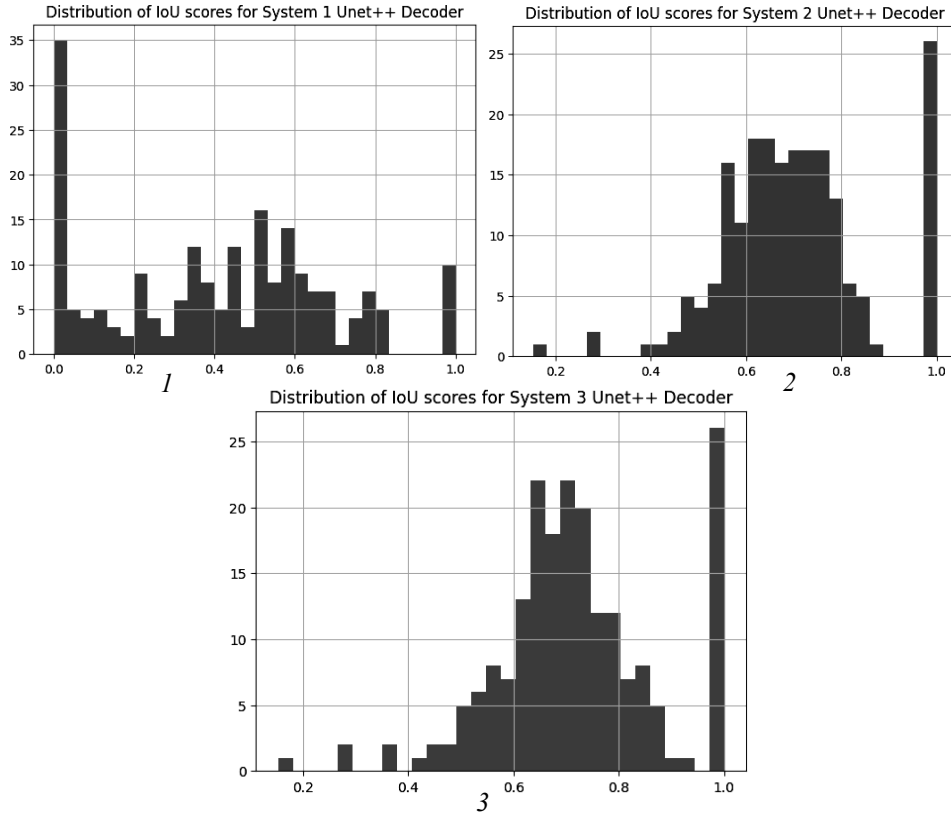
Fig. 6. IoU scores distribution for Systems 1, 2, and 3 with Unet++ decoder

Obtained results show fewer scans segmented with very poor scores and many more scans segmented with nearly ideal scores.

Visual results of segmentation can be seen in Figs. 7, 8.

According to visual results, the model correctly reacts to positive and negative clicks. Additionally, the model does not remove the correct segmentation if negative clicks are placed near correctly segmented regions. However, there is still space for improvement. As we can see from Fig. 7, the model is pretty conservative in segmenting additional areas after a positive click for some scans.

Feedback Score (equation (2)) is outlined only for interactive systems (second and third) in Table 2.

T a b l e 2. Number of all feedback types and resulting Feedback Score

System and Decoder	Number of Positive Clicks ↓	Number of Negative Clicks ↓	Number of Masks Erasements ↓	Feedback Score ↓
System 2 Unet++ Decoder	3024	**0**	**0**	3024
System 2 DeepLabV3+ Decoder	3024	**0**	**0**	3024
System 3 Unet++ Decoder	**1637**	284	1384	**2916.4**
System 3 DeepLabV3+ Decoder	1730	248	1344	2948.8

From Table 2: System 2 requires only positive clicks because there is no initial mask approximation, while System 3 requires correction of initial results, so it has all types of feedback. Considering weighting coefficients from equation (2), we see that System 3 again outperforms System 2 with all decoders.
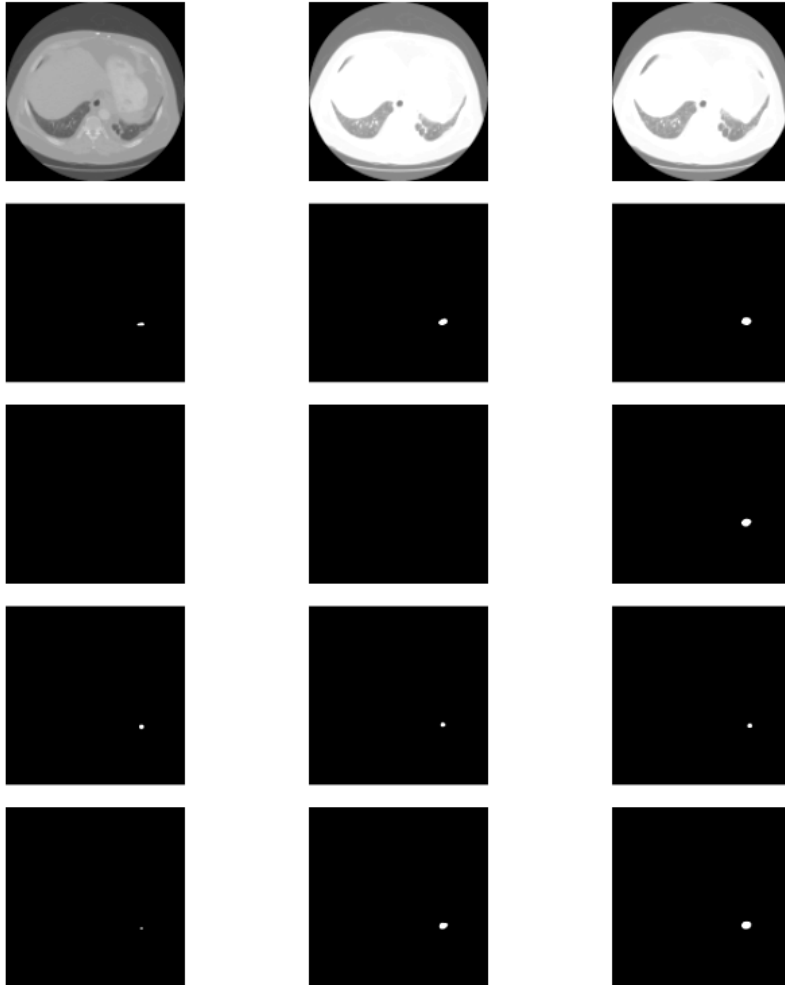
Fig. 7. Results of segmentation from Sytem 3 Decoder Unet++. First row — original scans. Second row — annotation. Third row — initial masks from H. Fourth row — positive clicks. Fifth row — corrected masks with H_I

Considering both quality and feedback criteria, we can conclude that System 3 with Unet++ decoder is a rational choice for the lung cancer segmentation task.

Finally, let's investigate the systems' performance on more interactive feedback iterations in Fig. 9.

From the received plots, System 2 outperforms System 3 in mean IoU only from the third feedback iteration while still losing in feedback score. These results are logical because System 2 always relies on expert feedback, while System 3 has initial mask approximation, which is not conditioned on feedback. On the other hand, there is still an issue with the "ideal" behavior for users' feedback simulation, and this issue will be addressed in future works.
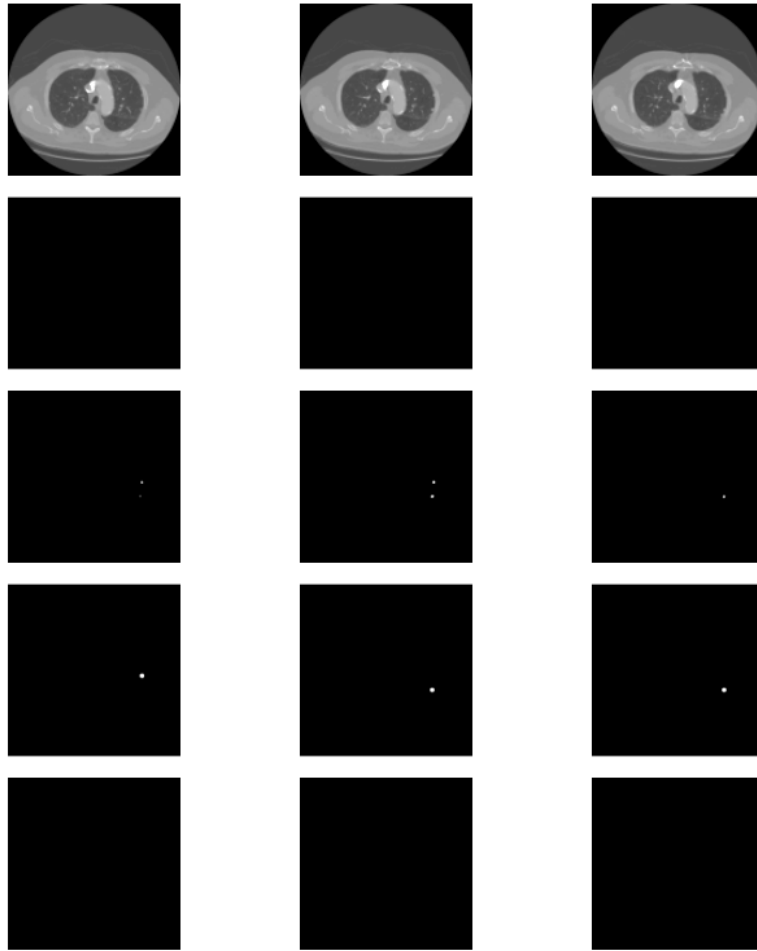
Fig. 8. Results of segmentation from Sytem 3 Decoder Unet++. First row — original scans. Second row — annotation. Third row — initial masks from H. Fourth row — negative clicks. Fifth row — corrected masks with H_I
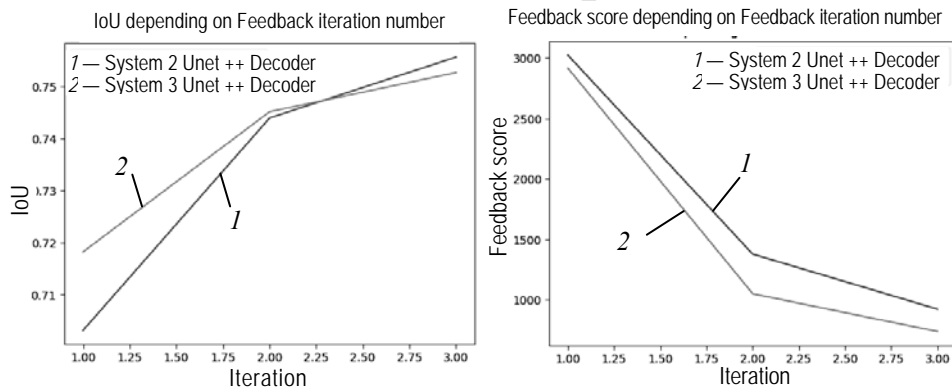
Fig. 9. Mean IoU and Feedback Score depending on feedback iteration number for Systems 2 and 3 with Unet++ Decoder

CONCLUSIONS

This paper has studied different IDSS for lung cancer segmentation, proposed evaluation criteria, and the algorithm for users' feedback simulation. Finally, a

system that outperforms previous approaches by all criteria is proposed. However, it may have less quality increase with feedback iterations compared to previous systems. This issue will be addressed in future works. It is important to mention that the proposed system is a combination of 2 other systems, so it is possible that there is a huge room for improvement. Another issue that requires further research is the users' feedback simulation algorithm. Its behavior is too "ideal," and there should be randomness conditioned on previous mask approximation results.

REFERENCES

1. R.T. Sutton, D. Pincock, D.C. Baumgart, D.C. Sadowski, R.N. Fedorak, and K.I. Kroeker, "An overview of clinical decision support systems: benefits, risks, and strategies for success," *NPJ Digit. Med.*, pp. 3–17, 2020 Feb 6. doi: 10.1038/s41746-020-0221-y.

2. E. Walling, C. Vaneeckhaute, "Developing successful environmental decision support systems: Challenges and best practices," *Journal of Environmental Management*, 264, 110513, 2020. doi: 10.1016/j.jenvman.2020.110513.

3. M. Rashidi, M. Ghodrat, B. Samali, and M. Mohammadi, "Decision Support Systems," *Management of Information Systems*, 2018. doi: 10.5772/intechopen.79390.

4. N. Shahid, T. Rappon, and W. Berta, "Applications of artificial neural networks in health care organizational decision-making: A scoping review," *PLOS ONE*, 14(2), e0212356, 2019. doi: 10.1371/journal.pone.0212356.

5. S. Mahadevan, P. Voigtlaender, and B. Leibe, "Iteratively Trained Interactive Segmentation," *ArXiv*, 2018. Available: /abs/1805.04398

6. M.Z. Zghurovskyi, N.D. Pankratova, *Systems Analysis: Problems, Methodology, Applications*. K.: Naukova dumka, 2005.

7. S. Walsh et al., "Decision Support Systems in Oncology," *JCO Clinical Cancer Informatics*, vol. 3, pp. 1–9, 2019. doi: 10.1200/CCI.18.00001.

8. G. Yu, Z. Chen, J. Wu, and Y. Tan, "Medical decision support system for cancer treatment in precision medicine in developing countries," *Expert Systems with Applications*, 186, 115725, 2021. doi: 10.1016/j.eswa.2021.115725.

9. T. Mukherjee, O. Pournik, S.N. Lim Choi Keung, and T.N. Arvanitis, "Clinical Decision Support Systems for Brain Tumour Diagnosis and Prognosis: A Systematic Review," *Cancers 2023*, 15(13), 3523. doi: 10.3390/cancers15133523.

10. B.V. Chapaliuk, Y.P. Zaychenko, "Medical image segmentation methods overview," *System Research and Information Technologies*, no. 1, pp. 72–81, 2018. doi: 10.20535/SRIT.2308-8893.2018.1.05.

11. O. Ronneberger, P. Fischer, and T. Brox, "U-Net: Convolutional Networks for Biomedical Image Segmentation," *ArXiv*, 2015. Available: /abs/1505.04597

12. T. Lin, P. Dollár, R. Girshick, K. He, B. Hariharan, and S. Belongie, "Feature Pyramid Networks for Object Detection," *ArXiv*, 2016. Available: /abs/1612.03144

13. L. Chen, G. Papandreou, I. Kokkinos, K. Murphy, and A.L. Yuille, "DeepLab: Semantic Image Segmentation with Deep Convolutional Nets, Atrous Convolution, and Fully Connected CRFs," *ArXiv*, 2016. Available: /abs/1606.00915

14. Z. Zhou, M.M. Siddiquee, N. Tajbakhsh, and J. Liang, "UNet++: A Nested U-Net Architecture for Medical Image Segmentation," *ArXiv*, 2018. Available: /abs/1807.10165

15. H. Huang et al., "UNet 3+: A Full-Scale Connected UNet for Medical Image Segmentation," *ArXiv*, 2020. Available: /abs/2004.08790

16. A. Hatamizadeh et al., "UNETR: Transformers for 3D Medical Image Segmentation," *ArXiv*, 2021. Available: /abs/2103.10504

17. Y. Zaychenko, G. Hamidov, and B. Chapaliuk, *The Application of CNN and Hybrid Networks in Medical Images Processing and Cancer Classification*. Cambridge Scholars Publishing, 2023.

18. A. Kirillov et al., "Segment Anything," *ArXiv,* 2023. Available: /abs/2304.02643

19. T. Sakinis et al., "Interactive segmentation of medical images through fully convolutional neural networks," *ArXiv*, 2019. Available: /abs/1903.08205

20. M. Carbonneau, V. Cheplygina, E. Granger, and G. Gagnon, "Multiple Instance Learning: A Survey of Problem Characteristics and Applications," *Pattern Recognition*, 2016. doi: 10.1016/j.patcog.2017.10.009.
21. M. Tan, Q.V. Le, "EfficientNet: Rethinking Model Scaling for Convolutional Neural Networks," *ArXiv*, 2019. Available: /abs/1905.11946
22. L. Chen, Y. Zhu, G. Papandreou, F. Schroff, and H. Adam, "Encoder-Decoder with Atrous Separable Convolution for Semantic Image Segmentation," *ArXiv, 2018*. Available: /abs/1802.02611
23. D.P. Kingma, J. Ba, "Adam: A Method for Stochastic Optimization," *ArXiv*, 2014. Available: /abs/1412.6980
24. S. Li et al., "PyTorch Distributed: Experiences on Accelerating Data Parallel Training," *ArXiv*, 2020. Available: /abs/2006.15704
25. J. Bertels et al., "Optimizing the Dice Score and Jaccard Index for Medical Image Segmentation: Theory & Practice," *Medical Image Computing and Computer Assisted Intervention – MICCAI 2019*. doi: https://doi.org/10.1007/978-3-030-32245-8_11
26. Q. Xie, M. Luong, E. Hovy, and Q.V. Le, "Self-training with Noisy Student improves ImageNet classification," *ArXiv*, 2019. Available: /abs/1911.04252
27. M. Kimura, "Understanding Test-Time Augmentation," in *Neural Information Processing. ICONIP 2021. Lecture Notes in Computer Science*, vol. 13108. Springer, Cham, 2021. doi: https://doi.org/10.1007/978-3-030-92185-9_46
28. S.G. Armato III et al., "Data From LIDC-IDRI [Data set]," *The Cancer Imaging Archive*, 2015. doi: http://10.0.31.1/K9/TCIA.2015.LO9QL9SX
29. Matthew C. Hancock, Jerry F. Magnan, "Lung nodule malignancy classification using only radiologist quantified image features as inputs to statistical learning algorithms: probing the Lung Image Database Consortium dataset with two statistical learning methods," *Journal of Medical Imaging*, 3(4), 044504, 8 December 2016. doi: https://doi.org/10.1117/1.JMI.3.4.044504
30. H. Rezatofighi, N. Tsoi, J. Gwak, A. Sadeghian, I. Reid, and S. Savarese, "Generalized Intersection over Union: A Metric and A Loss for Bounding Box Regression," *ArXiv*, 2019. Available: /abs/1902.09630
31. Z. Wu, C. Shen, and A. van den Hengel, "Bridging category-level and instance-level semantic image segmentation," *arXiv preprint*, 2016. Available: https://doi.org/10.48550/arXiv.1605.06885

INFORMATION ON THE ARTICLE

Volodymyr S. Sydorskyi, ORCID: 0000-0001-9697-7403, National Technical University of Ukraine "Igor Sikorsky Kyiv Polytechnic Institute", Ukraine, e-mail: volodymyr.sydorskyi@gmail.com

ІНТЕРАКТИВНА СИСТЕМА ПІДТРИМАННЯ ПРИЙНЯТТЯ РІШЕНЬ ДЛЯ СЕГМЕНТАЦІЇ РАКУ ЛЕГЕНІВ / В.С. Сидорський

Анотація. Досліджено клінічні інтелектуальні системи підтримання прийняття рішень (ІСППР) для сегментації раку легень, які базуються на глибинних нейронних мережах. Запропоновано нову інтерактивну ІСППР і порівняно її з попередніми підходами. Обговорено проблему невизначеності цілей під час створення інтерактивних систем і запропоновано критерії для оцінювання якості та кількості зворотного зв'язку від експерта. Для автоматизації оцінювання системи використано спеціальний алгоритм для симуляції зворотного зв'язку експерта. Запропонована інтерактивна ІСППР перевершила попередні підходи (як інтерактивні, так і неінтерактивні) у завданні сегментації раку легень. Цей підхід перспективний як щодо якості, так і зручності використання експертом. Водночас обговорено низку можливих модифікацій, які можна виконати для покращення як критеріїв оцінювання, так і запропонованої ІСППР у майбутніх працях.

Ключові слова: клінічні системи підтримання прийняття рішень, глибинне навчання, відкрита система, інтерактивна сегментація.

AN IMPROVED APPROACH TO ORGANISING MOBILE EDGE COMPUTING IN A 5G NETWORK

A. ASTRAKHANTSEV, L. GLOBA, O. FEDOROV, D. DEGTIAROV, Y. ROMANKO, K. ROMANII

Abstract. Mobile edge computing is an important element in ensuring the efficiency of the 5G network as a whole, as it enables data storage and computing at the network edge. Existing solutions do not fully address the issues of load distribution between computing nodes, and most solutions do not offer methods for verifying computations and controlling errors. Accordingly, this paper aims to develop an approach to the organization of mobile edge computing in a 5G mobile network that would authenticate distribution servers and computing nodes, manage the process of distributing computing nodes, have a procedure for verifying the correctness of calculations, and take into account the parameters of computing nodes during distribution. To achieve this goal, we propose to use the developed method. The method of load balancing and selection of computing nodes for edge computing via 5G allows for identifying available nodes and distributing computing blocks among them. It also provides mutual authentication of elements and includes a method of data verification and error detection for the MEC system. The provided solution allows for controlling errors during calculations and protecting the server from incorrect data. These methods are optimized according to minimum network resources and computing time criteria. These improvements increase the efficiency of mobile edge computing in a 5G network.

Keywords: 5G network, mobile edge computing, task allocation scheme, call flow, load balancing, task verification.

INTRODUCTION

The new 5G cellular networks are expected to face a sharp increase in mobile traffic and IoT user demands due to the massive growth in the number of mobile devices and the emergence of new computing applications. Running resource-intensive computing applications on resource-constrained mobile devices has recently become a major challenge, given the stringent requirements for computing time and the limited storage capacity of the devices.

Cloud computing allows you to store and process data on remote servers. A large number of different applications that generate an ever-increasing amount of data, which significantly increases network latency, uses them and places differentiated demands on data security and manageability. Mobile Edge Computing (MEC) technology can help prevent these problems from getting worse.

Mobile edge computing has recently emerged as a key technology to overcome these challenges, as it enables the provision of cloud computing services such as data storage and computing at the edge of the network. MECs have the potential to run computationally intensive applications such as augmented and virtual reality [1]. MEC is also an important component of the Internet of Things (IoT), as it allows to reduce the power consumption of mobile devices.

Mobile edge computing is a data management technology that involves storing and processing data close to the source. This allows for faster response to real-time computing needs and helps to guarantee the availability of information. In general, MEC is a decentralized computing infrastructure in which some signal processing, storage, management and computing applications are distributed in the most efficient and logical way between the data source and the cloud [2]. Mobile edge computing extends the concept of cloud computing by bringing the benefits of the cloud closer to users in the form of the network edge, which provides lower end-to-end latency.

The goal of the presented work is to organize mobile edge computing in a 5G network by performing authentication of distribution servers and computing nodes. It is also necessary to ensure the management of the process of distributing computing units, including the procedure for checking the correctness of calculations and taking into account the parameters of computing nodes during distribution.

In this regard, the following tasks were solved within the framework of an improved approach to the organization of mobile edge computing in the 5G network:

- Development of a method for load balancing and selection of computing nodes for MEC. The implementation of this method should not require additional physical elements in the network.

- Developing a method for data verification and error detection, as a computing node may report incorrect calculation results.

- Determining a method of mutual authentication for different types of equipment in the 5G network for the process of mobile edge computing without the use of a trusted third party.

At the same time, there are currently no existing technical solutions that would solve all of the above problems.

ANALYSIS OF EXISTING SOLUTIONS FOR MEC IN THE 5G NETWORK

The problems that arise when organizing mobile edge computing covered in a large number of publications. For example, [3] describes a typical MEC architecture and its main elements, as well as the problems associated with the distribution of computing tasks. Paper [4] focuses on the problems of transmission delay and computation delay with a large number of IoT devices. It also analyses the possibility of overloading peripheral clouds due to the spatially heterogeneous distribution of IoT tasks. To address these issues, it use game-theoretic methods to investigate load balancing problems to minimize transmission and computation delays in the task distribution process, given the limited bandwidth and computing resources in the edge clouds.

Work [5] solves a more complex problem of parallel offloading and load balancing with several shared MEC servers and delay-sensitive load. A similar

problem is solved in [6], but it proposes a two-level model of task distribution with delay minimization and computational cost estimation. In [5], a long-term stochastic programming problem with an average system cost is formulated under the conditions of stability of the battery level and delay constraints.

Another work by the same authors [7] partially solves one of the problems studied in proposed research — it helps to create a secure reward mechanism using blockchain technology that can help to balance the load between computing nodes.

Some works [8] propose to solve the problem of clustering and load balancing based on the charge level of computing nodes and geolocation tags.

In addition to the solutions that solve the problem of load distribution between the computing nodes of the MEC and which are presented in the above publications, it is necessary analyzing patented solutions separately. For example, patent [9] proposes a cloud platform with a pool of resources that connects to the main network via a transmission network. This solution requires a special distribution hub (RRH). In this article, to eliminate this drawback, it is proposed to use a flat structure divided into zones and use the base station as an arbiter (no additional equipment is required).

Patent [10] proposes a solution based on the availability of a map that stores information about the location, computing power and available storage of each of the computing nodes. The disadvantage of the solution is the need for a dynamically updated map with a list of nodes. This disadvantage can be overcome by using a broadcast of the request from the MEC server. In this case, the response of the base station to the computing nodes allows not to use the map, route table or database — saving network resources.

The patent [11] is devoted to determining the optimal number of required physical resource blocks during distribution, while the procedure for selecting computing nodes is not described. In [12], the distribution of computing tasks and resources is based on reducing the failure rate during handover, but the procedure for allocating network resources is also not described and there is no data verification and error control. The solution [13] offers a centralized implementation of edge computing, where a central computer or a cloud macro base station will perform the main distribution tasks. This requires additional costs. In addition, this solution uses only delay as a distribution criterion. The patent [14] also requires a hierarchical structure and does not provide for the identification and authentication of computing nodes. In addition, this solution lacks data verification and error control.

The patent [15] describes only the process of creating a session for mobile edge computing, does not provide solution for data verification and error control, and does not describe procedures for load balancing and selection of computing nodes.

Solutions [16; 17] do not provide for security measures (no identification and authentication). In addition, in both cases, a central database is required. In [18], it is described how a computing node should be rewarded for a completed operation, but the data verification procedure is not described and there is no support for the 5G network, as well as no secure channel for transferring rewards.

To summarize, most solutions for selecting computing nodes and load balancing use additional physical elements, which requires additional costs. The con-

sidered technical solutions require dynamically updated maps or databases, which requires additional network resources and increases the load on the network. In addition, many of these publications lack authentication procedures for participants.

PROBLEM STATEMENT

Let us identify the main participants in the process of distributed mobile edge computing (Table) and their functions according to the approach proposed in this paper. A similar list of process participants, but with a different set of functions, is given in [3; 19; 20].

Main participants in the process of distributed edge computing

Participant marking	Participant functions and components
MEC MEC Server	MEC Server: gather data flow from one/multiple sensors; has 5G supported radio module; run MEC supported application; has identity and billing entity.
Computing Node	Computing Node: process MEC Server Application Programming Interface (API) call; has 5G supported radio module; has CPU that support operability of MEC framework; has identity and billing entity.
Base station (Cell)	Cell: assign radio resource, verify identity, sign transaction, secure connection; support computing unit selection; support peer-to-peer communication; secure and sign transaction MEC Server → Computing node;

The solution of the tasks set in this paper done by simulation and mathematical modelling for the architecture shown in Table, taking into account the shortcomings of existing solutions discussed in the previous section. In order to prepare the proposed technical solution, a set of input data, a set of constraints, dependencies between them, and a set of output values were determined. Let us consider them in more detail.

Let the following data received at the input of the load balancing system for distributed boundary computing:

n — a set of computing nodes available to the MEC with computing capacities r_i and an initial level of trust d_i;

d_i — initial level of trust in the computing node;

$p(x_i)$ — the probability of an error during calculations by the i-th node;

T_p — time for the distribution of computing tasks;

Res — the amount of network resources involved in the distribution of tasks;

T_o — the expected calculation time;

T_{def} — the restriction for the expected calculation time;

V — the amount of calculations to be performed.

When distributing computational tasks for execution, it is necessary to ensure the minimum probability of calculation error $p(n)$ and minimize the network resources used during their distribution and processing in computing nodes: $(\text{Res} \rightarrow \min)$, subject to restrictions on the expected computing time $(T_o \leq T_{\text{def}})$. A weighted average used to determine the probability of a calculation error:

$$p(n) = \frac{1}{n} \sum_i^n p(x_i).$$

As a result, the proposed method should provide:

$y \in n(0, n)$ — a set of devices that perform the calculation of distributed computing with load balancing based on capacity r_i;

$w \in n(0, n - y)$ — a setoff additional devices that will provide redundancy and reliability of distributed computing;

Δd_i — change in the level of trust in the i-th node based on the results of its work.

The expected calculation time will consist directly of the calculation time and the time for distributing the calculation tasks defined as:

$$T_o = \frac{V}{nr} + T_p,$$

or considering the set of devices that perform the calculation and the set of additional devices:

$$T_o = \frac{V}{\sum_i^y (y_i\, r_i) + \sum_i^w (w_i\, r_i)} + T_p.$$

In this paper, we propose a method for organizing distributed computing that performs the following steps:

- a broadcast request from the MEC server to perform distributed computing;
- a response from at least one computing node to the base station containing a set of parameters (request ID, timestamp, etc.);
- the base station checks the available resources and provides network parameters for the MEC session of at least one computing node, which will allow for further point-to-point connection;
- the MEC server can verify the results of the calculations by means of data validation, mirroring and control code.

The essence of the method described above showed in Figs. 1, 2.
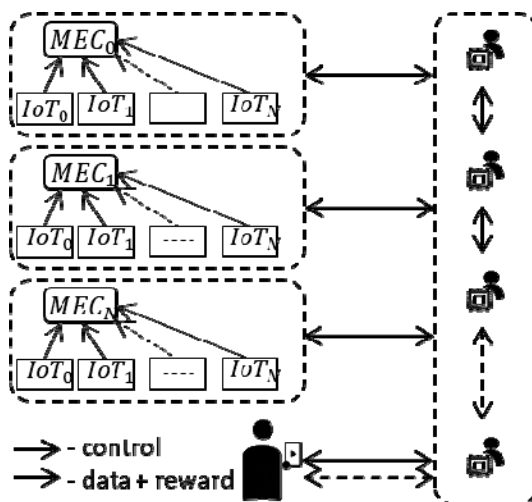
Fig. 1. Visualization of the principle of the proposed method

The proposed approach is based on two new methods:

• a method of load balancing and selection of computing nodes for edge computing via 5G, which allows to identify available nodes and distribute computing blocks among them, as well as provide mutual authentication of elements;

• a method of data verification and error detection for the MEC system, which allows to control the occurrence of errors during calculations, protect the server from incorrect data, and prioritize and reward nodes based on the results of the calculations performed.

Let us consider the principle of the proposed methods in more detail.

METHOD OF LOAD BALANCING AND SELECTION OF COMPUTING NODES IN A 5G NETWORK

The principle of the load balancing method includes two stages: 1) the authentication stage and 2) the point-to-point channel establishment and the computation and verification stage.

The first stage of authentication and channel creation (Fig. 2) involves the following steps:
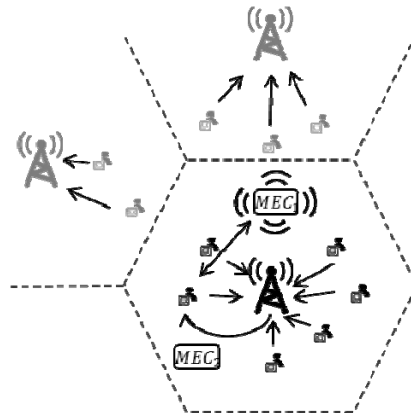
Fig. 2. The sequence of actions at the first stage of distributed computing — authentication and channel creation

1. The MEC server broadcasts a request to perform calculations with the following information:

• MEC identifier (temporary or permanent identifier);

• type of calculation.

2. Each computing node upon receiving paging device, reply to base station (cell) with:

$$E = F(C_{id}, T_{last}, E_{id}),$$

where (C_{id}) — identifier of the serving cell (base station); (T_{last}) — the time-stamp of the last received slot for performing calculations; (E_{id}) — network identifier (temporary or permanent).

3. The base station selects computing nodes and assigns a radio channel:

• selects a computing node based on the received values of E;

• assigns a radio channel based on available resources;

- notifies the MEC server and the computing node of the established information exchange channel.

The second stage, where calculations and their verification are performed, includes the following steps (Fig. 3):
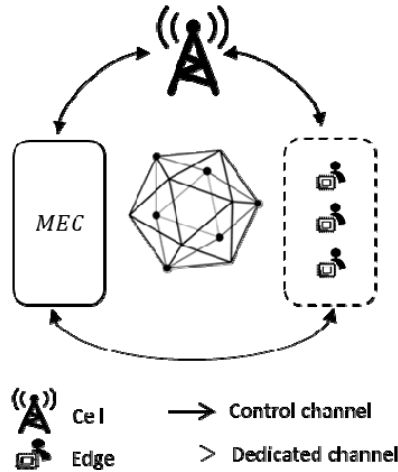
Fig. 3. The sequence of actions at the second stage of distributed computing — performing calculations and verifying results

1. The MEC server and the computing node establish a radio channel. The radio channel is formed based on the channel configuration parameters that each participant receives from the base station.

2. The MEC server and the computing node then perform a synchronization procedure.

3. Based on ETSI, the computing node makes an API call (Fig. 4) and sends a report to the base station after the computation is complete.
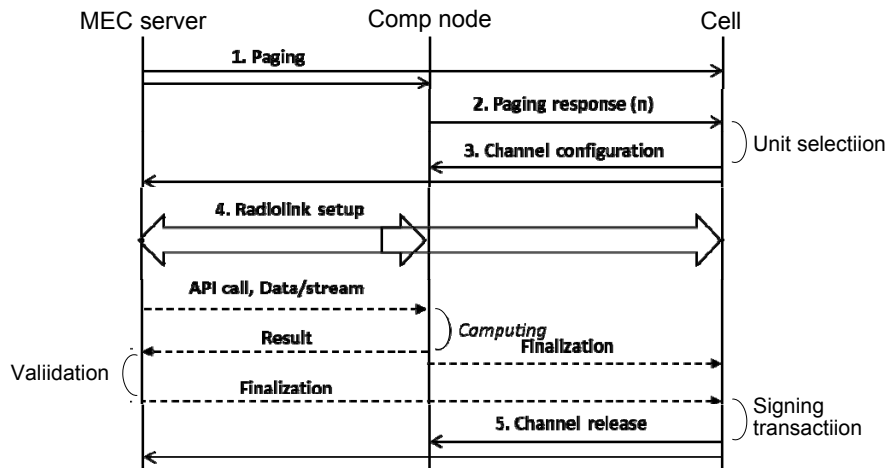
Fig. 4. The sequence of actions during an API call at the second stage

4. After verifying the result, the MEC server reports to the base station.

5. The reward for performing computations is calculated based on the complexity of the operation, execution time, and the amount of disk space consumed. To provide the compulsoriness of the workflow a blockchain technology is used. The participants are rewarded proportionally their fitness/ activities.

As mentioned above, during the second stage, the MEC server must check the calculations for correctness and errors, and assign a certain level of trust to each computing node. These procedures provided in the proposed method of data verification and error detection for the MEC system.

DATA VALIDATION AND ERROR FOUNDING METHOD FOR MEC SYSTEM

Each task that will be processed on the MEC server contains parts that can be performed independently. These parts are added to the task by software developers in the form of an API call. The results of such external computations carry the risks of computational errors and various types of attacks. In this paper, we propose a combined system for verifying the results of work, which includes the analysis of confidence levels and redundancy.

The proposed method for verifying the results of calculations and finding errors includes the following steps:

1. The computing device of the MEC server generates an error control code in the form of a set of low-computing level functions.

The control code (Fig. 5) is an automatically created task with the same complexity, format and length of input data as the real task, with the only difference being that the MEC server knows the exact result, so it can be checked.

2. The MEC server distributes tasks between the MEC computing nodes with additional redundancy.

Redundancy (Fig. 6) additionally helps to avoid mistakes in computing even on trusted devices. MEC server will apply calculation results and grant rewards only after at least 51% current network nodes will present the same results.

3. The MEC server updates its trust level after the task is successfully completed (Fig. 7).

Fig. 5. Using a control code to check the correctness of calculations
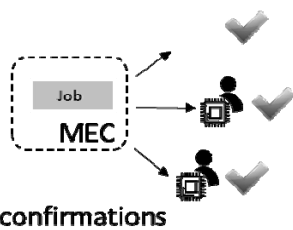
Fig 6. Use of additional redundancy to protect calculations from errors
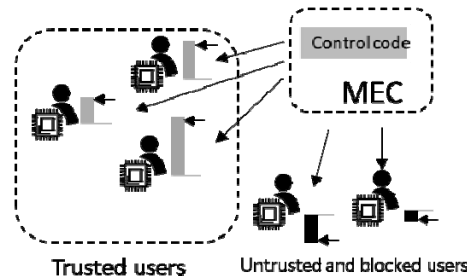
Fig. 7. Using the trust level to select computing nodes

Each MEC server has its own "trust level", depended on the control code execution and the results of previously completed tasks. If the results of the check code execution are correct, the trust level (Fig. 7) for this computing node increases. Otherwise, if the device calculates the check code with errors, the level of trust decreases until the node is completely blocked.

ADVANTAGES OF THE PROPOSED APPROACH

The benefits of the proposed approach consist of two parts: the benefits to the user and the benefits to the mobile operator. For the user, the proposed approach provides:

- *Ease of setup:* common network identifiers (e.g. IMSI) or blockchain wallet number can be used as the user's device identifier.
- *Mobility*: MEC calculation can be done without bidding for mobile phones/locations.
- *High level of security*: The transaction is signed using blockchain technology. Mutual authentication allows verifying MEC server.
- *High reliability*: Data verification, mirroring and check code are used to protect against fraud and detect errors.
- Network operator benefits:
- *Network resource economy* (compare to existing solutions [9–18])*:* Dynamic map with node list (or another database / route table) does not need.
- *Low cost* (compare to existing solutions [9–18])*:* no additional hardware is required; a software upgrade can resolve this problem.
- *Easy UE selection and MEC load balancing:* base station make a decision based on the set of computing requirements.
- *Increasing Spectral Efficiency:* peer-to-peer communication release high load on cellular network.

CONCLUSION

The proposed approach for distributed edge computing in 5G allows identifying and authenticating MEC participants, allocating additional resources for MEC from the mobile network, including preparing point-to-point communications. The method also assigns computing nodes and balances the load of edge computing by modifying the messaging protocol between the base station and mobile devices.

The originality of the proposed approach is provided by two methods that are further improvements to the methods of load balancing, selection of computing nodes for edge computing in a 5G network, data verification and error detection for the MEC system. These methods are optimized according to the criteria of minimum network resources usage and have a time constraint.

The proposed approach allows the MEC server to verify the results of calculations and distribute data for computation according to the capacity of the computing nodes.

Implementation of this approach allows the service provider to save network resources and low cost of deployment. It also provides easy load balancing between computing nodes. This approach is more convenient for the user, as it does not require the creation of additional identifiers and provides a high level of security through the introduction of mutual authentication.

REFERENCES

1. F. Vhora, J. Gandhi, "A Comprehensive Survey on Mobile Edge Computing: Challenges, Tools, Applications," *2020 Fourth International Conference on Computing*

Methodologies and Communication (ICCMC), Erode, India, 2020, pp. 49–55. doi: 10.1109/ICCMC48092.2020.ICCMC-0009

2. S.S.D. Ali, H. Ping Zhao, and H. Kim, "Mobile Edge Computing: A Promising Paradigm for Future Communication Systems," *TENCON 2018 - 2018 IEEE Region 10 Conference, Jeju, Korea (South), 2018*, pp. 1183–1187. doi: 10.1109/TENCON.2018.8650169

3. L.A. Haibeh, M.C.E. Yagoub, and A. Jarray, "A Survey on Mobile Edge Computing Infrastructure: Design, Resource Management, and Optimization Approaches," in *IEEE Access*, vol. 10, pp. 27591–27610, 2022. doi: 10.1109/ACCESS.2022.3152787

4. D. Liu, A. Hafid, and L. Khoukhi, "Workload Balancing in Mobile Edge Computing for Internet of Things: A Population Game Approach," in *IEEE Transactions on Network Science and Engineering*, vol. 9, no. 3, pp. 1726–1739, 1 May-June 2022. doi: 10.1109/TNSE.2022.3150755

5. W. Zhang, G. Zhang, and S. Mao, "Joint Parallel Offloading and Load Balancing for Cooperative-MEC Systems With Delay Constraints," in *IEEE Transactions on Vehicular Technology*, vol. 71, no. 4, pp. 4249–4263, April 2022. doi: 10.1109/TVT.2022.3143425

6. J. Ren et al., "An Efficient Two-Layer Task Offloading Scheme for MEC System with Multiple Services Providers," *IEEE INFOCOM 2022 - IEEE Conference on Computer Communications, London, United Kingdom, 2022*, pp. 1519–1528. doi: 10.1109/INFOCOM48880.2022.9796843

7. W. Zhang, W. Fan, G. Zhang, and S. Mao, "Learning-based joint service caching and load balancing for MEC blockchain networks," in *China Communications*, vol. 20, no. 1, pp. 125–139, Jan. 2023. doi: 10.23919/JCC.2023.01.011

8. H. Wu, L. Chen, C. Shen, W. Wen, and J. Xu, "Online Geographical Load Balancing for Energy-Harvesting Mobile Edge Computing," *2018 IEEE International Conference on Communications (ICC), Kansas City, MO, USA, 2018*, pp. 1–6. doi: 10.1109/ICC.2018.8422299

9. "The Radio Access Network and its resource allocation method calculated based on mixing fog," Patent App. CN108243245A, 2020.

10. Debashish Purkayastha, Xavier De Foy, Robert G. Gazda, "Systems and methods to create slices at a cell edge to provide computing services," Patent App. WO2018089417A1.

11. "Resource allocation methods based on mobile edge calculations," Patent App. CN109041130A, 2021.

12. "A kind of data distribution method based on MEC auxiliary in 5G networks," Patent App. CN108174421A, 2020.

13. "A kind of edge calculations method for 5G super-intensive networking scenes," Patent App. CN107333267A, 2019.

14. "A kind of 5G method of mobile communication and system based on MEC and layering SDN," Patent App. CN107404733A, 2020.

15. John Juha Antero Rasanen, Pekka Kuure, "Method and apparatus for implementing mobile edge application session connectivity and mobility," US Patent App. US16/072,901 (US 2019/0045409 A1).

16. Mehran Moshfeghi, "System and method for discount deal referral and reward sharing," US Patent App. US13/484,261 (US20120316939A1).

17. Willem Jacobus van Niekerk, Marc van Niekerk, Brendon van Niekerk, Ernst Kleinhans, "Method and system for online redistribution of data and rewards," US Patent App. US15/464,934 (US20170255981A1).

18. Dennis Detwiller, Robert Sparks, "Rewarding Users for Sharing Digital Content," US Patent App. US13/106,716 (US20120290308A1).

19. Pavel Mach, Zdenek Becvar, *Mobile Edge Computing: A Survey on Architecture and Computation Offloading*. Available: https://arxiv.org/abs/1702.05309

20. Q.V. Pham et al., "A Survey of Multi-Access Edge Computing in 5G and Beyond: Fundamentals, Technology Integration, and State-of-the-Art," *IEEE Access*, 2020. doi: https://doi.org/10.1109/ACCESS.2020.3001277

INFORMATION ON THE ARTICLE

Andrii A. Astrakhantsev, ORCID: 0000-0002-6664-3653, National Technical University of Ukraine "Igor Sikorsky Kyiv Polytechnic Institute", Ukraine, e-mail: andrii.astrakhantsev@nure.ua

Larysa S. Globa, ORCID: 0000-0003-3231-3012, National Technical University of Ukraine "Igor Sikorsky Kyiv Polytechnic Institute", Ukraine, e-mail: lgloba@its.kpi.ua

Oleksandr V. Fedorov, National Technical University of Ukraine "Igor Sikorsky Kyiv Polytechnic Institute", Ukraine

Dmytro V. Degtiarov, National Technical University of Ukraine "Igor Sikorsky Kyiv Polytechnic Institute", Ukraine

Yevgen O. Romanko, Interregional Academy of Personnel Management, Ukraine

Kyrylo A. Romanii, National Technical University of Ukraine "Igor Sikorsky Kyiv Polytechnic Institute", Ukraine

УДОСКОНАЛЕНИЙ ПІДХІД ДО ОРГАНІЗАЦІЇ МОБІЛЬНИХ ПЕРИФЕРІЙНИХ ОБЧИСЛЕНЬ У МЕРЕЖІ 5G / А.А. Астраханцев, Л.С. Глоба, О.В. Федоров, Д.В. Дегтярьов, Є.О. Романко, К.А. Романій

Анотація. Мобільні периферійні обчислення є важливим елементом забезпечення ефективності мережі 5G в цілому, оскільки дозволяють зберігати дані та виконувати обчислення на периферії мережі. В існуючих технічних рішеннях для систем зв'язку не в повному обсязі вирішені питання розподілу навантаження між обчислювальними вузлами; у більшості таких рішень не пропонується метод балансування обчислювального навантаження з контролем помилок у децентралізованій обчислювальній інфраструктурі з динамічно змінюваним набором обчислювальних вузлів. Метою дослідження є розроблення підходу до організації мобільних периферійних обчислень у мобільній мережі 5G, який би виконував перевірку справжності серверів розподілу та обчислювальних вузлів, керував процесом розподілу обчислювальних блоків, мав процедуру перевірки коректності розрахунків та враховував параметри обчислювальних вузлів під час розподілу. Для досягнення мети пропонується застосувати метод балансування навантаження та вибору обчислювальних вузлів для периферійних обчислень в мережі 5G, який дозволяє визначити наявні вузли та здійснити розподіл обчислювальних блоків між ними, а також забезпечити взаємну автентифікацію елементів інфраструктури з перевіркою даних та пошуком помилок для системи МЕС, який дає змогу контролювати появу помилок під час обчислень, захищати сервер від некоректних даних. Указаний метод оптимізовано за критеріями мінімуму використовуваних ресурсів мережі і мінімального часу виконання обчислень. Такі вдосконалення дозволяють підвищити ефективність мобільних периферійних обчислень у 5G мережі.

Ключові слова: мережі 5G, мобільні периферійні обчислення, розподіл завдань, протокол обміну, балансування навантаженням, верифікація обчислень.

EXPANSION OF THE MATHEMATICAL APPARATUS OF DISCRETE-CONTINUOUS NETWORKS FOR THE AUTOMATION OF THEIR SYNTHESIS PROCEDURES

A.A. GURSKIY, A.V. DENISENKO, A.E. GONCHARENKO

Abstract. The paper deals with a model of an intelligent system related to the automatic synthesis of Petri nets and presents a certain stage of developing this model. The peculiarity of the extended mathematical apparatus is that it contains a combination of Petri net incidence matrices to represent various algorithms. This combination of matrices is part of the equations describing the logic control device of a complex system. Accordingly, the work also presents a well-known mathematical description of discrete-continuous systems with a controlled structure, which includes certain logical control devices. This mathematical description, based on means of discrete-continuous networks, is associated with the incidence matrix of the Petri net, which is formed as a result of a particular synthesis algorithm. At the same time, the formed Petri net represents the corresponding logical control algorithm that should ensure the effective functioning of the corresponding system. The final part of the work presents various structural schemes of logic-dynamic models of systems related to the automatic synthesis of Petri nets. Here, we determine the features of the advanced mathematical apparatus based on discrete-continuous networks to develop an intelligent system that forms logical control algorithms. It is also noted that such systems can be used to create certain control algorithms that ensure increased efficiency of the functioning of some objects in difficult and unpredictable conditions.

Keywords: Petri nets, system with controlled structure, discrete-continuous network, automatic synthesis of Petri nets.

INTRODUCTION

Petri nets, as an applied mathematical apparatus, are quite well-known in the field of modeling and analysis of discrete dynamic or logic-dynamic systems. Petri nets were first proposed by Carl Adam Petri in 1962 as part of his dissertation work – "Communication with automata". Petri's work became a significant contribution to the development of parallel and distributed computing. Such a concept as the automatic synthesis of Petri nets can be found in the work of James Peterson [1] as a direction related to the development of certain algorithms. At the same time, the development of methods for the automatic synthesis of Petri nets entails the need to expand the mathematical apparatus for describing complex systems, functioning algorithms that can be represented by Petri nets.

REVIEW OF DISCRETE-CONTINUOUS NETWORKS

Nowadays, Petri nets are greatly expanded. So, for example, there are many varieties of Petri nets, such as: time Petri nets, inhibitor Petri nets, colored Petri nets, hybrid Petri nets, and others [2; 3].

The history of the corresponding scientific direction and the corresponding scientific thought, starting with Carl Adam Petri, is quite long, so there is no need to consider separate stages of development or less important elements. But, in this case, it is necessary to note the invention of a discrete-continuous network [4]. Discrete continuous network (DC-net) proposed in 1990–1993, is essentially a synthesis of structural schemes of automatic control systems and Petri nets, which are not the usual extension such as, for example, hybrid Petri nets. DC-net is primarily a tool for describing, modeling and analyzing logic-dynamic systems and systems with a controlled structure.

The description and modeling of systems by means of discrete-continuous networks allows us to imagine a certain class of systems called discrete-continuous with a controlled structure (DCCS). In English-language publications, such systems are called hybrid systems, and both traditional Petri nets and their variants, in individual cases, hybrid Petri nets are used to study such systems [5; 6].

DC-nets, like Petri nets, is an applied mathematical apparatus and we extent it in order to develop the technique of automatic synthesis of Petri nets.

The development of models based on such an advanced mathematical apparatus will allow solving complex problems related to the development of certain algorithms. As an example, it is worth noting the so-called "smart ant" problem, which is presented in works [7; 8]. An ant builds an automaton of its behavior with the help of trial and error and mutations. Thus, assume that a model built with the use of DC-nets, can synthesize an automaton of its behavior or an algorithm of some logical control; then we advise to use such a model at the stage of automated development of control algorithms, control systems, or as a certain intelligent system [9].

So, it can be noted that in this case it is necessary to expand the mathematical apparatus while developing methods of automatic synthesis of Petri nets. The paper is relevant due to the development of certain systems that provide the synthesis of Petri nets with the use of modern intelligent technologies such as fuzzy logic, artificial neural networks, genetic algorithms, etc. [10; 11].

Purpose of work: The purpose of this work is to minimize time and automate the process of synthesis of some control algorithms of complex systems.

To achieve the goal, we expand the mathematical apparatus of discrete-continuous networks, taking into account the procedure of automatic synthesis of Petri nets.

MAIN PART

Description of the system with a controlled structure

Modeling tools of DC-nets allow to present a model of complex technical systems consisting of two parts: continuous-event part (CEP) and discrete-event part (DEP) in a structural unity. Such a system was called a system with a controlled structure (SCS). The continuous-event part of the model represents the control object with a controlled structure (COCS) and the DEP of DC-net represents the logical control device (LCD).

The COCS is represented by the state and output equations:

$$\dot{x}(t) = f(\Xi(t_k), x(t), u(t)); \tag{1}$$

$$y(t) = f(\Xi(t_k), x(t)), \tag{2}$$

where $u(t)$ is continuous control vector; $x(t)$ is state vector; $y(t)$ is output vector; $\Xi(t_k)$ is vector function for controlling the structure of COCS (functioning modes). Accordingly, in such a system it is possible to identify a generalized input effect:

$$U = (u(t), \Xi(t_k)).$$

The LCD is represented by a finite state machine (3),(4) characterized by the equations:

$$a_k = \lambda(a_{k-1}, \upsilon_k), \tag{3}$$

$$\beta_k = \gamma(a_k, \beta_k), \tag{4}$$

where $A = \{a_1, a_2, ..., a_k, ... a_i\}$ is a finite set of internal states, $\{\upsilon_1, \upsilon_2, ..., \upsilon_k, ..., \upsilon_j\}$ is an iput alphabet, $\{\beta_1, \beta_2, ..., \beta_k, ..., \beta_v\}$ is an output alphabet, λ is a transition function (from state to another state), γ is an output function.

The presented formal form of equations (1)–(4) is appropriate without taking into account the procedure for automatic synthesis of LCD control algorithm and, accordingly, the automatic generation of a Petri net during the operation of SCS.

Mathematical description of discrete-continuous systems with a controlled structure with the use of the DC-net

The mathematical description of a discrete-continuous system with a controlled structure, taking into account the means of DC-net, can be obtained from a set of equations.

Dynamics of COCS in continuous space $X(t,|t_k|)$ can be represented in matrix-differential form by the equation of state:

$$\dot{X}(t,|t_k|) = A_o \cdot \Xi_1(^d u_o(t_k)) \cdot X(t,|t_k|) + B_o \cdot \Xi_2(^d u_o(t_k)) \cdot u(t,|t_k|), \tag{5}$$

output equation

$$Y(t,|t_k|) = C_o \cdot \Xi_3(^d u_o(t_k)) \cdot X(t,|t_k|), \tag{6}$$

equation of state of the LCD

$$^d X_L(t_k) = {}^d X_L(t_{k-1}) + |A_L| \cdot {}^d v_L(t_k) + {}^d u_L(t_k) + {}^d w_L(t_k), \tag{7}$$

and the LCD output equation

$$^d Y_L(t_k) = \Lambda \cdot {}^d X_L(t_k), \tag{8}$$

where $X(t,|t_k|)$ is vector of continuous event state of COCS; $Y(t,|t_k|)$ is continuous event output vector; $u(t,|t_k|)$ is continuous exposure vector; $A_0 = \begin{vmatrix} A_1^0 & A_2^0 & ... & A_N^0 \end{vmatrix}$; $B_0 = \begin{vmatrix} B_1^0 & B_2^0 & ... & B_N^0 \end{vmatrix}$; $C_0 = \begin{vmatrix} C_1^0 & C_2^0 & ... & C_N^0 \end{vmatrix}$; $A_1^0, A_2^0 ... A_N^0$, $B_1^0, B_2^0 ... B_N^0$ and $C_1^0, C_2^0 ... C_N^0$ — matrices of states, controls and

outputs of different structural operating modes; $\Xi(^d u_o(t_k))$ — vector function for managing structural changes (functioning modes of SCS); $\Xi_1(^d u_o(t_k)) = \left| \xi_1^1 \quad \xi_2^1 \quad ... \quad \xi_N^1 \right|^{\mathrm{T}}$ and $\Xi_2(^d u_o(t_k)) = \left| \xi_1^2 \quad \xi_2^2 \quad ... \quad \xi_N^2 \right|^{\mathrm{T}}$ is vector-functions of structure control depending on the discrete state $X_0^d(t_k)$ continuous event part. They implement the selection of a specific structure from a variety of structures $\{\Sigma_i\}_{i=1}^N$ using matrix multiplication A_0, B_0, C_0. Vector function control $\Xi(^d u_o(t_k))$ is a matrix of dimension $n \times 1$, that contains only one non-zero element. The dimension of the control function vector is consistent with the dimension of the matrices A_0, B_0, C_0; $^d u_o(t_k)$ is a discrete component of the control influence on CEP, transferring the system from one structure to another; $^d w_L(t_k)$ is external control action; $^d X_L(t_k)$, $^d X_L(t_{k-1})$ — preliminary and subsequent discrete state (labeling) of the Petri net; $|A_L|$ is incidence matrix reflecting the relationship of elements in DC-net; $^d v_L(t_k)$ is control vector in DC-net. A simplified block diagram of the SCS, according to the given mathematical description, is presented in Fig. 1.
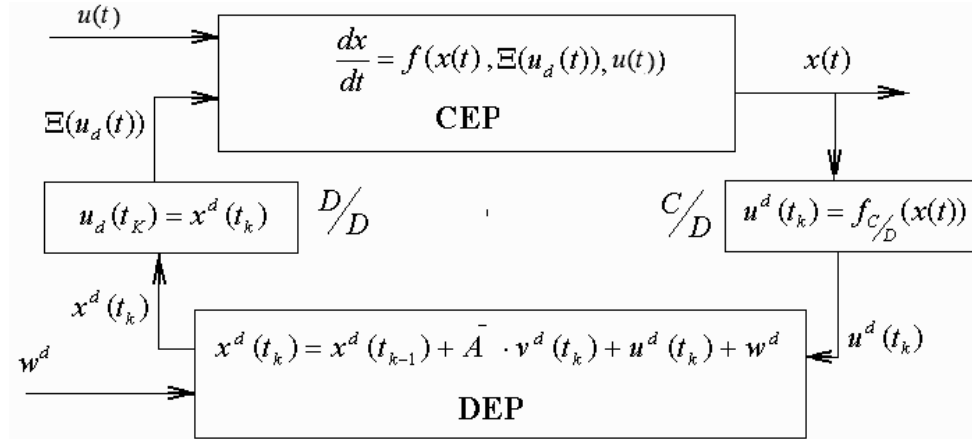
Fig. 1. Simplified block diagram of the logic-dynamic model

Expansion of the mathematical apparatus for describing complex systems based on procedures for automatic synthesis of Petri nets

These equations (5)–(8) are the basis for expanding the mathematical apparatus taking into account the procedures for automatic synthesis of Petri nets.

During the automatic synthesis of a Petri net, the dimension of vectors $^d X_L(t_k)$, $^d u_L(t_k)$ and matrices $|A_L|$ may not change, but the elements of the matrix must change during different runs of the system model. In this case, the incidence matrix $|A_L|$ may be $|A_{L1}|$, $|A_{L2}|$. Thus $|A_L| \in |A_{L1}|, |A_{L2}|, ..., |A_{Ln}|$, in this case, the value of n is unknown in advance and depends on the task at hand.

Matrix selection $\left|A_{Li}\right|$, where $i=1,\ldots,n$, depends on initial conditions $\overline{S}$, where $\overline{S}=[s_1 \quad s_2 \quad \ldots \quad s_n]^{\mathrm{T}}$ — a vector of initial conditions generated by some expert system. Taking into account the automatic synthesis of the Petri net, equation (7) will take the following form:

$$^dX_L(t_k)=^dX_L(t_{k-1})+(W_L\cdot{}^dS(^du_S(t_k)))^d\cdot v_L(t_k)+^du_L(t_k)+^dw_L(t_k), \quad (9)$$

where $W_L=[\left|A_{L1}\right| \quad \left|A_{L2}\right| \quad \ldots \quad \left|A_{Ln}\right|]$; according $W_L\cdot{}^dS(^du_S(t_k))=\left|A_{Li}\right|$, where

$i=1,\ldots,n$, $^dS(^du_S(t_k))=[s_1 \quad s_2 \quad \ldots \quad s_n]^T$, $\bigcup\limits_{i=1}^{n}s_i=1$, $\bigcap\limits_{i=1}^{n}s_i=0$.

Vector function $S(^du_S(t_k))$ contains elements

$$s_i=\begin{cases}1 & \text{at} \quad ^du_S(t_k)=^du_S(t_k)_{given}; \\ 0 & \text{at} \quad ^du_S(t_k)\neq{}^du_S(t_k)_{given},\end{cases}$$

where $^du_S(t_k)=[^du_{S1} \quad ^du_{S2} \quad \ldots \quad ^du_{Sm}]$; $^du_{Si}=f_{C/D}(\Delta J(t),w)$; $^du_S(t_k)_{given}$ — tasks vector; $\Delta J(t)=\int\limits_{t_1}^{t_2}f(y,u,t)dt-\int\limits_{t_3}^{t_4}f(y,u,t)dt$ is an/the increment of the system perfomance criterion; w — external influence from the expert; $f_{C/D}$ — function of continuous-discrete transformation of variables.

The equation (9) implies that the simplified block diagram presented in Fig. 1 is transformed as shown in Fig. 2.
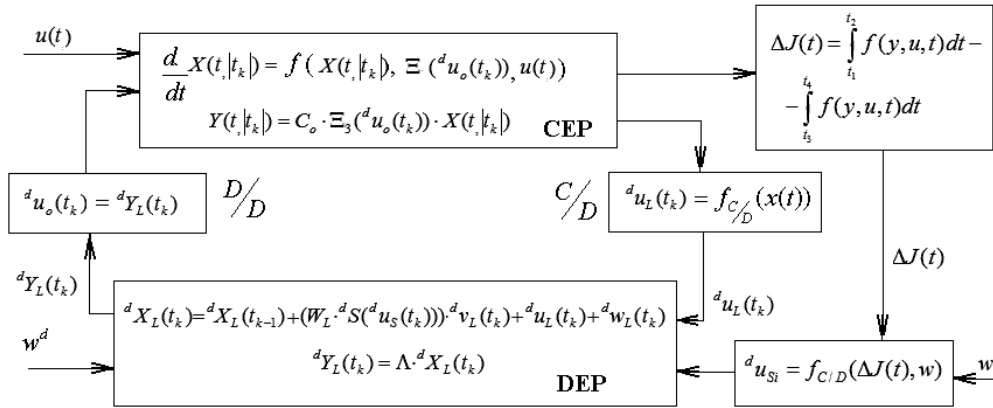
Fig. 2. Simplified block diagram of the logical-dynamic model of the system, implementing the automatic synthesis of Petri nets

To visualize the Petri net synthesis process, state variables $^dX_L(t_k)$, $^dX_L(t_{k-1})$ and increase in the value of the system performance criterion ΔJ can be output using a parametric file to the visualization platform, as shown in [12]. Visualization of the process of Petri net synthesis based on the corresponding Flash or Unity platform is an important component of the interaction of an expert with an intelligent system.

Research results

The consideration of the extended mathematical description of complex systems provides the basis for constructing a model of an intelligent system intended for the formation of some logical control algorithms.

These algorithms are formed according to certain methods through the automatic synthesis of Petri nets. Combination of different incidence matrices $\left|A_{Li}\right|$, where $i = 1, \ldots, n$, that are included in equation (9) represents a set of various algorithms that can be adjusted during the functioning of the intelligent system. The block diagram presented in Fig. 2 can represent this intelligent system, taking into account the additional procedure for correcting the incidence matrix; $\left|A_{Li}\right|$ implemented, as shown in [11], taking into account the functioning of an artificial neural network and its training. Such a system can be used to form certain control algorithms that provide increased operating efficiency in some objects.

CONCLUSIONS

In this work we expand the mathematical description of complex technological systems with the use of DC-nets, taking into account the automatic synthesis of Petri nets.

Expanding the mathematical description of complex technological systems with the use of DC-nets makes it possible to approach the solution of a practical problem associated with the development of an intelligent system that automatically synthesizes some logical control algorithms.

In turn, the use of such an intelligent system makes it possible to achieve a certain goal of work, which is to minimize the time and material costs for the development of logical control algorithms.

Further scientific research should be related to the development of methods for the synthesis of Petri nets and some algorithms used in control systems.

REFERENCES

1. J.L. Peterson, *Teorija setej Petri i modelirovanie sistem [Petri net theory and the modeling of systems]*. M.: Mir, 1984, 264 p.
2. K. Jensen, G. Rozenberg, *High-level Petri nets: theory and application*. Springer Science & Business Media, 2012, 721 p. doi: 10.1007/978-3-642-84524-6
3. P.V. Skorodumov, "Analysis of future expansions of Petri networks," *Science and World*, vol. 1, no. 10(14), pp. 66–68, 2014.
4. M.Z. Zgurovsky, V.A. Denisenko, *Diskretno neprerivnie sistemi c upravlyaemoi strukturi [Discrete-continuous system with controlled structure]*. Kyiv: Naukova dumka, 1998, 350 p.
5. Z. Yang, M. Blanke, "A unified approach to controllability analysis for hybrid control systems," *Nonlinear Analysis: Hybrid Systems*, vol. 1, issue 2, pp. 212–222, 2007. doi: 10.1016/j.nahs.2006.08.002
6. M.A. Drighiciu, "Hybrid Petri nets: A framework for hybrid systems modeling," *2017 International Conference on Electromechanical and Power Systems (SIELMEN) – IEEE, 2017*, pp. 020–025. doi: 10.1109/SIELMEN.2017.8123285
7. F.N. Tsarev, A.A. Shalito, *Primenenie geneticheskogo programmirovaniya dlya generacii avtomata v zadache ob "Umnom murave" [Application of genetic programming for automatic construction of an automaton in the problem of "intelligent ants"]*. M.: Fizmatlit, 2007, pp. 590–597.

8. A.V. Aleksandrov, "Generacija konechnyh avtomatov dlja upravlenija model'ju bespilotnogo samoleta [Generation of state machine creation for unmanned airplane controlling]," *Scientific and Technical Journal of Information Technologies, Mechanics and Optics*, vol. 2(72), pp. 3–8, 2011.

9. A.A. Gurskij, A.E. Goncharenko, and A.V. Denisenko, "Generaciya seti Petri na baze sredstv diskretno-nepreryvnyh setej pri formirovanii algoritma avtomaticheskoj nastrojki koordiniruyushchej sistemy upravleniya [Petri net generation by means of the resource of the discrete-continuous nets in the algorithm formation for the self-tuning of the coordinating control system]," *Electrotechnic and Computer Systems*, no. 26(102), pp. 78–87, 2017.

10. D.W. He, B. Strege, H. Tolle, and A. Kusiak, "Decomposition in automatic generation of Petri nets for manufacturing system control and scheduling," *International Journal of Production Research*, vol. 38, issue 6, pp. 1437–1457, 2000. doi: 10.1080/002075400188942

11. A.A. Gurskiy, A.V. Denisenko, "The automatic synthesis of Petri nets based on the functioning of artificial neural network," *Radio Electronics, Computer Science, Control*, issue 2/2021, pp. 84–92, 2021. doi: 10.15588/1607-3274-2021-2-9

12. A. Denisenko, A. Gurskiy, "Information technology of visualization for technological processes for research modes of complex technological systems functioning," *System Research and Information Technologies*, no. 2, pp. 74–83, 2021. doi: 10.20535/SRIT.2308-8893.2021.2.06

INFORMATION ON THE ARTICLE

Alexander A. Gurskiy, ORCID: 0000-0001-5158-2125, Odessa National University of Technology, Ukraine, e-mail: gurskiya2017@gmail.com

Andrey V. Denisenko, ORCID: 0000-0002-8610-0082, National University "Odessa Polytechnics", Ukraine, e-mail: denisenko.a.v@op.edu.ua

Alexander E. Goncharenko, ORCID: 0000-0003-4959-6469, Odessa National University of Technology, Ukraine, e-mail: kholod.automatic@gmail.com

РОЗШИРЕННЯ МАТЕМАТИЧНОГО АПАРАТУ ДИСКРЕТНО-НЕПЕРЕРВНИХ МЕРЕЖ ДЛЯ АВТОМАТИЗАЦІЇ ПРОЦЕДУР ЇХ СИНТЕЗУ / О.О. Гурський, А.В. Денисенко, О.Є. Гончаренко

Анотація. Подано певний етап розроблення моделі інтелектуальної системи, пов'язаної з автоматичним синтезом мереж Петрі. Розглянуто розширений математичний опис складних систем на основі засобів дискретно-неперервних мереж, який покладено в основу розроблення такої інтелектуальної системи, спрямованої передусім на формування алгоритмів логічного керування. Особливість розширеного математичного апарату полягає у тому, що у його складі є комбінація матриць інцидентності мереж Петрі для подання різноманітних алгоритмів. Ця комбінація матриць входить до складу рівнянь, що описує пристрій логічного керування складної системи. Відповідно подано відомий математичний опис дискретно-неперервних систем із керованою структурою, що включають певні пристрої логічного керування. Цей математичний опис на основі засобів дискретно-неперервних мереж, пов'язаний з матрицею інцидентності мережі Петрі, що формується в результаті певного алгоритму синтезу. Сформовано мережу Петрі — відповідний алгоритм логічного керування для забезпечення процесу ефективного функціонування відповідної системи. Подано різні структурні схеми логіко-динамічних моделей систем з автоматичним синтезом мереж Петрі. Визначено особливість розширеного математичного апарату на основі дискретно-неперервних мереж для розроблення інтелектуальної системи, що формує алгоритми логічного керування. Такі системи можна використовувати для формування певних алгоритмів керування, які забезпечують підвищену ефективність функціонування деяких об'єктів.

Ключові слова: мережі Петрі, система з керованою структурою, дискретно-неперервна мережа, автоматичний синтез мереж Петрі.

DECENTRALIZED LEADER-FOLLOWING CONSENSUS CONTROL DESIGN FOR DISCRETE-TIME MULTI-AGENT SYSTEMS WITH SWITCHING TOPOLOGY

Y.I. DOROFIEIEV, L.M. LYUBCHYK, M.M. MALKO

Abstact. The problem of consensus control of linear discrete-time multi-agent systems (MASs) with switching topology is considered in the presence of a leader. The goal of consensus control is to bring the states of all agents to the leader state while providing stability for local agents, as well as the MAS as a whole. In contrast to the traditional approach, which uses the concept of an extended dynamic multi-agent system model and communication topology graph Laplacian, this paper proposes a decomposition approach, which provides a separate design of local controllers. The control law is chosen in the form of distributed feedback with discrete PID controllers. The problem of local controllers' design is reduced to a set of semidefinite programming problems using the method of invariant ellipsoids. Sufficient conditions for agents' stabilization and global consensus condition fulfillment are obtained using the linear matrix inequality technique. The availability of information about a finite set of possible configurations between agents allows us to design local controllers offline at the design stage. A numerical example demonstrates the effectiveness of the proposed approach.

Keywords: multi-agent system, consensus control, switching topology, PID controller, invariant ellipsoids method, linear matrix inequality, semidefinite programming problem.

INTRODUCTION

Recently, consensus control of multi-agent systems (MAS) with networked structures has attracted the great attention of many researchers from different fields of science and engineering [1; 2]. In the field of automatic control, the development of consensus control theory is stimulated, in particular, by the rapid development of unmanned mobile vehicles and ensuring their coordinated behavior in accordance with the common goal [3]. Similar problems also arise under the control of large-scale systems with networked structures, such as complex technological and automated production systems, supply and logistics chains, and energy and transport systems as well.

The main problem of consensus control of MAS is the design of a control law, which allows all agents to reach the agreed values of their state or output variables, using the information obtained from other agents. Here, the control law is constructed based on a consensus protocol [2; 4]. The protocol design assumes

that the control for each local agent is formed on the basis of information about the deviations of the state or output vector of any agent from the corresponding vectors of neighbouring agents directly related to it. In this case, the corresponding control system also has a network structure wherein the rules for information exchange between each local agent and its directly connected neighbours are determined by the network topology.

A topology model usually describes the MAS structure as connections between agents in the form of a directed graph, in that the nodes of which correspond to the controlled local agents, where the graph edges describe the information transfer channels between them. Usually, a consensus protocol is taken in the form of a linear deviation feedback between local agent states or outputs and the weighted average vector of states or outputs of its immediate neighbours. In such a case, the control problem is reduced to finding a set of feedback gain matrices from the stability condition for both local controlled agents and the MAS as a whole, considering the relationship between them, as well as the condition of reaching a consensus.

Taking into account the peculiarities of practical problems of MAS control leads to the need to complicate the problems under consideration. In reality, due to breaks in communication channels, the topology of connections can be arbitrarily changed by switching between elements of a finite set of possible configurations, which leads to the need for consensus control design under switching topology conditions.

REVIEW AND ANALYSIS OF INFORMATION SOURCES

In the last years, consensus problem research has developed very rapidly and numerous results have been obtained concerning distributed consensus protocols for MAS design (see [5; 6] and references therein).

The usual approach to solving consensus control problems is based on a dynamic model of MAS with an extended state vector composed of the state vectors of local agents, thus constructing a model using the concept of the Laplacian of the communication topology graph [7]. At that, the Kronecker product of the dynamic matrices of local agents describes the matrix of the extended MAS model dynamics.

Efficient methods for studying the stability of such systems have been developed; for the synthesis of consensus control, modern methods for controllers' design in state space, including the methods of linear matrix inequalities (LMIs), are widely used. In [8], using the LMI technique, a new form of state-feedback consensus control based on the aggregate Laplacian is proposed and sufficient conditions of stabilization are established using the Lyapunov stability theory.

Early work in this area dealt mainly with the problem of ensuring consensus, represented in the form of balance ratios of an agent's state vectors so that all agents are driven to converge to a common state, determined by the consensus conditions. Further development of consensus control is associated with an additional condition of following the leader, which is considered an agent that imposes the desired behavior on others [5]. A number of works have been devoted to the consensus control problems in multi-agent systems with a leader, see links in [9].

A large number of works are devoted to the consensus control design problem under switching topology conditions; systematized results are given in [10]. In [11], it was shown that under certain assumptions, consensus can be achieved asymptotically under dynamically changing interaction topologies if the union of the collection of interaction graphs across some time intervals has a spanning tree frequently enough. Consensus of MAS in a continuous time domain under fixed and switching topology was studied in [12], where the dynamics of local and leader agents are considered linear; the design technique was based on Riccati inequality and Lyapunov inequality. These results have also been generalized to discrete-time systems. In [13], sufficient conditions for the solvability of consensus problems for discrete-time multi-agent systems with switching topology and time-varying delays have been presented. In [14], the consensus problem for MAS was also considered in the discrete-time domain, the topology of interactions between agents was assumed to be switched and undirected. In [15], the cooperative control problem of discrete-time multi-agent systems is discussed, bounded uncertain time delay and directed switching topology are considered, and sufficient conditions for asymptotic consensus of the system under directed switching topology are obtained. State-of-the-art survey on consensus control of network systems with switching network topologies, presented in [16] with emphasis on the relationships between the switching among different topology candidates and the networked control stability.

The architectural features of networked consensus control systems, combined with a natural desire to reduce the computational resources required to calculate controls in real time, stimulated an increase in interest in building distributed multi-agent systems with decentralized consensus control. From the viewpoint of the practical implementation of consensus control, a decentralized approach is of great interest, in which the local control for each agent is designed only using locally available information, so it requires less computational effort and is relatively more scalable with respect to the number of agents. A decentralized approach to asymptotic consensus control design for discrete MAS, where local agents exchange information only with their nearest neighbours is studied in detail by a number of researchers. In [17], for agents of the first order, a heuristic approach is proposed based on an analogy with the Vicsek model of the motion of a group of particles on a plane. In [18], an adaptive procedure for constructing control for each agent is proposed using only information from its neighbours in the network topology. The consensus problem for a multi-agent system with high-order linear dynamics and a fully decentralized consensus algorithm is proposed in [19], which allows each agent to reach the consensus value using only a finite number of steps of its past state information, but the solution is obtained under the condition that the system has a time-invariant topology. A fully decentralized algorithm that allows any agent to compute the consensus value of the whole network in a finite time using only the minimal number of successive values of its own history was proposed in [20], where was shown, that this minimal number of steps is related to a Jordan block decomposition of the network dynamics. However, this minimum number of steps is related to graph theoretical notions that can be directly computed from the Laplacian matrix of the graph and from the minimum external equitable partition. Decentralized event-triggered finite-time consensus control under a directed graph was investigated in [21], and an adaptive law is designed to counteract the effect of uncertainties and external disturbances.

The quality of consensus control in transients, which is especially important in leader-following tracking problems, can be significantly improved using more complex dynamic consensus protocols, in which control actions depend not only on the current but also on previous deviations. As such control laws, multivariable Proportional-Integral-Derivative (PID) controllers are widely used, which make it possible to significantly improve the quality of consensus control in comparison with static protocols.

Despite its well-known benefits, PID control is lightly addressed in the decentralized MAS control and they are mainly dealt with homogeneous MASs (see e.g. [22] and references therein). For instance, a robust PID consensus control strategy has been proposed in [23] for a system of linear high-order agents under the restrictive assumption of an undirected communication graph. A PD protocol is proposed in [24] to solve, instead, the problem of the average consensus under a fast arbitrarily switching topology for the case of first-order nonlinear homogeneous MASs with Lipschitz dynamics. To solve the leader tracking for uncertain high-order homogeneous MASs, robust PID protocols have been investigated [25]. Nevertheless, practical applications of the networked MASs require heterogeneous models due to the presence of mismatches and differences among the agents. In this context, only a few decentralized protocols aim to extend the PID-control advantages to the heterogeneous MAS framework. In [26] it was investigated the use of distributed PID actions to achieve consensus in networks of homogeneous and heterogeneous linear systems. The convergence of the strategy is proven for both cases using appropriate state transformations and Lyapunov functions. A multiplex proportional–integral approach for solving consensus problems in networks with heterogeneous node dynamics affected by constant disturbances was proposed in [27]. The proportional and integral actions are deployed on two different layers across the network, each with its own topology. Sufficient conditions for convergence are derived that depend upon the structure of the network, the parameters and topologies characterizing the control layers, and the node dynamics. Fully-distributed PID control strategy was proposed in [28], whose stability is analytically proven by exploiting the controller equations and the Static Output Feedback procedure adapted to the MASs framework.

In this paper, the problem of decentralized PID controller design for leader-following consensus control of networked heterogeneous MASs is considered under the assumption that sharing information between agents is carried out via switching communication topology. In this work, we use a distributed consensus protocol in the form of local dynamic feedback with a PID controller using the signal of deviation of local agent states from the weighted average states of its neighbours, with which the agent exchanges information in the current period. The synthesis of local PID controllers is based on the method of invariant ellipsoids. To analyze the stability of closed-loop controlled local agents, as well as the stability of the whole MAS, the second Lyapunov method and LMI technique were used. This allowed us to reduce a local controller problem design to a problem of semidefinite programming to find the optimal gain values for each agent by numerically solving the optimization problem. This, in turn, makes it possible to simplify the solution in comparison with other well-known approaches, for example, with the descriptor method [29].

In summary, the main features of the proposed approach and contributions of the work are:

- Within the framework of the principle of decentralized consensus control, a method of local controllers' design is proposed, which ensures the stability of individually controlled agents and the networked multi-agent systems as a whole under conditions of a switching communication network topology.

- Based on the sufficient conditions of local-controlled agents' stability and reaching consensus as well as leader-following tracking in LMI form, a computational procedure for optimizing the parameters of local controllers by solving a set of semidefinite programming problems is proposed; while controller parameters optimization is performed offline during the design phase.

- A decentralized optimal dynamic consensus control strategy with a recurrent form of the PID control law is proposed, which makes it possible to abandon the construction of an extended model of a closed local agent, which is usually used for discrete systems with PID controllers, which makes it possible to reduce the optimization problem dimension.

- Availability of information about a finite set of topology variations of connections between agents allows solving the problem of calculating the feedback gain matrix before the start of the control process. Thus, to determine the control action at each step of the MAS operation from the resulting set of solutions, the appropriate one is selected depending on which neighbours the agent exchange information in the current step.

PROBLEM FORMULATION

Consider a MAS represented by a network of N agents as a set of multivariable discrete-time linear dynamic systems, where each i-th agent is described by the difference equation

$$x_i(k+1) = A_i x_i(k) + B_i u_i(k), \ i = 1,...,N , \qquad (1)$$

where $k = 0,1,2,...$ is time instant; $x_i(k) \in \mathbf{R}^n$, $u_i(k) \in \mathbf{R}^m$ are state and control vectors of i-th agent at time k; A_i, B_i are constant matrices of appropriate dimensions such that the system (1) is controllable.

The connection topology of a networked MAS is described by an undirected graph $G = (V,E)$, where $V = \{1,...,N\}$ is a set of nodes (i.e., agents), and $E \subset V \times V$ is the set of edges. The presence of an edge (i,j) in the graph G means that agents i and j exchange information. $D = [d_{ij}]$ is the adjacency matrix of graph G and has dimension $N \times N$.

Since the topology of the connections between agents can change during the system dynamics, the graph G can switch at arbitrary time moments among a finite set $G_1, G_2,..., G_K$, each of which is an undirected graph, containing a spanning tree. This means that the graph G will have the form G_1 during a certain time interval, then $G_j, j \in \{1,...,K\}$, and so on, moreover, switching occurs arbitrarily.

A set of agents achieves consensus if the agents' states satisfy the consensus condition

$$\lim_{k \to \infty} (x_i(k) - x_j(k)) = 0, \ i,j = 1,...,N . \qquad (2)$$

The control law $u_i(k)$, hereafter the consensus protocol, solves the consensus control problem if all agents achieve consensus under this control.

We construct a distributed consensus protocol in the form of local feedback to a PID controller using the signal of deviation of local agent states from the weighted average states of its neighbours

$$u_i(k) = K_P \Sigma_i \sum_{j=1, j \neq i}^{N} \delta_{ij}(k)(x_i(k) - x_j(k)) + K_I \Sigma_i \sum_{j=1, j \neq i}^{N} \delta_{ij}(k) \sum_{l=0}^{k-1}(x_i(l) - x_j(l)) +$$

$$+ K_D \Sigma_i \sum_{j=1, j \neq i}^{N} \delta_{ij}(k)((x_i(k) - x_j(k)) - (x_i(k-1) - x_j(k-1))), \qquad (3)$$

where $\Sigma_i = 1 \Big/ \sum_{j=1, j \neq i}^{N} d_{ij}$; $K_P, K_I, K_D \in \mathbf{R}^{m \times n}$ are the gain matrices of the proportional, integral, and differential parts of the controller, respectively; $\delta_{ij}(k)$ is binary variable, the value of which determines whether information about the state of the j -th agent is available to the i -th agent at a time k :

$$\delta_{ij}(k) = \begin{cases} 0, & \text{agent } i \text{ does not receive information from agent } j, \\ 1, & \text{otherwise.} \end{cases}$$

The recurrent form of control law (3) is more convenient for practical implementation, so the current value of the control action is determined by its previous value and the correction

$$u_i(k) = u_i(k-1) + K_{0_i} \Sigma_i \sum_{j=1, j \neq i}^{N} d_{ij} \delta_{ij}(k)(x_i(k) - x_j(k)) +$$

$$+ K_{1_i} \Sigma_i \sum_{j=1, j \neq i}^{N} d_{ij} \delta_{ij}(k)(x_i(k-1) - x_j(k-1)) +$$

$$+ K_{2_i} \Sigma_i \sum_{j=1, j \neq i}^{N} d_{ij} \delta_{ij}(k)(x_i(k-2) - x_j(k-2)), \qquad (4)$$

where $K_{0_i}, K_{1_i}, K_{2_i} \in \mathbf{R}^{m \times n}$ are feedback coefficient matrices.

Introduce block matrix $K_i = [K_{0_i}, K_{1_i}, K_{2_i}]$ and the composite vectors $v_{ij}(k) = \text{col}\{(x_i(k) - x_j(k)), (x_i(k-1) - x_j(k-1)), (x_i(k-2) - x_j(k-2))\}, \quad i, j = 1, ..., N, \quad j \neq i$. Then, the consensus protocol (4) takes the form

$$u_i(k) = u_i(k-1) + \Sigma_i K_i \sum_{j=1, j \neq i}^{N} \delta_{ij}(k) v_{ij}(k) . \qquad (5)$$

The control law for the agent, acting as the leader, differs from (5) by addition the deviation term between the leader's state and the set point x^*

$$u_i^{leader}(k) = u_i(k) + K_{0_i}(x_i(k) - x^*) .$$

The model of a closed-loop local agent with the consensus protocol (5) will take the form with one-step control lag

$$x_i(k+1) = (A_{iC} + B_i K_i) \Sigma_i \sum_{j=1, j \neq i}^{N} \delta_{ij}(k) v_{ij}(k) + A_i \sum_{j=1, j \neq i}^{N} \delta_{ij}(k) x_j(k) + B_i u_i(k-1), \quad (6)$$

where $A_{iC} = [A_i \mathbin{\vdots} 0_{n \times n} \mathbin{\vdots} 0_{n \times n}]$ is a block matrix, $0_{n \times m}$ is the null matrix of the corresponding dimension. For the agent that is a leader, equation (6) differs by presence of the term $B_i K_{0_i}(x_i(k) - x^*)$.

For a linear closed-loop discrete MAS with local feedback described by equation (6) under the conditions of an arbitrarily switching topology described by a finite set of undirected connected graphs $G_1, G_2, ..., G_K$, the problem of decentralized consensus control is considered. Such a problem is reduced to the choice of feedback gain matrices $K_i, i = 1, ..., N$ that ensure the stabilization of closed-loop local agents, the stability of the controlled MAS as a whole, as well as the fulfilment of the consensus conditions (2).

CONSENSUS CONTROL DESIGN

The approach based on the second Lyapunov method, which allows us to obtain sufficient stability conditions for closed-loop local subsystems, is used to calculate the gain matrices of local controllers. The development of the theory of linear matrix inequalities [30] makes it possible to apply a similar approach to the synthesis of consensus control of multi-agent systems.

The main idea of linear feedback controller design using LMI is as follows. The control goal is formulated as an inequality with respect to the quadratic Lyapunov function built on the solutions of the closed-loop system. The resulting inequality is reduced to the LMI form with respect to the unknown matrix of the controller parameters. The specified constraints are also reduced to the LMI form. A certain criterion of optimality is used and the corresponding convex optimization problem is solved numerically, because of which the optimal parameters of the controllers are determined.

The considered technique is implemented based on the invariant ellipsoid's method [31]. Consider the ellipsoid described by the equation

$$\varepsilon_i(Q_i) = \{x \in \mathbf{R}^n : x_i^{\mathrm{T}}(k)Q_i x_i(k) \le 1\}, \tag{7}$$

where $0 \prec Q_i \in \mathbf{R}^{n \times n}$ is ellipsoid matrix; $M \succ 0$ ($M \succeq 0$) means that the matrix M is positive (nonnegative) definite.

The ellipsoid (7) is called state invariant for the system (6) if any trajectory of the system, having started in the ellipsoid, remains in it for any time moment $k \ge 0$.

The stabilization problem of system (6) comes down to calculating the block matrices of feedback gain $K_i, i = 1, ..., N$ such that the consensus protocol (5) provides minimization of ellipsoid (7) by some optimality criterion. We choose as a criterion the length squares sum of the ellipsoid semiaxes which is equal to the trace of its matrix Q_i.

Consider a quadratic function constructed from the solutions of the system (6)

$$V_i(k) = x_i^{\mathrm{T}}(k)P_i x_i(k), \quad 0 \prec P_i = P_i^{\mathrm{T}} \in \mathbf{R}^{n \times n}. \tag{8}$$

It is well known that function (8) is a Lyapunov function for system (6) if the conditions are fulfilled:

(i) the function values are non-negative for any $x_i(k) \neq 0$;

(ii) the function values decrease monotonically over time.

If equality holds

$$Q_i = P_i^{-1}, \tag{9}$$

then the invariant ellipsoid (7) is the level set of Lyapunov function candidate (8).

It was shown in [38] that for a stable and controllable discrete-time dynamical system, the solution of the minimization problem by some criterion of quadratic Lyapunov function under the constraint specified by the Lyapunov inequality, is achieved by the solution of the Lyapunov equation. Thus, such an approach allows reducing the robust control design problems with respect to the described class of system topology uncertainty, to solve the problem of minimizing a linear function under constraints that can be represented in the form of linear matrix inequalities, that is, to solve a semidefinite programming problem.

The hypothesis on the basis of which the design problem of consensus control for MAS with switching topology in the presence of a leader is solved is that for any version of the topology described by a finite set of undirected graphs $G_1, G_2, ..., G_K$, each of which contains a spanning tree, the statements of the following theorem are fulfilled.

Theorem. If for linear stable discrete-time system (6) matrices $\hat{Q}_i$, $\hat{Y}_{0i}$, $\hat{Y}_{1i}$, $\hat{Y}_{2i}$ are obtained by solving the optimization problem

$$\text{trace}(Q_i) \to \min \tag{10}$$

subject to

$$
\left[
\begin{array}{ccccc|cccc}
Q_i & \overbrace{A_i Q_i \quad A_i Q_i \quad \dots \quad A_i Q_i}^{N-1} & & & & \overbrace{\Delta_{ij}(A_{iQ}+B_iY_i) \quad \dots \quad \Delta_{ij}(A_{iQ}+B_iY_i)}^{N-1} & & & B_i \\
* & Q_i & 0_{n\times n} & \dots & 0_{n\times n} & 0_{n\times 3n} & \dots & 0_{n\times 3n} & 0_{n\times m} \\
* & * & 0_{n\times n} & \dots & 0_{n\times n} & 0_{n\times 3n} & \dots & 0_{n\times 3n} & 0_{n\times m} \\
\vdots & & \vdots & & & & \vdots & & \vdots \\
* & * & * & * & 0_{n\times n} & 0_{n\times 3n} & \dots & 0_{n\times 3n} & 0_{n\times m} \\
* & * & * & * & * & 0_{n\times 3n} & \dots & 0_{n\times 3n} & 0_{n\times m} \\
\vdots & & \vdots & & & & \vdots & & \vdots \\
* & * & * & * & * & * & * & 0_{n\times 3n} & 0_{n\times m} \\
* & * & * & * & * & * & * & * & 0_{m\times m}
\end{array}
\right] \succeq 0 \tag{11}
$$

on matrix variables $0 \prec Q_i \in \mathbf{R}^{n\times n}$, $Y_i = [Y_{0i}, Y_{1i}, Y_{2i}]$, $Y_{0i}, Y_{1i}, Y_{2i} \in \mathbf{R}^{m\times n}$, where $\Delta_{ij} = \Sigma_i \delta_{ij}$, $A_{iQ} = [A_i Q_i \ \vdots \ 0_{n\times n} \ \vdots \ 0_{n\times n}]$, «$*$» denotes the symmetric terms in then inequality matrix, then:

(i) for any initial state $x_i(0) \in \varepsilon_i(\hat{Q}_i)$ closed-loop system (6) is asymptotically stable;

(ii) among all consensus protocols of the form (5), the protocol with gain matrices

$$K_{0i} = \hat{Y}_{0i}\,\hat{Q}^{-1}, \quad K_{1i} = \hat{Y}_{1i}\,\hat{Q}^{-1}, \quad K_{2i} = \hat{Y}_{2i}\,\hat{Q}^{-1} \tag{12}$$

delivers the minimum of the matrix trace criterion for the invariant ellipsoid (7) of the closed-loop system (6) and hence guaranties the fulfillment of consensus condition (2).

Proof. The first of the conditions, which are necessary for a candidate (8) to be a Lyapunov function for the system (6), is satisfied due to the positive definiteness of the matrix P_i. Hence, the consensus protocol (5) should ensure that the second property is satisfied.

We calculate the difference of the candidates in the Lyapunov function (8) with respect to k and require that the value of the function decrease over time

$$V_i(k+1) - V_i(k) = s_i^{\mathrm{T}}(k) M_i s_i(k) \le 0, \tag{13}$$

where $s_i(k) = \mathrm{col}\{x_i(k), ..., x_N(k), v_{ij}(k), ..., v_{iN}(k), u_i(k-1)\} \in \mathbf{R}^{4Nn-3n+m}$,

$$M_i =$$

$$= \begin{bmatrix}
A_i^{\mathrm{T}} P_i A_i - P_i & \overbrace{A_i^{\mathrm{T}} P_i A_i \quad \dots \quad A_i^{\mathrm{T}} P_i A_i}^{N-1} & \overbrace{A_i^{\mathrm{T}} P_i \Delta_{ij}\Omega_i \quad \dots \quad A_i^{\mathrm{T}} P_i \Delta_{iN}\Omega_i}^{N-1} & A_i^{\mathrm{T}} P_i B_i \\
* & A_i^{\mathrm{T}} P_i A_i \quad \dots \quad A_i^{\mathrm{T}} P_i A_i & A_i^{\mathrm{T}} P_i \Delta_{ij}\Omega_i \quad \dots \quad A_i^{\mathrm{T}} P_i \Delta_{iN}\Omega_i & A_i^{\mathrm{T}} P_i B_i \\
\vdots & \vdots & \vdots & \vdots \\
* & * \quad * \quad A_i^{\mathrm{T}} P_i A_i & A_i^{\mathrm{T}} P_i \Delta_{ij}\Omega_i \quad \dots \quad A_i^{\mathrm{T}} P_i \Delta_{iN}\Omega_i & A_i^{\mathrm{T}} P_i B_i \\
* & * \quad * \quad * & \Delta_{ij}\Omega_i^{\mathrm{T}} P_i \Delta_{ij}\Omega_i \quad \dots \quad \Delta_{ij}\Omega_i^{\mathrm{T}} P_i \Delta_{iN}\Omega_i & \Delta_{ij}\Omega_i^{\mathrm{T}} P_i B_i \\
* & * \quad * \quad * & * \quad \dots \quad \Delta_{ij}\Omega_i^{\mathrm{T}} P_i \Delta_{iN}\Omega_i & \Delta_{ij}\Omega_i^{\mathrm{T}} P_i B_i \\
\vdots & \vdots & \vdots & \vdots \\
* & * \quad * \quad * & * \quad * \quad \Delta_{iN}\Omega_i^{\mathrm{T}} P_i \Delta_{iN}\Omega_i & \Delta_{iN}\Omega_i^{\mathrm{T}} P_i B_i \\
* & * \quad * \quad * & * \quad * \quad * & B_i^{\mathrm{T}} P_i B_i
\end{bmatrix},$$

$$\Omega_i = A_{iC} + B_i K_i.$$

Inequality (13) is equivalent to the matrix inequality $M_i \preceq 0$. Let us represent the inequality matrix in the form

$$M_i = \begin{bmatrix} A_i^{\mathrm{T}} \\ \vdots \\ A_i^{\mathrm{T}} \\ \Delta_{ij}\Omega_i^{\mathrm{T}} \\ \vdots \\ \Delta_{iN}\Omega_i^{\mathrm{T}} \\ B_i^{\mathrm{T}} \end{bmatrix} \cdot P_i \cdot \begin{bmatrix} A_i & \dots & A_i & \Delta_{ij}\Omega_i & \dots & \Delta_{iN}\Omega_i & B_i \end{bmatrix} +$$

$$+ \begin{bmatrix} -P_i & 0_{n \times (4(N-1)n+m)} \\ * & 0_{(4(N-1)n+m) \times (4(N-1)n+m)} \end{bmatrix}.$$

Using the Schur complement [32], inequality takes the form

$$
\begin{bmatrix}
-P_i^{-1} & \overbrace{A_i \quad A_i \quad \ldots \quad A_i}^{N-1} & \overbrace{\Delta_{ij}\Omega_i \quad \ldots \quad \Delta_{ij}\Omega_i}^{N-1} & B_i \\
* & -P_i \quad 0_{n\times n} \quad \ldots \quad 0_{n\times n} & 0_{n\times 3n} \quad \ldots \quad 0_{n\times 3n} & 0_{n\times m} \\
* & * \quad\; 0_{n\times n} \quad \ldots \quad 0_{n\times n} & 0_{n\times 3n} \quad \ldots \quad 0_{n\times 3n} & 0_{n\times m} \\
\vdots & \qquad \vdots & \qquad \vdots & \vdots \\
* & * \quad * \quad * \quad 0_{n\times n} & 0_{n\times 3n} \quad \ldots \quad 0_{n\times 3n} & 0_{n\times m} \\
* & * \quad * \quad * \quad * & 0_{n\times 3n} \quad \ldots \quad 0_{n\times 3n} & 0_{n\times m} \\
\vdots & \qquad \vdots & \qquad \vdots & \vdots \\
* & * \quad * \quad * \quad * & * \quad\; * \quad\; 0_{n\times 3n} & 0_{n\times m} \\
* & * \quad * \quad * \quad * & * \quad\; * \quad\; * & 0_{m\times m}
\end{bmatrix} \preceq 0.
$$

By multiplying the left and right parts of the inequality by -1, performing substitution (9) and applying a congruent transformation to the inequality matrix with $\mathrm{block\,diag}\{I_n, \underbrace{Q_i, ..., Q_i}_{4(N-1)}, I_m\}$, where I_n is identity matrix of the corresponding dimension, we obtain the matrix inequality, which is nonlinear with respect to the matrix variables Q_i and K_i. We introduce matrix variables $Y_{0i} = K_{0i}Q_i$, $Y_{1i} = K_{1i}Q_i$, $Y_{2i} = K_{2i}Q_i$. Whence, by virtue of $Q_i \succ 0$ the matrices K_{0i}, K_{1i}, K_{2i} recovers uniquely in accordance with (12). Then, we finally obtain the linear matrix inequality (11).

Thus, if there exist matrices $\hat{Q}_i, \hat{Y}_{0i}, \hat{Y}_{1i}, \hat{Y}_{2i}$, being a solution of the optimization problem (10) subject to (11), then (8) is a Lyapunov function for system (6), and the consensus protocol (5) with matrices calculated in accordance with (12), provides the fulfilment of stabilization (13) and consensus (2) conditions for the system (6). The theorem is proved.

Remark. The optimization problem (10) subject to (11) is a semidefinite programming problem that is solved numerically using freely distributed software packages developed based on MATLAB, for example, cvx [33] or SeDuMi [34].

NUMERICAL EXAMPLE

As an example, we consider a linear discrete-time MAS of 6 homogeneous agents, which was studied in [35] and solve the consensus control problem using the proposed approach. We deliberately consider a homogeneous MAC to reduce the amount of calculation.

During the system dynamics, the connection topology between agents switches randomly among the set of options represented by connected graphs $G_1,...,G_5$, as shown in Fig. 1. The reference set point x^* is received externally at the input of agent 1, which is a leader.

The dimensions of the agent model are $n = 2$, $m = 1$. The dynamics and control matrices are $A_i = \begin{bmatrix} 0 & 1 \\ 0{,}25 & 0 \end{bmatrix}$, $B_i = \begin{bmatrix} 1 \\ 1 \end{bmatrix}$, $i = 1,...,6$. All agents are Shur stable and controllable. The initial states of the agents are chosen:

$$x_1(0) = \text{col}\{50, -100\}, \ x_2(0) = \text{col}\{30, -60\}, \ x_3(0) = \text{col}\{10, -20\},$$

$$x_4(0) = \text{col}\{-10, 20\}, \ x_5(0) = \text{col}\{-30, 60\}, \ x_6(0) = \text{col}\{-50, 100\}.$$
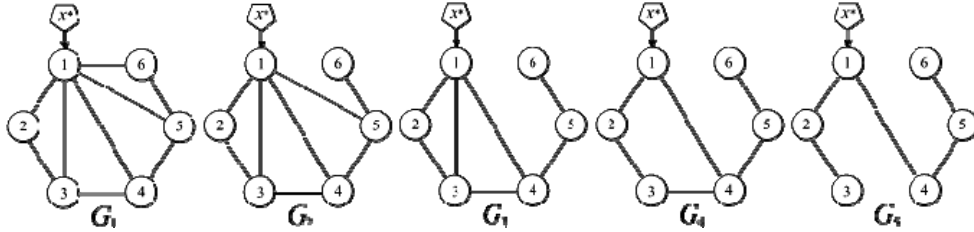
Fig. 1. The set of graphs describing the topology of connections in the MAS

We calculate the numerical solution of problem (10) subject to (11) for all versions of the MAS topology, which is presented in Fig. 1. As a result, the matrices of feedback gains, which determine the consensus protocol (5), were calculated for all agents. The analysis of the obtained results allowed to conclude that the hypothesis, put forward about the fulfilment of the statements of the proved theorem for any version of topology, described by a finite set of connected directed graphs, was experimentally confirmed, since the values of the local feedback matrices depend only on the number of neighbours with which the agent exchanges information in the current period.

For example, in a graph G_1 agents 2 and 6 are connected with two neighbours, while agents 3, 4, and 5 are connected with three neighbours. Therefore, we obtain $K_2(G_1) = K_6(G_1)$, $K_3(G_1) = K_4(G_1) = K_5(G_1)$. In a graph G_4, agents 1, 2, 3 and 5 are connected with two neighbours, and only agent 4 — with three neighbours. Accordingly, we obtain $K_1(G_4) = K_2(G_4) = K_3(G_4) = K_5(G_4) = K_2(G_1)$, $K_4(G_4) = K_3(G_1)$. Thus, for the considered network, we obtained:

$$K_{0i} = [-0,324 \ -0,558], \ K_{1i} = [-0,099 \ -0,206], \ K_{2i} = [-0,047 \ -0,057], \quad (14)$$

$$K_{0i} = [-0,301 \ -0,480], \ K_{1i} = [-0,023 \ -0,059], \ K_{2i} = [-0,031 \ -0,046],$$

$$K_{0i} = [-0,439 \ -0,762], \ K_{1i} = [-0,019 \ -0,027], \ K_{2i} = [-0,024 \ -0,041],$$

$$K_{0i} = [-0,634 \ -1,059], \ K_{1i} = [-0,012 \ -0,019], \ K_{2i} = [-0,019 \ -0,037],$$

$$K_{0i} = [-0,752 \ -1,342], \ K_{1i} = [-0,10 \ -0,017], \ K_{2i} = [-0,010 \ -0,026], (15)$$

where (14) corresponds to an agent exchanging information with one neighbour in the network, and (15) — to an agent with five neighbours, respectively.

Thus, it is sufficient to solve the optimization problem (10) subject to (11) for only one agent, sequentially changing the values of the binary variables δ_{ij}, $j = 1,...,N$, $j \neq i$ that determine the number of neighbours with which the agent exchanges information, to calculate the values of the feedback matrices for all possible cases: from having one neighbour before having $(N-1)$ neighbours.

The plots of the changes in the values of the first and second components of the agent's state vectors with fixed topology in the absence of setting action are shown in Fig. 2. The simulation results provided that the variant of the connection topology between agents at each step was chosen randomly among the versions presented in Fig. 1, are shown in Fig. 3. Clearly in both experiments, all agents achieve a consensus, but the consensus value in the second case differs from zero, that is, there is a static error.
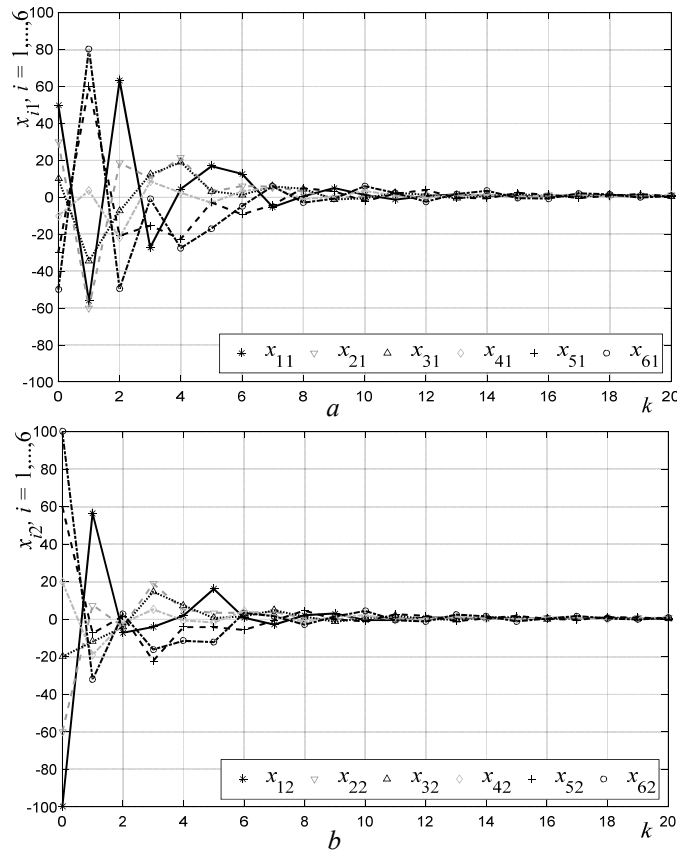
Fig. 2. Values of agents' states with fixed topology in the absence of setting action: *a* — first components of state vectors; *b* — second components of state vectors
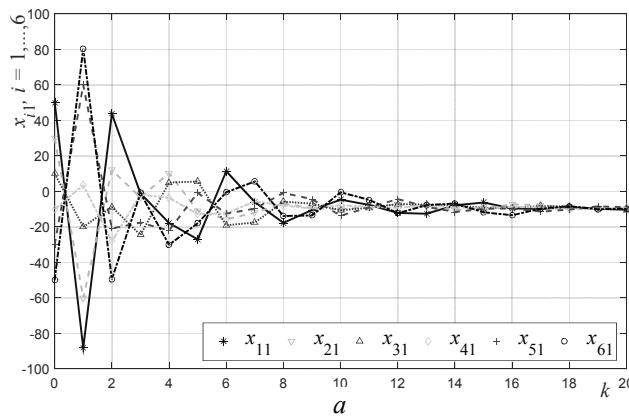
Fig. 3. Values of agents' states with switching topology in the absence of setting action: *a* — first components of state vectors; *b* — second components of state vectors
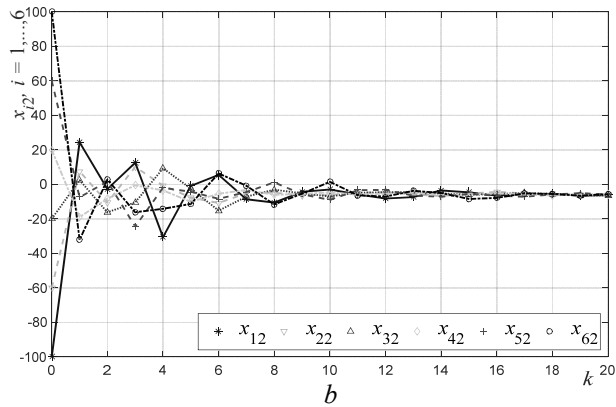
Fig. 3. Values of agents' states with switching topology in the absence of setting action: *a* — first components of state vectors; *b*— second components of state vectors. *End*

The simulation results of MAS with fixed topology, when the input of agent1, which is a leader, is supplied with a constant setting action $x^* = \text{col}\{500, 500\}$, is shown in Fig. 4. Fig. 5 shows the results obtained for MAS with switching topology in the presence of a reference setting.
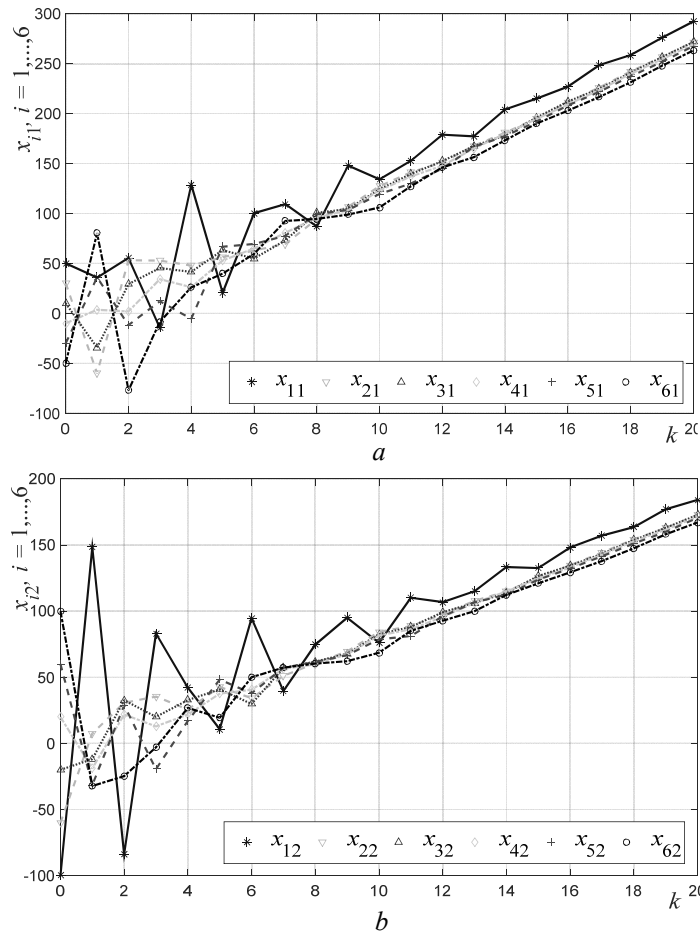
Fig. 4. Values of agents' states with fixed topology in the presence of setting action: *a* — first components of state vectors; *b* – second components of state vectors
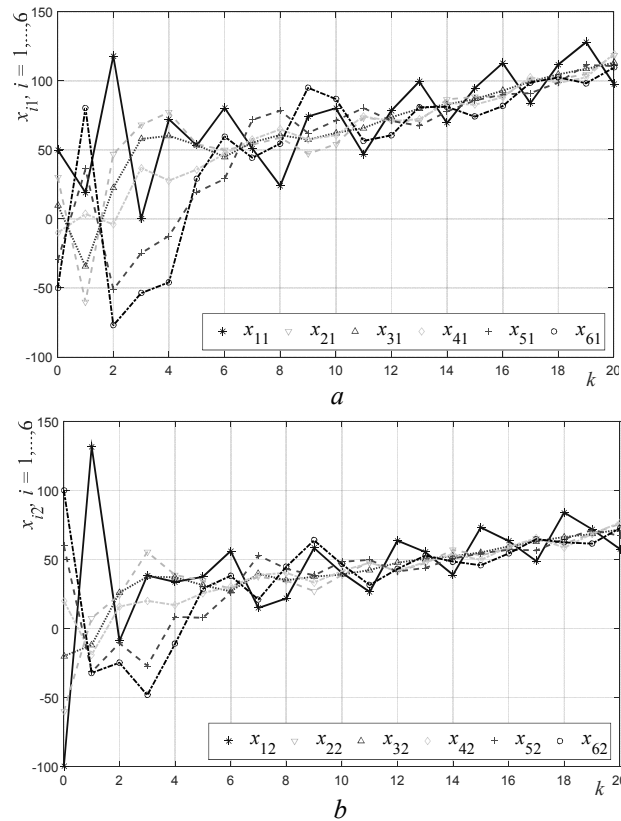
Fig. 5. Values of agent's states with switching topology in the presence of setting action: *a* — first components of state vectors; *b* — second components of state vectors

The analysis of the obtained results makes it possible to conclude that the consensus protocol (5) with the gain matrices calculated in accordance with the proposed decentralized method, can achieve consensus in a finite number of steps for any variant of the interconnection topology between agents from a given finite set.

CONCLUSIONS

The problem of decentralized consensus control of linear discrete-time multi-agent systems with switching topology in the presence of a leader is solved in this paper. A consensus protocol providing coordinating control is constructed in a feedback form with a PID controller using the deviation signal of the local agent state vector from the weighted average state vector of its neighbours. The discrete PID controller equation is presented in a recurrent form. The sufficient conditions for stabilization of the closed-loop local agent and the global consensus by constructing the quadratic Lyapunov function are obtained. Based on the invariant ellipsoid's method, the problem of local controller design is reduced to the problem of semidefinite programming, which is solved numerically. Analysis of the obtained results allowed us to conclude that the values of the gain matrices of local controllers depend on the number of neighbours with which the agent exchanges information in the current period. The significance of this study is to develop a practically realizable method for solving the consensus control problem of

discrete-time multi-agent systems with switching topology based on a decentralized approach, which does not require using the graph Laplacian that describes the connection topology between agents. The proposed approach may be further expanded to solve the consensus control problems of multi-agent systems in the presence of delays in measurements or in the process of information exchange between agents.

REFERENCES

1. J. Lunze, *Networked control of multi-agent systems*; 2nd edition, 2022, 725 p.
2. M. Mahmoud, M. Oyedeji, and Y. Xia, *Advanced distributed consensus for multi-agent systems*, 2020, 394 p.
3. Z. Qu, *Cooperative control of dynamical systems: applications to autonomous vehicles*. Springer, 2009, 325 p.
4. R.O. Saber, R.M. Murray, "Consensus protocols for networks of dynamic agents," *Proceedings of the 2003 American Control Conference*, pp. 951–956, 2003. doi: 10.1109/ACC.2003.1239709.
5. Z. Li, Z. Duan, *Cooperative control of multi-agent systems: a consensus region approach*. CRC Press, 2017, 262 p.
6. Y. Li, C. Tan, "A survey of the consensus for multi-agent systems," *Systems Science and Control Engineering*, vol. 7, no. 1, pp. 468–482, 2019. doi: 10.1080/21642583.2019.1695689.
7. M. Mesbahi, M. Egerstedt, *Graph theoretic methods in multi-agent networks*. Princeton University Press, 2010, 424 p.
8. M.S. Mahmoud, G.D. Khan, "LMI consensus condition foe discrete-time multi-agent systems, *IEEE/CAA Journal of Automatica Sinica*, vol. 5, no. 2, pp. 509–513, 2018. doi: 10.1109/JAS.2016.7510016.
9. X. Deng, X. Sun, and S. Liu, "Leader-following consensus control of nonlinear multi-agent systems with input constraint," *International Journal of Aeronautical and Space Sciences*, vol. 20, pp. 195–203, 2019. doi: 10.1007/s42405-018-0100-9.
10. L. Dong, S.K. Nguang, (Eds.) *Consensus tracking of multi-agent systems with switching topologies*. Academic Press, 2020, 257 p.
11. W. Ren, R.W. Beard, "Consensus seeking in multi-agent systems under dynamically changing interaction topologies," *IEEE Transactions on Automatic Control*, vol. 50, no. 5, pp. 655–661, 2005. doi: 10.1109/TAC.2005.846556.
12. W. Ni, D.Z. Cheng, "Leader-following consensus of multi-agent systems under and fixedn and switching topologies," *System and Control Letters*, vol. 59. no. 3–4, pp. 209–217. 2010. doi: 10.1016/j.sysconle.2010.01.006.
13. F. Xiao, L. Wang, "State consensus for multi-agent systems with switching topologies and time-varying delays," *International Journal of Control*, vol. 79, no. 10, pp. 1277–1284, 2006. doi: 10.1080/00207170600825097.
14. L.X. Gao, C.F. Tong, and L.Y. Wang, "H∞ dynamic output feedback consensus control for discrete-time multi-agent systems with switching topologies," *Arabian Journal for Science and Engineering*, vol. 39, no. 2, pp. 1477–1478, 2013. doi: 10.1007/s13369-013-0807-7.
15. C. Wang, J. Wang, P. Wu, and J. Gao, "Consensus problem and formation control for heterogeneous multi-agent systems with switching topologies," *Electronics*, vol. 11, no. 16, 2598, 2022. doi: 10.3390/electronics11162598.
16. G. Wen, X. Yu, W. Yu, and J. Lu, "Coordination and control of complex network systems with switching topologies: a survey," *IEEE Transactiions on Systems, Man, and Cybernetics: Systems*, vol. 51, no. 10, pp. 6242–6357, 2021. doi: 10.1109/TSMC.2019.2961753.

17. Q. Li, Z.P. Jiang, "Two decentralized heading consensus algorithms for nonlinear multi-agent systems," *Asian Journal of Control*, vol. 10, no. 2, pp. 187–200, 2008. doi: doi.org/10.1002/asjc.18.

18. S. Ge, C. Yang, Y. Li, and T.-H. Lee, "Decentralized adaptive control of a class of discrete-time multi-agent systems for hidden leader following problem," *2009 IEEE/RSJ International Conference on Intelligent Robots and Systems*, pp. 5065–5070, 2009. doi: 10.1109/IROS.2009.5354393.

19. Z. Hu, D. Fu, and H.-T. Zhang, "Decentralized finite time consensus for discrete-time high-order linear multi-agent system," *2019 Chinese Control Conference*, pp. 6154–6159, 2019. doi: 10.23919/ChiCC.2019.8866099.

20. Y. Yuan, G.-B. Stan, L. Shi, M. Barahona, and J. Goncalves, "Decentralized minimum-time consensus," *Automatica*, vol. 49, pp. 1227–1235, 2013. doi: 10.1016/j.automatica.2013.02.015.

21. C. Xu, B. Wu, D. Wang, and Y. Zhang, "Decentralized event-triggered finite-time attitude consensus control of multiple spacecraft under directed graph", *Journal of the Franklin Institute*, vol. 358, no. 18, pp. 9794–9817, 2021. doi: 10.1016/j.jfranklin.2021.10.019.

22. H. Gu, P. Liu, J. Lü, and Z. Lin, "PID control for synchronization of complex dynamical networks with directed topologies," *IEEE Transactions on Cybernetics*, vol. 51, no. 3, pp. 1334–1346, 2021. doi: 10.1109/TCYB.2019.2902810.

23. C.-X. Shi, G.-H. Yang, "Robust consensus control for a class of multi-agent systems via distributed PID algorithm and weighted edge dynamics," *Applied Mathematics and Computation*, vol. 316, pp. 73–88, 2018. doi: 10.1016/j.amc.2017.07.069.

24. D. Wang, N. Zhang, J. Wang, and W. Wang, "A PD-like protocol with a time delay to average consensus control for multi-agent systems under an arbitrarily fast switching topology," *IEEE Transactions on Cybernetics*, vol. 47, pp. 898–907, 2017. doi: 10.1109/TCYB.2016.2532898.

25. G. Fiengo, D.G. Lui, A. Petrillo, S. Santini, and M. Tufo, "Distributed robust PID control for leader tracking in uncertain connected ground vehicles with v2v communication delay," *IEEE/ASME Transactions on Mechatronics*, vol. 24, pp. 1153–1165, 2019. doi: 10.1109/TMECH.2019.2907053.

26. D.A. Burbano Lombana, M. di Bernardo, "Distributed PID control for consensus of homogeneous and heterogeneous networks," *IEEE Transactions on Control of Network Systems*, vol. 2, no. 2, pp. 154–163, 2015. doi: 10.1109/TCNS.2014.2378914.

27. D.A. Burbano Lombana, M. di Bernardo, "Multiplex PI control for consensus in networks of heterogeneous linear agents," *Automatica*, vol. 67, pp. 310–320, 2016. doi: 10.1016/j.automatica.2016.01.039.

28. D.G. Lui, A. Petrillo, and S. Santini, "An optimal distributed PID-like control for the output containment and leader-following of heterogeneous high-order multi-agent systems," *Information Sciences*, vol. 541, pp. 166–184, 2020. doi: 10.1016/j.ins.2020.06.049.

29. L. Lyubchyk, Y. Dorofieiev, "Consensus control of multi-agent systems with input delays: a descriptor model approach," *Mathematical Modeling and Computing*, vol. 6, no. 2, pp. 333–343, 2019. doi: 10.23939/mmc2019.02.333.

30. G. Herrmann, M.C. Turner, and I. Postlethwaite, "Linear matrix inequalities in control," in Turner M.C., Bates D.G. (eds), *Lecture Notes in Control and Information Sciences*, vol. 367, pp. 123–142, 2007.

31. A. Poznyak, A. Polyakov, and V. Azhmyakov, *Attractive ellipsoids in robust control*. Birkhäuser. Springer International Publishing, 2014, 348 p.

32. F. Zhang, "The Schur complement and its applications," *Numerical Methods and Algorithms*, vol. 4, Springer, 2005. doi: 10.1007/b105056.

33. M. Grant, S. Boyd, CVX: *MATLAB software for disciplined convex programming, version* 2.2, January 2020. Available: https://cvxr.com/cvx

34. J.F. Sturm, "Using SeDuMi 1.02, a MATLAB toolbox for optimization over symmetric cones," *Optimisation Methods and Software*, vol. 11, pp. 625–653, 1999. doi: 10.1080/10556789908805766.

35. Y.I. Dorofieiev, L.M. Lyubchyk, and A.A. Nikulchenko, "Consensus decentralized control of multi-agent networked systems using vector Lyapunov functions," *9th IEEE Intern. Conf. on Intelligent Data Acquisition and Advanced Computing Systems: Technolgy Application*, vol. 1, pp. 60–65, 2017. doi: 10.1109/IDAACS.2017.8095050.

INFORMATION ON THE ARTICLE

Yurii I. Dorofieiev, ORCID: 0000-0002-7964-1286, National Technical University "Kharkiv Polytechnic Institute", Ukraine, e-mail: yurii.dorofieiev@khpi.edu.ua

Leonid M. Lyubchyk, ORCID: 0000-0003-0237-8915, National Technical University "Kharkiv Polytechnic Institute", Ukraine, e-mail: leonid.liubchyk@khpi.edu.ua

Maxim M. Malko, ORCID: 0000-0002-0125-2141, National Technical University "Kharkiv Polytechnic Institute", Ukraine, e-mail: maxim.malko@khpi.edu.ua

СИНТЕЗ ДЕЦЕНТРАЛІЗОВАНОГО КОНСЕНСУСНОГО КЕРУВАННЯ ДЛЯ МУЛЬТИАГЕНТНИХ ДИСКРЕТНИХ СИСТЕМ З КОМУТАЦІЙНОЮ ТОПОЛОГІЄЮ ЗА НАЯВНОСТІ ЛІДЕРА / Ю.І. Дорофєєв, Л.М. Любчик, М.М. Малько

Анотація. Розглянуто задачу консенсусного керування лінійними мультиагентними дискретними системами (МАС) з комутаційною топологією за наявності лідера. Мета консенсусного керування полягає у зведенні станів усіх агентів до стану лідера з одночасним забезпеченням стійкості локальних агентів, а також МАС у цілому. На відміну від традиційного підходу, який використовує концепцію розширеної динамічної моделі мультиагентної системи та лапласіан графу комунікаційної топології, запропоновано підхід на основі декомпозиції, який передбачає незалежне проєктування локальних регуляторів. Закон керування вибирається у вигляді розподіленого зворотного зв'язку з дискретними ПІД-регуляторами. Задачу синтезу локальних регуляторів за допомогою методу інваріантних еліпсоїдів зведено до набору задач напіввизначеного програмування. Достатні умови стабілізації агентів та досягнення глобального консенсусу отримано за допомогою техніки лінійних матричних нерівностей. Наявність інформації про кінцевий набір можливих конфігурацій зв'язків між агентами дозволяє синтезувати локальні регулятори в автономному режимі на етапі проєктування. Ефективність запропонованого підходу продемонстровано за допомогою числового прикладу.

Ключові слова: мультиагентна система, консенсусне керування, комутаційна топологія, ПІД регулятор, метод інваріантних еліпсоїдів, лінійна матрична нерівність, задача напіввизначеного програмування.

ПРОЕКЦІЯ ГРАДІЄНТА: СПРОЩЕННЯ ОБЛАСТІ МІНІМІЗАЦІЇ АФІННИМ ПЕРЕТВОРЕННЯМ

І.Я. СПЕКТОРСЬКИЙ

Анотація. Розглянуто класичну задачу оптимізації у скінченновимірному просторі, тобто знаходження мінімуму функції на непорожній множині. Пошук точного розв'язку цієї задачі аналітичними методами потребує множинних обчислювальних ресурсів або взагалі неможливий. Для реальних задач частіше застосовують методи пошуку наближеного розв'язку, серед яких одним з найпростіших і найвідоміших для задач безумовної оптимізації є метод градієнтного спуску. Узагальненням методу градієнтного спуску на випадок умовної оптимізації є запропонований у 1964 р. метод проекції градієнта. Для деяких типів множини (відрізок, паралелепіпед, куля) проекцію точки на множину можна знайти простими явними формулами, проте для складніших (напр., еліпс) проектування стає окремою задачею мінімізації. Однак у деяких випадках обчислення проекції не можна спростити афінним перетворенням — напр., еліпс афінним (і навіть лінійним) перетворенням можна звести до кулі. Спрощено задачу мінімізації функції на множині застосуванням афінного перетворення $F(x) = Ax+b$, де A — невироджена квадратна матриця, b — фіксований вектор відповідної розмірності.

Ключові слова: проекція градієнта, мінімізація, афінне перетворення.

ВСТУП

Класичною задачею оптимізації у скінченновимірному просторі є знаходження мінімуму функції $f : \mathbb{R}^n \to \mathbb{R}$ на непорожній множині $D \subset \mathbb{R}^n$ (тут і надалі символ «$\subset$» позначає нестроге вкладення, тобто можливий випадок $D = \mathbb{R}^n$ — задача безумовної оптимізації). Як правило, пошук точного розв'язку цієї задачі аналітичними методами потребує надто багато обчислювальних ресурсів або взагалі неможливий. Тому для реальних задач найчастіше застосовують методи пошуку наближеного розв'язку, серед яких одним з найпростіших і найвідоміших для задач безумовної оптимізації є метод градієнтного спуску (див., напр., [1–6]). Узагальненням методу градієнтного спуску на випадок умовної оптимізації ($D \subset \mathbb{R}^n$) є запропонований у 1964 р. метод проекції градієнта (див. [7]). Для деяких типів множини D (відрізок, паралелепіпед, куля) проекцію точки $x \in \mathbb{R}^n$ на D можна знайти простими явними формулами, проте для дещо складніших областей (напр., якщо $D \subset \mathbb{R}^2$ — еліпс) проектування стає окремою задачею мінімізації. Однак у деяких випадках обчислення проекції на D можна спростити афінним перетворенням — напр., еліпс афінним (і навіть лінійним) перетворенням можна звести до кулі.

Мета роботи — звести задачу мінімізації функції $f : \mathbb{R}^n \to \mathbb{R}$ на множині $D \subset \mathbb{R}^n$ до мінімізації функції $\widetilde{f}(\widetilde{x}) = f(F^{-1}(\widetilde{x}))$ на множині

$$\widetilde{D} = \{Ax + b : x \in D\} = F(D), \text{ де } F(x) = Ax + b, \quad A \text{ — невироджена матриця}$$

розмірності $n \times n$, $b \in \mathbb{R}^n$ — фіксований вектор.

ОПУКЛІ МНОЖИНИ ТА ФУНКЦІЇ

Означення 1. Множину $D \subset \mathbb{R}^n$ називають опуклою, якщо $\lambda x + (1-\lambda)y \in D$ для будь-яких $x \in D, y \in D, \lambda \in [0,1]$. Інакше кажучи, D є опуклою, якщо разом з точками $x \in D, y \in D$ містить відрізок $[x, y]$:

$$\left.\begin{array}{l} x \in D, \\ y \in D \end{array}\right\} \Rightarrow [x, y] = \{\lambda x + (1-\lambda)y : \lambda \in [0,1]\} \subset D.$$

Приклад 1. На площині (простір $\mathbb{R}^2$) будь-який круг є опуклою фігурою (множиною), будь-яке коло — ні (рис. 1). Інші приклади опуклих та неопуклих фігур зображено на рис. 2.
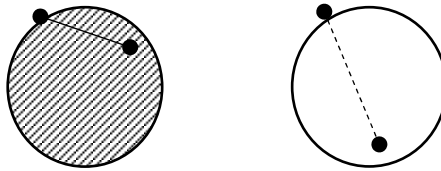
Круг — опукла фігура   Коло — неопукла фігура

Рис. 1. Круг і коло — властивість опуклості
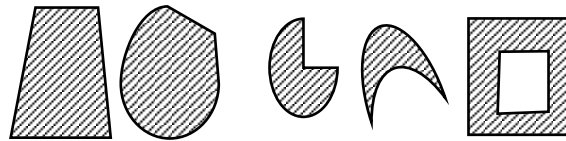
Опуклі фігури   Неопуклі фігури

Рис. 2. Опуклі та неопуклі фігури

Зауваження 1. Надалі вважатимемо, що будь-який еліпс та будь-який багатокутник містять внутрішню ділянку, яку вони обмежують. Таким чином, еліпс та трикутник завжди є опуклими фігурами, однак чотирикутник може не бути опуклим (рис. 3).
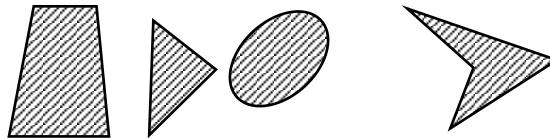
Опуклі фігури   Неопуклі фігури

Рис. 3. Еліпс та багатокутники — властивість опуклості

Означення 2. Функцію $f : \mathbb{R}^n \to \mathbb{R}$ називають опуклою, якщо для будь-яких $x \in D, y \in D, \lambda \in [0,1]$ справджується нерівність

$$f(\lambda x + (1-\lambda)y) \le \lambda f(x) + (1-\lambda)f(y). \tag{1}$$

Означення 3. Функцію $f : \mathbb{R}^n \to \mathbb{R}$ називають строго опуклою, якщо для будь-яких $x \in D, y \in D, \lambda \in (0,1)$, таких, що $x \ne y$, справджується нерівність

$$f(\lambda x + (1-\lambda)y) < \lambda f(x) + (1-\lambda)f(y).$$

Приклад 2. 1. Одновимірна ($n=1$) лінійна функція $f_1(x) = bx + c$ за будь-яких фіксованих констант $b \in \mathbb{R}$, $c \in \mathbb{R}$ є опуклою, але не строго опуклою, оскільки для будь-якої $\lambda \in [0,1]$ нестрога нерівність (1) виконується, проте перетворюється в рівність:

$$f_1(\lambda x + (1-\lambda)y) = b(\lambda x + (1-\lambda)y) + c =$$

$$= \lambda(bx + c) + (1-\lambda)(by + c) = \lambda f_1(x) + (1-\lambda)f_1(y). \qquad (2)$$

2. Одновимірна квадратична функція $f_2(x) = ax^2$ ($a \in \mathbb{R}$ — фіксована константа) є опуклою тоді і тільки тоді, коли $a \geq 0$. Дійсно, для будь-якої $\lambda \in [0,1]$ маємо:

$$f_2(\lambda x + (1-\lambda)y) = a(\lambda x + (1-\lambda)y)^2 = a\lambda^2 x^2 + a(1-\lambda)^2 y^2 + 2a\lambda(1-\lambda)xy =$$

$$= a\lambda x^2 + a(1-\lambda)y^2 - a\lambda(1-\lambda)x^2 - a\lambda(1-\lambda)y^2 + 2a\lambda(1-\lambda)xy = \qquad (3)$$

$$= \lambda f_2(x) + (1-\lambda)f_2(y) - a\lambda(1-\lambda)(x-y)^2.$$

Очевидно, у випадку $a > 0$ функція $f_2(x) = ax^2$ є строго опуклою. Зазначимо, що отриманий результат з урахуванням рівностей (2) та (3) легко поширити на загальну одновимірну квадратичну функцію $f_3(x) = ax^2 + bx + c$; функція опукла, якщо $a \geq 0$ (зокрема, строго опукла, якщо $a > 0$); константи $b \in \mathbb{R}$, $c \in \mathbb{R}$ на опуклість (строгу опуклість) функції $ax^2 + bx + c$ не впливають.

Із означень 1 та 2 негайно випливає простий факт, що пов'язує обидва означення: функція $f : \mathbb{R}^n \to \mathbb{R}$ опукла тоді і тільки тоді, коли її надграфік $\mathrm{Epi}\, f = \{(x,y) \in \mathbb{R}^n \times \mathbb{R} : f(x) = y\}$ є опуклою множиною в просторі $\mathbb{R}^{n+1} = \mathbb{R}^n \times \mathbb{R}$. На рис. 4 схематично показано надграфіки функцій $f_1(x) = bx + c$ та $f_3(x) = ax^2 + bx + c$.
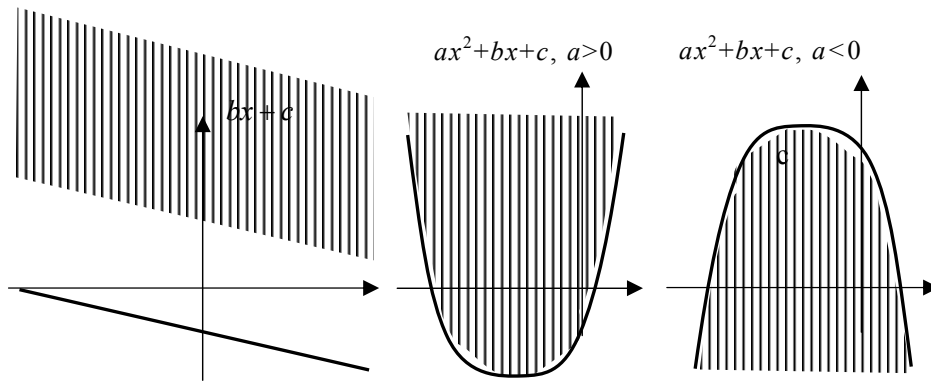
Рис.4. Надграфіки лінійної та квадратичної функцій

Означення 4. Функцію $f : \mathbb{R}^n \to \mathbb{R}$ називають сильно опуклою з параметром $\theta > 0$, якщо для будь-яких $x \in D$, $y \in D$, $\lambda \in [0,1]$ справджується нерівність

$$f(\lambda x + (1-\lambda)y) \leq \lambda f(x) + (1-\lambda)f(y) - \tfrac{1}{2}\theta\lambda(1-\lambda)\|x-y\|^2.$$

Приклад 3. Квадрат евклідової норми $\| x \|^2$ як функція $\| \cdot \|^2 : \mathbb{R}^n \to \mathbb{R}$ є сильно опуклою з параметром $\theta = 2$. Дійсно, для будь-якої $\lambda \in [0,1]$ аналогічно (3) отримуємо:

$$\| \lambda x + (1-\lambda) y \|^2 = (\lambda x + (1-\lambda) y, (\lambda x + (1-\lambda) y) =$$

$$= \lambda^2 \| x \|^2 + (1-\lambda)^2 \| y \|^2 + 2\lambda(1-\lambda)(x,y) =$$

$$= \lambda \| x \|^2 + (1-\lambda) \| y \|^2 - \lambda(1-\lambda) \| x - y \|^2 .$$

Зауваження 2. Деякі автори (напр., [4, 5, 8]), визначаючи сильну опуклість функції, випускають коефіцієнт $\frac{1}{2}$ у доданку перед параметром опуклості, що зменшує параметр опуклості вдвічі. Так, згідно з таким визначенням, функція $\| x \|^2$ є сильно опуклою з параметром $\theta = 1$.

Відомі критерії опуклості для гладких функцій. Так, для двічі неперервно диференційовної функції $f : \mathbb{R}^n \to \mathbb{R}$ справджуються логічні еквівалентності (див., напр., [2, 4–6, 8]):

• Функція f опукла тоді й тільки тоді, коли $(f'' h, h) \geq 0$ для будь-якого $h \in \mathbb{R}^n$ (гесіан f'' є невід'ємно визначеною матрицею).

• Функція f сильно опукла з параметром $\theta > 0$ тоді і тільки тоді, коли $(f'' h, h) \geq \theta \| h \|^2$ для будь-якого $h \in \mathbb{R}^n$ (матриця $f'' - \theta I_n$ є невід'ємно визначеною матрицею).

Для строго опуклих функцій аналогічна еквівалентність неправильна, проте справджується наслідок: для строгої опуклості функції f достатньо, щоб $(f'' h, h) > 0$ для будь-якого ненульового $h \in \mathbb{R}^n$ (гесіан f'' є додатно визначеною матрицею).

Приклад 4. Одновимірна функція $f(x) = x^4$ опукла, і навіть строго опукла. Дійсно, враховуючи строгу (навіть сильну) опуклість функції $g(x) = x^2$ (див. приклад 3) та строгу монотонність $g(x) = x^2$ на $[0,+\infty)$, отримуємо:

$$f(x) = g(g(x)) = (\lambda x + (1-\lambda) y)^4 = ((\lambda x + (1-\lambda) y)^2)^2 < (\lambda x^2 + (1-\lambda) y^2)^2 <$$

$$< \lambda^2 x^4 + (1-\lambda)^2 y^4 \leq \lambda x^4 + (1-\lambda) y^4 = \lambda f(x) + (1-\lambda) f(y)$$

для будь-якої $\lambda \in (0,1)$. Проте функція $f(x) = x^4$ не сильно опукла, оскільки для будь-якої константи $\theta > 0$ нерівність $f''(x) = 12 x^2 \geq \theta$ не справджується для $| x | \leq \sqrt{\frac{\theta}{12}}$.

Сформулюємо у вигляді лем три відомі (див., напр., [2, 4, 5, 8]) властивості щодо мінімізації опуклої функції на опуклій множині.

Лема 1. Нехай $D \subset \mathbb{R}^n$ — опукла множина, . $f : \mathbb{R}^n \to \mathbb{R}$ — опукла функція, $x^* \in D$ — локальний мінімум f на D, тобто існує таке $\varepsilon > 0$, що $f(x^*) \leq f(x)$ для всіх $x \in D$, для яких $\| x - x^* \| < \varepsilon$. Тоді $x^* \in D$ — глобальний мінімум f на D, тобто $f(x^*) \leq f(x)$ для всіх $x \in D$.

Доведення. Нехай $x^* \in D$ — локальний мінімум f на D, $\varepsilon > 0$ — таке число, що $f(x^*) \le f(x)$ для всіх $x \in D$, для яких $\|x - x^*\| \le \varepsilon$. Зафіксуємо довільне $a \in D$. Тоді для $\lambda = \frac{\varepsilon}{2} \min\left(\frac{1}{\|x^*\|}, \frac{1}{\|a\|}\right)$ маємо: $\|(\lambda a + (1-\lambda)x^*) - x^*\| =$ $= \|\lambda a - \lambda x^*\| \le \lambda(\|a\| + \|x^*\|) \le \varepsilon$, звідки, з урахуванням опуклості множини D та функції f, $f(x^*) \le f(\lambda a + (1-\lambda)x^*) \le \lambda f(a) + (1-\lambda)f(x^*)$. Отже, $f(x^*) \le \lambda f(a) + (1-\lambda)f(x^*)$, звідки $\lambda f(x^*) \le \lambda f(a)$ і, оскільки $\lambda > 0$, $f(x^*) \le f(a)$. Таким чином, ураховуючи довільність вибору $a \in D$, точка $x^* \in D$ дійсно є глобальним мінімумом функції f на D. $\square$

Лема 2. Нехай $D \subset \mathbb{R}^n$ — опукла множина, . $f : \mathbb{R}^n \to \mathbb{R}$ — строго опукла функція. Тоді f досягає глобального мінімуму на D не більш ніж в одній точці.

Доведення. Припустимо, що f досягає глобального мінімуму y^* на D принаймні у двох різних точках $m_1 \in D$, $m_2 \in D$, тобто $f(m_1) =$ $= f(m_2) = y^*$, та $m_1 \ne m_2$. Тоді, враховуючи опуклість D та строгу опуклість f, отримуємо, що $\frac{m_1 + m_2}{2} \in D$ та $f\left(\frac{m_1 + m_2}{2}\right) < \frac{1}{2}(f(m_1) + f(m_2)) = y^*$, що суперечить глобальності мінімуму $f(m_1) = f(m_2) = y^*$ на множині D. $\square$

Лема 3. Нехай $D \subset \mathbb{R}^n$ — опукла множина, . $f : \mathbb{R}^n \to \mathbb{R}$ — сильно опукла функція. Тоді f досягає глобального мінімуму на D у точності в одній точці.

Доведення (див., напр., [4, 5, 8]) спирається на обгрунтуванні обмеженості знизу множин Лебега $D_v = \{\forall x \in D : f(x) \le v\}$ та неперервності f на $\mathbb{R}^n$.

Детальніше про властивості опуклих множин і функцій див., [2, 4–6, 8].

АФІННЕ ПЕРЕТВОРЕННЯ ОПУКЛИХ МНОЖИН ТА АРГУМЕНТІВ ОПУКЛИХ ФУНКЦІЙ

Уведемо до розгляду афінне перетворення $F : \mathbb{R}^n \to \mathbb{R}^n$, тобто відображення $F(x) = Ax + b$, де A — фіксована невироджена матриця розмірності $n \times n$, $b \in \mathbb{R}^n$ — фіксований вектор. Зазначимо, що завдяки невиродженості A існує обернене (також афінне) перетворення $F^{-1}(x) = A^{-1}x - A^{-1}b$.

Лема 4. Нехай $D \subset \mathbb{R}^n$ — непорожня опукла множина. Тоді опуклою є також множина $\widetilde{D} = \{Ax + b : x \in D\} = F(D)$.

Доведення. Нехай $\widetilde{x} \in \widetilde{D}, \widetilde{y} \in \widetilde{D}$. За визначенням множини $\widetilde{D}$, маємо елементи $x \in D$, $y \in D$, такі, що $\widetilde{x} = Ax + b$, $\widetilde{y} = Ay + b$, звідки $x = A^{-1}\widetilde{x} - A^{-1}b \in$ $\in D$, $y = A^{-1}\widetilde{y} - A^{-1}b \in D$. Тоді, зафіксувавши довільну $\lambda \in [0,1]$, отримуємо:

$$\lambda \widetilde{x} + (1-\lambda)\widetilde{y} = \lambda(Ax + b) + (1-\lambda)(Ay + b) =$$

$$= A(\lambda x + (1-\lambda)y + b) = F(\lambda x + (1-\lambda)y) \in \widetilde{D},$$

оскільки $\lambda x + (1-\lambda) y \in D$ завдяки опуклості D. Отже, $\lambda \widetilde{x} + (1-\lambda) \widetilde{y} \in \widetilde{D}$, що доводить опуклість множини $\widetilde{D}$.

Приклад 5. Розглянемо в $\mathbb{R}^2$ множину, обмежену прямокутником (сторони повернуті відносно координатних осей):

$$D = \left\{ \begin{pmatrix} x_1 \\ x_2 \end{pmatrix} : \begin{cases} 2 \le 3x_1 + 4x_2 \le 5 \\ 2 \le -4x_1 + 3x_2 \le 10 \end{cases} \right\}.$$

Очевидно, область D можна отримати афінним (навіть лінійним) перетворенням із прямокутника $\widetilde{D}$, сторони якого паралельні координатним осям: $\begin{pmatrix} 3x_1 + 4x_2 \\ -4x_1 + 3x_2 \end{pmatrix} = \begin{pmatrix} 3 & 4 \\ -4 & 3 \end{pmatrix} \begin{pmatrix} x_1 \\ x_2 \end{pmatrix} = 5 \begin{pmatrix} 0.6 & 0.8 \\ -0.8 & 0.6 \end{pmatrix} \begin{pmatrix} x_1 \\ x_2 \end{pmatrix}$. Таким чином, афінне перетворення $\begin{pmatrix} \widetilde{x}_1 \\ \widetilde{x}_2 \end{pmatrix} = F\left(\begin{pmatrix} x_1 \\ x_2 \end{pmatrix} \right) = \begin{pmatrix} 0.6 & 0.8 \\ -0.8 & 0.6 \end{pmatrix} \begin{pmatrix} x_1 \\ x_2 \end{pmatrix}$ (у даному випадку — поворот) переводить повернутий прямокутник $D = \left\{ \begin{pmatrix} x_1 \\ x_2 \end{pmatrix} : \begin{cases} 2 \le 3x_1 + 4x_2 \le 5 \\ 2 \le -4x_1 + 3x_2 \le 10 \end{cases} \right\}$

у прямокутник $\widetilde{D} = \left\{ \begin{pmatrix} \widetilde{x}_1 \\ \widetilde{x}_2 \end{pmatrix} : \begin{cases} 2 \le 5\widetilde{x}_1 \le 5 \\ 2 \le 5\widetilde{x}_2 \le 10 \end{cases} \right\} = \left\{ \begin{pmatrix} \widetilde{x}_1 \\ \widetilde{x}_2 \end{pmatrix} : \begin{cases} 0.4 \le \widetilde{x}_1 \le 1 \\ 0.4 \le \widetilde{x}_2 \le 2 \end{cases} \right\} = F(D)$,

сторони якого паралельні координатним осям (рис. 5).
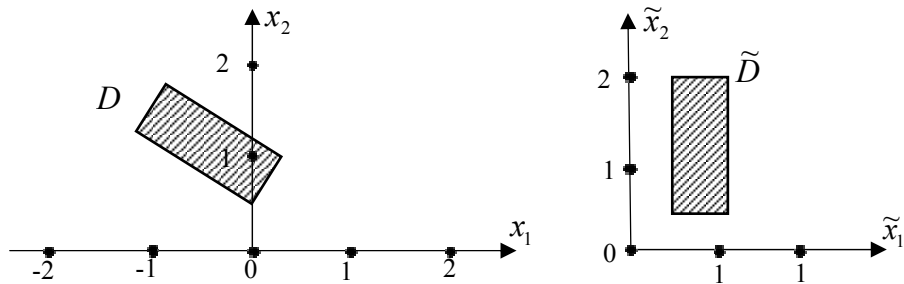
Рис. 5. Область $D = \left\{ \begin{pmatrix} x_1 \\ x_2 \end{pmatrix} : \begin{cases} 2 \le 3x_1 + 4x_2 \le 5 \\ 2 \le -4x_1 + 3x_2 \le 10 \end{cases} \right\}$ — повернутий прямокутник, область

$\widetilde{D} = \left\{ \begin{pmatrix} \widetilde{x}_1 \\ \widetilde{x}_2 \end{pmatrix} : \begin{cases} 0.4 \le \widetilde{x}_1 \le 1 \\ 0.4 \le \widetilde{x}_2 \le 2 \end{cases} \right\}$ — прямокутник, сторони якого паралельні координатним осям

Приклад 6. Розглянемо в $\mathbb{R}^2$ множину, обмежену кривою другого порядку:

$$D = \left\{ \begin{pmatrix} x_1 \\ x_2 \end{pmatrix} : 34(x_1 - 5)^2 + 41(x_2 + 10)^2 + 24(x_1 - 5)(x_2 + 10) \le 1 \right\} =$$

$$= \left\{ \begin{pmatrix} x_1 \\ x_2 \end{pmatrix} : \left(\begin{pmatrix} 34 & 12 \\ 12 & 41 \end{pmatrix} \begin{pmatrix} x_1 - 5 \\ x_2 + 10 \end{pmatrix}, \begin{pmatrix} x_1 - 5 \\ x_2 + 10 \end{pmatrix} \right) \le 1 \right\}.$$

Процедурою діагоналізації отримуємо:

$$\begin{pmatrix} 34 & 12 \\ 12 & 41 \end{pmatrix} = \begin{pmatrix} 0.6 & -0.8 \\ 0.8 & 0.6 \end{pmatrix} \begin{pmatrix} 50 & 0 \\ 0 & 25 \end{pmatrix} \begin{pmatrix} 0.6 & 0.8 \\ -0.8 & 0.6 \end{pmatrix}.$$

Оскільки матриця $\begin{pmatrix} 34 & 12 \\ 12 & 41 \end{pmatrix}$, як і матриця $\begin{pmatrix} 50 & 0 \\ 0 & 25 \end{pmatrix}$, є додатно визначеною, область D є повернутим та зсунутим еліпсом і може бути отримана афінним перетворенням з одиничного круга $\widetilde{D} = \left\{ \begin{pmatrix} \widetilde{x}_1 \\ \widetilde{x}_2 \end{pmatrix} : \widetilde{x}_1{}^2 + \widetilde{x}_2{}^2 \le 1 \right\}$, рис. 6.
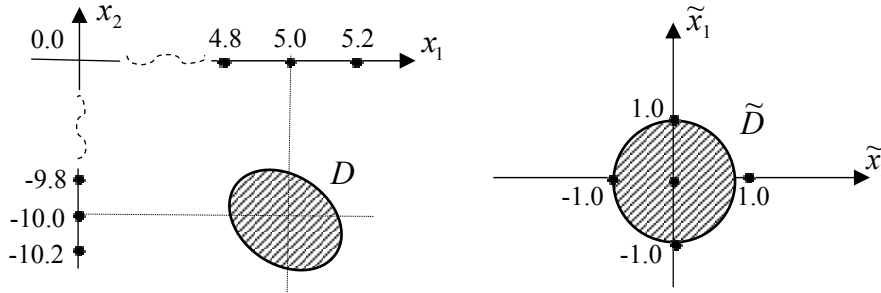
Рис. 6. Область D — еліпс $34(x_1 - 5)^2 + 41(x_2 + 10)^2 + 24(x_1 - 5)(x_2 + 10) \le 1$, область $\widetilde{D} = \left\{ \begin{pmatrix} \widetilde{x}_1 \\ \widetilde{x}_2 \end{pmatrix} : \widetilde{x}_1{}^2 + \widetilde{x}_2{}^2 \le 1 \right\}$ — одиничний круг

Еліптичну криву $34(x_1 - 5)^2 + 41(x_2 + 10)^2 + 24(x_1 - 5)(x_2 + 10) = 1$, або, у записі через квадратичну форму, $\left(\begin{pmatrix} 34 & 12 \\ 12 & 41 \end{pmatrix} \begin{pmatrix} x_1 - 5 \\ x_2 + 10 \end{pmatrix}, \begin{pmatrix} x_1 - 5 \\ x_2 + 10 \end{pmatrix} \right) = 1$, можна отримати з одиничного кола $x_1{}^2 + x_2{}^2 = 1$ послідовно зсувом, повертанням та розтягненням:

$$\left(\begin{pmatrix} 34 & 12 \\ 12 & 41 \end{pmatrix} \begin{pmatrix} x_1 - 5 \\ x_2 + 10 \end{pmatrix}, \begin{pmatrix} x_1 - 5 \\ x_2 + 10 \end{pmatrix} \right) = 1 \Leftrightarrow$$

$$\Leftrightarrow \left(\begin{pmatrix} 0.6 & -0.8 \\ 0.8 & 0.6 \end{pmatrix} \begin{pmatrix} 50 & 0 \\ 0 & 25 \end{pmatrix} \begin{pmatrix} 0.6 & 0.8 \\ -0.8 & 0.6 \end{pmatrix} \begin{pmatrix} x_1 - 5 \\ x_2 + 10 \end{pmatrix}, \begin{pmatrix} x_1 - 5 \\ x_2 + 10 \end{pmatrix} \right) = 1 \Leftrightarrow$$

$$\Leftrightarrow \left(\begin{pmatrix} 50 & 0 \\ 0 & 25 \end{pmatrix} \begin{pmatrix} 0.6 & 0.8 \\ -0.8 & 0.6 \end{pmatrix} \begin{pmatrix} x_1 - 5 \\ x_2 + 10 \end{pmatrix}, \begin{pmatrix} 0.6 & 0.8 \\ -0.8 & 0.6 \end{pmatrix} \begin{pmatrix} x_1 - 5 \\ x_2 + 10 \end{pmatrix} \right) = 1 \Leftrightarrow$$

$$\Leftrightarrow \left(\begin{pmatrix} 5\sqrt{2} & 0 \\ 0 & 5 \end{pmatrix} \begin{pmatrix} 5\sqrt{2} & 0 \\ 0 & 5 \end{pmatrix} \begin{pmatrix} 0.6 & 0.8 \\ -0.8 & 0.6 \end{pmatrix} \begin{pmatrix} x_1 - 5 \\ x_2 + 10 \end{pmatrix}, \begin{pmatrix} 0.6 & 0.8 \\ -0.8 & 0.6 \end{pmatrix} \begin{pmatrix} x_1 - 5 \\ x_2 + 10 \end{pmatrix} \right) = 1 \Leftrightarrow$$

$$\Leftrightarrow \left(\begin{pmatrix} 5\sqrt{2} & 0 \\ 0 & 5 \end{pmatrix} \begin{pmatrix} 0.6 & 0.8 \\ -0.8 & 0.6 \end{pmatrix} \begin{pmatrix} x_1 - 5 \\ x_2 + 10 \end{pmatrix}, \begin{pmatrix} 5\sqrt{2} & 0 \\ 0 & 5 \end{pmatrix} \begin{pmatrix} 0.6 & 0.8 \\ -0.8 & 0.6 \end{pmatrix} \begin{pmatrix} x_1 - 5 \\ x_2 + 10 \end{pmatrix} \right) = 1.$$

Отже, афінне перетворення

$$\begin{pmatrix} \widetilde{x}_1 \\ \widetilde{x}_2 \end{pmatrix} = F\left(\begin{pmatrix} x_1 \\ x_2 \end{pmatrix} \right) = \begin{pmatrix} 5\sqrt{2} & 0 \\ 0 & 5 \end{pmatrix} \begin{pmatrix} 0.6 & 0.8 \\ -0.8 & 0.6 \end{pmatrix} \begin{pmatrix} x_1 - 5 \\ x_2 + 10 \end{pmatrix} = \begin{pmatrix} 3\sqrt{2} & 4\sqrt{2} \\ -4 & 3 \end{pmatrix} \begin{pmatrix} x_1 \\ x_2 \end{pmatrix} + \begin{pmatrix} 25\sqrt{2} \\ 50 \end{pmatrix}$$

пов'язує одиничний круг $\widetilde{D} = \left\{ \begin{pmatrix} \widetilde{x}_1 \\ \widetilde{x}_2 \end{pmatrix} : \left(\begin{pmatrix} \widetilde{x}_1 \\ \widetilde{x}_2 \end{pmatrix}, \begin{pmatrix} \widetilde{x}_1 \\ \widetilde{x}_2 \end{pmatrix} \right) \leq 1 \right\} = \left\{ \begin{pmatrix} \widetilde{x}_1 \\ \widetilde{x}_2 \end{pmatrix} : \widetilde{x}_1^{\,2} + \widetilde{x}_2^{\,2} \leq 1 \right\}$ і

зсунутий повернутий еліпс

$$D = \left\{ \begin{pmatrix} x_1 \\ x_2 \end{pmatrix} : \left(\begin{pmatrix} 34 & 12 \\ 12 & 41 \end{pmatrix} \begin{pmatrix} x_1 - 5 \\ x_2 + 10 \end{pmatrix}, \begin{pmatrix} x_1 - 5 \\ x_2 + 10 \end{pmatrix} \right) \leq 1 \right\} =$$

$$= \left\{ \begin{pmatrix} x_1 \\ x_2 \end{pmatrix} : 34(x_1 - 5)^2 + 41(x_2 + 10)^2 + 24(x_1 - 5)(x_2 + 10) \leq 1 \right\} =$$

$$= \left\{ \begin{pmatrix} x_1 \\ x_2 \end{pmatrix} : \left(F \left(\begin{pmatrix} x_1 \\ x_2 \end{pmatrix} \right), F \left(\begin{pmatrix} x_1 \\ x_2 \end{pmatrix} \right) \right) \leq 1 \right\} = \left\{ F^{-1} \left(\begin{pmatrix} \widetilde{x}_1 \\ \widetilde{x}_2 \end{pmatrix} \right) : \widetilde{x}_1^{\,2} + \widetilde{x}_2^{\,2} \leq 1 \right\} = F^{-1}(\widetilde{D}).$$

Для матриці A уведемо позначення $\lambda_{\max} = \max\limits_{x \in \mathbb{R}^n \,: \|x\| = 1} (AA^{\mathrm{T}} x, x)$ та

$\lambda_{\min} = \min\limits_{x \in \mathbb{R}^n \,: \|x\| = 1} (AA^{\mathrm{T}} x, x)$ відповідно максимальне та мінімальне власне чи-

сло матриці AA^{T}; нагадаємо, що матриці AA^{T} та $A^{\mathrm{T}} A$ мають однаковий набір додатних (завдяки невиродженості A) власних чисел.

Лема 5. Нехай функція $f : \mathbb{R}^n \to \mathbb{R}$ — опукла (строго опукла, сильно опукла з параметром $\theta > 0$). Тоді функція $\widetilde{f} : \mathbb{R}^n \to \mathbb{R}$, $\widetilde{f}(\widetilde{x}) = f(F^{-1}(\widetilde{x})) = f(A^{-1}\widetilde{x} - A^{-1}b)$ теж опукла (відповідно строго опукла, сильно опукла з параметром $\theta \lambda_{\max}^{-1} > 0$).

Доведення. 1. Нехай функція $f : \mathbb{R}^n \to \mathbb{R}$ опукла. Зафіксувавши $\lambda \in [0,1]$, дістаємо:

$$\widetilde{f}(\lambda \widetilde{x} + (1-\lambda)\widetilde{y}) = f(\lambda(A^{-1}\widetilde{x} - A^{-1}b) + (1-\lambda)(A^{-1}\widetilde{y} - A^{-1}b)) \leq$$

$$\leq \lambda f(A^{-1}\widetilde{x} - A^{-1}b) + (1-\lambda)f(A^{-1}\widetilde{y} - A^{-1}b) = \lambda \widetilde{f}(\widetilde{x}) + (1-\lambda)\widetilde{f}(\widetilde{y})$$

для довільних $\widetilde{x} \in \mathbb{R}^n, \widetilde{y} \in \mathbb{R}^n$, що доводить опуклість функції g. $\qquad \square$

2. Нехай функція $f : \mathbb{R}^n \to \mathbb{R}$ строго опукла; $\widetilde{x} \in \mathbb{R}^n, \widetilde{y} \in \mathbb{R}^n$ і $\widetilde{x} \neq \widetilde{y}$. За умовою, матриця A невироджена, а отже, матриця A^{-1} існує і невироджена, звідки $A^{-1}\widetilde{x} - A^{-1}b \neq A^{-1}\widetilde{y} - A^{-1}b$. Зафіксувавши $\lambda \in (0,1)$, маємо

$$\widetilde{f}(\lambda \widetilde{x} + (1-\lambda)\widetilde{y}) = f(\lambda(A^{-1}\widetilde{x} - A^{-1}b) + (1-\lambda)(A^{-1}\widetilde{y} - A^{-1}b)) <$$

$$< \lambda f(A^{-1}\widetilde{x} - A^{-1}b) + (1-\lambda)f(A^{-1}\widetilde{y} - A^{-1}b) = \lambda \widetilde{f}(\widetilde{x}) + (1-\lambda)\widetilde{f}(\widetilde{y})$$

для довільних $\widetilde{x} \in \mathbb{R}^n, \widetilde{y} \in \mathbb{R}^n$, що доводить строгу опуклість функції $\widetilde{f}$. $\qquad \square$

3. Нехай функція $f : \mathbb{R}^n \to \mathbb{R}$ сильно опукла з параметром $\theta > 0$. Зазначимо, що матриця AA^T симетрична і, завдяки невиродженості матриці A, додатно визначена. Це означає, що всі власні числа матриці AA^T дійсні до-

датні числа. Очевидно, $\lambda_{\max}^{-1} = \min\limits_{x \in \mathbb{R}^n : \|x\|=1} ((AA^T)^{-1}x, x)$ — мінімальне власне

число матриці $(AA^T)^{-1}$. Отже, зафіксувавши $\lambda \in [0,1]$, отримуємо:

$$\widetilde{f}(\lambda\widetilde{x} + (1-\lambda)\widetilde{y}) = f(\lambda(A^{-1}\widetilde{x} - A^{-1}b) + (1-\lambda)(A^{-1}\widetilde{y} - A^{-1}b)) \leq$$

$$\leq \lambda f(A^{-1}\widetilde{x} - A^{-1}b) + (1-\lambda)f(A^{-1}\widetilde{y} - A^{-1}b) - \lambda(1-\lambda)\tfrac{\theta}{2}\| A^{-1}(\widetilde{x} - \widetilde{y})\|^2 =$$

$$= \lambda\widetilde{f}(\widetilde{x}) + (1-\lambda)\widetilde{f}(\widetilde{y}) - \lambda(1-\lambda)\tfrac{\theta}{2}(A^{-1}(\widetilde{x} - \widetilde{y}), A^{-1}(\widetilde{x} - \widetilde{y})) =$$

$$= \lambda\widetilde{f}(\widetilde{x}) + (1-\lambda)\widetilde{f}(\widetilde{y}) - \lambda(1-\lambda)\tfrac{\theta}{2}((AA^T)^{-1}(\widetilde{x} - \widetilde{y}),(\widetilde{x} - \widetilde{y})) \leq$$

$$\leq \lambda\widetilde{f}(\widetilde{x}) + (1-\lambda)\widetilde{f}(\widetilde{y}) - \lambda(1-\lambda)\tfrac{\theta}{2}\lambda_{\max}^{-1}$$

для довільних $\widetilde{x} \in \mathbb{R}^n$, $\widetilde{y} \in \mathbb{R}^n$, що доводить сильну опуклість функції $\widetilde{f}$ з параметром $\theta\lambda_{\max}^{-1}$.

Приклад 7. Нехай $f : \mathbb{R}^n \to \mathbb{R}$, $f(x) = \| x \|^2$. Функція $f(x) = \| x \|^2$ сильно опукла з параметром $\theta = 2$ (див. приклад 3), а отже, функція $\widetilde{f}(\widetilde{x}) = = \| F^{-1}(\widetilde{x})\|^2 = \| A^{-1}\widetilde{x} - A^{-1}b\|^2$ є сильно опуклою з параметром $\theta\lambda_{\max}^{-1} > 0$. Цікаво, що у випадку $b = 0$ білінійний функціонал $\langle \widetilde{x}, \widetilde{y} \rangle = ((AA^{\mathrm{T}})^{-1}\widetilde{x}, \widetilde{y})$, завдяки симетричності та додатній визначеності матриці $(AA^{\mathrm{T}})^{-1}$, визначає інший скалярний добуток, а функція $\langle\langle \widetilde{x}, \widetilde{x} \rangle\rangle = g(\widetilde{x}) = \| F^{-1}(\widetilde{x})\|^2 = \| A^{-1}\widetilde{x} \|^2$ іншу норму в $\mathbb{R}^n$.

У [4] наведено теорему про збереження опуклості функції (без умови строгої чи сильної опуклості) за застосування до аргумента довільного перетворення $Ax + b$.

ПРОЕКЦІЯ ТОЧКИ НА МНОЖИНУ

Означення 5. Проекцією точки $a \in \mathbb{R}^n$ на непорожню множину $D \subset \mathbb{R}^n$ називають точку $\mathrm{Pr}_D\, a \in D$, найближчу до a серед усіх точок $x \in D$:

$$\| \mathrm{Pr}_D\, a - a \| = \inf_{x \in D} \| x - a \|. \tag{4}$$

Оскільки норма $\| \cdot \|$ невід'ємна, рівність (4) можна подати через квадрат норми $\| \cdot \|^2$:

$$\| \mathrm{Pr}_D\, a - a \|^2 = \inf_{x \in D} \| x - a \|^2. \tag{5}$$

Очевидно, $\mathrm{Pr}_D\, a = a$ тоді й тільки тоді, коли $a \in D$.

Приклад 8. Для кола $D = \left\{ \begin{pmatrix} x_1 \\ x_2 \end{pmatrix} : (x_1 - x_{0,1})^2 + (x_2 - x_{0,2})^2 = r^2 \right\} \subset \mathbb{R}^2$

радіуса $r > 0$ із центром у $x_0 = \begin{pmatrix} x_{0,1} \\ x_{0,2} \end{pmatrix}$ проекцію точки $a = \begin{pmatrix} a_1 \\ a_2 \end{pmatrix} \neq \begin{pmatrix} x_{0,1} \\ x_{0,2} \end{pmatrix}$

можна обчислити за формулою $\mathrm{Pr}_D\, a = x_0 + \frac{r}{\|a-x_0\|}(a-x_0)$, тобто $\mathrm{Pr}_D\, a$

міститься на перетині відрізка $[x_0, a]$ з колом D (див. рис.7, *а, б*).; проекцією центра кола $a = x_0$ є кожна точка кола (рис. 7, *в*).
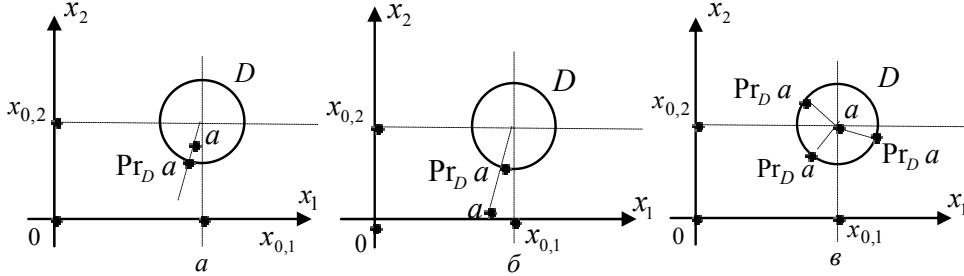
Рис. 7. Проекція точки на коло

Приклад 9. Для відкритого круга

$$D = \left\{ \begin{pmatrix} x_1 \\ x_2 \end{pmatrix} : (x_1 - x_{0,1})^2 + (x_2 - x_{0,2})^2 < r^2 \right\} \subset \mathbb{R}^2$$

радіуса $r > 0$ із центром в $x_0 = \begin{pmatrix} x_{0,1} \\ x_{0,2} \end{pmatrix}$ проекції точки $a \notin D$ ($\|a\| \geq r$) не
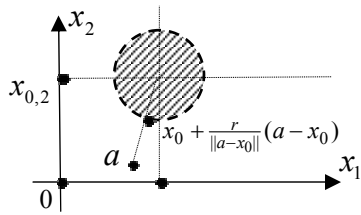
Рис. 8. Проекція точки на відкритий круг не існує

існує. Дійсно, $\inf\limits_{x \in D} \|x - a\| = \|x_0 - a\| + r$ міг би досягатись лише в точці $x_0 + \frac{r}{\|a-x_0\|}(a-x_0)$ (рис. 8), але $x_0 + \frac{r}{\|a-x_0\|}(a-x_0) \notin D$, оскільки

$$\|(x_0 + \frac{r}{\|a-x_0\|}(a-x_0)) - x_0\| = \|(\frac{r}{\|a-x_0\|}(a-x_0)\| =$$
$$= \frac{r}{\|a-x_0\|}\|a - x_0\| = r.$$

У загальному випадку точка $a \in \mathbb{R}^n$ може мати кілька проекцій на множину $D \subset \mathbb{R}^n$ (приклад 8) або не мати жодної (приклад 9). Проте відомий класичний факт (див., напр., [1, 4, 5]), який наводимо як лему.

Лема 6. 1. Нехай множина $D \subset \mathbb{R}^n$ непорожня і замкнена. Тоді будь-яка точка $a \in \mathbb{R}^n$ має принаймні одну проекцію на D.

2. Нехай множина $D \subset \mathbb{R}^n$ опукла. Тоді будь-яка точка $a \in \mathbb{R}^n$ має не більше однієї проекції на D.

Доведення. 1. Проекція $\mathrm{Pr}_D\, a$ на замкнену множину D існує за теоремою Веєрштраса: неперервна функція $\|\cdot\|:\mathbb{R}^n \to \mathbb{R}$ досягає свого найменшого значення $\inf\limits_{x \in D} \|x - a\| = \min\limits_{x \in D} \|x - a\|$ на непорожній замкненій множині $D \subset \mathbb{R}^n$.

2. Функція $\|\cdot\|^2:\mathbb{R}^n \to \mathbb{R}$ є строго (і навіть сильно) опуклою (див. приклад 3) і, за лемою 2, має не більше одного глобального мінімуму на опуклій множині $D \subset \mathbb{R}^n$. □

Приклад 10. 1. Нехай $D = \{x : \| x - x_0 \| \le r\} \subset \mathbb{R}^2$ замкнений круг раді-уса $r > 0$ із центром в $x_0 \in \mathbb{R}^2$. Очевидно, D опукла і замкнена і, за лемою 6, для будь-якого $a \in \mathbb{R}^2$ існує єдина проекція $\mathrm{Pr}_D\, a =$

$$= \begin{cases} a, \ a \in D; \\ x_0 + \frac{r}{\|a - x_0\|}(a - x_0), \ a \notin D \end{cases}$$ точки $a \in \mathbb{R}^2$ на множину D (див. приклад 8).

2. Нехай $D = \{x : m_i \le x_i \le M_i\, (i = 1,2)\} \subset \mathbb{R}^2$ прямокутник (рис. 9), визначений точками $m \in \mathbb{R}^2$, $M \in \mathbb{R}^2$, $m_i \le M_i\, (i = 1,2)$. Очевидно, D опукла і замкнена, і, за лемою 6, для будь-якого $a \in \mathbb{R}^2$ існує єдина проекція $\mathrm{Pr}_D\, a\ (i = 1,2)$:

$$(\mathrm{Pr}_D\, a)_i = \begin{cases} m_i; \\ a_i, m_i < a_i < M_i; \\ M_i, a_i \ge M_i, \end{cases}$$

Формули для проекцій на круг і прямокутник (сторони якого паралельні координатним осям), наведені у прикладі 10, природним чином узагальнюються на кулю та паралелепіпед у $\mathbb{R}^n$. Детальніше про проекції на деякі прості множини $D \subset \mathbb{R}^n$ (куля, паралелепіпед, півпростір та ін.) див., напр. [5]. Однак для проекцій на більш складні множини (зокрема, на еліпс) надати прості явні формули неможливо.
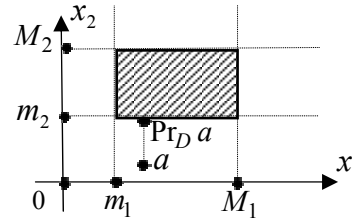
Рис. 9. Проекція точки на прямокутник

Приклад 11. Нехай

$$D = \left\{ \begin{pmatrix} x_1 \\ x_2 \end{pmatrix} : 34(x_1 - 5)^2 + 41(x_2 + 10)^2 + 24(x_1 - 5)\,(x_2 + 10) \le 1 \right\}$$

повернутий еліпс (див. приклад 6), $a = \begin{pmatrix} 5 \\ -9.7 \end{pmatrix}$. Оскільки $a \notin D$, проекція $\mathrm{Pr}_D\, a$ лежить на еліптичній кривій $34(x_1 - 5)^2 + 41(x_2 + 10)^2 + 24(x_1 - 5)\,(x_2 + 10) = 1$, яка обмежує область D. Застосовуючи до пошуку екстремуму у рівності (5) метод множників Лагранжа, запишемо відповідну функцію Лагранжа:

$$L(x_1, x_2, \lambda) = (x_1 - 5)^2 + (x_2 + 9.7)^2 - \lambda(34(x_1 - 5)^2 +$$
$$+ 41(x_2 + 10)^2 + 24(x_1 - 5)\,(x_2 + 10) - 1).$$

Мінімум функції $L(x_1, x_2, \lambda)$ можливий лише в нулях часткових похідних:

$$L'_{x_1}, L'_{x_2}, L'_\lambda : \begin{cases} 2(x_1 - 5) - \lambda(68(x_1 - 5) + 24(x_2 + 10)) = 0 \\ 2(x_2 + 9.7) - \lambda(24(x_1 - 5) + 82(10 + x_2)) = 0 \\ 34(x_1 - 5)^2 + 41(x_2 + 10)^2 + 24(x_1 - 5)\,(x_2 + 10) - 1 = 0 \end{cases} \quad (6)$$

Легко перевірити, що аналітичне розв'язання системи (6) зводиться до рівняння 4-го степеня відносно λ — такі рівняння, хоч і допускають явний розв'язок, але відповідні формули складні і містять радикали до 4-го степеня включно. Тому раціональним бачиться чисельне розв'язання системи (6), у результаті чого, після відкидання «зайвих» коренів (які не можуть бути мінімумом правої частини рівності (5)), отримуємо: $\mathrm{Pr}_D\, a \approx \begin{pmatrix} 4.9757 \\ -9.8381 \end{pmatrix}$ (множник $\lambda \approx -0.0218$, але це значення безпосередньо не входить до $\mathrm{Pr}_D\, a$), рис. 10.
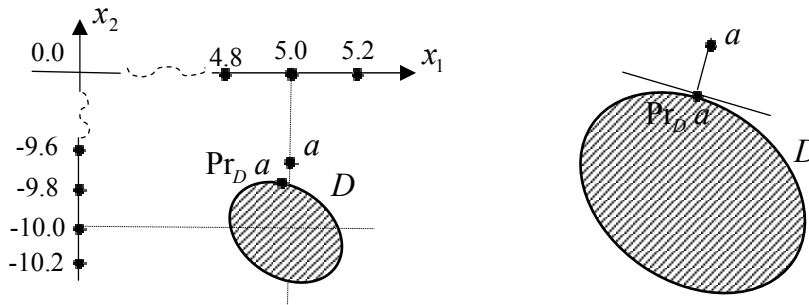
Рис. 10. Проекція точки на еліпс $34(x_1 - 5)^2 + 41(x_2 + 10)^2 + 24(x_1 - 5)(x_2 + 10) \le 1$

Приклад 12. Нехай $D = \left\{ \begin{pmatrix} x_1 \\ x_2 \end{pmatrix} : \begin{cases} 2 \le 3x_1 + 4x_2 \le 5 \\ 2 \le -4x_1 + 3x_2 \le 10 \end{cases} \right\}$ повернутий прямокутник (див. приклад 5), $a = \begin{pmatrix} 1 \\ 4 \end{pmatrix}$.

Для обчислення $\mathrm{Pr}_D\, a$ проаналізуємо розташування точки a відносно пар паралельних прямих $3x_1 + 4x_2 = 2$ і $3x_1 + 4x_2 = 5$ та $-4x_1 + 3x_2 = 2$ і $-4x_1 + 3x_2 = 10$. Оскільки $3 \cdot 1 + 4 \cdot 4 = 19 \ge 5$, проекція $\mathrm{Pr}_D\, a$ лежить на прямій $3x_1 + 4x_2 = 5$. Оскільки $2 < -4 \cdot 1 + 3 \cdot 4 = 8 < 10$, проекція $\mathrm{Pr}_D\, a$ ле-

жить на прямій, яка проходить через точку a та паралельна прямим $-4x_1 + 3x_2 = 2$ і $-4x_1 + 3x_2 = 10$, тобто на прямій $-4(x_1 - 1) + 3(x_2 - 4) = 0$, або, в іншому вигляді, на прямій $-4x_1 + 3x_2 = 8$. Розв'язуючи систему $\begin{cases} 3x_1 + 4x_2 = 5 \\ -4x_1 + 3x_2 = 8 \end{cases}$, дістаємо: $\mathrm{Pr}_D\, a =$
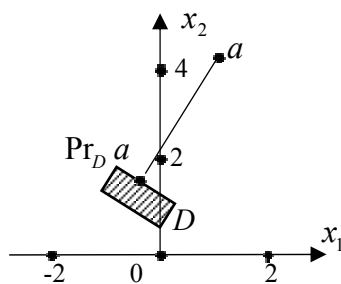
Рис. 11. Проекція точки на прямокутник $\begin{cases} 2 \le 3x_1 + 4x_2 \le 5 \\ 2 \le -4x_1 + 3x_2 \le 10 \end{cases}$

$= \begin{pmatrix} -\frac{17}{25} \\ \frac{44}{25} \end{pmatrix} = \begin{pmatrix} -0.68 \\ 1.76 \end{pmatrix}$, рис. 11.

Зауваження 3. У прикладах 11 і 12 вектор $a - \mathrm{Pr}_D\, a$ ортогональний дотичній у точці a до кривої, що обмежує область D (рис. 10 та 11 відповідно). Така властивість є загальною і поширюється на множини D з негладкою межею (див., напр., [1, 4, 5]).

АФІННЕ ПЕРЕТВОРЕННЯ В ОПЕРАТОРІ ПРОЕКТУВАННЯ

Нехай $D \subset \mathbb{R}^n$ — непорожня опукла та замкнена множина, a довільна точка в $\mathbb{R}^n$. Згідно з лемою 6, проекція $\mathrm{Pr}_D\, a$ існує і єдина, тобто інфімум у рівності (4) досягається у єдиній точці $\mathrm{Pr}_D\, a = \underset{x \in D}{\arg\min} \| x - a \|$.

Розглянемо заміну змінних $\widetilde{x} = F(x)$ за афінним перетворенням $F : \mathbb{R}^n \to \mathbb{R}^n$, $F(x) = Ax + b$ (A — невироджена матриця розмірності $n \times n$, $b \in \mathbb{R}^n$). Позначивши, як і в п. 0, $\widetilde{D} = \{ F(x) : x \in D \} = F(D)$, $\widetilde{x} = F(x)$, $\widetilde{a} = F(a)$, уведемо оператор $\mathrm{Pr}_D^F\, a$, пов'язаний з обчисленням проекції $\mathrm{Pr}_{\widetilde{D}}\, \widetilde{a}$ з подальшою заміною змінних $\widetilde{x} = F(x)$:

$$\mathrm{Pr}_D^F\, a = F^{-1}(\mathrm{Pr}_{\widetilde{D}}\, \widetilde{a}) \qquad (7)$$

Очевидно, множина $\widetilde{D} = F(D)$ є непорожньою, за лемою 4 $\widetilde{D} = F(D)$ є опуклою і, завдяки замкненості множини D та неперервності відображення F — замкненою. Таким чином, проекція $\mathrm{Pr}_{\widetilde{D}}\, \widetilde{a}$ за лемою 6 існує і єдина.

Ураховуючи визначення оператора $\mathrm{Pr}_D\, a$, подамо рівність (7) через $\arg\min$:

$$\mathrm{Pr}_D^F\, a = F^{-1}(\underset{\widetilde{x} \in \widetilde{D}}{\arg\min} \| \widetilde{x} - \widetilde{a} \|) = \underset{\widetilde{x} \in \mathbb{R}^n : F^{-1}(\widetilde{x}) \in F^{-1}(\widetilde{D})}{\arg\min} \| F(x) - F(a) \| =$$

$$= \underset{x \in D}{\arg\min} \| (Ax + b) - (Aa + b) \| = \underset{x \in D}{\arg\min} \| A(x - a) \| = \underset{x \in D}{\arg\min} \| x - a \|_F .$$

Отже, оператор $\mathrm{Pr}_D^F\, a$, як і оператор $\mathrm{Pr}_D\, a$, визначає на D точку, найближчу до a, але найближчу — у сенсі метрики, визначеної нормою $\| x \|_F = \| A x \|$ (див. також приклад 7). Зазначимо, що норма $\| x \|_F = \| A x \|$ (а отже, і оператор $\mathrm{Pr}_D^F\, a$) визначається матрицею A і не залежить від b. Очевидно, що у випадку ортогональної матриці A маємо рівність норм:

$$\| x \|_F^2 = \| A x \|^2 = (Ax, Ax) = (x, x) = \| x \|^2 ,$$

а отже, $\mathrm{Pr}_D^F\, a = \mathrm{Pr}_D\, a$.

Приклад 13. Розглянемо в $\mathbb{R}^2$ еліпс (див. приклади 6 і 11):

$$D = \left\{ \begin{pmatrix} x_1 \\ x_2 \end{pmatrix} : 34(x_1 - 5)^2 + 41(x_2 + 10)^2 + 24(x_1 - 5)(x_2 + 10) \le 1 \right\} =$$

$$= \left\{ \begin{pmatrix} x_1 \\ x_2 \end{pmatrix} : \left(\begin{pmatrix} 34 & 12 \\ 12 & 41 \end{pmatrix} \begin{pmatrix} x_1 - 5 \\ x_2 + 10 \end{pmatrix}, \begin{pmatrix} x_1 - 5 \\ x_2 + 10 \end{pmatrix} \right) \le 1 \right\} =$$

$$= \left\{ \begin{pmatrix} x_1 \\ x_2 \end{pmatrix} : \left(\begin{pmatrix} 3\sqrt{2} & 4\sqrt{2} \\ -4 & 3 \end{pmatrix} \begin{pmatrix} x_1 \\ x_2 \end{pmatrix} + \begin{pmatrix} 25\sqrt{2} \\ 50 \end{pmatrix}, \begin{pmatrix} 3\sqrt{2} & 4\sqrt{2} \\ -4 & 3 \end{pmatrix} \begin{pmatrix} x_1 \\ x_2 \end{pmatrix} + \begin{pmatrix} 25\sqrt{2} \\ 50 \end{pmatrix} \right) \le 1 \right\} .$$

Очевидно (див. також приклад 6), еліпс D пов'язаний з одиничним кругом $\widetilde{D} = \left\{ \begin{pmatrix} \widetilde{x}_1 \\ \widetilde{x}_2 \end{pmatrix} : \widetilde{x}_1{}^2 + \widetilde{x}_2{}^2 \le 1 \right\}$ афінним перетворенням $\begin{pmatrix} \widetilde{x}_1 \\ \widetilde{x}_2 \end{pmatrix} = F\begin{pmatrix} x_1 \\ x_2 \end{pmatrix} =$

$= \begin{pmatrix} 3\sqrt{2} & 4\sqrt{2} \\ -4 & 3 \end{pmatrix}\begin{pmatrix} x_1 \\ x_2 \end{pmatrix} + \begin{pmatrix} 25\sqrt{2} \\ 50 \end{pmatrix} : \ D = F^{-1}(\widetilde{D})$, або $\widetilde{D} = F(D)$.

Обчислимо $\operatorname{Pr}_D^F a$ для $a = \begin{pmatrix} 5 \\ -9.7 \end{pmatrix}$. Оскільки $\widetilde{a} = F(a) \approx \begin{pmatrix} 1,70 \\ 0.90 \end{pmatrix} \notin \widetilde{D}$,

отримуємо (див. приклад 10, п. 1):

$$\operatorname{Pr}_{\widetilde{D}} \widetilde{a} = \begin{cases} \widetilde{a}, \ \widetilde{a} \in \widetilde{D}; \\ 0 + \dfrac{1}{\|\widetilde{a} - 0\|}(\widetilde{a} - 0), \ \widetilde{a} \notin \widetilde{D} \end{cases} = \dfrac{\widetilde{a}}{\|\widetilde{a}\|} \approx \begin{pmatrix} 0.46 \\ 0.89 \end{pmatrix},$$

звідки остаточно маємо:

$$\operatorname{Pr}_D^F a = F^{-1}(\operatorname{Pr}_{\widetilde{D}} \widetilde{a}) = \begin{pmatrix} 3\sqrt{2} & 4\sqrt{2} \\ -4 & 3 \end{pmatrix}^{-1} \left(\dfrac{\widetilde{a}}{\|\widetilde{a}\|} - \begin{pmatrix} 25\sqrt{2} \\ 50 \end{pmatrix} \right) =$$

$$= \dfrac{1}{50}\begin{pmatrix} 3\sqrt{2} & -8 \\ 4\sqrt{2} & 6 \end{pmatrix}\left(\dfrac{\widetilde{a}}{\|\widetilde{a}\|} - \begin{pmatrix} 25\sqrt{2} \\ 50 \end{pmatrix} \right) \approx \begin{pmatrix} 5 \\ -9.84 \end{pmatrix}.$$

Зауважимо, що $\operatorname{Pr}_D^F a \ne \operatorname{Pr}_D a$ (рис. 12).
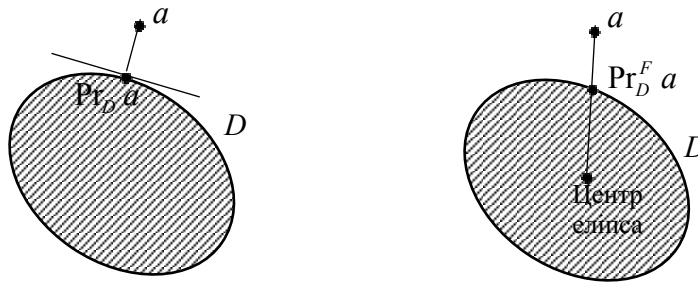
Рис. 12. Оператори $\operatorname{Pr}_D a$ і $\operatorname{Pr}_D^F a$ для еліпса $34(x_1 - 5)^2 + 41(x_2 + 10)^2 + 24(x_1 - 5) \times$
$\times (x_2 + 10) \le 1$

Приклад 14. Розглянемо в $\mathbb{R}^2$ повернутий прямокутник (див. також приклади 5 та 12) $D = \left\{ \begin{pmatrix} x_1 \\ x_2 \end{pmatrix} : \begin{cases} 2 \le 3x_1 + 4x_2 \le 5 \\ 2 \le -4x_1 + 3x_2 \le 10 \end{cases} \right\}$. Оскільки

$\begin{pmatrix} 3x_1 + 4x_2 \\ -4x_1 + 3x_2 \end{pmatrix} = 5\begin{pmatrix} 0.6 & 0.8 \\ -0.8 & 0.6 \end{pmatrix}\begin{pmatrix} x_1 \\ x_2 \end{pmatrix}$, область D пов'язана афінним перетво-

ренням $\begin{pmatrix} \widetilde{x}_1 \\ \widetilde{x}_2 \end{pmatrix} = F\left(\begin{pmatrix} x_1 \\ x_2 \end{pmatrix}\right) = \begin{pmatrix} 0.6 & 0.8 \\ -0.8 & 0.6 \end{pmatrix}\begin{pmatrix} x_1 \\ x_2 \end{pmatrix}$ із прямокутником $\widetilde{D} =$

$= \left\{ \begin{pmatrix} \widetilde{x}_1 \\ \widetilde{x}_2 \end{pmatrix} : \begin{cases} 0.4 \le \widetilde{x}_1 \le 1 \\ 0.4 \le \widetilde{x}_2 \le 2 \end{cases} \right\} = F(D)$, сторони якого паралельні координатним

осям (детальніше див. приклад 5). У цьому випадку, оскільки матриця

$A = \begin{pmatrix} 0.6 & 0.8 \\ -0.8 & 0.6 \end{pmatrix}$ є ортогональною (матрицею повороту), оператор $\mathrm{Pr}_D^F a$

збігається із проекцією: $\mathrm{Pr}_D^F a = \mathrm{Pr}_D a$ для довільного $a \in \mathbb{R}^n$ (див. приклад 12, рис. 11).

МЕТОД ПРОЕКЦІЇ ГРАДІЄНТА З АФІННИМ ПЕРЕТВОРЕННЯМ

Нехай $D \subset \mathbb{R}^n$ — непорожня опукла та замкнена множина, $f : \mathbb{R}^n \to \mathbb{R}$ диференційовна строго опукла функція на $\mathbb{R}^n$ За сформульованих умов, згідно з лемою 3, існує єдиний мінімум функції f на D: $x^* = \underset{x \in D}{\arg\min} f(x)$. Аналітичне обчислення x^* у практичних випадках є складним і почасти неможливим. Для чисельного розв'язання задачі $x^* = \underset{x \in D}{\arg\min} f(x)$ у 1964 р. американським вченим А. Голдштейном був запропонований (див. [7]) ітераційний метод, нині відомий як метод проекції градієнта:

- $x^0 \in \mathbb{R}^n$ — обрана початкова точка;
- $x^{k+1} = \mathrm{Pr}_D(x^k + \alpha^k h^k)$ ($k \geq 0$), де $h^k = -f'(x^k)$ напрямок кроку (антиградієнт), $a^k \in \mathbb{R}^n$ — довжина кроку (обирається залежно від модифікації методу).

Одним з найпоширеніших методів вибору довжини кроку є метод найшвидшого спуску: $\alpha^k = \underset{\alpha > 0}{\arg\min} f(x^k + \alpha h^k)$, який, разом з додатковими умовами на f і D, забезпечує збіжність $x^k \xrightarrow[k \to +\infty]{} x^*$; сформулюємо відомий (див., напр. [4]) результат у вигляді теореми.

Теорема 1. Нехай $D \subset \mathbb{R}^n$ — непорожня опукла та замкнена множина, $f : \mathbb{R}^n \to \mathbb{R}$ функція на $\mathbb{R}^n$, яка задовольняє умови:

- неперервна диференційовність на $\mathbb{R}^n$;
- сильна опуклість з параметром $\theta > 0$;
- градієнт є ліпшицевим з константою L, тобто $\| f'(x) - f'(y) \| \leq \leq L \| x - y \|$.

Тоді рекурентно задана послідовність

- $x^0 \in \mathbb{R}^n$ довільно обрана початкова точка,
- $x^{k+1} = \mathrm{Pr}_D(x^k + \alpha^k h^k)$ ($k \geq 0$), де $h^k = -f'(x^k)$, $\alpha^k = \underset{\alpha > 0}{\arg\min} f(x^k + \alpha h^k)$ збігається до x^* з геометричною швидкістю: $x^k \xrightarrow[k \to +\infty]{} x^*$, $\| x^{k+1} - x^* \| \leq q \| x^k - x^* \|$ ($k \geq k_0$), де $q \in [0,1)$ — фіксована константа, k_0 — фіксований номер.

Доведення див., напр. у [4].

Зауваження 4. Очевидно, умова геометричної швидкості (або лінійної швидкості) $\|x^{k+1} - x^*\| \le q\|x^k - x^*\|$ ($k \ge k_0$) еквівалентна умові $\|x^k - x^*\| \le$ $\le Cq^k$ ($k \ge 0$), де $q \in [0,1)$, $C \ge 0$ — фіксовані константи.

Метод проекції градієнта пов'язаний з обчисленням проекції точки x^k на множину D, що нескладно у простих випадках (наприклад, якщо D круг або прямокутник, див. приклад 10), проте ускладнюється до окремої задачі мінімізації для складніших випадків (наприклад, якщо D еліпс, див. приклад 11).

Для спрощення задачі проектування застосуємо у задачі пошуку $x^* = \underset{x \in D}{\arg\min} f(x)$ заміну змінних, пов'язану з афінним перетворенням $F : \mathbb{R}^n \to \mathbb{R}^n$, $F(x) = Ax + b$ (A — невироджена матриця розмірності $n \times n$, $b \in \mathbb{R}^n$). Позначивши, як і в п. 2, $\widetilde{D} = \{F(x) : x \in D\} = F(D)$, $\widetilde{x} = F(x)$, $\widetilde{f}(\widetilde{x}) = f(F^{-1}(\widetilde{x})) = f(A^{-1}\widetilde{x} - A^{-1}b)$, отримуємо область $\widetilde{D} \subset \mathbb{R}^n$ і функцію $\widetilde{f} : \mathbb{R}^n \to \mathbb{R}$. Таким чином, пошук $x^* = \underset{x \in D}{\arg\min} f(x)$ можна звести до пошуку $\widetilde{x}^* = \underset{\widetilde{x} \in \widetilde{D}}{\arg\min} \widetilde{f}(\widetilde{x})$, $\widetilde{x}^* = F^{-1}(x^*)$, з подальшим «поверненням» до $x = F^{-1}(\widetilde{x})$.

Теорема 2. Нехай функція $f : \mathbb{R}^n \to \mathbb{R}$ і область $D \subset \mathbb{R}^n$ задовольняють умови теореми 1, $x^{F,0} \in \mathbb{R}^n$ — довільна початкова точка, $x^{F,k+1} == \mathrm{Pr}_D^F(F^{-1}(F(x^{F,k}) + \widetilde{\alpha}^k \widetilde{h}^k))$ ($k \ge 0$), де $\widetilde{h}^k = -(A^T)^{-1} f'(x^{F,k})$, $\widetilde{\alpha}^k = \underset{\widetilde{\alpha} > 0}{\arg\min} f(x^{F,k} + \widetilde{\alpha}\widetilde{h}^k)$. Тоді послідовність $x^{F,k}$ ($k \ge 0$) збігається до $x^* = \underset{x \in D}{\arg\min} f(x)$ зі швидкістю геометричної прогресії:

$$x^{F,k} \xrightarrow[k \to +\infty]{} x^*, \ \|x^{F,k} - x^*\| \le C(q^F)^k \ (k \ge 0),$$

де $q^F \in [0,1)$, $C \ge 0$ — фіксовані константи.

Доведення. Розглянемо (див. також п. 2 і 4) отримані заміною змінних $\widetilde{x} = F(x)$ область $\widetilde{D} = \{\widetilde{x} = F(x) : x \in D\} = F(D)$ та функцію $\widetilde{f}(\widetilde{x}) =$ $= f(F^{-1}(\widetilde{x})) = f(A^{-1}\widetilde{x} - A^{-1}b)$.

Оскільки область D за умовою непорожня, опукла та замкнена, область $\widetilde{D} = F(D)$ за побудовою також є непорожньою, за лемою 4 опуклою, за неперервністю відображення F замкненою. Оскільки f за умовою є сильно опуклою з параметром $\theta > 0$, функція $\widetilde{f}$ за лемою 5 є сильно опуклою з параметром $\theta\lambda_{\max}^{-1} > 0$. Функція f за умовою є неперервно диференційовною, тоді функція $\widetilde{f}$ теж є диференційовною як композиція диференційовних відображень f і F^{-1}. Для обчислення $\widetilde{f}'$ знайдемо $(\widetilde{f}', d)$ для довільного фіксованого $d \in \mathbb{R}^n$:

$$(\widetilde{f}'(\widetilde{x}), d) = (f'(A^{-1}\widetilde{x} - A^{-1}b), A^{-1}d) = ((A^T)^{-1}f'(A^{-1}\widetilde{x} - A^{-1}b), d),$$

звідки, враховуючи довільність $d \in \mathbb{R}^n$, отримуємо, що $\widetilde{f}'(\widetilde{x}) = = ((A^T)^{-1}f'(F^{-1}(\widetilde{x}))$ є неперервним, і функція $\widetilde{f}$ є неперервно диференційовною. Нарешті, із ліпшицевості f' з константою L, для $\widetilde{f}'$ маємо:

$$\| \widetilde{f}'(\widetilde{x}) - \widetilde{f}'(\widetilde{y}) \|^2 = \| (A^T)^{-1}f'(A^{-1}\widetilde{x} - A^{-1}b) - (A^T)^{-1}f'(A^{-1}\widetilde{y} - A^{-1}b) \|^2 =$$

$$= ((A^T A)^{-1}(f'(A^{-1}\widetilde{x} - A^{-1}b) - f'(A^{-1}\widetilde{y} - A^{-1}b)),$$

$$f'(A^{-1}\widetilde{x} - A^{-1}b) - f'(A^{-1}\widetilde{y} - A^{-1}b)) \leq$$

$$\leq \lambda_{\min} \| f'(A^{-1}\widetilde{x} - A^{-1}b) - f'(A^{-1}\widetilde{y} - A^{-1}b)) \|^2 \leq$$

$$\leq \lambda_{\min} L^2 \| A^{-1}(\widetilde{x} - \widetilde{y}) \|^2 \leq \lambda_{\min}^2 L^2 \| \widetilde{x} - \widetilde{y} \|^2,$$

де $\lambda_{\min} = \min\limits_{x \in \mathbb{R}^n : \|x\|=1} (A^T A x, x)$ — мінімальне власне число матриці AA^T. Таким чином, $\widetilde{f}'$ ліпшицевий з константою $\lambda_{\min}L$. Отже, область $\widetilde{D}$ і функція $\widetilde{f}$ задовольняють умови теореми 1, тобто рекурентно задана послідовність $\widetilde{x}^k$ ($k \geq 0$), де $\widetilde{x}^0 \in \mathbb{R}^n$ довільно обрана початкова точка, $\widetilde{x}^{k+1} = \Pr_{\widetilde{D}}(\widetilde{x}^k + \widetilde{\alpha}^k \widetilde{h}^k)$, $\widetilde{h}^k = -\widetilde{f}'(\widetilde{x}^k) = -(A^T)^{-1}f'(F^{-1}(\widetilde{x}^k))$, $\widetilde{\alpha}^k = \arg\min\limits_{\widetilde{\alpha} > 0} \widetilde{f}(\widetilde{x}^k + \widetilde{\alpha}\widetilde{h}^k)$ збігається до x^* з геометричною швидкістю: $\widetilde{x}^k \xrightarrow[k \to +\infty]{} \widetilde{x}^*$, $\| \widetilde{x}^{k+1} - \widetilde{x}^* \| \leq \widetilde{q} \| \widetilde{x}^k - \widetilde{x}^* \|$ ($k \geq 0$), де $\widetilde{q} \in [0,1)$ фіксована константа. Увівши позначення $x^{F,k} = = F^{-1}(\widetilde{x}^k)$, дістаємо: $x^{F,0} = F^{-1}(\widetilde{x}^0)$ (початкова точка),

$$x^{F,k+1} = F^{-1}(\widetilde{x}^{k+1}) = F^{-1}(\Pr_{\widetilde{D}}(\widetilde{x}^k + \widetilde{\alpha}^k \widetilde{h}^k) = \Pr_D^F(F^{-1}(F(x^{F,k}) + \widetilde{\alpha}^k \widetilde{h}^k)).$$

Оскільки за лемою 3 існує єдиний $\widetilde{x}^* = \arg\min\limits_{\widetilde{x} \in \widetilde{D}} \widetilde{f}(\widetilde{x})$, за побудовою маємо зв'язок $\widetilde{x}^* = F(x^*)$, звідки $x^{F,k} \xrightarrow[k \to +\infty]{} x^*$. Нарешті, оцінимо швидкість збіжності $x^{F,k} \xrightarrow[k \to +\infty]{} x^*$:

$$\| x^{F,k+1} - x^* \| \leq \| F^{-1}(\widetilde{x}^{k+1}) - F^{-1}(\widetilde{x}^*) \| = \| A^{-1}(\widetilde{x}^{k+1} - \widetilde{x}^*) \| =$$

$$= ((AA^T)^{-1}(\widetilde{x}^{k+1} - \widetilde{x}^k), \widetilde{x}^{k+1} - \widetilde{x}^*) \leq$$

$$\leq \frac{1}{\lambda_{\min}} \| \widetilde{x}^{k+1} - \widetilde{x}^* \| \leq \frac{\widetilde{q}}{\lambda_{\min}} \| \widetilde{x}^k - \widetilde{x}^* \| = C\widetilde{q}^k,$$

тобто $x^{F,k} \xrightarrow[k \to +\infty]{} x^*$ із лінійною швидкістю, що завершує доведення теореми. □

Зауваження 5. Послідовності x^k ($k \geq 0$) та $x^{F,k}$ ($k \geq 0$) мають однакову границю x^*, однак, взагалі кажучи, поточково розрізняються, тобто найчастіше $x^k \neq x^{F,k}$.

Приклад 15. Нехай $f : \mathbb{R}^2 \to \mathbb{R}$, $f\left(\begin{pmatrix} x_1 \\ x_2 \end{pmatrix}\right) = (x_1 - 6)^2 + (x_2 + 11)^2 +$

$+ (x_1 - 6)^4$. Функція f сильно опукла з параметром $\theta = 2$, оскільки

$f''\left(\begin{pmatrix} x_1 \\ x_2 \end{pmatrix}\right) = \begin{pmatrix} 2 + 12(x_1 - 6)^2 & 0 \\ 0 & 2 \end{pmatrix}$.

Розглянемо задачу мінімізації функції f на множині $D \subset \mathbb{R}^2$ в еліпсі (див. приклади 6, 11 і 13):

$$D = \left\{ \begin{pmatrix} x_1 \\ x_2 \end{pmatrix} : 34(x_1 - 5)^2 + 41(x_2 + 10)^2 + 24(x_1 - 5)(x_2 + 10) \leq 1 \right\} =$$

$$= \left\{ \begin{pmatrix} x_1 \\ x_2 \end{pmatrix} : \left(\begin{pmatrix} 34 & 12 \\ 12 & 41 \end{pmatrix} \begin{pmatrix} x_1 - 5 \\ x_2 + 10 \end{pmatrix}, \begin{pmatrix} x_1 - 5 \\ x_2 + 10 \end{pmatrix} \right) \leq 1 \right\} =$$

$$= \left\{ \begin{pmatrix} x_1 \\ x_2 \end{pmatrix} : \left(\begin{pmatrix} 3\sqrt{2} & 4\sqrt{2} \\ -4 & 3 \end{pmatrix} \begin{pmatrix} x_1 \\ x_2 \end{pmatrix} + \begin{pmatrix} 25\sqrt{2} \\ 50 \end{pmatrix}, \begin{pmatrix} 3\sqrt{2} & 4\sqrt{2} \\ -4 & 3 \end{pmatrix} \begin{pmatrix} x_1 \\ x_2 \end{pmatrix} + \begin{pmatrix} 25\sqrt{2} \\ 50 \end{pmatrix} \right) \leq 1 \right\},$$

який пов'язаний афінним перетворенням

$$\begin{pmatrix} \tilde{x}_1 \\ \tilde{x}_2 \end{pmatrix} = F\left(\begin{pmatrix} x_1 \\ x_2 \end{pmatrix}\right) = \begin{pmatrix} 3\sqrt{2} & 4\sqrt{2} \\ -4 & 3 \end{pmatrix} \begin{pmatrix} x_1 \\ x_2 \end{pmatrix} + \begin{pmatrix} 25\sqrt{2} \\ 50 \end{pmatrix}$$

з кругом $\tilde{D} = \left\{ \begin{pmatrix} \tilde{x}_1 \\ \tilde{x}_2 \end{pmatrix} : \tilde{x}_1^2 + \tilde{x}_2^2 \leq 1 \right\} = F(D)$.

Оскільки область $D \subset \mathbb{R}$ непорожня, опукла і замкнена, можемо застосувати результат теореми 2; формулу для обчислення проекції точки на круг $\tilde{D}$ наведено у прикладі 10. У табл. 1 подано результати роботи класичного методу проекції градієнта (послідовність x^k, $k \geq 0$) та методу проекції градієнта з афінним перетворенням (послідовність $x^{F,k}$, $k \geq 0$); в обох випадках для збіжності з точністю до 10^{-5}. За початкову точку взято центр еліпса: $x^0 = x^{F,0} = \begin{pmatrix} 5 \\ -10 \end{pmatrix}$ (те ж саме спостерігається і за інших початкових точок).

Таблиця 1

k	**0**	**1**	**2**	**3**	**4**	**5**
x^k	$\begin{pmatrix} 5.00000 \\ -10.00000 \end{pmatrix}$	$\begin{pmatrix} 5.10119 \\ -10.15950 \end{pmatrix}$	$\begin{pmatrix} 5.11600 \\ -10.15380 \end{pmatrix}$	$\begin{pmatrix} 5.11628 \\ -10.15380 \end{pmatrix}$	$\begin{pmatrix} 5.11629 \\ -10.15380 \end{pmatrix}$	$\begin{pmatrix} 5.11628 \\ -10.15380 \end{pmatrix}$
$x^{F,k}$	$\begin{pmatrix} 5.00000 \\ -10.00000 \end{pmatrix}$	$\begin{pmatrix} 5.10640 \\ -10.15750 \end{pmatrix}$	$\begin{pmatrix} 5.11568 \\ -10.15400 \end{pmatrix}$	$\begin{pmatrix} 5.11623 \\ -10.15380 \end{pmatrix}$	$\begin{pmatrix} 5.11626 \\ -10.15380 \end{pmatrix}$	$\begin{pmatrix} 5.11626 \\ -10.15380 \end{pmatrix}$

Отже, комп'ютерне моделювання підтверджує, що $\lim\limits_{k \geq 0} x^k =$

$= \lim\limits_{k \geq 0} x^{F,k} \approx \begin{pmatrix} 5.1627 \\ -10.15380 \end{pmatrix}$, що збігається зі значенням $x^* = \arg\min\limits_{x \in D} f(x)$ з точністю до 10^{-5}, проте траєкторії x^k і $x^{F,k}$ розрізняються.

Приклад 16. Нехай $f : \mathbb{R}^2 \to \mathbb{R}$, $f\left(\begin{pmatrix} x_1 \\ x_2 \end{pmatrix}\right) = (x_1 + 1)^2 + (x_2 - 1)^2 + (x_1 + 1)^4$.

Функція f сильно опукла з параметром $\theta = 2$, оскільки $f''\left(\begin{pmatrix} x_1 \\ x_2 \end{pmatrix}\right) =$

$$= \begin{pmatrix} 2 + 12(x_1 + 1)^2 & 0 \\ 0 & 2 \end{pmatrix}.$$

Розглянемо задачу мінімізації функції f на множині $D \subset \mathbb{R}^2$ у повернутому прямокутнику (див. приклади 5, 10 і 12) $D = \left\{ \begin{pmatrix} x_1 \\ x_2 \end{pmatrix} : \begin{cases} 2 \le 3x_1 + 4x_2 \le 5 \\ 2 \le -4x_1 + 3x_2 \le 10 \end{cases} \right\}$, який пов'язаний афінним перетворенням

$$\begin{pmatrix} \widetilde{x}_1 \\ \widetilde{x}_2 \end{pmatrix} = F\left(\begin{pmatrix} x_1 \\ x_2 \end{pmatrix}\right) = \frac{1}{5} \begin{pmatrix} 3 & 4 \\ -4 & 3 \end{pmatrix} \begin{pmatrix} x_1 \\ x_2 \end{pmatrix} = \begin{pmatrix} 0.6 & 0.8 \\ -0.8 & 0.6 \end{pmatrix} \begin{pmatrix} x_1 \\ x_2 \end{pmatrix}$$ із прямокутником

$\widetilde{D} = \left\{ \begin{pmatrix} \widetilde{x}_1 \\ \widetilde{x}_2 \end{pmatrix} : \begin{cases} 2 \le 5\widetilde{x}_1 \le 5 \\ 2 \le 5\widetilde{x}_2 \le 10 \end{cases} \right\} = \left\{ \begin{pmatrix} \widetilde{x}_1 \\ \widetilde{x}_2 \end{pmatrix} : \begin{cases} 0.4 \le \widetilde{x}_1 \le 1 \\ 0.4 \le \widetilde{x}_2 \le 2 \end{cases} \right\} = F(D)$, сторони якого паралельні координатним осям.

Оскільки область $D \subset \mathbb{R}$ непорожня, опукла і замкнена, можемо застосувати результат теореми 2, формула для обчислення проекції точки на прямокутник $\widetilde{D}$ наведена у прикладі 10. У табл. 2 наведено результати роботи класичного методу проекції градієнта (послідовність x^k, $k \ge 0$) та методу проекції градієнта з афінним перетворенням (послідовність $x^{F,k}$, $k \ge 0$); в обох випадках для збіжності з точністю до 10^{-5}. За початкову точку взято центр прямокутника: $x^0 = x^{F,0} = \begin{pmatrix} -0.54 \\ 1.28 \end{pmatrix} = F^{-1}\left(\begin{pmatrix} 0.7 \\ 1.2 \end{pmatrix}\right)$ (схоже спостерігається і за інших початкових точок).

Т а б л и ц я 2

k	**0**	**1**	**2**	**3**	**4**	**5**
x^k	$\begin{pmatrix} -0.54000 \\ 1.28000 \end{pmatrix}$	$\begin{pmatrix} -0.85268 \\ 1.13951 \end{pmatrix}$	$\begin{pmatrix} -0.87694 \\ 1.15770 \end{pmatrix}$	$\begin{pmatrix} -0.87626 \\ 1.15719 \end{pmatrix}$	$\begin{pmatrix} -0.87627 \\ 1.15720 \end{pmatrix}$	$\begin{pmatrix} -0.87627 \\ 1.15720 \end{pmatrix}$
$x^{F,k}$	$\begin{pmatrix} -0.54000 \\ 1.28000 \end{pmatrix}$	$\begin{pmatrix} -0.85268 \\ 1.13951 \end{pmatrix}$	$\begin{pmatrix} -0.87694 \\ 1.15770 \end{pmatrix}$	$\begin{pmatrix} -0.87626 \\ 1.15719 \end{pmatrix}$	$\begin{pmatrix} -0.87627 \\ 1.15720 \end{pmatrix}$	$\begin{pmatrix} -0.87627 \\ 1.15720 \end{pmatrix}$

Отже, комп'ютерне моделювання підтверджує, що $\lim\limits_{k \ge 0} x^k = \lim\limits_{k \ge 0} x^{F,k} \approx$

$\approx \begin{pmatrix} 5.1627 \\ -10.15380 \end{pmatrix}$, що збігається зі значенням $x^* = \arg\min\limits_{x \in D} f(x)$ з точністю до 10^{-5}, і траєкторії x^k і $x^{F,k}$ також збігаються, що пояснюється ортогональністю матриці $\begin{pmatrix} 0.6 & 0.8 \\ -0.8 & 0.6 \end{pmatrix}$, яка визначає $F\left(\begin{pmatrix} x_1 \\ x_2 \end{pmatrix}\right)$.

ВИСНОВКИ

1. Афінне перетворення координат у деяких випадках суттєво спрощує проектування точки на множину.

2. Афінне перетворення у методі проекції градієнта принаймні не погіршує швидкість збіжності методу.

3. Напрямом подальших досліджень може бути узагальнення отриманого результату на ширший клас перетворень; принциповим має бути зберігання опуклості множин та сильної опуклості функцій.

ЛІТЕРАТУРА

1. Andersen Ang, "Projected Gradient Algorithm," *Mathématique et recherche opérationnelle*, 2021. Available: https://angms.science/doc/CVX/CVX_PGD.pdf
2. Sébastien Bubeck, "Convex Optimization: Algorithms and Complexity," *Foundations and Trends in Machine Learning*, vol. 8, no. 3-4, pp. 232–357, 2015. doi: 10.1561/2200000050
3. H. Jongen, K. Meer, and E. Triesch, *Optimization Theory*. New York, Boston, Dordrechr, London, Moscow: Kluwer Academic Publisher, 2007, 443 p.
4. A. Sukharev, A. Timokhov, and V. Fedorov, *Course Optimization Methods*. M.: Nauka, 2005, 368 p.
5. F.P. Vasil'ev, *Numerical Methods for Solving Extremal Problems.* M.: Nauka, 1988, 552 p.
6. Y. Nesterov, *Introductory Lectures on Convex Optimization*. Boston, Dordrechr, London: Kluwer Academic Publisher, 2004, 236 p.
7. A. Goldstein, "Convex programming in Hilbert space," *Bulletin of the American Mathematical Society*, no. 70, pp. 709–710, 1964.
8. M.P. Moklyachuk, *Foundations of Convex Analysis: Textbook.* Kyiv: TViMS, 2004, 240 p.
9. A. Ahmadi, *Characterizations of convex functions, strict and strong convexity, optimality conditions for convex problems*. 2021. Available: http://www.princeton.edu/~aaa/Public/Teaching/ORF523/ORF523_Lec7.pdf
10. R. Rockafellar, *Convex Analysis*. Princeton: Princeton University Press, 2015, 472 p.

INFORMATION ON THE ARTICLE

Igor Ya. Spectorsky, ORCID: 0000-0003-4863-7986, Educational and Research Institute for Applied System Analysis of the National Technical University of Ukraine "Igor Sikorsky Kyiv Polytechnic Institute", Ukraine, e-mail: i.spectorsky@gmail.com

GRADIENT PROJECTION: SIMPLIFYING MINIMIZATION AREA BY AFFINE TRANSFORM / I.Ya. Spectorsky

Abstract. One of the classical problems of optimization theory in a finite-dimensional space is to find a minimum of a function on a nonempty set. Usually, finding the precise solution to this task analytically requires a lot of computational resources or is even impossible at all. So, approximate methods are used most often in practical cases. One of the simplest and the most well-known among such approximate methods for unconditional optimization is the method of gradient descent; its generalization for conditional optimization was found in 1964, the method of projected gradient. For some simple sets (line segment, parallelepiped, ball), the projection of the point on the set can be easily found by an explicit formula. However, for more complicated sets (e.g., an ellipse), projecting becomes a separate task. Nevertheless, sometimes computing projection can be simplified by affine transform; e.g., an ellipse can be transformed into a ball by affine (moreover, by linear) transformation. The paper aims to simplify the problem of minimizing function on the set by changing the condition set by affine transform $F(x) = Ax + b$, where A is a non-degenerated square matrix, and b is a fixed vector of proper dimension.

Keywords: gradient projection, minimization, affine transformation.

STUDY OF THE FACTOR INFLUENCE ON THE UNIFORMITY OF COFFEE GRAIN GRINDING BY METHODS OF STATISTICAL ANALYSIS

I.V. HRYHORENKO, S.I. KONDRASHOV, S.M. HRYHORENKO, O.S. OPRYSHKIN

Abstract. In order to assess the impact of each of the factors that affect the quality and uniformity of grinding coffee beans and to compare the impact of these factors, it is worth establishing a quantitative indicator of this impact. To solve this problem, dispersion analysis was used as a method of organizing sample data according to possible sources of dispersion. The chosen method made it possible to decompose the total dispersion into components caused by the influence of factor levels. Grinding time, geometric dimensions of the grain, moisture content of the grain, speed of rotation of the motor shaft were selected as factors influencing the homogeneity of grinding. The justification and assessment of the reliability of statistical conclusions about the informational significance of indicators affecting the homogeneity of coffee grinding was carried out to ensure the highest possible probability of the obtained result.

Keywords: dispersion analysis, homogeneity of grinding, factor influence, model, indicator of control, coffee bean.

INTRODUCTION

The problems of determining the factor influence on the quality and uniformity of grinding and the creation of systems for controlling the grinding process are of interest to both domestic scientists and the world scientific community. The paper [1] states that one of the most common problems in the preparation of coffee drinks in coffee machines is the unsatisfactory quality of coffee, which is associated with improper grinding of coffee beans, and the taste of the coffee drink depends on the size of the ground particles and the uniformity of coffee grinding. The paper [2] examines the influence of the origin of coffee beans and the temperature during the grinding of roasted coffee. It is noted that the extraction depends on the temperature, the chemical composition of the water, as well as the available surface area of the coffee. The study [3] reported that some physico-chemical characteristics such as extraction yield, total dissolved solids, total phenol content, pH, and titrated acidity can strongly depend on the degree of grinding of the coffee bean. The work [4; 5] is aimed at developing an experiment to study the key factors affecting different methods of coffee preparation. The need to obtain different degrees of grinding of coffee beans in order to be able to provide a high flow rate of coffee in the preparation of espresso is discussed in the paper [6].

The structure or scheme of an experiment is described, by the factors involved in it and the ways in which different levels of different factors are combined [7]. The variance is used here as the simplest measure of dispersion, provid-

ing an opportunity to compare the influence of the factor under study and the factor of chance [8]. If the dispersion is due to the joint action of random causes and the change in the levels of the factors, then by obtaining an estimate of the total response variance and the estimation of the variances of the factors, one can find an estimate of the residual variance, and then, using statistical variance comparison criteria, rank the factors according to the degree of their effect on the response dispersion.

PRESENTATION OF THE TASK

The quality of grinding coffee beans is influenced by a number of factors that negatively affect the uniformity of grinding, which are difficult to stabilize to reduce the impact on the original value. As previously mentioned, it is necessary to carry out a procedure for randomizing factors in order to make their impact random and to be able to use statistical criteria.

Suppose that H — is the parameter of the control object characterizing the homogeneity of coffee grinding, which needs to be determined; $F_1, \ldots F_n$ — factors affecting the quality of the grinding process (e.g. grinding time, speed of rotation of the motor shaft, temperature at the engine stator, distance between mills, grain moisture, geometry of the bean: width, thickness, length). The result that takes into account the action of each of the factors can be written in the form of a mathematical model in which the influencing factors are H and $(n-1)$ factors due to the variability of the remaining control indicators. This statement is due to the fact that the remaining indicators characterize quantitatively $(n-1)$ the physical properties of the control object and can be directly measured.

To assess the homogeneity of coffee grinding, consider the model of the effect on the measurement result of the control index F taking into account the effects of four factors (H and factors whose levels are quantified by the values of the three control indicators (grinding time, geometric grain sizes, grain moisture). Data in cross-classification are denoted by symbols with four indices $\alpha, \beta, \gamma, \delta$. Since the control indicators are not additive, it is necessary to introduce components into the model characterizing the interaction between the indicators. Thus, the mathematical model has the form:

$$F_{\alpha\beta\gamma\delta i} = \overline{F} + f_\alpha + A_\beta + B_\gamma + C_\delta + (fA)_{\alpha\beta} + (fB)_{\alpha\gamma} + (fC)_{\alpha\delta} + (AB)_{\beta\gamma} +$$
$$+ (AC)_{\beta\delta} + (BC)_{\gamma\delta} + (fAB)_{\alpha\beta\gamma} + (fAC)_{\alpha\beta\delta} + (fBC)_{\alpha\gamma\delta} +$$
$$+ (ABC)_{\beta\gamma\delta} + (fABC)_{\alpha\beta\gamma\delta} + \varepsilon_{\alpha\beta\gamma\delta i}. \tag{1}$$

where $\alpha, \beta, \gamma, \delta$ are the number of factor levels; $\overline{F}$ — is the general average; f_α — is the deviation of the measurement result of the control indicator F from its average value $\overline{F}$, which is due to the influence of the parameter H; $A_\beta, B_\gamma, C_\delta$ — deviation of the measurement result $F_{\alpha\beta\gamma\delta}$ from $\overline{F}$, due to three factors; $(fA)_{\alpha\beta}, (fB)_{\alpha\gamma}, (fC)_{\alpha\delta}, (AB)_{\beta\gamma}, (AC)_{\beta\delta}, (BC)_{\gamma\delta}$ — deviations due to pairwise interactions of all influencing factors; $(fAB)_{\alpha\beta\gamma}, (fAC)_{\alpha\beta\delta}, (fBC)_{\alpha\gamma\delta}, (ABC)_{\beta\gamma\delta}$ — deviations due to the interaction of three influencing factors; $(fABC)_{\alpha\beta\gamma\delta}$ — deviation, which is due to the interaction of four influencing fac-

tors; $\varepsilon_{\alpha\beta\gamma\delta i}$ — random residue; i — is the number of multiple measurement at fixed levels $\alpha, \beta, \gamma, \delta$.

The initial conditions for model (1) will be:

1. $\sum_\alpha f_\alpha = 0;\ \sum_\beta A_\beta = 0;\ \sum_\gamma B_\gamma = 0;\ \sum_\delta C_\delta = 0;$

$\sum_\alpha (fA)_{\alpha\beta} = 0;\ \sum_\beta (fA)_{\alpha\beta} = 0;\ \sum_\alpha (fB)_{\alpha\gamma} = 0;\ \sum_\gamma (fB)_{\alpha\gamma} = 0;\ \sum_\alpha (fC)_{\alpha\delta} = 0;$

2. $\sum_\delta (fC)_{\alpha\delta} = 0;\ \sum_\beta (AB)_{\beta\gamma} = 0;\ \sum_\gamma (AB)_{\beta\gamma} = 0;\ \sum_\beta (AC)_{\beta\delta} = 0;\ \sum_\delta (AC)_{\beta\delta} = 0;$

$\sum_\gamma (BC)_{\gamma\delta} = 0;\ \sum_\delta (BC)_{\gamma\delta} = 0;$

$\sum_\alpha (fAB)_{\alpha\beta\gamma} = \sum_\beta (fAB)_{\alpha\beta\gamma} = \sum_\gamma (fAB)_{\alpha\beta\gamma} = 0;$

$\sum_\alpha (fAC)_{\alpha\beta\delta} = \sum_\beta (fAC)_{\alpha\beta\delta} = \sum_\delta (fAC)_{\alpha\beta\delta} = 0;$

3. $\sum_\alpha (fBC)_{\alpha\gamma\delta} = \sum_\gamma (fBC)_{\alpha\gamma\delta} = \sum_\delta (fBC)_{\alpha\gamma\delta} = 0;$

$\sum_\beta (ABC)_{\beta\gamma\delta} = \sum_\gamma (ABC)_{\beta\gamma\delta} = \sum_\delta (ABC)_{\beta\gamma\delta} = 0;$

4. $\sum_\alpha (fABC)_{\alpha\beta\gamma\delta} = \sum_\beta (fABC)_{\alpha\beta\gamma\delta} = \sum_\gamma (fABC)_{\alpha\beta\gamma\delta} = \sum_\delta (fABC)_{\alpha\beta\gamma\delta} = 0;$

5. $\sum_\alpha \sum_\beta \sum_\gamma \sum_\delta \sum_i \varepsilon_{\alpha\beta\gamma\delta i} = 0.$

In addition to these conditions, restrictions are imposed on the random balance:

1) all $\varepsilon_{\alpha\beta\gamma\delta i}$ are mutually independent;

2) $M[d_{abcq}{}^2] = \sigma^2\ \ M[\varepsilon_{\alpha\beta\gamma\delta i}{}^2] = \sigma^2$;

3) random variables $\varepsilon_{\alpha\beta\gamma\delta i}$ are distributed according to the normal law.

Regarding the type of deviations f_α, A_β, B_γ, C_δ we note the following:

1) f_α — is a random variable because it reflects the effect of a priori uncertain levels of the parameter of the control object *H;*

2) A_β, B_γ, C_δ — are parameters by virtue of the metrological values of the control indicators.

Since due to the randomness of the levels of the parameter *H* the resulting model (1) is not exclusively parametric, but can be attributed to mixed models.

TRANSITION TO THE MOST COMMON FACTOR FUEL MODEL

It is a well-known fact that the multifactor model (1) requires for its study a sample size of $k^4 \cdot r$, where k — is the number of levels for each of the factors, and r — is the number of multiple observations for all possible combinations of levels of the influencing factors. In order for the results obtained during the variance analysis to be statistically significant, the value must satisfy the conditions $k > 4$, $r > 1$.

Thus, at $k = 5$, and $r = 2$ the minimum volume of the number of four-dimensional observations of the control index F should be $5^4 \cdot 2 = 1250$ values. It turns out that it is very difficult, and sometimes almost impossible to provide such a large number of non-standard samples of coffee beans while maintaining the complete uniformity of the measurement experiment.

In order to avoid this complexity, we simplify model (1), leaving only the main deviations f_α, $A_\beta, B_\gamma, C_\delta$ and the deviations caused by pairwise interactions $(fA)_{\alpha\beta}, (fB)_{\alpha\gamma}, (fC)_{\alpha\delta}$. The resulting model will contain an increased residual $\psi_{\alpha\beta\gamma\delta v}$, which also includes a random residual $\varepsilon_{\alpha\beta\gamma\delta i}$, and deviations caused by the action of three: $(fAB)_{\alpha\beta\gamma}, (fAC)_{\alpha\beta\delta}, (fBC)_{\alpha\gamma\delta}, (ABC)_{\beta\gamma\delta}$ and four — $(fABC)_{\alpha\beta\gamma\delta}$, influencing factors, as well as pairwise deviations $(AB)_{\beta\gamma}$, $(AC)_{\beta\delta}$, $(BC)_{\gamma\delta}$:

$$F_{\alpha\beta\gamma\delta v} = \overline{F} + f_\alpha + A_\beta + B_\gamma + C_\delta + (fA)_{\alpha\beta}, (fB)_{\alpha\gamma}, (fC)_{\alpha\delta} + \psi_{\alpha\beta\gamma\delta v} \qquad (2)$$

In order to reduce the complexity of the model (1) it can be reduced to three two-factor simplified cross-classification models:

$$F_{\alpha\beta v} = \overline{F} + f_\alpha + A_\beta + (fA)_{\alpha\beta} + \psi(A)_{\alpha\beta v}; \quad \gamma = \delta = i = v; \qquad (3)$$

$$F_{\alpha\gamma v} = \overline{F} + f_\alpha + B_\gamma + (fB)_{\alpha\gamma} + \psi(B)_{\alpha\gamma v}; \quad \alpha = \delta = i = v; \qquad (4)$$

$$F_{\alpha\delta v} = \overline{F} + f_\alpha + C_\delta + (fC)_{\alpha\delta} + \psi_{(C)\alpha\delta v}; \quad \beta = \gamma = i = v. \qquad (5)$$

where v — is the number of multiple measurements of the F indicator in the table cell with the original model data (3), (4) i (5); $\psi_{(A)\alpha\beta v}$, $\psi_{(B)\alpha\gamma v}$, $\psi_{(C)\alpha\delta v}$ — random residues due to three factors: grinding time, geometric grain size, grain moisture, respectively.

A comparison of the residuals of the presented models with the residuals of models (1) and (2) shows that simplifying the model obviously reduces its accuracy, because these residuals are more than $\psi_{\alpha\beta\gamma\delta v}$, a $\psi_{\alpha\beta\gamma\delta v} > \varepsilon_{\alpha\beta\gamma\delta i}$.

Let's analyze the condition that allows us to synthesize model (2) on the basis of models (3), (4), and (5). For each of these models, there is the same main deviation s, additional deviations $A_\beta, B_\gamma, C_\delta$, and deviations due to the effects of pairwise interaction.

The first and most important condition is to ensure that the standard deviations in models (3), (4), and (5) are equal to each other. To do this, the number of groups of observations of the control indicator F must be the same for all models, which corresponds to the same number of rows in the original data table. At the same time, the number of values of the control indicator F in each group should be the same b, and the value of $F_{\alpha\beta\gamma\delta}$ in the middle of each group should remain unchanged (where N — is the number of measurements) for any of the models (3), (4), and (5). The grouping of $F_{\alpha\beta\gamma\delta i}$ values should be carried out according to the specified groups of values of the parameter H.

It should be borne in mind that the method of forming columns (subgroups) in the table of the established source data should be determined by the established additional influencing factor, and provide a single procedure for selecting $F_{\alpha\beta\gamma\delta}$ values for each of the subgroups of the group with a fixed number $\alpha, \alpha = \overline{1, b}$. The

number of subgroups in each of the groups must also be the same m, for each of the models (3), (4) and (5). Each of the subgroups of any of the groups (cells of the source data table) will have the same $g = N/mb$ — the number of observations.

In order to model additional factor injection (based on all vortex data) on display F, you need to carry out the following operations:

– rank the intragroup values of the control indicator F_p, you need to carry out the following operations;

– break the ranked (for all b groups) series of values of the F_p indicator into m subgroups;

– in each of the subgroups, select the g values of the information index F corresponding to the g values of the F_p indicator and enter them into the source data cell.

The resulting $b \times m$ table of observation results of control measure F values with g multiple observations in each of $b \times m$ cells can now be used for variance analysis of any of the models (3), (4) and (5) cross classifications corresponding to a given additional factor influencing F_p, $p = \overline{1,3}$.

We will introduce the designation of these three factors through F_s, F_t, F_u . In general, we will denote any of these factors through F_p. Therefore, any of the models (3), (4), and (5) can be represented in the form:

$$F_{\alpha z v} = \overline{F} + f_\alpha + p_z + (fp)_{\alpha z} + \psi_{\alpha z v}, \qquad (6)$$

where $\psi_{\alpha z v}$ — is a random residue.

The complete decomposition of the sum of the squares of deviations of the values $F_{\alpha z v}$ from $\overline{F}$, under the initial conditions and constraints of the model (1), will have the following form:

$$W = W_f + W_p + W_{fp} + W_{\psi p} . \qquad (7)$$

The results of the variance analysis of the model (6) are presented in Table 1, where $F_{\alpha z v} = \overline{F}_\alpha, \overline{F}_z, \overline{F}_{\alpha z}$ — are the average values in rows, columns and in cells.

T a b l e 1. Results of dispersion analysis

Source of variability	Number of degrees of freedom k	Sum of squares
The main factor H	$b - 1$	$W_f = gp \sum\limits_{\alpha=1}^{b} (\overline{F}_\alpha - \overline{F})^2$
Additional factor F_p	$m - 1$	$W_p = gb \sum\limits_{z=1}^{m} (\overline{F}_z - \overline{F})^2$
Interaction between H and F_p	$(b{-}1)(m{-}1)$	$W_{fp} = g \sum\limits_{\alpha=1}^{b} \sum\limits_{z=1}^{m} (\overline{F}_{\alpha z} - \overline{F}_\alpha - \overline{F}_z + \overline{F})^2$
Remainder (in the middle of the cell)	$bm\,(g{-}1)$	$W_{\psi p} = \sum\limits_{\alpha=1}^{b} \sum\limits_{z=1}^{m} \sum\limits_{v=1}^{g} (F_{\alpha z v} - \overline{F}_{\alpha z})^2$
General	$N - 1$	$W = \sum\limits_{\alpha=1}^{b} \sum\limits_{z=1}^{m} \sum\limits_{v=1}^{g} (F_{\alpha z v} - \overline{F})^2$

Unfortunately, for models (3), (4) that (5), the same $\overline{F}$ and the sums of W and W_f is represented by the sum of squares from $F_{\alpha\beta\gamma\delta}$ from F model (2) as the union of the sum of (7), $p = \overline{1,3}$ with the fictitious residual sum W_ψ^*, which characterizes the influence of factors not taken into account in the model:

$$W = W_f + W_s + W_t + W_u + W_{fs} + W_{ft} + W_{fu} + W_\psi^* . \qquad (8)$$

The resulting ratio (8) makes it possible to simplify the previous model (2) and represent it in the following form:

$$F_{\alpha\beta\gamma\delta\nu} = \overline{F} + f_\alpha + A_\beta + B_\gamma + C_\delta + (fA)_{\alpha\beta} + (fB)_{\alpha\gamma} + (fC)_{\alpha\delta} + \psi_{\alpha\beta\gamma\delta\nu}^*, \qquad (9)$$

where $\psi_{\alpha\beta\gamma\delta\nu}^*$ — is a random residue due to the action of three factors: grinding time, geometric grain size, grain moisture. The values of the sums of the right part of the expression (8), in addition to W_ψ^* are calculated according to the equations of the sums of the squares of the tables of the results of the variance analysis of the models (3), (4) and (5), similar to Table 2, replacing the F_p factor with a specific additional factor — F_s, F_t, F_u. The sum of W_ψ^* can be calculated from any of the equations:

$$\begin{cases} W_\psi^* = W_{\psi\,s} - W_t - W_u - W_{f\,t} - W_{f\,u} ; \\ W_\psi^* = W_{\psi\,t} - W_s - W_u - W_{f\,s} - W_{f\,u} ; \\ W_\psi^* = W_{\psi\,u} - W_t - W_s - W_{f\,t} - W_{f\,s} ; \end{cases} \qquad (10)$$

$$W_\psi^* = W_{\psi\,s} + W_{\psi\,t} + W_{\psi\,u} + 2W_f + 2W . \qquad (11)$$

Table 2 presents the results of the variance analysis of the simplified model (9), the random residue of which will be fictitious (determines the sum of W_ψ^* in equation (8)).

T a b l e 2 . Results of the variance analysis with the model (8)

Source of variability	Source of variability	Sum of the squares of deviations
The main factor H	$k_f = b - 1$	$\overline{W}_f = W_f / k_f$
Factor F_s	$k_s = m - 1$	$\overline{W}_s = W_s / k_s$
Factor F_t	$k_t = m - 1$	$\overline{W}_t = W_t / k_t$
Factor F_u	$k_u = m - 1$	$\overline{W}_u = W_u / k_u$
Interaction HF_s	$k_{fs} = (b-1) \cdot (m-1)$	$\overline{W}_{fs} = W_{fs} / k_{fs}$
Interaction HF_t	$k_{ft} = (b-1) \cdot (m-1)$	$\overline{W}_{ft} = W_{ft} / k_{ft}$
Interaction HF_u	$k_{fu} = (b-1) \cdot (m-1)$	$\overline{W}_{fu} = W_{fu} / k_{fu}$
Remainder	$k_\psi = N - b((3m-2)$	$\overline{W}_\psi = W_\psi^* / k_\psi$
General	$k = N-1$	$\overline{W} = W / k$

We will conduct a study of the simplified model (9). This model, occupies an intermediate position between model (1) and models (3), (4) and (5). From (10) it follows that the residual sum of the simplified model (11) is less than the residual sums of the models (3), (4) and (5). This indicates the increased accuracy of this model compared to the cross-classification models (3), (4), and (5). Based on the results of Table. 2, we conclude that the number of degrees of freedom of the residual sum W_{ψ}^{*} decreases with an increase in the number of b groups (by the level of parameter H) and the number of m subgroups (by the level of additional factors F_s, F_t, F_u).

Let's write k_{ψ} from Table 2 in the following form:

$$k_{\psi} = N - b \cdot m \left(3 - \frac{b}{m} \right). \tag{12}$$

From the resulting expression (12) it follows that the number of degrees of freedom is the greater, at $b \cdot m = \text{const}$, the greater the ratio b/m.

This finding makes it possible to further plot the number of groups and subgroups in the tables of the original data of the models (3), (4), and (5). In this case, the number of b groups (subranges of measurement of the control parameter H (homogeneity) is desirable to increase, and the number of subgroups should be reduced, reducing m to a minimum. For example, take $m = 2$. This will increase the number of degrees of freedom of the residual sum W_{ψ}^{*}. Thus, it is obvious that the main advantage of the simplified model is the possibility of simultaneous testing of the H_0, hypothesis, that is, when the influence of factors H, F_s, F_t, F_u, on the information measure of control F is absent. In this way you can write H_0: $f_p = ... = f_b = 0$.

This is the main hypothesis and its components have the following form:

$$H_0^s : s_p = ... = s_m = 0 ; \quad H_0^{fs} : fs_p = ... = fs_{bm} = 0 ;$$

$$H_0^t : t_p = ... = t_m = 0 ; \quad H_0^{ft} : ft_p = ... = ft_{bm} = 0 ;$$

$$H_0^u : u_p = ... = u_m = 0 ; \quad H_0^{fu} : fu_p = ... = fu_{bm} = 0 .$$

The test of the hypotheses presented is done in relation to the corresponding mean squares $(\overline{W}_f, \overline{W}_s, \overline{W}_t, \overline{W}_u, ..., \overline{W}_{fu})$ to the mean residual square $\overline{W}_{\psi}$ followed by comparison of the obtained F — statistics with the corresponding percentage points for F — distributions.

This advantage of the simplified model (9) makes it possible to estimate the amount of expected information about the levels of parameter H for the information measure F when considering the levels of both influencing factors and their interactions:

$$I = \log \sqrt{1 + \left(\frac{\sigma_F}{\sigma_{\Delta F}} \right)^2} ,$$

where $\sigma_F^2 = \overline{W}_f$;

$$\sigma_F^2 = \overline{W}_f = \frac{1}{(n-1)}\sum_{i=1}^{n}(F_i - \overline{F})^2 \,,$$

where $\overline{F} = \frac{1}{n}\sum_{i=1}^{n}F_i$; $\sigma_{\Delta F}^2$ — is a function of the sum of the squares of deviations $(\overline{W}_f, \overline{W}_s, \overline{W}_t, \overline{W}_u, ..., \overline{W}_{fu})$ in Table 1 and Table. 2.

Table 3 presents the equation for calculating $\sigma_{\Delta F}^2$ for the simplified model (9) with different combinations of factors affecting the information indicator F.

T a b l e 3. Calculated Ratios for Parameter $\sigma_{\Delta F}^2$

Factorial influences taken into account	$\sigma_{\Delta F}^2$
Additional factor F_s	$(W_t + W_u + W_{fs} + W_{ft} + W_{fu} + W_\psi^*)\big/(k_t + k_u + k_{fs} + k_{ft} + k_{fu} + k_\psi)$
Additional factor F_t	$(W_s + W_u + W_{fs} + W_{ft} + W_{fu} + W_\psi^*)\big/(k_s + k_u + k_{fs} + k_{ft} + k_{fu} + k_\psi)$
Additional factor F_u	$(W_s + W_t + W_{fs} + W_{ft} + W_{fu} + W_\psi^*)\big/(k_s + k_t + k_{fs} + k_{ft} + k_{fu} + k_\psi)$
F_s, F_t	$(W_u + W_{fs} + W_{ft} + W_{fu} + W_\psi^*)\big/(k_u + k_{fs} + k_{ft} + k_{fu} + k_\psi)$
F_s, F_u	$(W_t + W_{fs} + W_{ft} + W_{fu} + W_\psi^*)\big/(k_t + k_{fs} + k_{ft} + k_{fu} + k_\psi)$
F_t, F_u	$(W_s + W_{fs} + W_{ft} + W_{fu} + W_\psi^*)\big/(k_s + k_{fs} + k_{ft} + k_{fu} + k_\psi)$
F_s, F_t, F_u	$(W_{fs} + W_{ft} + W_{fu} + W_\psi^*)\big/(k_{fs} + k_{ft} + k_{fu} + k_\psi)$
F_s, F_t, F_u, HF_s	$(W_{ft} + W_{fu} + W_\psi^*)\big/(k_{ft} + k_{fu} + k_\psi)$
F_s, F_t, F_u, HF_t	$(W_{fs} + W_{fu} + W_\psi^*)\big/(k_{fs} + k_{fu} + k_\psi)$
F_s, F_t, F_u, HF_u,	$(W_{fs} + W_{ft} + W_\psi^*)\big/(k_{fs} + k_{ft} + k_\psi)$
F_s, F_t, F_u, HF_s, HF_t, HF_u	$\overline{W}_\psi$

If we do not take into account all the influencing factors, and this corresponds to obtaining information under multifactorial influence, then

$$\sigma_{\Delta F}^2 = \frac{W_s + W_t + W_u + W_{fs} + W_{ft} + W_{fu} + W_\psi^*}{N - b - 2}.$$

In order to perform the verification of statistical findings, we present model (9) as a one-factor model of one-sided classification, i.e., when the influence of additional factors is determined solely by the magnitude of the random residue $\psi_{\alpha i}$:

$$F_{\alpha i} = \overline{F} + f_i + \psi_{\alpha i}, , \tag{13}$$

where $\alpha = \overline{1,b}$; $i = \overline{1,n}$; $n = N/b$.

In this case, the magnitude of n multifactorial observations in each of the b groups is the same.

Model (13), due to the uncertainty of the levels of the control parameter *H*, refers to the variance component models.

We will use the formal analysis of the model (13) and write the expression of the full sum of the squares of deviations *W* through the sum of the two terms

$$W_f = n \sum_{i=1}^{b} (\overline{F}_\alpha - \overline{F})^2 \;,$$

where $\overline{F}_\alpha$ — group mean values of the performance trait; $\overline{F}$ — is the overall average; *n* — is the number of units of the population in each group.

Residual variance (random) is the sum of the group sums of the squares of deviations of all variant of the resultant trait in groups from the mean values of the trait in them:

$$W_\psi = \sum_{\alpha=1}^{b} \sum_{i=1}^{g} (F_{\alpha i} - \overline{F}_\alpha)^2 \;.$$

Consider now the ratio of the mean squares for the recorded sums W_f and W_ψ :

$$F = \frac{W_f / (b-1)}{W_\psi / (N-b)} \;.$$

F-statistics can be used to test one of two hypotheses:

$$H_0 : M[\overline{F_1}] = ... = M[\overline{F_b}] \quad H_1 : M[\overline{F_1}] \neq ... \neq M[\overline{F_b}] .$$

A rule follows from the theory: if statistical conclusions indicate the validity of the main hypothesis H_0 , then the parameter *H* does not affect the change in the control indicator *F*. That is, the indicator *F* does not carry information about the change in the levels of the control parameter *H*, and if the hypothesis H_1, is valid, then the indicator *F* is informative in relation to the control parameter *H*. Decisions μ_0 (valid hypothesis H_0) and μ_1 (valid hypothesis H_1) are accepted, comparing the *F* statistic with the critical value F_K.

The conditional densities of the probability distribution of *F*-statistics are a linearly transformed random variable with central $F_{b-1, N-b}$, the distribution:

$$f(F/H_0) \approx F_{b-1, N-b} \;,$$

$$f(F/H_1) \approx \left(1 + g \frac{\sigma_f^2}{\sigma^2} \right) \cdot F_{b-1, N-b} \;, \tag{14}$$

where the variances σ_f^2 and σ^2 refer, respectively, to the random deviations of f_α і $\psi_{\alpha i}$ in the model (13).

The variance of σ_f^2 can be represented as the sum:

$$\sigma_f^2 = \sigma_H^2 + \sigma_r^2 \;,$$

where σ_H^2 — the variance of the control parameter *H*, which is due to the uncertainty of its values in the measurement range D_H ; σ_r^2 — the variance of the

measurement result of the values of the control parameter *H*, which is due to the uncertainty of the reproduction of the values of *H* by the technical means of control (in fact, this is the variance of the measurement result).

Testing hypotheses about the significance of the effects of factors and their interactions is carried out using the Fisher criterion. To do this, calculate the ratio of the corresponding mean squares to the remaining middle square. The obtained values are compared with the F_K values found in the *F*-distribution tables for the accepted significance level $\alpha = 0,05$, or higher (0,01 – 0,001) and the number of degrees of freedom.

Hence, if the control measure *F* is sensitive to a change in the level of the control parameter *H* over the entire range of its measurements, then the *F*-statistic will be characterized by the distribution density (14) for all measured levels of the indicator *H*.

Now consider the problem of one-sided testing of the parameter *H* within the implementation of the alternative hypothesis H_1. This hypothesis must be represented as a complex one, which will check the correspondence between the real value *f* of the control parameter *H* and the control value f_0:

$$H_1^0 : \ f \le f_0 \ \text{(parameter *H* is normal)};$$

$$H_1^1 : \ f > f_0 \ \text{(parameter *H* is not normal)}.$$

Such situations must correspond to the choice of one of two solutions:

$$\mu_0 : \ F \le F_K \,,$$

where *F* — calculated value of the *F*-criterion; F_K — tabular value of the *F*-criterion. Then the influence of the factor on the control parameter is not proven, but the absence of influence of the factor is not proven.

If:

$$\mu_1 : \ F > F_K \,,$$

then statistical observation proves with a given probability the influence of the factor on the control parameter.

Enter the following designations: Ω_1 and Ω_2 — probabilities of errors of the first and second kind:

$$\Omega_1 = P(\mu_1 / f \le f_0) \,; \quad \Omega_2 = P(\mu_0 / f > f_0) \,.$$

Then the probabilities of choosing solutions μ_0, μ_1 are respectively determined by the expressions:

$$P[F > F_K] \ge 1 - \Omega_2 \,, \tag{15}$$

$$P[F > F_K] \le \Omega_1 \,. \tag{16}$$

The fragment *F* has distribution (14), then from the expressions (15) and (16) it flows

$$\begin{cases} P[F_{b-1,N-b} > F_K (1 + n v_1^2)^{-1}] \ge 1 - \Omega_2; \\ P[F_{b-1,N-b} > F_K (1 + n v_0^2)^{-1}] > \Omega_1, \end{cases} \tag{17}$$

where

$$\begin{cases} \nu_1^2 = \dfrac{\sigma_H^2 + \sigma_r^2}{\sigma^2}; \\[3mm] \nu_0^2 = \dfrac{\sigma_r^2}{\sigma^2}. \end{cases} \qquad (18)$$

Considering the system of equations (17), one can find the value of F_K that satisfies both of these expressions. To do this, it is necessary to ensure that the condition is fulfilled

$$\frac{F_{b-1,N-b,1-\Omega_1}}{F_{b-1,N-b,\Omega_2}} \le \frac{1+n\nu_1^2}{1+n\nu_0^2}. \qquad (19)$$

The numerator and denominator of the left side of the inequality (19) are $(1-\Omega_1)$ and Ω_2 — are the percentage points of the central F — the distribution with $(b-1)$ and $(N-b)$ degrees of freedom.

It can be shown now that the expression that (19) corresponds to the expression:

$$\frac{\chi_{b-1,1-\Omega_1}^2}{\chi_{b-1,\Omega_2}^2} \le \frac{\nu_1^2}{\nu_0^2}, \qquad (20)$$

where $\chi_{b-1,1-\Omega_1}^2$, χ_{b-1,Ω_2}^2 — percentage points of the central χ^2 distribution with $(b-1)$ degrees of freedom.

From formula (20) it follows that given number of levels b of control parameter H (groups of results of observations of parameter F of model (13)) and given ratio $\nu_1^2 \big/ \nu_0^2 = A$ it is possible to estimate the reliability of decision-making μ_0 and μ_1

$$A = 1 - \frac{\Omega_1 + \Omega_2}{2},$$

fixed, for example, the value of Ω_1 (Naiman – Pearson criterion) and calculate Ω_2, as the interval:

$$\Omega_2 = \frac{1}{2^{\frac{b-1}{2}} \cdot \Gamma\left(\frac{b-1}{2}\right)} \int\limits_0^{z_{\min}} \chi^{\left(\frac{b-1}{2}-1\right)} \cdot e^{-\frac{\chi}{2}} \partial\chi,$$

where $z_{\min} = \chi_{b-1,1-\Omega_1}^2 \big/ A$; $\Gamma\left(\dfrac{b-1}{2}\right)$ — gamma function.

The relation A is determined from the formula (18):

$$A = 1 + \frac{\sigma_r^2}{\sigma^2}.$$

The results obtained already make it possible to move on to the practical use of the simplified model. At the same time, it must be remembered that in the practice of variance analysis, there may be cases when the number of replicates obtained for each combination of levels of the factors under study is different and

equal m_{ij}; m_{ij} numbers can have any value, including zero, but each row and column must have at least one, and some have two non-zero values. In this case, there are possible situations in which it is impossible to obtain unbiased estimates for all parameters of the model. The need to introduce a system of weight coefficients into the calculated ratios complicates the calculations, the analysis of such plans involves, as a rule, the use of a computer.

SUMMARIES

When executing the partition, the following results are obtained:

− to assess the homogeneity of coffee grinding, a mathematical model of the influence of four factors on the result of measuring the control indicator has been developed;

− a simplified model of cross-classifications was proposed for further use and investigated, which took into account the effects of simultaneous interaction of four factors (grinding time, geometric grain size, grain moisture, speed of rotation of the motor shaft) on the result of measurement of the unit control indicator (uniformity of coffee grinding);

− obtained equations that allow to evaluate the reliability of statistical conclusions in relation to the informational significance of control indicators for the proposed simplified model of cross-classification;

− analytical ratios are obtained, which allow to estimate the amount of information on each of the control indicators under the factor influence on the proposed linear function of the transformation of these indicators.

− the advantages of the chosen approach are that it makes it possible to assess the validity of multiparameter control results of three or more levels of the control indicator and to select the most informative subsets of these values.

REFERENCES

1. V.P. Misyats, M.M. Rubanka, and S.A. Demishonkova, "System of adaptive control of the drive of automatic coffee machines," *Bulletin of the Khmelnytskyi National University*, no. 1, pp. 151–159, 2021 (293). doi: 10.31891/2307-5732-2021-293-1-151-159.
2. E. Uman et al., "The effect of bean origin and temperature on grinding roasted coffee," *Sci. Rep.*, vol. 6, 24483, 2016. doi: https://doi.org/10.1038/srep24483.
3. Nancy Cordoba, Laura Pataquiva, Coralia Osorio, Fabian Leonardo Moreno Moreno, and Ruth Yolanda Ruiz, "Effect of grinding, extraction time and type of coffee on the physicochemical and flavor characteristics of cold brew coffee," *Sci. Rep.*, 9, 8440, 2019. doi: https://doi.org/10.1038/s41598-019-44886-w.
4. Jonathan D. Walston, Daniel L. Short, and M. Affan Badar, "An Experimental Design on Coffee Extraction Factors Impacting the Measurable Percent of Total Dissolved Solids in Solution," *Asia-Pacific Journal of Management Research and Innovation*, pp. 1–11, 2023. doi: 10.1177/2319510X221136690.
5. Anderson G. Costa, Eudócio R.O. da Silva, Murilo M. de Barros, and Jonatthan A. Fagundes, "Estimation of percentage of impurities in coffee using a computer vision system," *Brazilian Journal of Agricultural and Environmental Engineering*, vol. 26, no. 2, pp. 142–148, 2022. doi: http://dx.doi.org/10.1590/1807-1929/agriambi.v26n2p142-148.
6. G. Angeloni et al., "Test of an innovative method to prepare coffee powder puck, improving espresso extraction reliability," *Eur. Food Res. Technol.*, 248, pp. 163–170, 2022. doi: https://doi.org/10.1007/s00217-021-03868-x.

7. Ihor Hryhorenko, Elena Tverytnykova, Svitlana Hryhorenko, and Viktoria Krylova, "Temperature sensor research as a part of a microprocessor system by statistical analysis method," *2022 IEEE 3rd KhPI Week on Advanced Technology (KhPIWeek), 2022, Kharkiv, Ukraine*, pp. 102–107. doi: 10.1109/ХПИНеделя57572.2022.9916478.

8. I. Hryhorenko, S. Kondrashov, and O. Opryshkin, "Formation of test impacts for the first level of the information and measurement system," *Bulletin of the National Technical University «KhPI». Series: New solutions in modern technology*, no. 1 (15), pp. 19–26, 2023. doi: https://doi.org/10.20998/2413-4295.2023.01.03.

INFORMATION ON THE ARTICLE

Ihor V. Hryhorenko, ORCID: 0000-0002-4905-3053, National Technical University "Kharkiv Polytechnic Institute", Ukraine, e-mail: grigmaestro@gmail.com

Serhii I. Kondrashov, ORCID: 0000-0002-5191-8562, National Technical University "Kharkiv Polytechnic Institute", Ukraine, e-mail: Serhii.Kondrashov@khpi.edu.ua

Svitlana M. Hryhorenko, ORCID: 0000-0003-0150-4844, National Technical University "Kharkiv Polytechnic Institute", Ukraine, e-mail: sngloba@gmail.com

Oleksandr S. Opryshkin, ORCID: 0009-0008-7094-5129, National Technical University "Kharkiv Polytechnic Institute", Ukraine, e-mail: Aleksandr.Opryshkin@cit.khpi.edu.ua

ДОСЛІДЖЕННЯ ФАКТОРНОГО ВПЛИВУ НА ОДНОРІДНІСТЬ ПОМЕЛУ ЗЕРНА КАВИ МЕТОДАМИ СТАТИСТИЧНОГО АНАЛІЗУ / І.В. Григоренко, С.І. Кондрашов, С.М. Григоренко, О.С. Опришкін

Анотація. Для оцінювання впливу кожного із факторів, які впливають на якість та однорідність помелу зерна кави, і порівняння впливу цих факторів варто встановити кількісний показник цього впливу. Для цього використано дисперсійний аналіз як метод організації вибіркових даних відповідно до можливих джерел розсіювання. Обраний метод дозволив розкласти загальне розсіювання на складові, зумовлені впливом рівнів факторів. Факторами, що впливають на однорідність помелу, обрано: час помелу, геометричні розміри зерна, вологість зерна, швидкість обертання валу двигуна. Проведено обґрунтування та оцінювання достовірності статистичних висновків про інформаційну значущість показників, що впливають на однорідність помелу кави для забезпечення максимально високої вірогідності отриманого результату.

Ключові слова: дисперсійний аналіз, однорідність помелу, факторний вплив, модель, показник контролю, зерно кави.

ВІДОМОСТІ ПРО АВТОРІВ

Андреєва Тетяна Василівна,

асистент кафедри інженерії програмного забезпечення Національного авіаційного університету, Україна, Київ

Астраханцев Андрій Анатолійович,

доцент, кандидат технічних наук, доцент кафедри інформаційних технологій в телекомунікаціях Навчально-наукового Інституту телекомунікаційних систем КПІ ім. Ігоря Сікорського, Україна, Київ

Баран Данило Романович,

аспірант КПІ ім. Ігоря Сікорського, Україна, Київ

Ворохобін Ігор Ігорович,

професор, доктор технічних наук, директор Навчально-наукового інституту навігації Національного університету «Одеська морська академія», Україна, Одеса

Глоба Лариса Сергіївна,

професор, доктор технічних наук, професор кафедри інформаційних технологій в телекомунікаціях Навчально-наукового Інституту телекомунікаційних систем КПІ ім. Ігоря Сікорського, Україна, Київ

Гончаренко Олександр Євгенович,

кандидат технічних наук, доцент кафедри автоматизації технологічних процесів і робото-технічних систем Одеського національного технологічного університету, Україна, Одеса

Григоренко Ігор Володимирович,

професор, кандидат технічних наук, професор кафедри інформаційно-вимірювальних технологій і систем Національного технічного університету «Харківський політехнічний інститут», Україна, Харків

Григоренко Світлана Миколаївна,

доцент, кандидат технічних наук, доцент кафедри комп'ютерних та радіоелектронних систем контролю та діагностики Національного технічного університету «Харківський політехнічний інститут», Україна, Харків

Гріненко Олена Олександрівна,

кандидат технічних наук, в.о. завідувача кафедри інженерії програмного забезпечення Національного авіаційного університету, Україна, Київ

Гурський Олександр Олександрович,

кандидат технічних наук, доцент кафедри автоматизації технологічних процесів і робототехнічних систем Одеського національного технологічного університету, Україна, Одеса

Дегтярьов Дмитро Володимирович,

студент магістратури кафедри інформаційних технологій в телекомунікаціях Навчально-наукового Інституту телекомунікаційних систем КПІ ім. Ігоря Сікорського, Україна, Київ

Денисенко Андрій Володимирович,

кандидат технічних наук, старший викладач кафедри інформаційних систем Національного університету «Одеська політехніка», Україна, Одеса

Дорофєєв Юрій Іванович,

професор, доктор технічних наук, завідувач кафедри системного аналізу та інформаційно-аналітичних технологій Національного технічного університету «Харківський політехнічний інститут», Україна, Харків

Зайченко Юрій Петрович,

професор, доктор технічних наук, професор кафедри математичних методів системного аналізу ІПСА КПІ ім. Ігоря Сікорського, Україна, Київ

Іванова Ірина Миколаївна,

викладач кафедри експлуатації портів і технології вантажних робіт Одеського національного морського університету, Україна, Одеса

Кондрашов Сергій Іванович,

професор, доктор технічних наук, професор кафедри інформаційно-вимірювальних технологій і систем Національного технічного університету «Харківський політехнічний інститут», Україна, Харків

Корбан Дмитро Вікторович,

доцент, кандидат технічних наук, доцент кафедри управління судном Національного університету «Одеська морська академія», Україна, Одеса

Любчик Леонід Михайлович,

професор, доктор технічних наук, професор кафедри комп'ютерної математики та аналізу даних Національного технічного університету «Харківський політехнічний інститут», Україна, Харків

Малько Максим Миколайович,

доцент, кандидат технічних наук, професор кафедри системного аналізу та інформаційно-аналітичних технологій Національного технічного університету «Харківський політехнічний інститут», Україна, Харків

Мельник Олексій Миколайович,

доцент, кандидат технічних наук, доцент кафедри судноводіння і морської безпеки Одеського національного морського університету, Україна, Одеса

Онищенко Олег Анатолійович,

професор, доктор технічних наук, професор кафедри технічної експлуатації флоту Національного університету «Одеська морська академія», Україна, Одеса

Опришкін Олександр Сергійович,

аспірант Національного технічного університету «Харківський політехнічний інститут», Україна, Харків

Панкратов Євген Володимирович,

аспірант КПІ ім. Ігоря Сікорського, Україна, Київ

Панкратова Наталія Дмитрівна,

член-кореспондент НАН України, професор, доктор технічних наук, заступник директора з наукової роботи ІПСА КПІ ім. Ігоря Сікорського, Україна, Київ

Писарчук Олексій Олександрович,

професор, доктор технічних наук, професор кафедри обчислювальної техніки КПІ ім. Ігоря Сікорського, Україна, Київ

Романій Кирило Анатолійович,

студент магістратури кафедри інформаційних технологій в телекомунікаціях Навчально-наукового Інституту телекомунікаційних систем КПІ ім. Ігоря Сікорського, Україна, Київ

Романко Євген Олегович,

студент магістратури кафедри інформаційних технологій Міжрегіональної Академії управління персоналом, Україна, Київ

Сидорський Володимир Сергійович,

аспірант КПІ ім. Ігоря Сікорського, Україна, Київ

Спекторський Ігор Якович,

доцент, кандидат фізико-математичних наук, доцент кафедри математичних методів системного аналізу ІПСА КПІ ім. Ігоря Сікорського, Україна, Київ

Старовойт Тетяна Василівна,

аспірант ІПСА КПІ ім. Ігоря Сікорського, Україна, Київ

Стеценко Максим Сергійович,

судновий механік 1-го розряду, Навчально-науковий інститут інженерії Національного університету «Одеська морська академія», Україна, Одеса

Терновський Валентин Борисович,

професор, доктор фізико-математичних наук, професор кафедри навігації і керування судном Одеського національного морського університету, Україна, Одеса

Тимчик Григорій Семенович,

професор, доктор технічних наук, декан приладобудівного факультету КПІ ім. Ігоря Сікорського, Україна, Київ

Федоров Олександр Володимирович,

студент магістратури кафедри інформаційних технологій в телекомунікаціях Навчально-наукового Інституту телекомунікаційних систем КПІ ім. Ігоря Сікорського, Україна, Київ

ПРАВИЛА ОФОРМЛЕННЯ СТАТЕЙ

для журналу

«СИСТЕМНІ ДОСЛІДЖЕННЯ ТА ІНФОРМАЦІЙНІ ТЕХНОЛОГІЇ»

1. Стаття з анотаціями та іншою інформацією подається з використанням веб-сайту журналу (http://journal.iasa.kpi.ua).

Назва статті, прізвище та ініціали автора (авторів), а також анотація (від 700 до 1000 символів) подаються українською та англійською мовами.

2. Текст статті набирається в редакторі Microsoft Word 2003 шрифтом Times New Roman із вирівнюванням по ширині.

3. На початку статті вказується індекс УДК, назва статті, ініціали та прізвище автора (авторів).

4. Список літератури подається в порядку посилання після тексту статті. Якщо є можливість, у списку вказується DOI кожного посилання.

5. Набір формул здійснюється в редакторі формул «Equations». Для змінних з індексами та без індексів застосовуються дужки клавіатурного набору, наприклад $(x_i^j, y_k^l), [x_i^j, y_k^l]$.

6. Символи у формулах (крім особливих випадків) набираються курсивом. Допускаються прямі символи, але їх треба розмітити або включити до списку спеціальних символів.

7. Нумерувати необхідно тільки ті формули (винесені на середину рядків), на які є посилання в тексті.

8. Таблиці та рисунки виконуються в одному стилі, їм надається номер, назва і розташовуються після посилань у тексті. Не слід повторювати в статті підписи до рисунків та таблиць.

9. Стаття разом із таблицями, рисунками і списком літератури має бути не більше 15 сторінок. Оглядові статті обсягом до 25 сторінок приймаються за домовленістю із редколегією.

10. До рукопису додаються відомості про кожного автора: країна, місто, місце роботи, службова посада, вчений ступінь та звання, сфера наукових досліджень, контактні телефони, адреса та e-mail.